Increase Service Life at Bridge Ends through Improved Abutment and Approach Slab Details and Water Management Practices

Final Report
October 2023

BRIDGE ENGINEERING CENTER

IOWA STATE UNIVERSITY
Institute for Transportation

Sponsored by
Iowa Highway Research Board
(IHRB Projects TR-722 and TR-739)
Iowa Department of Transportation
(InTrans Projects 17-605 and 17-637)

About the Bridge Engineering Center

The mission of the Bridge Engineering Center (BEC) is to conduct research on bridge technologies to help bridge designers/owners design, build, and maintain long-lasting bridges.

About the Institute for Transportation

The mission of the Institute for Transportation (InTrans) at Iowa State University is to save lives and improve economic vitality through discovery, research innovation, outreach, and the implementation of bold ideas.

Iowa State University Nondiscrimination Statement

Iowa State University does not discriminate on the basis of race, color, age, ethnicity, religion, national origin, pregnancy, sexual orientation, gender identity, genetic information, sex, marital status, disability, or status as a US veteran. Inquiries regarding nondiscrimination policies may be directed to the Office of Equal Opportunity, 3410 Beardshear Hall, 515 Morrill Road, Ames, Iowa 50011, telephone: 515-294-7612, hotline: 515-294-1222, email: eooffice@iastate.edu.

Disclaimer Notice

The contents of this report reflect the views of the authors, who are responsible for the facts and the accuracy of the information presented herein. The opinions, findings and conclusions expressed in this publication are those of the authors and not necessarily those of the sponsors.

The sponsors assume no liability for the contents or use of the information contained in this document. This report does not constitute a standard, specification, or regulation.

The sponsors do not endorse products or manufacturers. Trademarks or manufacturers' names appear in this report only because they are considered essential to the objective of the document.

Iowa DOT Statements

Federal and state laws prohibit employment and/or public accommodation discrimination on the basis of age, color, creed, disability, gender identity, national origin, pregnancy, race, religion, sex, sexual orientation or veteran's status. If you believe you have been discriminated against, please contact the Iowa Civil Rights Commission at 800-457-4416 or Iowa Department of Transportation's affirmative action officer. If you need accommodations because of a disability to access the Iowa Department of Transportation's services, contact the agency's affirmative action officer at 800-262-0003.

The preparation of this report was financed in part through funds provided by the Iowa Department of Transportation through its "Second Revised Agreement for the Management of Research Conducted by Iowa State University for the Iowa Department of Transportation" and its amendments.

The opinions, findings, and conclusions expressed in this publication are those of the authors and not necessarily those of the Iowa Department of Transportation.

Technical Report Documentation Page

1. Report No.	2. Government Accession No.	3. Recipient's Catalog No.
IHRB Projects TR-722 and TR-739		

4. Title and Subtitle	5. Report Date
Increase Service Life at Bridge Ends through Improved Abutment and Approach Slab Details and Water Management Practices	October 2023
	6. Performing Organization Code
7. Author(s)	**8. Performing Organization Report No.**
Behrouz Shafei (orcid.org/0000-0001-5677-6324), Brent Phares (orcid.org/0000-0001-5894-4774), Weizhuo Shi (orcid.org/0000-0001-8193-0098), and Shadi Azad (orcid.org/0009-0004-9911-5568)	InTrans Projects 17-605 and 17-637
9. Performing Organization Name and Address	**10. Work Unit No. (TRAIS)**
Bridge Engineering Center Iowa State University 2711 South Loop Drive, Suite 4700 Ames, IA 50010-8664	**11. Contract or Grant No.**
12. Sponsoring Organization Name and Address	**13. Type of Report and Period Covered**
Iowa Highway Research Board Iowa Department of Transportation 800 Lincoln Way Ames, IA 50010	Final Report
	14. Sponsoring Agency Code
	IHRB Projects TR-722 and TR-739

15. Supplementary Notes

Visit https://intrans.iastate.edu for color pdfs of this and other research reports.

16. Abstract

Integral and semi-integral abutment bridges have become increasingly popular in Iowa and across the country because they eliminate joints at the bridge ends. Expansion joints in bridge decks allow water to seep in and corrode bearings along with other structural elements in conventional bridge construction. An integral abutment connects the bridge deck and girders with the substructure in one piece to reduce maintenance and increase service life. The abutment moves with the rest of the bridge, and this movement introduces new issues with water drainage, soil settlement, soil erosion, and concrete cracking. The objective of this research was to evaluate improved bridge end details to increase service life and investigate limitations placed on the use of semi-integral abutment bridges. Research methods include a literature review, visual inspections, field monitoring, and finite element simulations.

The extensive literature review identified research relevant to improving the performance of bridge ends. Abutments, approach slabs, geotechnical aspects, drainage, and expansion joints were evaluated in detail. It was found that innovative bridge abutments allow for the elimination of conventional bearings and attempt to reduce issues associated with integral construction. Semi-integral abutment bridges and those with approach slabs attached to the abutment were inspected across the state of Iowa to assess the performance of current design methods. The condition and performance of tied joints was found to be unsatisfactory in some instances, with measured openings much larger than those built during initial construction. Joints between wingwalls and approach slabs were also found to be in poor condition. Four bridges were outfitted with a multitude of sensors, including strain gauges and displacement transducers, to measure concrete expansion and bridge displacement. Finite element models were also created to investigate the movement of approach slabs on the soil below. Simulated bridge expansion provided insights into approach slab behavior and tie bar stresses due to friction. Parametric studies were completed on various approach slab properties, including friction with soil, soil stiffness, tie bar style, and bridge skew.

17. Key Words	18. Distribution Statement
expansion joint—integral abutment bridge—semi-integral abutment	No restrictions.

19. Security Classification (of this report)	20. Security Classification (of this page)	21. No. of Pages	22. Price
Unclassified.	Unclassified.	222	NA

Form DOT F 1700.7 (8-72) **Reproduction of completed page authorized**

INCREASE SERVICE LIFE AT BRIDGE ENDS THROUGH IMPROVED ABUTMENT AND APPROACH SLAB DETAILS AND WATER MANAGEMENT PRACTICES

Final Report
October 2023

Principal Investigator
Behrouz Shafei, Associate Professor
Bridge Engineering Center, Iowa State University

Co-Principal Investigator
Brent Phares, Bridge Research Engineer
Bridge Engineering Center, Iowa State University

Graduate Research Assistants
Douglas Krapf and Conor Duffy

Authors
Behrouz Shafei, Brent Phares, Weizhuo Shi, and Shadi Azad

Sponsored by
Iowa Highway Research Board and Iowa Department of Transportation
(IHRB Projects TR-722 and TR-739)

Preparation of this report was financed in part
through funds provided by the Iowa Department of Transportation
through its Research Management Agreement with the
Institute for Transportation
(InTrans Projects 17-605 and 17-637)

A report from
Bridge Engineering Center
Institute for Transportation at Iowa State University
2711 South Loop Drive, Suite 4700
Ames, IA 50010-8664
Phone: 515-294-8103 / Fax: 515-294-0467
https://bec.iastate.edu

TABLE OF CONTENTS

ACKNOWLEDGMENTS xv
EXECUTIVE SUMMARY xvii
CHAPTER 1. INTRODUCTION 19
1.1. Overview 19
1.2. Research Needs and Motivations 20
1.3. Research Objectives 20
1.4. Report Outline 20
CHAPTER 2. LITERATURE REVIEW 22
2.1. Overview 22
2.2. Abutment Details 22
2.3. Approach Slab Details 40
2.4. Geotechnical Design 46
2.5. Bridge End Drainage 48
2.6. Expansion Joints 51
2.7. Approach Slab Performance 52
2.8. Recommendations for Mitigating Approach Slab Failure 56
2.9. Inventory of Iowa Approach Slab Performance 59
CHAPTER 3. BRIDGE VISUAL INSPECTIONS 78
3.1. 1215 Polk 78
3.2. 111 Pottawattamie 80
3.3. 113 Cass 82
3.4. 213 Cass 83
3.5. 310 Jasper (Northbound and Southbound) 84
3.6. 208 Bremer (Northbound and Southbound) 85
3.7. 108 Blackhawk 88
3.8. Joint Condition 89
CHAPTER 4. BRIDGE INSTRUMENTATION AND DATA 90
4.1. Sensor Descriptions 90
4.2. Jasper County 118 92
4.3. Story County 118 111
4.4. Polk County 120 127
4.5. Butler County 118 136
CHAPTER 5. FINITE ELEMENT MODELING 148
5.1. Jasper County 118 FE Model 149
5.2. Story County 118 FE Model 164
5.3. Additional Models for Investigation of Settlement and Erosion 183
5.4. Shelby County 118 FE Model 197
5.5. Washington County FE Model 200
CHAPTER 6. CONCLUSIONS AND RECOMMENDATIONS 213

6.1. Literature Review.....213
6.2. Inspections 215
6.3. Field Monitoring 215
6.4. Finite Element Analysis.....217

REFERENCES 219

LIST OF FIGURES

Figure 1.1. Factors contributing to a “bump” at the end of a bridge 19
Figure 2.1. Proposed strong-axis alternative pile orientation for Illinois integral abutment bridges founded on H-piles 25
Figure 2.2. H-pile summary: permissible IDOT integral abutment bridge lengths versus skew (100 ft intermediate spans).....26
Figure 2.3. Integral abutment pile selection chart based on EEL 27
Figure 2.4. Earth pressure behind the abutment 29
Figure 2.5. Comparison of horizontal stress behind abutment after fourth cycle of 30 mm bridge expansion 30
Figure 2.6. Comparison of total displacement in backfill after bridge deck contracting to original length following fourth cycle of 30 mm bridge expansion.....31
Figure 2.7. Details of Louisiana Department of Transportation and Development (LaDOTD) prototype semi-integral abutment bridge design.....32
Figure 2.8. Proposed dependent backwall configuration, i.e., construction joint over the backwall face at the span side with continuous bottom reinforcement.....33
Figure 2.9. Deck sliding over backwall 34
Figure 2.10. Semi-integral abutment details 35
Figure 2.11. Deck extension 36
Figure 2.12. Example detail of Virginia Abutment 37
Figure 2.13. Cross section at abutment showing elastic inclusion 38
Figure 2.14. Proposed buttress at semi-integral abutment bridges 38
Figure 2.15. VDOT rub plate example design calculations.....39
Figure 2.16. Abutment and approach slab cross section.....39
Figure 2.17. Elevation view of precast approach slab 43
Figure 2.18. Reinforcement details of an embedded beam approach slab.....45
Figure 2.19. Proposed new integral abutment bridge design alternatives 47
Figure 2.20. Proposed abutment backfill drainage system with geomembrane and graded granular filter (units in mm).....49
Figure 2.21. Cross section of a wingwall and drainage system 50
Figure 2.22. Voiding under approach slab.....53
Figure 2.23. Diagram summarizing frequent problems at several bridge sites 53
Figure 2.24. Problems leading to the formation of a bump 54
Figure 2.25. Structural movement due to thermal effects.....54
Figure 2.26. Transverse cracking of approach.....55
Figure 2.27. Examples of voiding at integral abutment bridges 56
Figure 2.28. Differential settlement at barrier 60
Figure 2.29. Differential settlement at joint.....61
Figure 2.30. Examples of spalling 61
Figure 2.31. Transverse cracking.....62
Figure 2.32. Asphalt patch.....62
Figure 2.33. Cracking/Differential settlement at barrier.....63
Figure 2.34. Cracking at barrier.....63
Figure 2.35. General information about the bridge.....64
Figure 2.36. Bridge plan sheet location 64

Figure 2.37. Bridge plan sheet—design number 65
Figure 2.38. Bridge plan sheet—abutment type 65
Figure 2.39. Bridge plan sheet—approach slab details.....66
Figure 2.40. Bridge inspection photographs—approach slabs 66
Figure 2.41. Bridge inspection photographs—barriers.....67
Figure 2.42. Bridge inspection sheet location.....67
Figure 2.43. Bridge issues entries 68
Figure 2.44. Bridges with stub abutments 68
Figure 2.45. Different types of joints in stub abutments.....69
Figure 2.46. Bridge plan sheet—approach slab information 69
Figure 2.47. Bridge inspection photographs 70
Figure 2.48. Table of bridge issues 70
Figure 2.49. Bridge issues table and bridge inspection photographs.....71
Figure 2.50. Bridge issues according to abutment type 72
Figure 2.51. General properties of the investigated bridges 73
Figure 3.1. South bridge-deck-to-approach-slab joint with excess sealant (left) and water and abutment staining at the outermost girder (right).....79
Figure 3.2. North abutment face 80
Figure 3.3. Transverse approach slab crack (left) and bridge-deck-to-approach-slab joint (right).....81
Figure 3.4. Void at the intersection of bridge-deck-to-approach-slab joint and barrier 81
Figure 3.5. Approach-slab-to-wingwall joint showing separation (left) and misaligned wingwall and barrier (right) 82
Figure 3.6. Iowa DOT curb E joint detail 83
Figure 3.7. Abutment face showing the new backwall on top of the old footing.....83
Figure 3.8. Concrete cracking at the end of the wingwall (left) and additional cracking at the end of the wingwall (right).....84
Figure 3.9. Blocked embankment drainage (left) and additional blocked embankment drainage (right).....85
Figure 3.10. Deck-to-approach-slab joint showing severe spalling (left) and additional deck-to-approach-slab joint showing severe spalling (right).....86
Figure 3.11. Typical embankment condition (left) and embankment condition at the abutment (right).....87
Figure 3.12. Horizontal void created by the embankment pulling away from the abutment 87
Figure 3.13. Measuring tape showing the vertical depth of the void.....88
Figure 4.1. Jasper County 118—east and west abutments 92
Figure 4.2. Jasper County 118—approach slab dimensions and section view 92
Figure 4.3. Jasper County 118—instrumentation plan (typical of east and west ends).....93
Figure 4.4. Jasper County 118—EP1-W earth pressure sensor after installation.....94
Figure 4.5. Jasper County 118—typical strain gauge installation 95
Figure 4.6. Jasper County 118—crackmeter without protective cover (left) and crackmeter with protective cover installed (right).....96
Figure 4.7. Jasper County 118—displacement transducer with reference post (left) and longitudinal and transverse displacement transducers attached at the acute bridge corner (right) 97

Figure 4.8. Jasper County 118—daily maximum and minimum air temperatures, August 30, 2018, to May 8, 2019 99
Figure 4.9. Jasper County 118—east longitudinal displacement....100
Figure 4.10. Jasper County 118—west longitudinal displacement....100
Figure 4.11. Jasper County 118—total measured, theoretical, and modified bridge expansion 101
Figure 4.12. Jasper County 118—air and concrete temperatures over time....103
Figure 4.13. Jasper County 118—west end joint expansion (southwest bridge corner)....104
Figure 4.14. Jasper County 118—west end joint expansion (northwest bridge corner)....104
Figure 4.15. Jasper County 118—east end joint expansion (northeast bridge corner)....105
Figure 4.16. Jasper County 118—east end joint expansion (southeast bridge corner)....105
Figure 4.17. Jasper County 118—east abutment transverse displacement....106
Figure 4.18. Jasper County 118—west abutment transverse displacement....106
Figure 4.19. Jasper County 118—east longitudinal and transverse displacement relationship....107
Figure 4.20. Jasper County 118—west longitudinal and transverse displacement relationship....107
Figure 4.21. Jasper County 118—EP2-E earth pressure for full monitoring period 109
Figure 4.22. Jasper County 118—EP2-W earth pressure for full monitoring period....109
Figure 4.23. Jasper County 118—EP1-W earth pressure for full monitoring period....110
Figure 4.24. Story County 118—approach slab section and dimensions 111
Figure 4.25. Story County 118—approach slab instrumentation plan....112
Figure 4.26. Story County 118—strain gauges installed on the longitudinal rebar and tie bars 113
Figure 4.27. Story County 118—crackmeter installation across the barrier rail joint....114
Figure 4.28. Story County 118—crackmeter approach slab side blockout location 115
Figure 4.29. Story County 118—air and concrete slab temperatures....116
Figure 4.30. Story County 118—measured and theoretical longitudinal bridge expansion....117
Figure 4.31. Story County 118—approach-slab-to-sleeper-slab joint expansion....118
Figure 4.32. Story County 118—approach-slab-to-sleeper-slab joint expansion....118
Figure 4.33. Story County 118—approach-slab-to-sleeper-slab joint expansion....119
Figure 4.34. Story County 118—bridge-barrier-to-approach-slab-barrier joint expansion....120
Figure 4.35. Story County 118—bridge-barrier-to-approach-slab-barrier joint expansion....120
Figure 4.36. Story County 118—bridge-barrier-to-approach-slab-barrier joint expansion....121
Figure 4.37. Story County 118—bridge-barrier-to-approach-slab-barrier joint expansion....121
Figure 4.38. Story County 118—representative slab strain gauge behavior 122
Figure 4.39. Story County 118—SG10-S measured strains 123
Figure 4.40. Story County 118—curb gap at the barrier end (typical)....124
Figure 4.41. Story County 118—open barrier joint (typical) 125
Figure 4.42. Iowa DOT E joint....125
Figure 4.43. Story County 118—approach slab modified subbase condition immediately before concrete pouring....126
Figure 4.44. Story County 118—large void under the south abutment corner....126
Figure 4.45. Story County 118—visible exposed rebar and foundation pile....127
Figure 4.46. Polk County 120—approach slab section and dimensions....128
Figure 4.47. Polk County 120—approach slab instrumentation plan....128

Figure 4.48. Polk County 120—strain gauges in tie 129
Figure 4.49. Polk County 120—strain gauges installed on the longitudinal rebar and tie bars 129
Figure 4.50. Polk County 120—crackmeter installation across the abutment-to-approach-slab joint 130
Figure 4.51. Polk County 120—air and concrete slab temperatures 131
Figure 4.52. Polk County 120—measured longitudinal bridge expansion at east end 131
Figure 4.53. Polk County 120—measured longitudinal bridge expansion at west end 132
Figure 4.54. Polk County 120—measured strains, EA5 and EA6 132
Figure 4.55. Polk County 120—measured strains, WA5 and WA6 133
Figure 4.56. Polk County 120—measured strains, EA7 and EA8 133
Figure 4.57. Polk County 120—measured strains, WA7 and WA8 134
Figure 4.58. Polk County 120—measured strains, EA10 and EA11 134
Figure 4.59. Polk County 120—measured strains, WA10 and WA11 135
Figure 4.60. Polk County 120—measured strains in the ties, EA4 and EA9 135
Figure 4.61. Polk County 120—measured strains in the ties, WA4 and WA9 136
Figure 4.62. Butler County 118—approach slab section and dimensions 137
Figure 4.63. Butler County 118—approach slab instrumentation plan 138
Figure 4.64. Butler County 118—strain gauges installed on the longitudinal rebars 139
Figure 4.65. Butler County 118—crackmeter installation across the abutment-to-approach-slab joint 139
Figure 4.66. Butler County 118—air and concrete slab temperatures 140
Figure 4.67. Butler County 118—measured longitudinal bridge expansion at east end 141
Figure 4.68. Butler County 118—measured longitudinal bridge expansion at west end 141
Figure 4.69. Butler County 118—measured strains at the approach-slab-to-sleeper-slab joint 142
Figure 4.70. Butler County 118—measured strains at the approach-slab-to-bridge-deck joint, middle 143
Figure 4.71. Butler County 118—measured strains at the approach-slab-to-bridge-deck joint, corners 145
Figure 4.72. Butler County 118—measured strains at the east approach-slab-to-bridge-deck joint 146
Figure 4.73. Butler County 118—transverse crack on the east approach slab 147
Figure 5.1. Jasper County 118—finite element model geometry 149
Figure 5.2. Iowa DOT modified subbase grain size distribution 150
Figure 5.3. Jasper County 118—finite element model mesh 151
Figure 5.4. Jasper County 118—finite element model boundary conditions 152
Figure 5.5. ABAQUS friction behavior verification 153
Figure 5.6. Jasper County 118—equivalent thermal coefficient of expansion 155
Figure 5.7. Jasper County 118—modified (tied) finite element model boundary conditions 156
Figure 5.8. Jasper County 118—modified (tied) finite element model with tie bars 156
Figure 5.9. Jasper County 118—Case 2 displacement magnitude 158
Figure 5.10. Jasper County 118—Case 3 X displacement 158
Figure 5.11. Jasper County 118—Case 4 X displacement 159
Figure 5.12. Jasper County 118—Cases 1 and 2 approach slab movement 160
Figure 5.13. Jasper County 118—Cases 3 and 4 approach slab movements 160

Figure 5.14. Jasper County 118—Case 3 soil contact pressure contour plot 161
Figure 5.15. Jasper County 118—Case 4 soil contact pressure contact plot 162
Figure 5.16. Jasper County 118—tied approach slab load-displacement (X direction) 163
Figure 5.17. Jasper County 118—tied approach slab transverse load-displacement (expansion) 164
Figure 5.18. Story County 118—approach slab mesh density sensitivity 165
Figure 5.19. Story County 118—approach slab strain comparison 166
Figure 5.20. Story County 118—tie bar strain comparison 167
Figure 5.21. Story County 118—approach slab corner displacement comparison.....167
Figure 5.22. Story County 118—tied approach expansion comparison 168
Figure 5.23. Story County 118—soil friction load-displacement comparison 170
Figure 5.24. Story County 118—von Mises stress for varying coefficients of friction (contraction) 171
Figure 5.25. Story County 118—soil stiffness study approach slab concrete stresses 172
Figure 5.26 Iowa DOT BR-205 standard tied connection 173
Figure 5.27. Story County 118—tie bar study approach slab stresses.....174
Figure 5.28. Story County 118—tie bar study von Mises stresses (contraction) 175
Figure 5.29. Story County 118—tie bar study von Mises stresses (expansion) 176
Figure 5.30. Story County 118—approach slab plan view for changing skew angle from 30 to 0 degrees (left to right).....177
Figure 5.31. Story County 118—skew angle study load-displacement.....178
Figure 5.32. Story County 118—skew angle study concrete stresses 178
Figure 5.33. Story County 118—concrete stress contours for 30 degree skew for contraction (left) and expansion (right) 179
Figure 5.34. Story County 118—skew angle study von Mises stress range (contraction) 180
Figure 5.35. Story County 118—von Mises distribution for 0 degree skew 181
Figure 5.36. Story County 118—von Mises distribution for 15 degree skew 182
Figure 5.37. Story County 118—von Mises distribution for 30 degree skew 183
Figure 5.38. Story County 118—FE assembly and mesh.....185
Figure 5.39. Jasper County model stress distribution.....189
Figure 5.40. Initial vertical settlement for Story County approach slab 190
Figure 5.41. Initial stress values for Story County model (top).....190
Figure 5.42. Initial stress values for Story County model (bottom) 191
Figure 5.43. Stress concentrations at dowel connection 191
Figure 5.44. Story County 8 ft void scenario.....192
Figure 5.45. Maximum vertical displacement versus void length 193
Figure 5.46. Concrete tensile stress in joint versus void length.....193
Figure 5.47. Maximum tensile stress in bottom of span versus void length.....194
Figure 5.48. Tensile stresses in connection joint (13 ft void).....195
Figure 5.49. Locations of damage-based failure in 16 ft void model 195
Figure 5.50. Maximum principal stress in each model 196
Figure 5.51. Shelby County 118—model geometry and boundary conditions.....198
Figure 5.52. Shelby County 118—load displacement plot 199
Figure 5.53. Shelby County 118—maximum principal stress 199
Figure 5.54. Shelby County 118—von Mises stress distribution 200
Figure 5.55. Washington County—south approach slab spalling location.....201

Figure 5.56. Bridge 606890 location map 202
Figure 5.57. Washington County—general layout of precast panels 203
Figure 5.58. Washington County—layout of precast panels at abutment 203
Figure 5.59. Washington County—longitudinal section of approach and abutment.....204
Figure 5.60. Washington County—rebar layout for Panel 1A 205
Figure 5.61. Washington County—rebar and connection dowels 206
Figure 5.62. Washington County—general layout and meshing of model components 207
Figure 5.63. Washington County—loading scenario.....208
Figure 5.64. Washington County—stress concentrations on bottom of slab.....209
Figure 5.65. Washington County—areas of tensile stress on top surface of approach slab 209
Figure 5.66. Concrete failure in Washington County connection joint 210
Figure 5.67. Washington County—stress concentrations in dowels and precast panels 210
Figure 5.68. Washington County—approach slab settlement 211
Figure 5.69. Washington County—stress concentrations after approach slab settlement.....212

LIST OF TABLES

Table 2.1. Ranking analysis of mitigation techniques for bridge approach settlement 41
Table 2.2. Relationships among different bridge issues 74
Table 2.3. Common issues in bridges with different abutment types.....76
Table 2.4. Common issues in bridges with different slab types 76
Table 3.1. Joint measurements and design plan values 89
Table 4.1. Peak total expansion values and range percent error.....101
Table 5.1. Iowa DOT modified subbase gradation.....150
Table 5.2. Jasper County 118—finite element model load cases 157
Table 5.3. Jasper County 118—approach slab corner displacements.....159
Table 5.4. Story County 118—approach slab mesh sensitivity results.....165
Table 5.5. Parametric study model variations.....169
Table 5.6. Story County 118—friction study tie bar and concrete stress results.....171
Table 5.7. Story County 118—soil stiffness study approach slab concrete stresses 172
Table 5.8. Story County 118—soil stiffness study tie bar von Mises stresses 173
Table 5.9. Story County 118—tie bar study approach slab concrete stresses 174
Table 5.10. Story County 118—tie bar study tie bar von Mises stresses 175
Table 5.11. Story County 118—skew angle study slab weights.....177

ACKNOWLEDGMENTS

The authors would like to acknowledge the Iowa Highway Research Program (IHRB) and Iowa Department of Transportation (DOT) for sponsoring this project.

Special thanks are due to Michael Nop, Curtis Carter, Lili Yang, Louie Caparelli, Dusten Olds, and Scott Ingersoll for their participation in the project's technical advisory committee (TAC). Additionally, the authors would like to recognize Doug Wood and Owen Steffens, staff members of the Structural Engineering Research Laboratory at Iowa State University (ISU), for their assistance with field instrumentation activities.

EXECUTIVE SUMMARY

Integral and semi-integral abutment bridges are currently limited to short and moderate span lengths, eliminating the need to accommodate excessive bridge movement. They are also limited to reasonable skews so that they are not subjected to excessive secondary forces. The limits placed on their use are different in every state and depend on many factors. As research continues to push the boundaries of jointless bridge design, there are many aspects of bridge design and detailing that need to catch up. For example, although research may show foundation piling to be sufficient to allow for integral abutment bridges over a given length, other bridge details like a tied approach slab connection, wingwalls, and drainage details may not be able to accommodate the expected bridge movements. There is no consensus on how best to detail most of the components listed, resulting in the variety seen when reviewing the current standards. This is the main motivation of the research presented in this report, which aimed to help the Iowa Department of Transportation (DOT) and other Midwestern transportation agencies improve the long-term performance of many key bridge aspects.

In order to address this issue, seven different bridge designs that used tied approach slabs, including nine different structures, were inspected for condition as it relates to service life. The 1/4 in. preformed tied approach joints used at every location measured between 3/8 in. and 1 5/8 in. The joints were found to be opening over time and not performing as intended. Decreased joint widths at the opposite ends of the approach slabs highlight the fact that the approach slabs are shifting away from the tied connection. Multiple bridges using the Iowa DOT BR-205 Standard Road Plan have been let within the past few years. The road plan includes the use of a tied approach with vertical paving notch dowels. Future inspections should be completed to determine the effectiveness of the tied approach joints. Ideally, inspections would take place at least one year after initial construction to allow the bridges to experience one full seasonal temperature cycle.

The condition and performance of the joints between the wingwalls and the approach slab curbs appeared unsatisfactory on multiple occasions. Noted problems included a 6 in. deep void at the intersection of the approach to the deck joint and wingwall, separation of the approach slab and wingwall and opening of the joint, concrete cracking at the beginning of the approach slab curb, and frequent poor drainage resulting in buildup of debris at the beginning of the curb. The poor performance of the joints between the wingwalls and the approach slabs together with recommendations made based on a review of the literature indicate that barrier rails should be placed on top of the approach slab when the approach slabs are tied to the abutments. Strip seals are recommended for new construction of integral and semi-integral abutments. An example of a curb “kick-up” detail is provided, and a similar detail would be required to accommodate the continuous curb on the sleeper slab.

Abutment drainage was largely free of debris and able to drain water from behind the abutments should it infiltrate the deck joints. A single bridge, 310 Jasper Southbound, had drain exits for which the openings were very close to becoming blocked, with debris piling up at the outlet and the northwest drain completely closed.

In addition, finite element (FE) models of various bridge ends were developed to study the effect of bridge thermal movement and the response of the approach slabs. Various parameters, such as approach slab friction, soil stiffness, tie bar style, and bridge skew, were systematically investigated through FE simulations. Key findings were as follows:

- Load-displacement curves produced for the Jasper County bridge approach slab with a tied connection show a lateral force in the tied joint of a similar magnitude to the longitudinal force. The force develops very quickly, with only a fraction of the maximum displacement required to realize the movement of the slab in both directions. Tied joint design should therefore account for large lateral forces. Limiting bridge expansion in the transverse direction using buttresses could eliminate transverse displacement of the slab.
- Comparisons of the Story County bridge model with field monitoring data show similar magnitudes of strain induced in the tie bars. However, tied approach joint expansion was slightly underestimated in the model. The model shows a deformation in the tie bars before the strain reaches a plateau and the entire approach slab begins sliding. In contrast, continuous opening of the joint was observed in the instrumentation data.
- Increasing the coefficients of friction between the concrete approach slab and soil only served to increase the total force required to pull the slab. The stresses in the tie bars also increased proportionally, while the force distribution across the bars remained relatively unchanged. The uncertainties involved in estimating approach slab friction were shown to have minimal effect on how forces are carried by the bars.
- While soil stiffness did not affect the concrete or tie bars stresses during bridge contraction, it was found that stiffer soil can considerably increase concrete and tie bar stresses (i.e., maximum values) at the full range of thermal expansion. Inclined tie bars experienced lower stresses than vertical tie bars during bridge contraction while pulling the approach slab. Concrete stresses showed no notable trends with regard to bar orientation. Also, the results of additional models indicated that, regardless of the magnitude of stress in the tied connection, there were stress concentrations at this connection point.
- Skew drastically changes the stress distribution in the tie bars across the tied approach joint. Force is shifted towards the acute approach slab corner/obtuse bridge corner. Stresses are simultaneously lowered in the obtuse slab corner, resulting in a greater range of stresses for increased skew angles. These results were consistent with the case of an extreme skew angle of 55 degrees (which exceeds the current Iowa DOT skew limit of 45 degrees), for which the Shelby County bridge model exhibited a similar variation in stress in the tie bars across the width of the tied approach joint during bridge contraction.

CHAPTER 1. INTRODUCTION

1.1. Overview

An increased focus on the life-cycle cost of infrastructure results in attempts to lower costs in areas other than just initial construction. There are additional aspects including maintenance, repair, operation, and disposal. The other component of life-cycle cost is service life. How long can the structure safely perform its intended function? By increasing service life, the costs are spread over a longer amount of time.

A major source of bridge maintenance problems and increased repair work is bearings and joints. Girders in bridges with stub abutments are placed on bearings, which are located directly below joints at the ends of the bridge. When joints degrade over time, they leak surface water and de-icing chemicals onto the bridge bearings (Hassiotis et al. 2006). Girder encasement in a reinforced concrete backwall (Fell 2022) provides "jointless" bridges that expand and contract as one piece during temperature changes, pushing on the soil at either end. The movement must be accommodated somehow and frequently presents design challenges that shorten the service life. The issue of unsatisfactory drainage remains, and designs often do not adequately remove water away from bridge components. Water that infiltrates the bridge ends may increase settlement or contribute to erosion of the embankment. The worst case involves water flowing under the abutment and exposing the steel piles, leading to corrosion and possibly compromising the structural capacity of the foundation. Many factors seen in Figure 1.1 contribute to a large number of metrics of poor performance, including a "bump" at the end of the bridge, which is a symptom of approach slab settlement (Briaud et al. 1997).

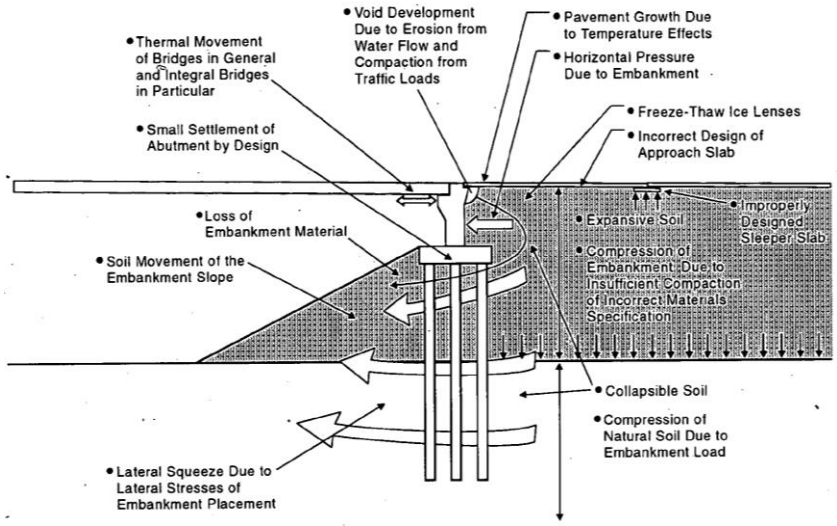

Briaud et al. 1997

Figure 1.1. Factors contributing to a "bump" at the end of a bridge

1.2. Research Needs and Motivations

Integral and semi-integral abutment bridges are currently limited to short and moderate span lengths so they are not subjected to excessive bridge movement. They are also limited to reasonable skews to limit secondary forces (Bakeer et al. 2005). The limits placed on their use are different in every state and depend on many factors. As research continues to push the boundaries of jointless bridge design (e.g., DeJong et al. 2021a, 2021b; Karim and Shafei 2021, 2022; Shi et al. 2020), there are many aspects of bridge design and detailing that need to catch up. For example, although research may show foundation piling to be sufficient to allow for integral abutment bridges over a given length, other bridge details like a tied approach slab connection, wingwalls, and drainage details may not be able to accommodate the expected bridge movements (Olson et al. 2013). There is no consensus on how best to detail most of the parts listed, resulting in the variety seen when reviewing current standards. This is the main motivation of the research presented in this report, which aimed to help the Iowa Department of Transportation (DOT) and other Midwestern transportation agencies to improve the long-term performance of many key bridge aspects.

1.3. Research Objectives

Objectives included collection of information relevant to increasing bridge end service life and development of recommendations and guidelines. Information was accumulated through multiple tasks, including a comprehensive literature review, bridge inspections, field instrumentation and monitoring, and finite element (FE) modeling.

The process began with a thorough review of the current literature on relevant topics, including integral abutments, semi-integral abutments, tied approach slabs, bridge end erosion, and bridge drainage. Nine different bridges in the state of Iowa with semi-integral abutments or tied approach slabs were inspected for signs of soil settlement, concrete cracking, poor joint performance, and poor drainage. These inspections provided real examples of problems contributing to poor bridge service life. In order to support recommendations for increasing service life, four bridges were instrumented with an array of sensors to record various measurements over long periods of time. FE modeling also allowed for a parametric investigation of bridge properties to make additional design recommendations.

1.4. Report Outline

This report is organized into chapters according to the different tasks that were completed in order to accomplish the research objectives. Chapter 2 presents the information obtained from the literature review pertaining to the many complicated aspects of bridge ends. The chapter is split into subcategories covering abutments, approach slabs, soil and geotechnical engineering, bridge end drainage, and expansion joints. Chapter 3 presents the results of visual inspections performed on nine different bridges of varying ages, span lengths, skews, and traffic levels. The results of the inspections illustrate how poor design and detailing can lead to degradation and shorten service life, which in turn can lead to costly repair or replacement. Chapter 4 begins with a description of the techniques used to install strain gauges, crackmeters, earth pressure sensors,

and displacement transducers on four Iowa bridges for long-term monitoring. The resulting data reveal how the bridges respond to environmental and mechanical stressors. Chapter 5 details the creation and calibration of FE models and the parametric studies used to determine the effects of changes in bridge properties on concrete and steel stresses and other performance metrics. Chapter 6 provides the conclusions of the research efforts, including recommendations that the Iowa DOT can use to improve bridge end service life through revised abutment, approach slab, and drainage details.

CHAPTER 2. LITERATURE REVIEW

2.1. Overview

The goal of this literature review was to compile relevant research studies and systematically present the important findings of each after outlining important objectives, test methods, and limitations. The information is grouped into multiple categories related to the overall performance of integral and semi-integral abutment bridges. The reviewed research focused on abutment and backfill details, approach slab details, geotechnical performance and specifications, proper drainage, and expansion joint devices.

Furthermore, there are several key approach slab issues that are exacerbated by utilizing a jointless, moveable abutment bridge. The culmination of these negative side effects is a “bump” at the end of the bridge, an issue that several DOTs and previous authors have investigated numerous times via field investigations, instrumented monitoring of field bridges, literature reviews, and finite element analyses.

This literature review also serves to provide context for previous research in the area, emphasizing common issues with moveable abutments, the reasons for these issues, and recommendations for mitigating them in future designs.

Since the focus of the review is so broad and many important conclusions are included, the proper context in which the conclusions and recommendations are formulated is included where necessary.

2.2. Abutment Details

2.2.1. Length and Skew Limits

Mistry (2005) provided an excellent overview of jointless bridges, including the reason for transition away from conventional bridges, an explanation of what integral abutments are, the many advantages of jointless bridges, and an extensive list of best practices and details. Deck joints are sometimes not given the proper attention during installation and can lead to larger problems with rather expensive bearings. Eliminating joints and bearings can prevent future structural issues and additional costs. Jointless bridges simplify design, simplify widening and replacement, offer lower future maintenace costs, and can expedite construction, among other advantages. The most significant practice the author notes is the standardized use of sleeper slabs to control the crack between the approach slab and the pavement. Important design detail recommendations are made to tie approach slabs to abutments with hinge-type reinforcing, use generous shrinkage reinforcement in the deck slab above the abutment, design wingwalls as small as possible to make them easier to move with the bridge, and to use cantilevered turn-back wingwalls instead of transverse wingwalls for shallow superstructures.

Surveys are a useful tool to gain insight into the current practice of engineers across the country. Since the design of integral abutment bridges and approach slabs lacks a standard process, continuous surveys are required to stay up to date. Maruri and Petro (2005) summarized the results from a survey sent to all 50 states about their use of integral abutments and jointless bridges. Thirty-nine states responded. The survey included questions about the number of integral abutments designed, built, and in service; the criteria used for design and construction, including maximum span lengths, total lengths, skews, and curvature; and problems experienced with integral abutment bridges. A majority of states limit the total length and skew of integral abutment bridges; the variation and range of limits show the lack of uniformity and standardization among states. Ninety percent of states responded that their policy was to eliminate as many joints as possible and use jointless construction in new bridge design. White (2007) conducted a survey of bridge designers in seven European countries about the use of integral and semi-integral abutment bridges in their respective countries. The results were able to highlight some interesting differences in design practices between Europe and the United States. The design earth pressure for abutment backwalls varied between full passive pressure and a value between at-rest and passive pressure. Approach slabs were not required to be used with integral abutment bridges but were recommended by most countries. U-wingwalls parallel to the bridge centerline are in use, which is similar to practice in the United States, but wingwalls were cast both with the superstructure of a semi-integral abutment and with the stationary substructure of a semi-integral abutment. Overall, there are some significant differences between practices in Europe and the United States that appear to be driven by empirical results and the successful performance of past projects.

Surveys are especially helpful for recording the design limitations placed upon different types of jointless bridges. Length limitations of integral abutment bridges built on H-piles in sand were investigated by Dicleli and Albhaisi (2003). The authors used SAP2000 to create an FE model and complete a parametric study to examine the effects of various factors on the maximum displacement capacity of the bridge, which assumed a 0 degree skew. Displacement capacity was found to decrease with stiffer foundation soil and larger/stiffer bridges in terms of span lengths and cross-sectional stiffness. It was recommended that piles be placed in the strong axis direction for bending for low-cycle fatigue performance, but if the flexural capacity of the abutment controls displacement, then piles should be oriented with the weak axis in bending. Concrete bridges were determined to be less sensitive to temperature variations; the maximum length limit in cold climates was recommended to be 190 m (623 ft), while it was recommended that steel bridges in cold climates be limited to 100 m (328 ft).

Dunker and Abu-Hawash (2005) provided a history of the use and expansion of integral abutment bridges in Iowa. The simple cantilever pile model developed at Iowa State University (ISU) allowed for changes to the length and skew limits of integral abutment bridges. Thermal expansion and contraction of the bridge introduce second-order bending effects to the piles and increase stresses. Limiting the piles to elastic stresses was conservative, so piles were allowed to deform plastically. Allowing a hinge does not affect the pile strength since the strains are considered residual. The 2002 limits encompassed 90% of a particular group of bridges compared to 70% with the 1988 policy limits, which shows how effective the changes were in allowing for the construction of more jointless bridges. As part of its bridge design manual, the Idaho Transportation Department (ITD) produced a set of guidelines for the design of integral

abutment bridges (ITD 2008). Length limitations are set as 650 ft for concrete structures and 350 ft for steel structures. Wingwalls are to be parallel with the girders for all bridges, and piles are to be oriented for bending in the strong axis regardless of the bridge skew. Hassiotis et al. (2006) combined the results of bridge monitoring with a finite model created using ABAQUS, producing a design guide that limited integral designs to a length of 460 ft and skew of 30 degrees.

Olson et al. (2009) aimed to expand the limitations for integral abutment bridges in the state of Illinois. The study included FE modeling and the development of instrumentation plans for future Illinois bridges. LPILE and FTOOL were used for two-dimensional (2D) FE modeling and SAP2000 was used for three-dimensional (3D) modeling. It was found that a continuous connection between the approach slab and the abutment/deck results in stress well above the tensile rupture strength of typical concrete materials and a hinged connection provides much lower stresses. The FE models produced many recommendations for the Illinois DOT (IDOT), including the use of compacted select granular backfill behind the abutment. In order to increase integral abutment bridge limitations, it was recommended to predrill pile locations to 8 ft and either reduce the pile embedment in pile caps from 2 ft to 6 in. or include hinge details similar to those used by the Virginia DOT (VDOT). Length and skew limitations were provided for concrete piles and two sizes of steel piles for both strong and weak axis bending.

LaFave et al. (2016, 2017) completed a systematic study on the behavior of integral abutment bridges under thermal loading. The authors completed a parametric analysis of chosen primary and secondary parameters in the first study (2016) and compared the results of that analysis with field monitoring results from two Illinois bridges in the second study (2017). Primary parameters were abutment skew, pile size, span length, and number of spans, and the study used a matrix of 38 model batches to see trends in the overall behavior. Full bridge models were created using SAP2000 software, and approach slabs were not included since bridge behavior was not affected by their presence. Stress levels in the real bridge approach slabs were low magnitude and did not have significant effects. Overall bridge expansion in the models was around 90% of the free expansion predicted by the effective expansion length (EEL). Increasing skew created increasing thermal displacements at the acute bridge corners, a finding that was also confirmed by field data. Larger pile sizes, like HP16s and HP18s, were found to be feasible and allow for longer EELs so long as increased forces and moments in the abutment and superstructure could be accommodated.

Olson et al. (2013) continued the investigation into the IDOT length and skew limits for integral abutment bridges building off previous work by Olson et al. (2009). The main objective of the research was to use 3D SAP2000 models to complete a parametric study of the effects of different factors on integral abutment bridge behavior. Various parameters such as bridge length, skew, interior span length, pile type and size, live loading, and pile orientation were studied using 200 different full-bridge FE models. All models considered only a two-lane bridge, and in order to determine length and skew limits piles were taken to first yield as opposed to allowing plastic deformation, as some states do in design. Some general trends were found across the different models, including the fact that greater abutment rotation, due to less restraint, results in lower pile stresses. Longer intermediate spans between supports also increased pile stresses. Skew has large effects on integral abutment bridge behavior regardless of many other

parameters. The authors noted that the largest amount of bridge expansion occurs parallel to the bridges longitudinal axis, so it was proposed to place piles with webs parallel to that axis regardless of the bridge skew. This strong-axis alternate orientation, shown in Figure 2.1, provided pile stresses 20% to 30% lower than either weak-axis or strong-axis piles, and it was recommended that IDOT consider the use of strong-axis alternate orientation.

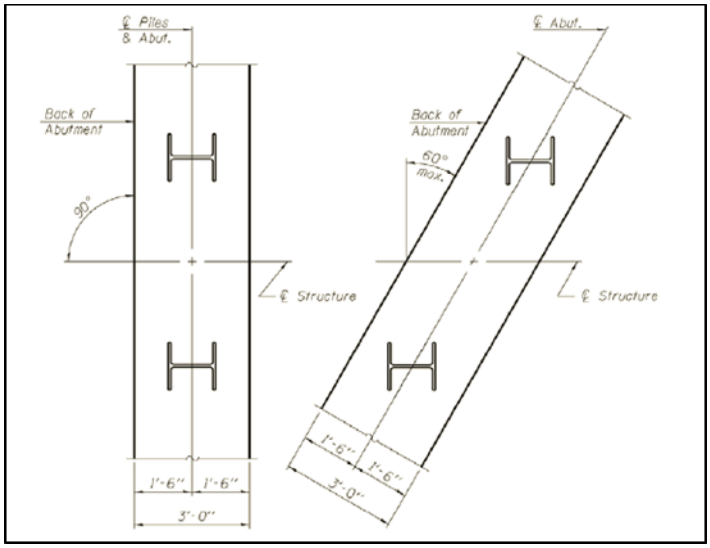

Olson et al. 2013

Figure 2.1. Proposed strong-axis alternative pile orientation for Illinois integral abutment bridges founded on H-piles

The limitations seen in Figure 2.2 are based strictly on the performance of the pile foundation and do not account for other structural or nonstructural bridge components. The study resulted in additional recommendations for IDOT, including the use of compacted granular backfill behind abutments. For skews less than 45 degrees, the passive pressure that develops resists thermal expansion, and the backwall friction helps to resist transverse abutment movements for all bridges regardless of skew.

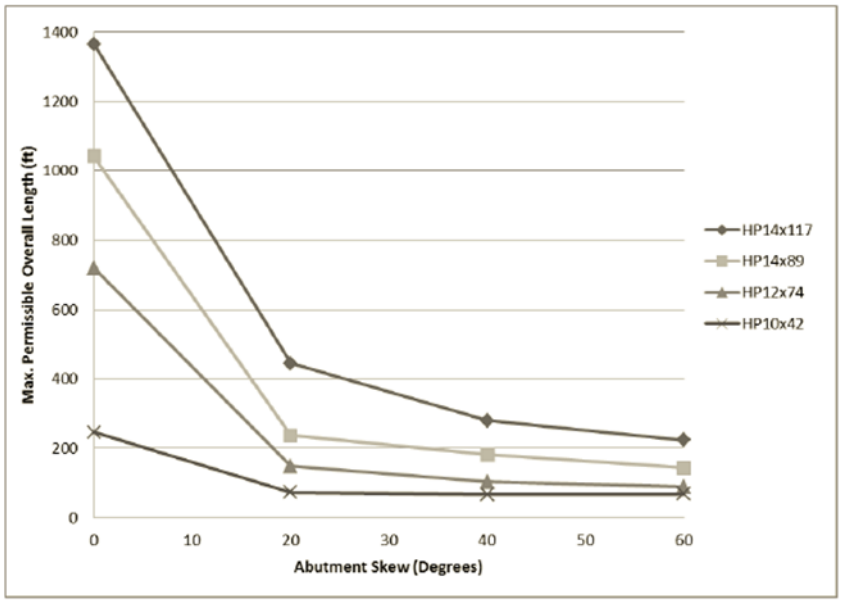

Olson et al. 2013

Figure 2.2. H-pile summary: permissible IDOT integral abutment bridge lengths versus skew (100 ft intermediate spans)

In 2012, IDOT issued a memorandum to all bridge designers (IDOT 2012). The memorandum adopted a new pile orientation for abutments that is the exact opposite of the strong-axis alternate proposed by Olson et al. (2013). The memorandum states that the "pile web is always perpendicular to the centerline of the structure." Integral abutment limits were increased to a length of 550 ft and skews up to 45 degrees. The corbel was eliminated and absorbed into the abutment cap. The integral abutment pile selection chart seen in Figure 2.3 is a function of EEL and skew. The EEL must be calculated accounting for the centroid of stiffness of the abutments. EEL is calculated the same for concrete and steel bridges and is equal to or greater than half the total expansion length, depending on whether the centroid of stiffness lies at the center of the bridge or is shifted towards one abutment.

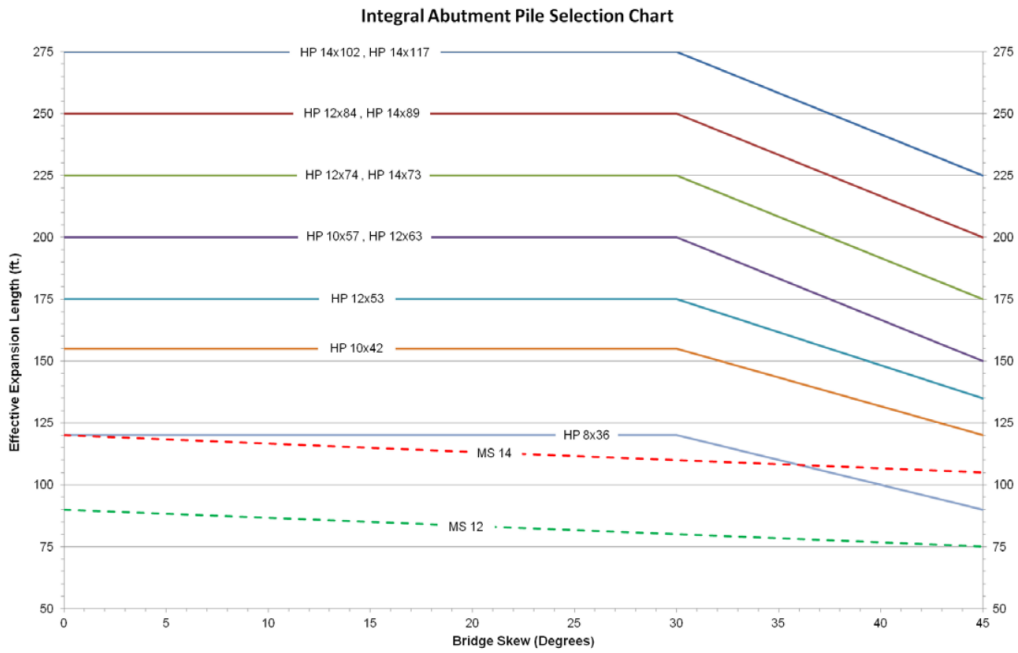

IDOT 2012

Figure 2.3. Integral abutment pile selection chart based on EEL

2.2.2. Earth Pressure and Forces on Abutments

The pressure experienced by an abutment backwall in an integral or semi-integral abutment bridge is an important yet complex issue. Hassiotis et al. (2006) worked with the New Jersey DOT (NJDOT) to fully evaluate integral abutments for use in place of bridges with bearings. The extremely extensive evaluation included monitoring of an integral abutment bridge and development of a finite element model, all culminating in recommendations and a design guide for integral abutment bridges. The review of the current practice at the time concluded that additional research was needed in the development of passive earth pressures behind the abutment due to cyclic loading. A 298 ft long integral abutment bridge with a 15 degree skew and piles oriented for weak-axis bending was fitted with a multitude of sensors. The results of the monitoring period combined with a finite element model created using ABAQUS led to a large number of recommendations for integral abutment bridges. The approach slab should be connected to the abutment with a moment connection allowing for rotation and should be designed as a simply supported span in case of a loss of soil support underneath a majority of the length. Since passive pressures behind the abutment can increase over time and were found to be larger than typical design values, passive pressure should be calculated with a maximum density of the soil and a maximum internal angle of friction. The obtuse corner of a skewed bridge will see a larger pressure than the acute corner due to unequal movement, and geosynthetics may be able to reduce passive pressure build-up.

Bonczar et al. (2005a, 2005b) examined the effects of soil properties on the behavior of piles and abutments using both 2D and 3D finite element models created using GT-STRUDL structural design and analysis software. Abutment backfill was modeled as nonlinear springs in the FE

models. Earth pressures were found to be higher when loose material was used to surround the tops of the piles due to lower constraint and higher movement. The equivalent cantilever method provided a great correlation for pile moments for bridge expansion and was conservative for contraction.

According to the ITD (2008), the earth pressure on the abutment is calculated using full passive pressure for the top third varying linearly to at-rest earth pressure at the bottom of the abutment. A design check for lateral forces is also provided that compares the lateral capacity of piles and the soil pressure on wingwalls to the moment created by the eccentricity of soil forces at either end of the bridge. Field monitoring of integral abutment bridges is rather common due to the insight the data can provide about the real-world performance of experimental details. However, monitoring is typically done for 1 to 2 years at the most, just enough to capture a full seasonal cycle.

Kim and Laman (2011) instrumented four bridges for which monitoring periods lasted between 2.5 and 7 years. Many responses were measured using the 240 total sensors, including abutment displacement and rotation, backfill pressure, girder rotation and moments, pile forces, and approach slab strain. Based on temperature readings, American Association of State Highway and Transportation Officials (AASHTO) LRFD (2010) design temperature ranges for concrete were found to be conservative, and the difference between ambient temperature and superstructure temperature was negligible. The thermal loading produced nonlinear and irreversibly increasing abutment displacements over time. Earth pressure in all four bridges reached passive pressure values, making it an appropriate design choice to use full passive pressure. A difference was observed in the girder rotation and abutment rotation values, indicating that the assumption of a fully fixed connection may not be entirely accurate and further investigation may be required. Thermal loading of the superstructure must be taken into account, as positive thermal loading creates negative bending in the girders and negative thermal loading creates positive bending.

Arenas et al. (2013) investigated the behavior of integral abutment bridges with mechanically stabilized earth (MSE) walls when subject to thermal movements. Only full integral abutments with MSE walls on three sides forming a U-back configuration were considered. The study included a survey of state DOTs across the United States, a 3D numerical model, an analysis of corrugated steel pipes that surround piles, and a parametric study to develop a spreadsheet to aid in design for thermal responses. The survey received responses from 21 agencies. It was discovered that almost all agencies used a skew limit of 30 degrees, and 71% of agencies oriented piles for weak-axis bending only. Abutment design earth pressures varied across the board between active, at-rest, passive, or a combination of earth pressures. The 3D numerical model created using FLAC3D software determined that surrounding piles with corrugated steel pipes and filling them with loose sand does not reduce pile loading due to stiffening after cyclic loading, so it was recommended that VDOT end the practice to reduce costs. Final conclusions noted that earth pressure increases during a one-year cycle to reach a peak value increase of up to 60% over the first year, with an increase of only 6% the following year, as seen in Figure 2.4. The use of elasticized expanded polystyrene (EPS), which was found to be rare in the completed survey, reduced lateral earth pressures according to the numerical analyses, which supported its

use by VDOT. The numerical analyses also showed that transverse displacements of skewed bridges reached magnitudes similar to longitudinal displacements.

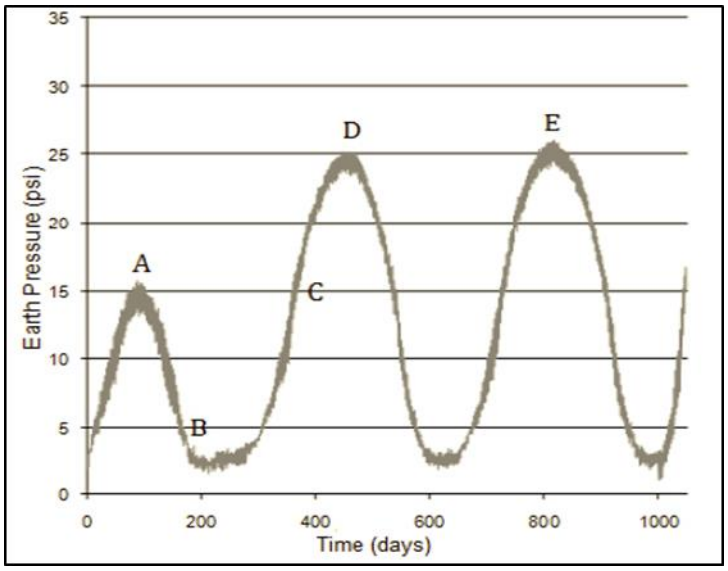

Arenas et al. 2013

Figure 2.4. Earth pressure behind the abutment

Kong et al. (2016) instrumented the first fully integral abutment bridge constructed in the state of Louisiana in 2011. Louisiana has unique soil conditions, which is why there was a lack of information on integral abutment bridge behavior for engineers to use. The Caminada Bay Bridge has long continuous spans, deep precast prestressed concrete piles, and very soft soil conditions, creating additional challenges. Monitoring was concentrated on the first 11 spans, with an integral abutment at one end, 10 bents rigidly connected to the 300 ft continuous slab, and simple support at the other end. Extensive temperature data showed a temperature variation at a central bent deck surface large enough to possibly cause cracking of the concrete deck with seasonal temperature variations within the design values of AASHTO LRFD. Soil behavior at the abutment proved to be nonlinear and extremely complicated, with restraints accumulating over time, but it was found that the effects of abutment movement were negligible at a distance of 6.9 ft away from the abutment.

Kong et al. (2016) continued studying the Caminada Bay Bridge in Louisiana. The monitoring data obtained were used to validate a 3D finite element model in the program ANSYS. A parametric study examined the effects of support conditions, soil types, and joint connections between the piles and bents on the overall bridge behavior. Free supports at the bridge ends allowed for larger displacements, inducing the largest positive and negative bending moment on the piles; however, high compressive strains developed in the bridge deck under fixed support conditions. This illustrates a trade-off between superstructure and substructure performance when examining where thermal expansion is accommodated. Loose sand backfill was found to result in lower backfill pressures when compared to dense sand. The soil surrounding the piles was found to have the largest effect on the bridge. When changing soft soil to stiff soil, the

maximum displacements decreased by 1.5 times, but the pile strains increased 70% and the slab negative strains increased by 48%.

Varmazyar et al. (2017) analyzed the performance of a new backfill method to improve interactions between the soil and the bridge structure during cyclic movements. The problem of high earth pressures and the "ratcheting" of backfill was outlined as a reason for the study. Ratcheting causes increasing earth pressures on an integral bridge abutment over time as the bridge contracts and the backfill collapses into the void before being compressed in the next expansion cycle. Traditional backfill is constructed in layers or lifts, and when combined with the need to cover the large area occupied by the approach slab, the result is a significant amount of time required for construction. The proposed solution used a compressible inclusion made of resilient EPS attached to the abutment backwall with a backfill consisting of cement-stabilized sand (CSS) or no-fines mass concrete behind it. The intent of this detail was to reduce lateral earth pressures, accommodate expansion and contraction movements, and prevent settlement or voids below the approach slab, all while reducing construction costs through reduced cost and time of installation. The authors created a 2D finite element model using PLAXIS 2D software that included the bridge abutment, foundation piles, the bridge deck, and backfill. Models were created for both a traditional backfill and the proposed solution so that results could be compared. Four cycles of expansion and contraction of 10, 30, and 100 mm were applied to simulate the thermal movements of a bridge. The model that featured a compressible inclusion with CSS showed decreased lateral earth pressures on the abutment, with a spike at the soil just below the abutment (Figure 2.5) and much lower residual total displacements, meaning a reduction of ratcheting effects (Figure 2.6). The proposed design performed better at a lower cost and would shorten construction times.

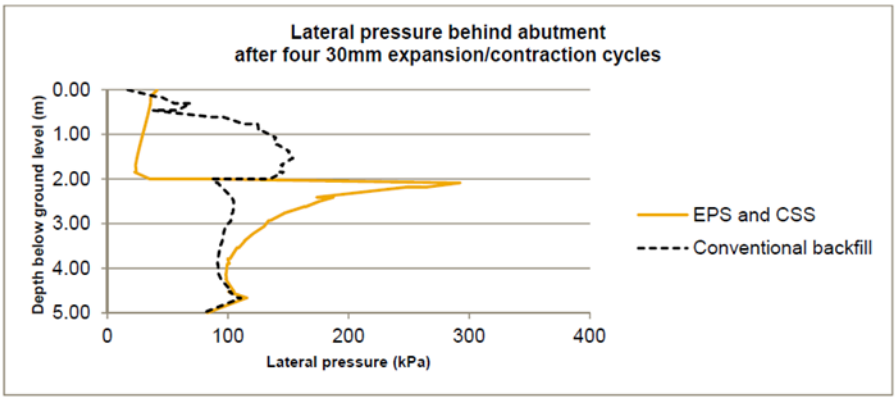

Varmazyar et al. 2017

Figure 2.5. Comparison of horizontal stress behind abutment after fourth cycle of 30 mm bridge expansion

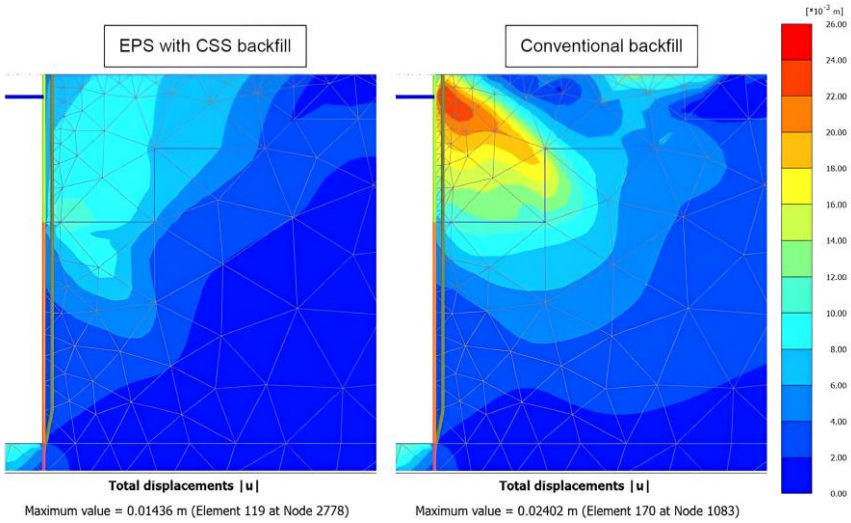

Varmazyar et al. 2017

Figure 2.6. Comparison of total displacement in backfill after bridge deck contracting to original length following fourth cycle of 30 mm bridge expansion

The first six prototype semi-integral abutment bridges constructed in the state of Louisiana were evaluated by Bakeer et al. (2005) to determine if they had performed satisfactorily since construction. All six bridges were inspected, and two were selected for a structural/geotechnical analysis and finite element analysis, respectively. All of the bridges used the same abutment design detail shown in Figure 2.7, which utilized geosynthetics to reinforce the embankment behind the abutment and allow for a gap between the abutment backwall and embankment. The gap's purpose was to accommodate longitudinal expansion of the abutment. During bridge inspections, it was found that the gaps were performing as intended and had not closed or filled with any significant amount of material. Additional results of the inspections showed the semi-integral abutment bridges outperforming similar conventional bridges based on a rating system of each bridge component. An ANSYS model was used to complete a parametric study examining the effects of thermal loading, settlement of the approach, and bridge skew. No overstressing was detected in any components for temperature gradient loading or for a skew of 30 degrees; however, cracking was seen in the approach settlement model and was the reason for a weak joint (sawcut joint) being included in the design of one of the bridges (Bridge I-2) at 10 ft away from the abutment backwall. Final recommendations include the use of a sleeper slab and a compressible joint at the end of the approach, a vertical gap of at least 6 in. behind the backwall, and the use of a weak joint as an internal hinge in the approach slab at one-quarter the length away from the backwall.

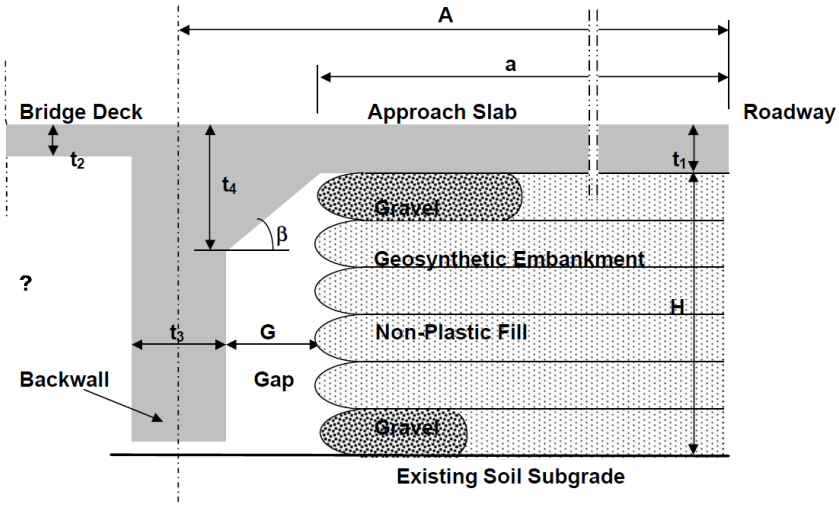

Bakeer et al. 2005

Figure 2.7. Details of Louisiana Department of Transportation and Development (LaDOTD) prototype semi-integral abutment bridge design

2.2.3. Unique Abutment Details

In cases where limitations disqualify the use of integral or semi-integral abutments, other options are available. Aktan et al. (2008) completed an extensive investigation of link slabs used in jointless bridges along with the performance and details at the ends of the bridges, including abutments and approach slabs. Two different bridge types were considered, including deck-sliding-over-backwall and semi-integral abutment. The literature review revealed that only continuous bottom reinforcement should be used to prevent moment transfer in deck-sliding-over-backwall bridges (Figure 2.8), and FE modeling confirmed that stresses over the abutment are reduced with the improved detail. For semi-integral abutments, an inclined bar should be used with a construction joint to serve the same purpose of moment and stress reduction by acting as a hinge allowing the approach slab end to rotate when the backfill inevitably settles. Friction between the approach slab and subgrade did not create any appreciable stresses in the approach slab in the FE models. It was recommended that the construction joint be placed at the span-side abutment face for deck-sliding-over-backwall bridges and at the approach-side abutment face for semi-integral abutment bridges.

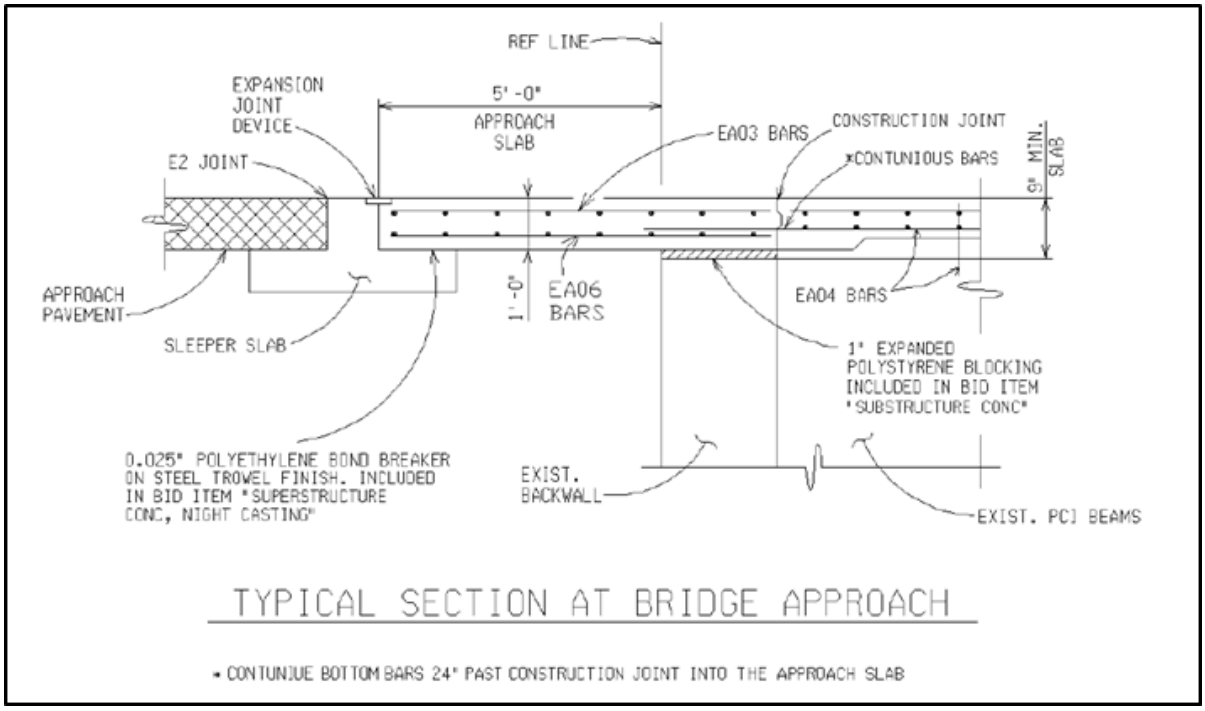

Aktan et al. 2008

Figure 2.8. Proposed dependent backwall configuration, i.e., construction joint over the backwall face at the span side with continuous bottom reinforcement

Aktan and Attanayake (2011) also investigated link slabs, deck-sliding-over-backwall abutments, and semi-integral abutments for bridges with a high skew (over 20 degrees). This study complements previous work by Aktan et al. (2008), which considered bridges with a skew of less than 20 degrees. The authors instrumented a bridge with a 42 degree skew in Michigan for load testing and measured displacements at different locations using a laser tracker. Skewed bridges expand and contract along an axis between the two acute bridge corners, instead of just longitudinally along the axis of the girders. The transverse movement of deck-sliding-over-backwall bridges can be restrained by restraining the center girder (or the two center girders in the case of bridges with an even number of girders) using concrete keys with rub plates. A 1 in. layer of expanded polystyrene is placed between the backwall and the bottom surface of the approach slab, as shown in Figure 2.9.

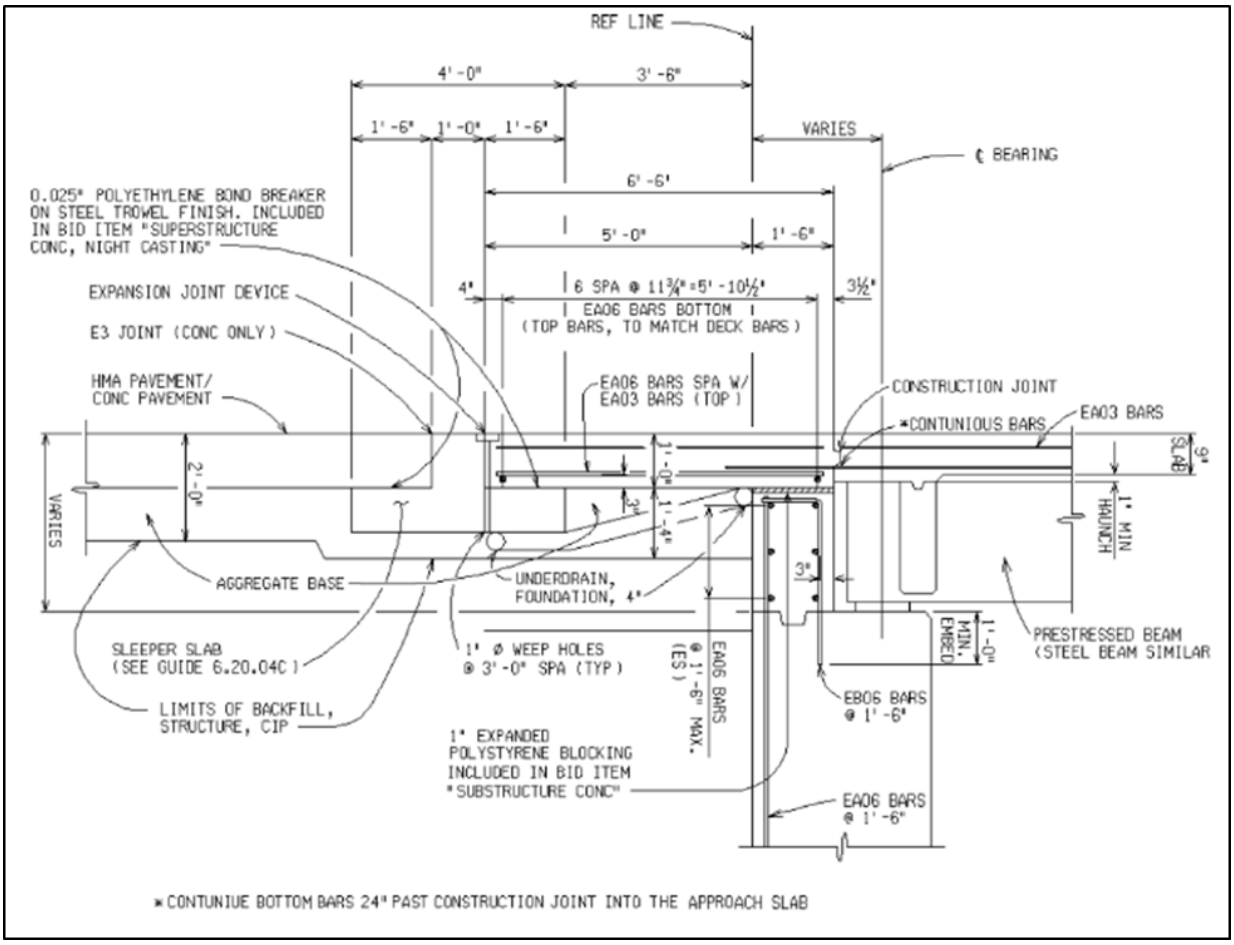

Aktan and Attanayake 2011

Figure 2.9. Deck sliding over backwall

A similar longitudinal restraint concept applies for semi-integral abutments (Figure 2.10), except transverse movement is restrained by rub plates on a wingwall at the acute corner. The use of an EPS layer behind the backwall was recommended to reduce passive pressures. The use of a 0.025 in. thick polyethylene layer beneath the approach slab can reduce friction, something that should be done for all surfaces of the approach slab to facilitate free movement.

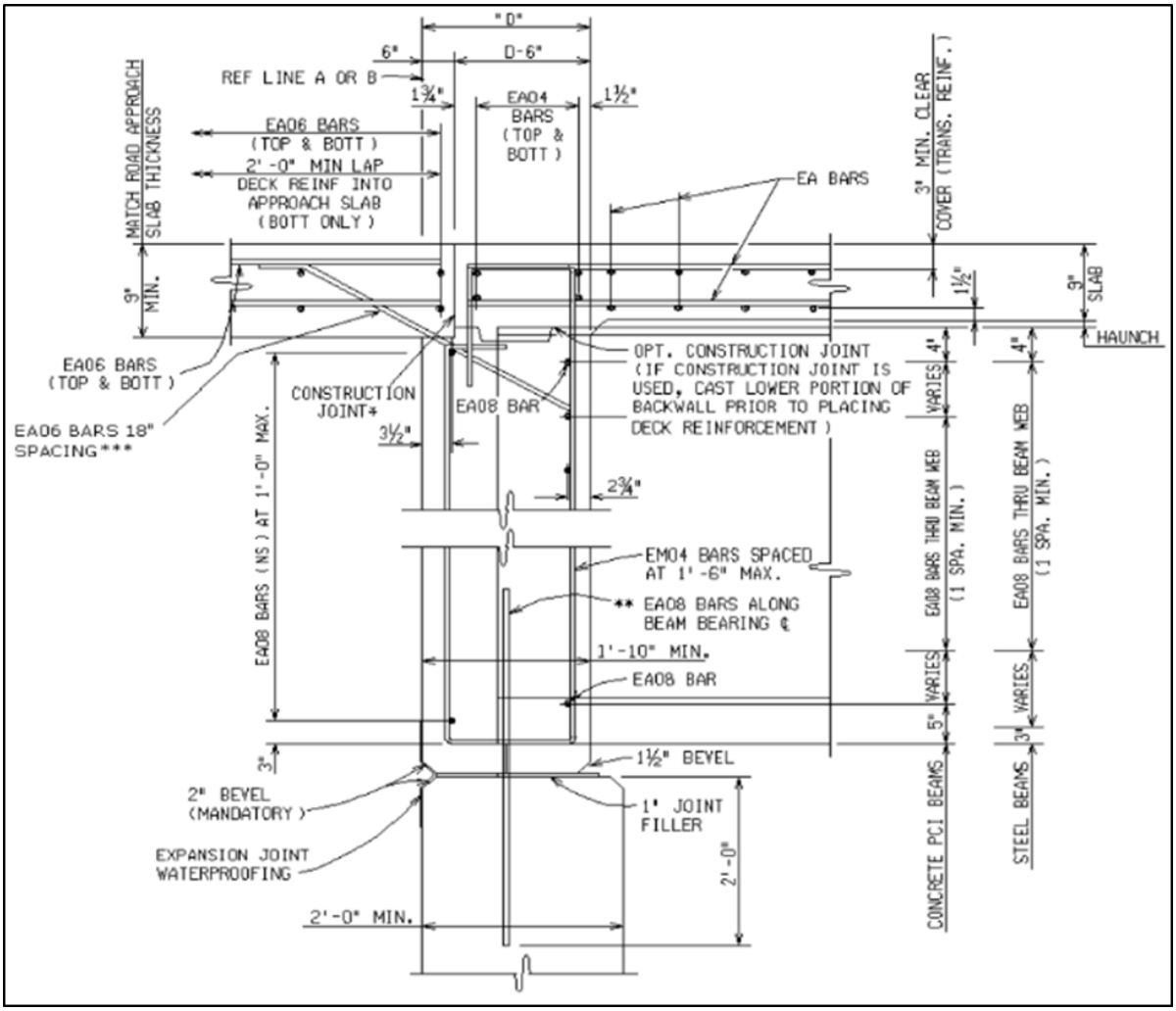

Aktan and Attanayake 2011

Figure 2.10. Semi-integral abutment details

Like the Michigan DOT (MDOT), VDOT also has jointless bridge design options that are not traditional integral or semi-integral designs. Weakley (2005) covered a set of guidelines for designing jointless bridges for VDOT. Three different types, integral, semi-integral, and deck-sliding-over-backwall, are used depending on length, skew, and anticipated abutment movement limits. The backwall for fully integral abutment bridges is designed to handle passive earth pressures. If the bridge is skewed, the piles must accommodate lateral loading as well. Semi-integral designs are used when the minimum pile length of 25 ft cannot be used for construction of a fully integral abutment bridge. Skewed bridges result in lateral movements that must be resisted so that movement is limited to the longitudinal direction. Rub plates made of stainless steel are placed at the acute corners of bridges to bear on wingwalls, and the wing haunch is a vertical cantilever and must be reinforced more heavily to account for this loading. A deck extension configuration (Figure 2.11) eliminates the deck joint at the abutment by extending the bridge deck over the backwall. The joint is relocated, and a 1/2 in. layer of polystyrene is placed horizontally between the abutment and deck above. Lateral movement and rotation due to skew may still occur, so rub plates are used as they are for semi-integral abutment bridges. VDOT uses

elasticized EPS to replace backfill in contact with the abutment backwall to reduce passive pressures and settlement. The use of the elasticized EPS mitigates the effect of ratcheting, which occurs during bridge shrinkage. The previous connection between the approach slab and abutment used two layers of bars continuing into the bridge deck. Cracking problems occurred, with cracks appearing at the ends of the bars due moments caused by settlement, so the change was made to a single layer of bars angled into the abutment to allow rotation.

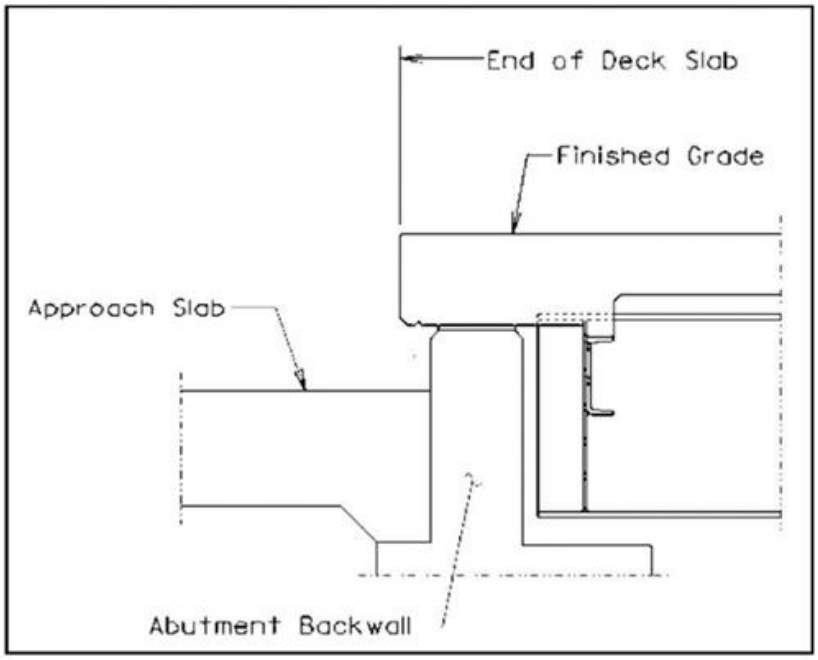

Weakley 2005

Figure 2.11. Deck extension

A new jointless bridge detail known as the "Virginia Abutment" was created to work in any scenario that includes a double backwall with a large drainage area and an expansion joint between the semi-integral-like abutment and second backwall. The Virginia Abutment (Figure 2.12) uses an isolated backwall located behind an integral backwall. A tooth joint is located at the bridge deck surface between the two abutment walls. There is a large void space between the two, and the concrete is covered with an epoxy coating to facilitate drainage. The void space is large enough that it can be easily maintained and cleared of any possible debris. Thermal expansion and contraction of the bridge is accommodated without any interaction with the soil. There do not appear to have been any research studies done specifically on the Virginia Abutment; however, this design is in use by VDOT. The following is an excerpt from the VDOT *Manual of the Structure and Bridge Division*: "When beyond the limits of the selection criteria indicated above for full integral abutments, semi-integral abutments or conventional cantilever abutments with deck slab extensions and the decision is made not to pursue a design waiver, Virginia Abutments shall be used."

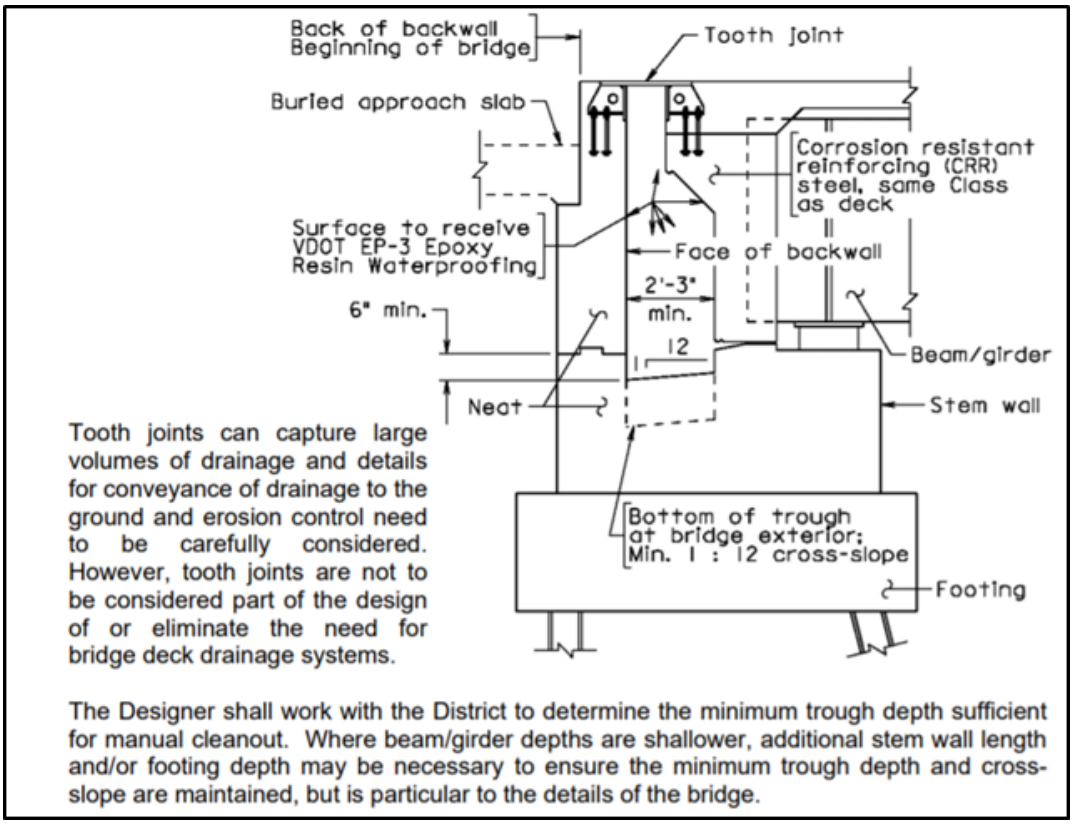

VDOT *Manual of the Structure and Bridge Division*, pp. 17.01–17.04

Figure 2.12. Example detail of Virginia Abutment

Hoppe and Eichenthal (2012) conducted field monitoring of a highly skewed semi-integral abutment bridge for VDOT. The 100 ft one-span bridge with a 45 degree skew was monitored for five years. One abutment utilized a 15 in. layer of EPS as an elastic inclusion per VDOT policy (Figure 2.13). The inclusion was combined with a well-graded backfill separated by geotextile drainage fabric, since VDOT had determined in previous studies that uniformly graded backfill was causing approach slab settlement. Piles were oriented for bending in the strong direction, since it was noted that semi-integral abutments do not transfer lateral thermal loading to the piles. Instead, this lateral load was resisted by a concrete buttress at the acute corner of the bridge, since highly skewed bridges tend to rotate with expansion. Approach slabs were not used in construction, and after the monitoring period the approach areas had performed well. A finite element model created in SAP2000 determined that a new buttress location in the abutment near the acute corner of the bridge, shown in Figure 2.14, may be more effective. The study also recommended that semi-integral abutment bridge limitations be increased from 30 to 45 degrees, K_h values with and without elastic inclusions should be modified, and wingwalls should be designed for larger earth pressures than K_a to prevent the cracking that was observed.

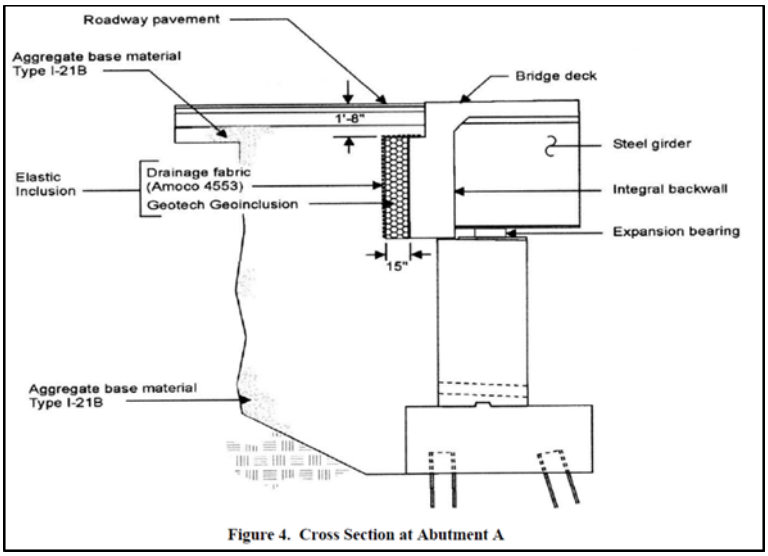

Hoppe and Eichenthal 2012

Figure 2.13. Cross section at abutment showing elastic inclusion

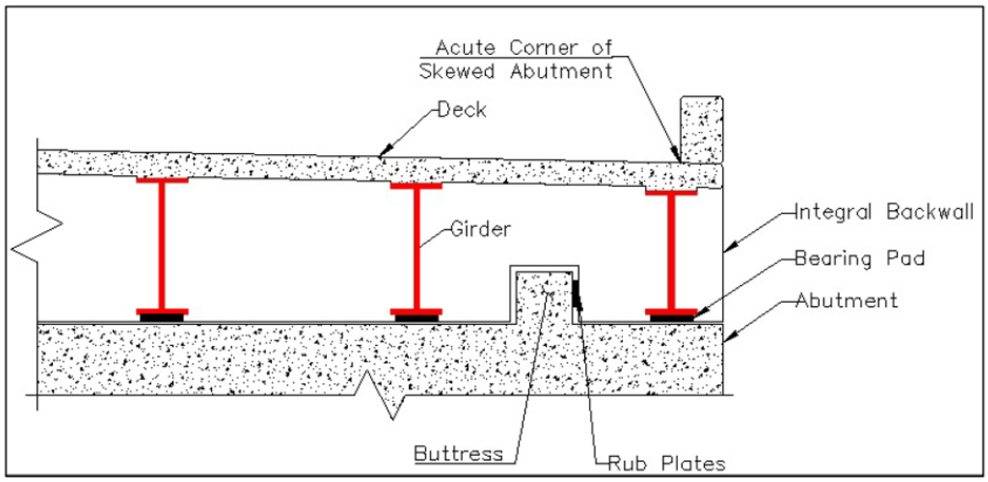

Hoppe and Eichenthal 2012

Figure 2.14. Proposed buttress at semi-integral abutment bridges

Hoppe et al. (2016) summarized the advancements in jointless bridge design implemented by VDOT. In addition to much of the work done in Hoppe and Eichenthal (2012), the authors explained the design priority of VDOT when choosing an abutment type. Fully integral is the primary choice for new bridges, but if length and skew restrictions require it, a semi-integral design is used. If limitations are still not satisfied, then the bridge design uses a deck extension first and finally the Virginia Abutment. The Virginia Abutment detail allows for jointless design in any scenario using a semi-integral abutment with an isolated backwall that does not apply any bridge movements to the backfill. A large recess exists between the two and is open on both sides to allow for drainage without the possibility of blockage due to its size. The four different jointless bridge types provide options for VDOT to utilize jointless design to lower life-cycle costs and adapt to unique and challenging conditions.

Rub plates (Figure 2.15) can be used with concrete end restraints to facilitate smooth movement and reduced friction. VDOT design uses two stainless steel rub plates cast into the concrete using shear studs. The plates are designed to resist horizontal forces due to thermal induced passive earth pressures and must accommodate longitudinal movement.

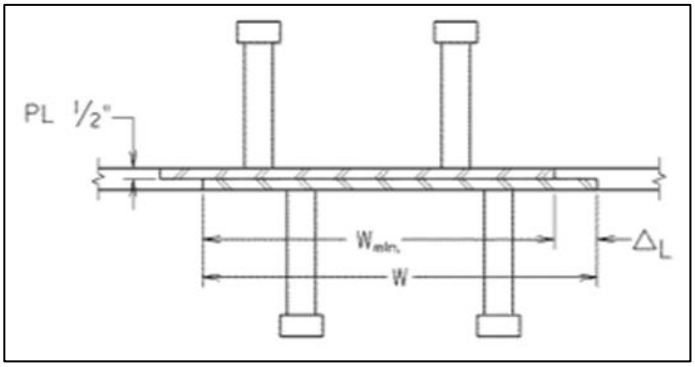

VDOT Manual of the Structure and Bridge Division, pp.17.08–17.22

Figure 2.15. VDOT rub plate example design calculations

Aktan and Attanayake (2011) included the use of rub plates with their recommended abutment details for MDOT. Rub plates can be placed on the deck or abutment or used in a concrete key system. The concrete key system was described as the most promising for deck-sliding-over-backwall abutments. MDOT has not yet adopted the girder end restraint details. Concrete shear key and rub plate details from the study are still under discussion by MDOT.

High skew angles can complicate bridge behavior and have a negative effect on performance if a bridge is not properly detailed. Biana (2010) presented a unique design completed in the United Kingdom to overcome some difficult design restraints (Figure 2.16).

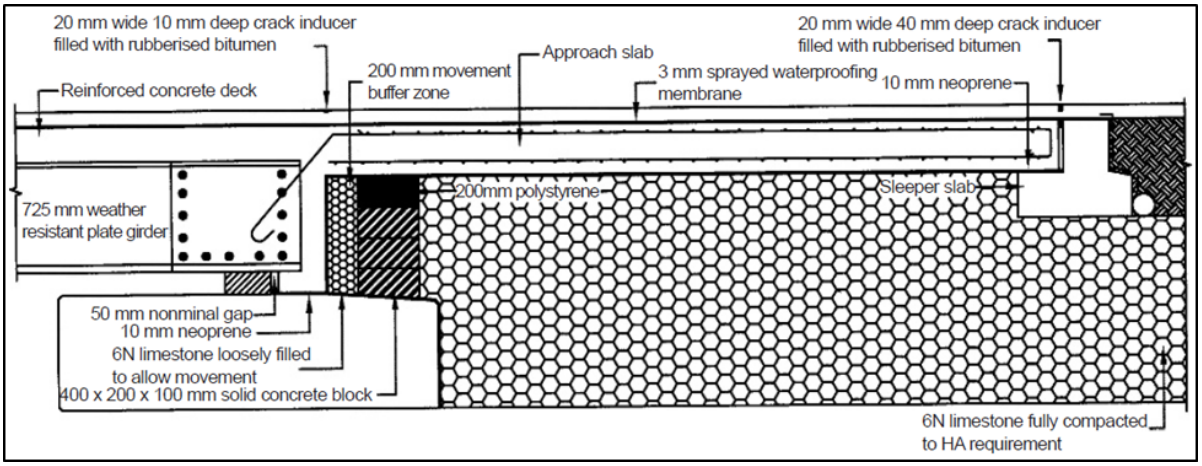

Biana 2010

Figure 2.16. Abutment and approach slab cross section

The result was a composite semi-integral abutment bridge with a high skew of 36 degrees. Longitudinally guided bearings control lateral movement of the bridge to keep it aligned. Behind the abutment, a loose limestone layer was intended to accommodate longitudinal movement, sandwiched between the abutment and a solid concrete block layer that holds back compacted limestone backfill. After 21 months, there were no signs of distress in the approach slab joint to the bridge deck.

2.3. Approach Slab Details

Approach slabs are intended to provide a smooth transition from the pavement road surface onto the bridge deck. If they are of sufficient length, a change in elevation at either end leads only to a small change in the slope of the slab. Approach slabs that are designed thick enough and with enough reinforcement are able to span gaps or voids caused by erosion. The overall performance of an approach slab used on an integral or semi-integral abutment bridge is affected by many factors, and much research has been done to remedy the problems associated with them. Seo et al. (2002) completed a thorough investigation of the bump at the end of the bridge in Texas. The study included a survey of Texas DOT (TxDOT) districts, FE models of the embankment soil under different conditions, monitoring of two bridges in Houston, and testing of a 1/20th scale bridge transition model, all resulting in a proposed approach slab design to improve performance. The results of the survey questionnaire highlight settlement of embankment fill followed by erosion as the top causes of the bump, though use of an approach slab minimizes the problem. The FE model created in ABAQUS used plane strain to simplify conditions and included many loading conditions using distributed and point loads. The numerical analyses found that 80% of the maximum settlement occurs in the first 20 ft of soil near the abutment for a uniform load case. Final recommendations included using quality backfill and compacting it to 95% of modified Proctor and using an approach slab that is at least 20 ft long.

Puppala et al. (2009) created a synthesis of practically all previous research and information on the performance of approach slabs. Causes of the bump include consolidation settlement, poor compaction of backfill, poor drainage and erosion, design detail specifics, skew, and seasonal temperature variations. In order to improve soil conditions, different methods can be used, such as replacement of embankment soil, use of surcharge loads, and dynamic compaction. Embankments can be reinforced using stone columns, compaction piles, driven piles, or, more commonly, geosynthetic reinforcement. MSE walls, lightweight fill, and flowable fill are all viable options for improving the performance of backfill behind an abutment. Approach slab design is extremely important as longer approach slabs are less sensitive to settlement at the ends, but they should be designed to span between the abutment and the other end. Using a thicker slab is the most effective way to reduce tensile stresses that can cause cracking, and proper compaction is necessary under sleeper slabs just as it is under the approach slab. After reviewing all previous research, the authors ranked all possible methods for preventing approach slab settlement, as shown in Table 2.1.

Table 2.1. Ranking analysis of mitigation techniques for bridge approach settlement

New or Maintenance Measure	Mitigation Method	Technique Feasibility (a)			Construction Requirements (b)			Cost Considerations (c)			Overall Performance (d)			Is This Method Recommended for Present Research?
		Ineffective	Effective but Under Research	Proven, Well Design Method	Low	Medium	High	Low	Medium	High	Not Proven	Ineffective	Effective	
Novel Methods for Foundation and Fill Improvement	MSE Walls/GRS		✓				✓			✓	✓			×
	Geofoam		✓			✓			✓		✓			✓
	Lightweight Fill		✓			✓			✓		✓			✓
	Flowable Fill		✓		✓				✓		✓			✓
	DSM*		✓		✓				✓				✓	✓
	CFA**		✓			✓			✓		✓			✓
	Concrete Injection Columns		✓			✓				✓	✓			×
	Geopiers		✓			✓			✓				✓	✓
Maintenance Measures	HMA Overlay			✓		✓		✓				✓		×
	Mud/Slab Jacking		✓		✓			✓					✓	✓
	Slab Replacement			✓		✓			✓			✓		×
	Grouting			✓	✓				✓		✓			×
	Urethane Injection		✓		✓					✓	✓			✓

Source: Puppala et al. 2009
* Deep soil mixing
** Continuous flight auger cast piles

Luna et al. (2004) sought to improve practices in Missouri related to approach slabs, since the Missouri DOT (MoDOT) was not satisfied with their performance based on a survey of MoDOT districts. Approach slabs were rated according to one of three designations, with only 68% performing with no apparent issues and 15% requiring corrective action. Two different bridges in two different areas of the state with differing soil conditions were examined, and finite element models were created using PLAXIS. The models provided an upper and lower bound for approach settlement and allowed for prediction of settlement based on conditions and construction staging. It was determined that construction sequencing and staging had a large effect on overall performance and that construction of the approach slab should be delayed as long as possible to allow for settlement of the embankment before placement of the final grade. A sleeper slab drain should be placed below the bottom of the sleeper slab, and 2 ft of crushed rock should be used below the sleeper and approach slabs. The abutment should not include any notches or overhangs and the backwall should be straight in order to facilitate good compaction. Finally, the backfill should be compacted to 95% for the entire height of the approach embankment under the approach slab, sleeper slab, and pavement.

The connection between the approach slab and abutment is extremely important due its location and the forces it experiences. A tied approach slab should move with the bridge during expansion and contraction, but the connection joint should not open to allow penetration by surface water. Greimann et al. (2008) tested multiple approach slab details by monitoring two bridges in Iowa. The bridges were identical three-span prestressed concrete girder bridges with different approach slabs. One bridge utilized a precast concrete approach slab that was anchored to the abutment using vertical reinforcing bars. The other bridge used a cast-in-place approach slab attached to the abutment in the same manner. The bridges were outfitted with many sensors to measure temperature, strain, and displacement in different locations such as on girders, on piles, and in slabs, and the sensors were set up to measure displacement of the abutments. Abutments may displace horizontally and rotate, but the results showed that the abutment's rotation was negligible and that displacement depended entirely upon the horizontal movement of the entire abutment. After calculating the coefficient of thermal expansion, it was possible to find the theoretical expansion and contraction of the bridge. The theoretical and experimental data followed the same trends until winter, when strain ratcheting may explain some deviations. Results showed that there are forces present in the approach slabs at the expansion joints that must be accounted for in design. The approach slabs performed well initially, and overall the bridges' behavior seemed to follow short- and long-term cycles as temperatures changed over time. Later inspections revealed an opening of the joint as time progressed. The construction of the two bridges differed only in the type and size of approach slab used and showed different behaviors, leading to the belief that the type and/or size of the approach slab plays a role in the behavior of not only the approach slab itself but also the bridge superstructure.

Nadermann et al. (2010) complemented the work of Greimann et al. (2008) by using a similar approach to study an approach-slab-to-abutment connection in the state of Iowa. The approach detail used precast panels with a cast-in-place shoulder and inclined tie bars between the abutment and appoach (Figure 2.17). The shoulders were instrumented with strain gauges, and crackmeters were placed at the joints. Similar trends in temperature were found as the slab acted as an insulator from daily extreme temperatures. Temperatures also followed short-term and long-term cycles over the course of the monitoring period. Based on the strains seen in the

approach slab, there is a force in the expansion joint. The coefficient of friction between the approach slab and the soil below reached much higher levels than in Greimann et al. (2008), and it is believed this is because low temperatures caused the soil to freeze to the slab. The approach slabs functioned well over the monitoring period from October 2008 to January 2010.

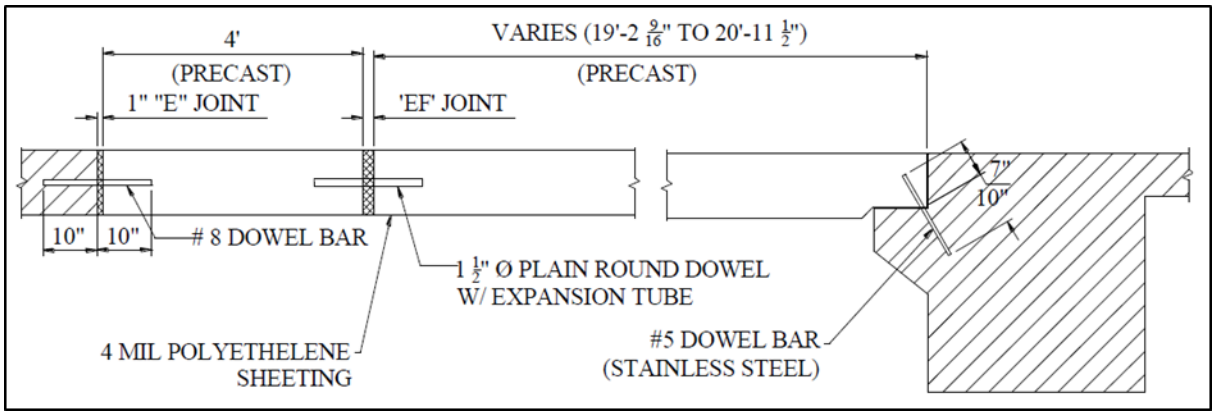

Nadermann et al. 2010

Figure 2.17. Elevation view of precast approach slab

Research has focused mainly on settlement of the approach slab and embankment, with little focus on the forces in the tie bars or the friction force under the approach slab. Often in finite element models the approach slab has been neglected due to its negligible effects on the movement of the abutments and the bridge, which have often been the focus of the study. LaFave et al. (2016) found that the approach slab had no impact on bridge behavior since forces were negligible in the superstructure due to approach slab friction under positive thermal loading. Their assumption from the parametric study was validated by monitoring results. According to Olson et al. (2009) the presence of an approach slab in their finite element model did not significantly affect stresses in the bridge deck. It is apparent that measures should still be taken to reduce friction, since sliding can affect the backfill and slab itself. According to Aktan and Attanayake (2011), it is vital to reduce friction on approach slab surfaces, which can be accomplished by placing a 0.025 in. thick polyethylene sheet between the backfill and the approach slab. Mistry (2005) and Thiagarajan et al. (2012) both recommended two layers of polyethylene sheets, and Phares and Dahlberg (2015) recommended one. There were no other friction reduction methods found in the literature search. Hassiotis et al. (2006) recommended ensuring that the surface of the subbase course follows and is parallel to the roadway grade and cross slope. A filter fabric “or some type of bond-breaker” such as polyethylene sheets was also recommended for placement between the subbase course and approach slab.

Oliva and Rajek (2011) used a parametric study to determine the effects of different design parameters on the rotation and strain of approach slabs. The goal was to determine the typical rotation that occurs so that it could be accounted for by engineers in designing approach slab connections at both ends. A finite element model was created using ABAQUS software that represented a typical integral abutment bridge. The model included a “settlement trench,” which was represented by a lack of backfill under a triangular portion of the approach slab and at the

abutment face. This trench accounted for the fact that due to settlement or erosion there is often a lack of support under the approach slab as the bridge ages.

The results of the parametric study were categorized and judged based on the flexural strain seen in the approach slab and the amount of rotation of the approach slab at the abutment. The settlement trench only had a significant impact when the length reached 6 ft or more, while the approach slab length had little effect on strain or rotation. Varying soil parameters were also investigated, and it was found that a loose soil condition introduced cracking of the approach slab under truck loading, the only condition to do so. The cracking was eliminated with the use of an 8 ksi strength concrete, suggesting that a precast approach slab could remedy the effects of poor soil conditions. Overall, rotations for all cases and parameters, except the loose soil condition, generally remained under 0.002 radians, which means that this is a magnitude that should be accounted for in design. As part of their parametric study, the authors also included approach slab length as a variable. After using three different lengths, they determined using approach slab strains that length only had a small effect on the behavior of the slab. All three cases used the same geometry as the base model and assumed moderately stiff soil. None of the lengths experienced cracking.

Nassif et al. (2009) compared the performance of the existing New Jersey standard approach details with two different prototype standards through field monitoring and finite element modeling. The two designs considered were embedded beam, shown in Figure 2.18, and continuous thickness. The continuous thickness design offers an increased thickness over the traditional design, and the embedded beam design places effective beams inside the slab every 1.8 meters in both directions to create plates that support only one wheel load of an HS-20 truck at a time. ABAQUS was used to create a 2D FE model using shell and spring elements along with a full 3D model of solid elements to model soil behavior. Both designs provided a minimum 2.8 times the cracking capacity of the existing New Jersey design, and the embedded beam design entrapped cracks within plates surrounded by effective beams. The embedded beam design was recommended for adoption by the NJDOT for future approach slabs.

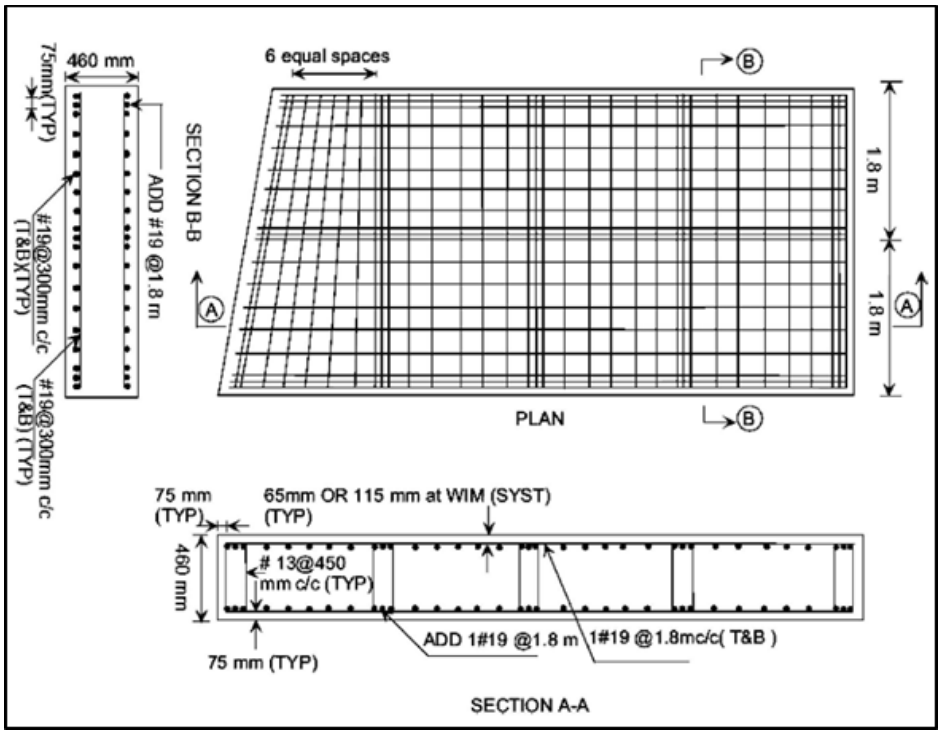

Nassif et al. 2009

Figure 2.18. Reinforcement details of an embedded beam approach slab

Yasrobi et al. (2016) surveyed 28 states about the issue of approach slab settlement. Settlement was found to be a common problem across the country, and states were organized into categories based on what percentage of bridges experienced settlement. The responses to many other questions could then be compared with the performance groups to determine whether certain practices were required in better performing states. If the responses did not correlate with the performance groups, then it could be inferred that the parameters in question most likely had little or no effect on approach slab settlement. The survey asked states what the cause of the observed settlement is, to which the most popular answer was poor construction, followed by high embankment fill. Based on an examination of the responses to each question, the authors were able to create a list of recommendations for design and construction that should have a tangible effect on approach slab settlement. Approach slabs should be 12 to 16 in. thick and less than 30 ft long to maintain proper structural stiffness and rigidity to avoid large deflections under load due to a loss of support, and a reinforced foundation should be used under a sleeper slab if one is included. Well-graded pervious backfill should be used in lieu of poorly graded backfill and should be compacted to 95% of standard Proctor density. It was recommended to use geotextile reinforcement under the approach slab, and construction requirements should be revised or developed for the optimal construction sequence, construction method, compaction method, and compaction control.

Chen and Abu-Farsakh (2016) experimented with a new approach slab design to replace Louisiana's current standard at the time due to problems with the bump at the end of the bridge. The plan was to create a stiffer slab by thickening and use of a higher reinforcement ratio, and to reinforce the soil under the sleeper slab using two geogrid layers. The approach slab was

intended to span the gap between the bridge abutment and sleeper slab when backfill support was inevitably lost. Both the new and old designs were implemented on the same bridge, one at each end, so that they could be directly compared. The new design, located on the west side, used a slab thickness of 16 in. and a length of 40 ft and was supported by a 3 ft 11 in. sleeper slab. The new design outperformed the old after 1.5 years, both visually and according to monitoring data. The roughness profile showed a smoother surface with less bump, and there was less cracking at the approach to the pavement joint. Sensors showed that earth pressures decreased over time as the load was spread out to the slab ends as intended on the new design, while earth pressures increased under the old design, possibly due to lower slab rigidity. The geogrid reinforcement under the sleeper slab performed well, and strains were measured to be under the typical manufacturer design value.

2.4. Geotechnical Design

Dupont and Allen (2002) outlined the causes of differential settlement of bridge approaches as follows: compression of embankment fill, settlement of foundation soil beneath the embankment, poor design or construction practices, and poor drainage practices. A look at current practice began with a survey of all 50 states, in which it was found that only 21 states used special procedures when backfilling around integral abutments and end bents. The authors noted that some states appeared to view the approach slab as the overall solution to bridge approach problems instead of as a design feature in need of additional improvement. Many conclusions were reached that were intended to alleviate future approach problems, including approach settlement periods/use of surcharge loading, lowered approach slabs with asphalt overlays, and the design of maintenance plans simultaneously with construction plans. Other more viable or effective methods included improving drainage on/around approaches, reducing embankment side slopes, and designing longer/stronger approach slabs.

Robison and Luna (2004) accurately modeled the deformation and settlement of bridge approach embankments in Missouri using PLAXIS software. By accurately modeling the staged construction process, the structurally important deflection, which occurs after the completion of the approach slab, could be determined and minimized on future projects. Other recommendations for MoDOT included enhanced soil exploration for high embankments (10 to 20 ft), the use of geosynthetics, and the use of select drainage material underneath the entire slab and sleeper beam. Some additional recommendations for better geotechnical performance of the embankment are provided by Luna et al. (2004). A recommendation was made to include exploratory boreholes 30 to 50 ft away from the abutment in the location of the approach embankment. Embankment slopes should be limited to 2.5H:1V to increase stability, and geosynthetic reinforcing should be considered for embankments higher than 10 ft.

Horvath (2005) examined the geotechnical issues that accompany integral abutment bridges. The author stated that the problems with integral abutment bridges are geotechnical in nature, so it would follow that the solutions should be geotechnical as well. Many solutions do not address the discontinuity between the moving structure and stationary soil. As the structure contracts in winter, a soil wedge moves inward and downward into the opening gap gehind the abutment. This creates a long-term problem in addition to the passive pressure on the abutment during the

summer. The ratcheting increases the passive pressure seen by the backwall over time. The movement of soil means that a loss of support will occur under the approach slab no matter what kind of soil is used or how well it is compacted. Compressible inclusions were found to be unable to hold back the active pressure of the slumping soil, since they were elastic enough to accommodate the expansion of the bridge in the first place. Two different details were proposed, as shown in Figure 2.19, with the first more promising and cost-effective than the second. The first uses a compressible inclusion in combination with an MSE embankment, which gives the soil enough strength to avoid falling into the void. The inclusion acts as a joint while also insulating the soil against temperature changes and possibly aiding in drainage. Passive pressures are reduced to increase cost savings in design. The second detail is intended for soft soil under the approach embankment and utilizes a wedge of EPS with a compressible layer. In conclusion, any successful solution must support the soil on a year-round basis and be able to fuction as an expansion joint between the abutment and soil.

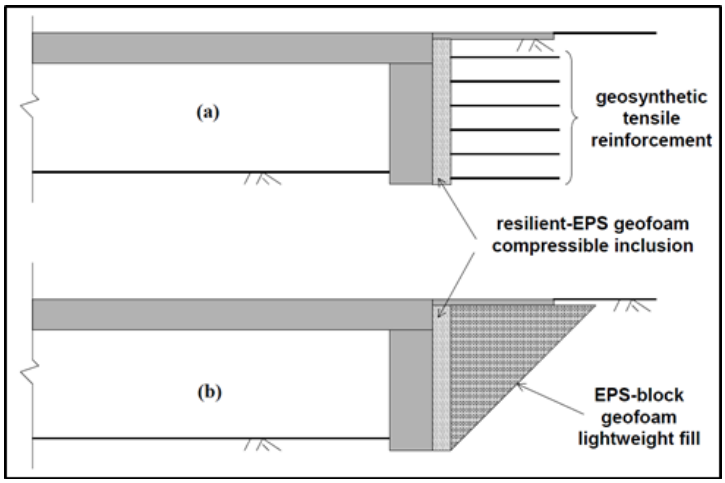

Horvath 2005

Figure 2.19. Proposed new integral abutment bridge design alternatives

Backfill is extremely important, since it interacts with both the abutment and the approach slab placed on top of it. Abu-Hejleh et al. (2008) evaluated the Colorado DOT bridge approach design methods to detemine their effectiveness and to provide recommendations moving forward. The practice at the time included three different methods for backfill: flowfill concrete, MSE Class 1 backfill, and MSE Class B free-draining backfill. Five different bridges were inspected, and forensic investigations were performed to determine the source of bridge bump problems. Approaches using the three then-current methods performed better than approaches using previous methods, but some settlement issues persisted. Flowfill was still recommended for unique scenarios where compaction is extremely difficult, but MSE Class B backfill had the lowest unit cost over the bridge's design life since there was no necessary repair reported. Final recommendations suggested optimum fill material compaction and the use of surchage preloading if possible. In order to better support the sleeper slab, two different methods were proposed. One included more MSE fill under the sleeper slab than the standard 4 ft at the time of the study. The other detail used piles to support the sleeper slab. The sleeper slab and expansion joint above it may be installed up to 1 in. higher in elevation than the design in order to account for post-construction settlement if approved by the hydraulic, structural, and roadway engineers.

The Nebraska DOT (NDOT) has a rather unique practice that includes the use of helical piles at the end of an approach slab, per correspondence with Mark Traynowicz of NDOT on September 13, 2018. Grade beams are used similarly to an approach slab and are almost always supported on piling. Nebraska allows H-piles, pipe, or concrete piles, but in the case of an approach slab replacement helical piles may be used as an alternative if they are the only piling required for the project.

2.5. Bridge End Drainage

Drainage is vital to bridge end design because of the effects poor drainage can have on the service life of a structure over time. An inspection of 74 Iowa bridges led to an investigation of approach slab performance by White et al. (2007). Void development due to backfill collapse, severe backfill erosion, poor surface and subsurface water management, and poor construction practices were identified as critical problems seen at some poorly performing bridge approaches. Elevation profiles of 38 bridge approaches were measured, and the majority were found to require maintenance or repair based on a 1/200 slope criterion. Four different backfill samples were tested in a laboratory, and bulking moisture contents ranged between 2% to 10%. Since field moisture contents were measured between 4% to 5%, the soils had a significant collapse potential, which would result in voids beneath the approach slab. Compacting poorly graded granular backfill at a moisture content outside the bulking moisture content would reduce the potential for collapse. In order to minimize erosion, a gradation with less than 60% passing the No. 8 sieve should be used. A full-height square abutment with a paving notch is easier to construct and would facilitate better compaction around the abutment.

Mekkawy et al. (2005) utilized the same bridge approach inspection results as White et al. (2007) to develop the Bridge Approach Drainage Model (BADM). The BADM is a 1/4 scale model of an abutment backwall, backfill, and approach slab used to test different drainage techniques. The BADM was created to evaluate designs on the basis of surface/subsurface drainage and erosion on embankment and backfill materials, which are the two major causes of approach settlement in Iowa. Steady-state flow from the expansion joint to the drainpipe was achieved for each of the 13 models and allowed to run for 4 hours. Flow and settlement were measured, and the models were inspected for void formation and erosion. The poorest performing model of the group was the one that simulated field practices. Three details performed much better than the rest: a geocomposite drain with backfill reinforcement and a moisture content above bulking, tire chips behind the bridge abutment, and porous backfill material for the entire depth behind the abutment.

All performance issues in jointless bridges, such as approach slab performance, embankment settlement, erosion, and abutment backwall earth pressures, are all related due to the thermal movement of the bridge itself. Drainage design can have a huge impact on the geotechnical aspects of the project. Miller et al. (2013) investigated the settlement of approach slabs in Oklahoma in order to provide recommendations to minimize settlement in future construction. After completing a literature review to determine the causes of settlement, a survey was sent to Oklahoma DOT Field Divisions to identify sites for inspection of bridge approach slabs.

Thirty different bridges were inspected visually, with fifteen showing representative examples of erosion and drainage concerns. Common issues included large voids appearing under approach slabs and abutments, and surface drainage was categorized as universally poor, with separated joints or cracks allowing water infiltration. Staining on abutment walls indicated that soil loss was occuring through cracks in the abutment in some locations. Two bridges performed very well due to design changes in the drainage detailing. Shields Boulevard over I-35 included a neoprene sheet at the base of the abutment to block the hydraulic short circuit and prevent drainage from escaping under the abutment. Another example of poor detailing is that drain outlets, even when performing well, were allowing expelled water to flow back into embankments because of the outlet location. One recommendation was made to outlet drains near the bottom of slope walls into erosion-resistant drainage ways and to check and maintain all drainage systems regularly. Geomembranes can eliminate unwanted drainage paths and prevent short circuits under the abutment, as shown in Figure 2.20. Construction of embankments should involve a complete settlement analysis, which will illustrate the importance of the soil properties and identify issues with wetting-induced compression. Compaction should be made more accurate through the use of a relative density-based specification instead of a standard Proctor-based specification.

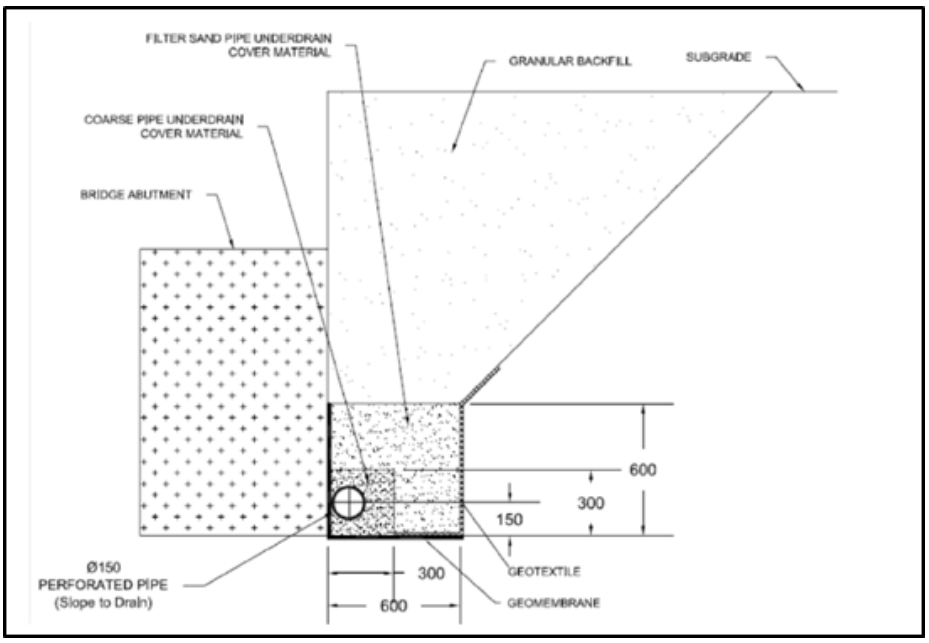

Miller et al. 2013

Figure 2.20. Proposed abutment backfill drainage system with geomembrane and graded granular filter (units in mm)

The practice of placing a concrete barrier rail on top of the approach slab is recommended for drainage purposes (Briaud et al. 1997). The detail shown in Figure 2.21 has been referenced many times in various studies and shows the problem with placing the barrier on the wingwall. The joint between the approach slab and wingwall allows for water infiltration, potentially leading to settlement or erosion of the embankment. There is no mention of possible consequences in terms of other aspects of approach slab performance.

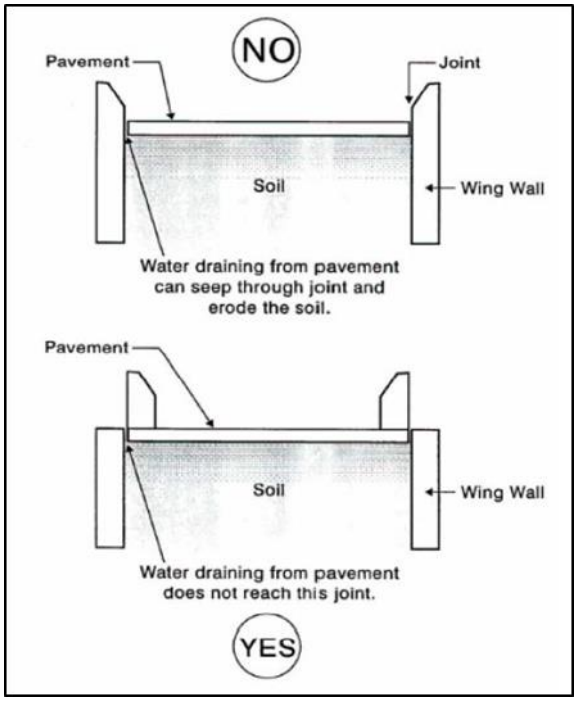

Briaud et al. 1997

Figure 2.21. Cross section of a wingwall and drainage system

Phares and Dahlberg (2015) evaluated the approach slab design used by the Wisconsin DOT (WisDOT) after WisDOT made a change from using three expansion joints to using a single expansion joint due to difficulties in constructing multiple joints. Twelve bridges were inspected, and a single soil sample was taken for laboratory analysis. Testing showed that increasing moisture content reduces the likelihood of collapse, an issue covered by White et al. (2007). The authors provided many general recommendations, including the continued use of polyethylene sheeting under the approach slab and sleeper slabs. In order to maintain proper drainage, several details were also recommended, including full-width approach slabs, tiled drainage near the approach-slab-to-pavement joint, surface drainage channels on embankments, drainage tiles in the embankments, drainage that can intercept water on the bridge deck before reaching the abutment-to-approach-slab joint, and a drainage path for water that does infiltrate joints. Proper drain maintenance is key and should be completed on a regular schedule.

According to Puppala et al. (2009), proper drainage is extremely important to prevent water infiltration into the approach slab embankment, which can result in erosion and a loss of support, so the authors recommended that deck surface water from the bridge be intercepted before it crosses the joint to the approach slab, as previously noted by Phares and Dahlberg (2015) and Abu-Hejleh et al. (2008). Impervious membranes with collector pipes can be used to collect water that penetrates cracks and joints. Membranes can be limited to locations under joints to lower costs. A half-circle PVC pipe under a joint can carry water to the sides of the approach and prevent infiltration.

Lenke (2006) conducted a thorough field evaluation of 19 bridges in New Mexico in conjuction with the New Mexico DOT (NMDOT). All 19 bridges were noted as having problems with their approaches. MSE walls showed fewer problems than other abutment systems due to the use of better compaction and high-quality fill for improved drainage. The NMDOT increased the use of wingwalls to reduce erosion and provide extra stability for backfill. The approach should be tied to barrier walls and wingwalls in order to prevent water intrusion into the fill below the approach. It was recommended that corbels should not be used to support the approach slab because they make proper compaction difficult near the abutment.

2.6. Expansion Joints

Due to the unsatisfactory performance of the Minnesota DOT (MnDOT) standard E8 expansion joint, Reza (2013) investigated the standard practices of other states in terms of approach slab joint materials and details. The E8 joint was designed to be used between the approach slab and pavement and consists of a 4 in. wide gap filled with a high-density foam product (Evazote) attached to the inside walls of the joint by adhesive. The joint has often failed in winter as the bridge contracts and the joint opens due to breakage of the thin asphalt seal or failure of the adhesive. Joints at three different bridges were monitored using crackmeters to determine the correct multiplier coefficient (ultimately determined to be 1.5) for calculating joint size. The multiplier is multiplied by the change in temperature, length, and coefficient of thermal expansion to obtain numbers that can be compared with the manufacturer ratings for joint types and sizes. The review of other states' practices showed that strip seals should be considered for the expansion joints for new integral and semi-integral abutment bridges based on previous performance and the fact that it is the most popular choice. However, using strip seals would require a new detail for where the joint meets the curb and increase costs slightly due to the need to extend the concrete barrier longer than the then-current practice. As a result of the studies by LaFave et al. (2016, 2017), it was recommended that IDOT consider alternative expansion joint details to its current strip seal, since longer bridges over 700 ft could experience movements larger than the strip seal limit of 2 in.

It appears that expansion joint issues are inevitable and unavoidable, thus the push for jointless bridge design. Miller et al. (2013) noted that "pavement surface joint seals were largely compromised and so the subsurface drainage must be designed with the expectation that water will enter the joints, potentially with enough erosive power to undermine approach slabs." There is little information available recommending any certain expansion device at the approach-slab-to-sleeper-slab joint; most studies simply state what joints are used and what problems are associated with them. In a set of design guidelines included as part of Idaho's bridge design manual, the ITD (2008) says, "The joint width at the end of the approach slab where it rests on the sleeper beam should only be large enough to prevent the joint from completely closing during hot weather, with an allowance for the minimum compressed width of the joint seal material. It is not necessary to design the joint for the full movement range that would be required in a typical joint design."

The review of state DOTs surrounding Minnesota by Reza (2013) included the kind of expansion device used at the approach-slab-to-sleeper-slab joint. South Dakota and Michigan used strip

seals. Ohio was using an asphalt pressure relief joint. Problems with ride quality over the pavement-bridge interface in Ohio led to a study at ISU by Phares et al (2011). Kansas utilized an approach slab overlapping 2 ft on an 8 ft sleeper slab with 6 ft of asphalt over the top. On the other side of the sleeper slab was another concrete slab overlapping 2 ft on the same sleeper slab that spanned to another sleeper slab. Polytite waterproofing membrane was applied on all concrete surfaces in contact with asphalt. Ontario chose its expansion device based on the expected movement at the joint. Movement less than 1 in. resulted in the use of an asphalt-impregnated fiber board sealed by rubber asphalt. A sleeper slab with a closed-cell neoprene seal was used for movement between 1 and 2 in. Movements greater than 2 in. called for a strip seal.

2.7. Approach Slab Performance

An effective way of determining areas of improvement for future moveable abutment designs is to take stock of how the approach slabs on previous projects are performing under field conditions. In a comprehensive review performed by Yasrobi et al. (2016), it was concluded that 46% of the 28 reviewed states were not satisfied with their current approach slab design. It was noted that the most common cause for the observed failures was inappropriate approach slab settlement, which many DOTs mainly attributed to poor construction practices. Further, this excessive settlement was often accompanied by poor drainage, which led to erosion and the occurrence of voids underneath the approach slab. As this runoff continued to make its way underneath the slab, the void continued to worsen, increasing the likelihood of structural issues with the slab. Based on the findings of Yasrobi et al. (2016), it was determined that backfill design and construction were the most important factors leading to approach slab settlement and failure. However, it was noted that properly designed backfill is not enough to eliminate approach slab issues on its own.

The findings presented above by Yasrobi et al. (2016) have been echoed by previous research. In a series of studies performed by White et al. (2005, 2007) that investigated 74 Iowa bridges to quantify common issues with failed approach slabs, it was determined that severe voids had developed under 25% of the inspected bridge approaches. In addition, severe erosion was present at 40% of the bridges, and 60% of the bridges had ineffective runoff. The majority of the bridges exceeded the recommended 1/200 slope proposed by Wahls (1990) and Long et al. (1998), and differential settlement of 2 to 6 in. was common at the end of the abutment wingwall. Runoff and erosion often accompany one another, as excess runoff typically leads to increased erosion underneath the approach slab. The erosion was found to typically leave a void ranging from 6 to 12 in. between the base of the slab and the geotextile-reinforced subbase (Figure 2.22).

White et al. 2007

Figure 2.22. Voiding under approach slab

While this voiding does not lead to immediate failure of the connection joint or approach slab, it does present other issues that may develop over time, including connection joint shearing, settlement and transverse cracking of the approach slab, and erosion and fracturing of the slope, embankment, and piles (Figure 2.23). Typically, void development was observed within the first year of service, and grouting underneath the slab to mitigate the issue was found to not necessarily prevent further settlement.

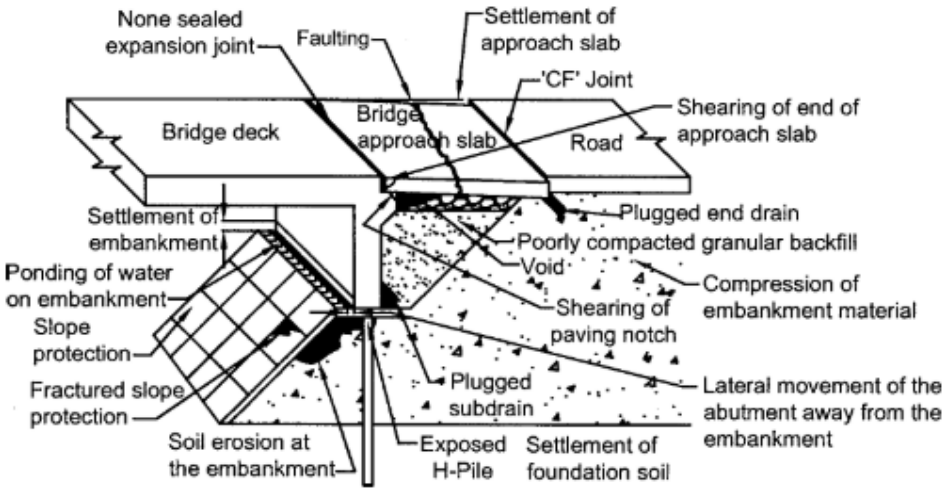

White et al. 2007

Figure 2.23. Diagram summarizing frequent problems at several bridge sites

The prevalence of a void directly adjacent to the abutment, as shown in Figure 2.24, is further aggravated by the introduction of integral abutments, which push and pull the backfill as the bridge structure expands and contracts with thermal effects. These thermal movements, reported by Schaefer and Koch (1992), create compaction in the soil as the bridge expands. However, once the bridge contracts and pulls away from the embankment, a void is left.

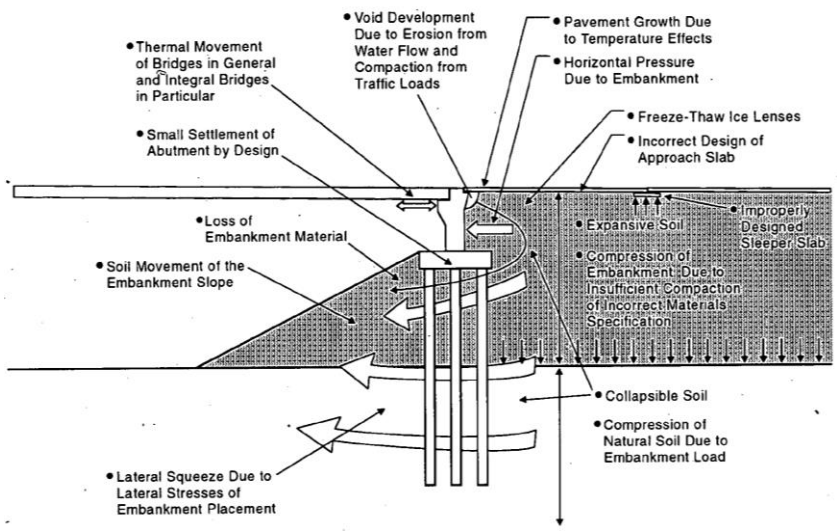

Briaud et al. 1997

Figure 2.24. Problems leading to the formation of a bump

Once this initial void is formed, the integral abutment is at a much higher risk for further erosion and voiding due to excess, mismanaged runoff. This cyclical nature of this movement has been verified by several subsequent studies via field inspection and approach slab instrumentation. In a project that monitored the temperature and displacement of two integral abutment connections, one with a precast slab and one with a cast-in-place slab, strain ratcheting was observed, as shown in Figure 2.25 (Greimann et al. 2008).

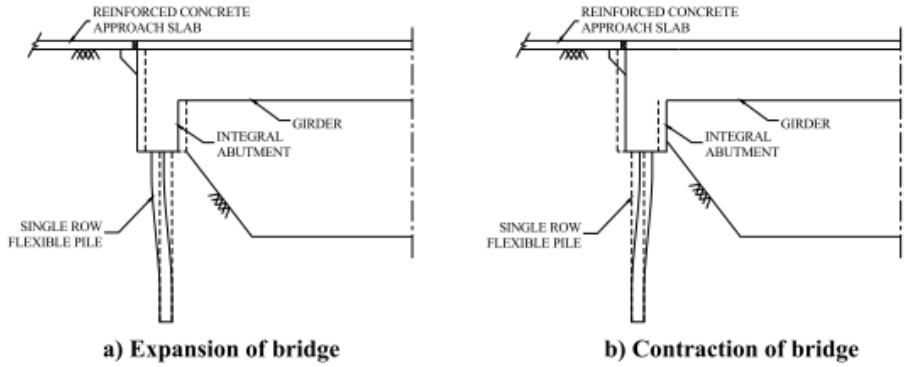

Greimann et al. 2008

Figure 2.25. Structural movement due to thermal effects

This ratcheting effect, which progressively worsens the voiding condition underneath the slab with time, provides an area where additional runoff may erode the subbase. Additionally, while the vertical reinforcing bar connection was initially found to work as intended, an opening in the joint formed over time. A 22 in. void was also documented underneath the doubly reinforced south approach slab, and transverse cracking of the slab was reported.

A similar study was performed by Nadermann et al. (2010), where it was observed that this temperature movement took the form of two patterns: a long-term cycle encompassing the general temperature movement throughout the year and a repeated short-term cycle as the temperature fluctuated throughout the course of each day. Again, while the tied connection observed in this study initially performed well, it was later shown to age poorly, excessively opening as time went on. The majority of the vertical tie bar connections investigated had not performed well in the long term, often opening more than twice their initial design width due to thermal movement. In addition, several of these bridges displayed transverse cracking similar to that shown in Figure 2.26, and it was hypothesized that this cracking and voiding would lead to inadequate drainage and further problems.

Figure 2.26. Transverse cracking of approach

In an effort to determine how widespread the settlement and voiding situation in Iowa approach slabs was, the Iowa DOT contracted Wiss, Janney, Elstner Associates, Inc. (WJE) to perform two empirical surveys of slab performance in the state (Rende and Donnelly 2011). The first study, performed in 2011 in the wake of a large amount of Missouri River flooding in western Iowa, utilized ground penetrating radar (GPR) and impulse-response (IR). In addition to these two forms of nondestructive evaluation, coring was performed to verify the accuracy of the acquired data. In total, 22 bridges (44 individual reinforced approach slabs) were investigated for voiding and vertical settlement, and the coring verification determined that GPR was a reliable way to scan and detect deficiencies in the soil beneath the approach slab.

Of the 44 slabs investigated, 3 experienced severe voiding ranging between 10 to 20 ft in length and 2 to 5 ft in depth. Soil tests conducted beneath these slabs indicated that none of the original subbase remained. However, none of these slabs displayed any visible signs of structural impairment to the approach slab. Of the remaining 41 approach slabs, 28 exhibited voiding,

although it typically spanned less than 10 ft from the face of the abutments with a depth of less than 2 in.; the original subbase, consisting of compacted sand or gravel, was typically present at these locations.

A second study with a similar intent was again conducted by WJE in 2018. In this case, the goal was to investigate the performance of 12 Iowa approach slabs with stub and integral abutments constructed between 2006 and 2015 following the implementation of design recommendations proposed by White et al. (2005). This second survey consisted of visual inspections and GPR and was supplemented by coring and borescope investigations to confirm the presence and extent of voiding. A large majority of the connection joints and expansion joints had fared poorly, differing from the design plans in opening width by as much as 3 in. The GPR and borescope inspections revealed similar performance to that documented in the 2011 report—the bridges with integral abutments displayed large voids adjacent to the abutments, likely from repeated thermal expansion and contraction. The approach slabs on these bridges were likely more susceptible to further erosion and damage as a result of these movement voids, such as the damage shown in Figure 2.27. However, it was recorded that many of these bridges were performing well structurally, although several did show signs of transverse cracking and pavement spalling. The maximum settlement and differential settlement were recorded as 1 in. and 0.4 in., respectively. Investigation of the performance of the stub abutment bridges displayed a stark contrast to the performance of the integrally connected bridges, with the stub abutment bridges showing much less voiding in general.

Iowa DOT

Figure 2.27. Examples of voiding at integral abutment bridges

2.8. Recommendations for Mitigating Approach Slab Failure

Given the nature of the failures described in the section above, the main factors contributing to approach slab/connection joint failure in moveable abutment bridges stem from geotechnical problems related to soil settlement and erosion. Typically, design techniques to anticipate and prepare for these failures are split between two overarching categories: soil preparation and structural design considerations.

2.8.1. Soil Preparation and Design

Standard design recommendations for the subbase beneath approach slabs is centered around limiting settlement and limiting loss of the original subbase. Exact recommendations vary, but most researchers agree that a stiff, well-drained soil performs best. According to the study performed by Yasrobi et al. (2016), backfill should consist of a well-graded pervious material with a minimum 95% compacted standard Proctor density. It was also recommended that in situ density tests be performed on the proposed soil in order to gauge the possibility of future settlement. In a finite element analysis run as a part of an approach slab performance study at the University of Wisconsin–Madison, it was found that soil stiffness had a notable impact on concrete cracking (Oliva and Rajek 2011). As soil stiffness decreased, the amount of both settlement and slab rotation at the abutment increased; these responses were followed by a higher likelihood of transverse cracking. The same was true for void occurrence. As the length of the void increased, the likelihood of structural failure increased as the slab was required to span the longer settlement trenches. A similar study was conducted by Nassif et al. (2002) that determined that edge settlement led to tensile stress concentrations in the top of the slab, whereas settlement in the middle of the slab led to tensile stress concentration in the bottom of the slab. In order to improve subgrade performance and ensure optimal stiffness, Phares et al. (2011) recommended improving compaction effort via a light vibratory compactor on granular backfill to mitigate settlement. By providing a sufficiently stiff soil, the entire length of the approach slab is consistently supported and deflection is limited.

Should soil with an appropriate stiffness be used, it is also important to prevent future erosion due to poor drainage. It is often recommended that proper water drainage be an integral part of design (Phares and Dahlberg 2015, White et al. 2007). To reduce the overall forces present within the slab due to thermal movement, steps should also be taken to lower the friction factor between the base of the slab and the subgrade underneath. The most common recommendation is the use of polyethylene sheeting between these two components (Mistry 2005, Aktan and Attanayake 2011, Phares and Dahlberg 2015). By lowering the amount of friction force required for the approach slab to slide across the underlying subbase, the amount of force transferred through the abutment connection is reduced, lowering the likelihood of a connection failure.

The inclusion of a sleeper slab has also been suggested to overcome settlement at the far end of an approach slab (Phares et al. 2011, Yasrobi et al. 2016). Unlike the side of the slab adjacent to the bridge, which rests on a seat provided by the abutment, the majority of the slab is supported only by the soil underneath. Therefore, areas farther from the abutment are at a higher risk for settlement.

The inclusion of a sleeper slap provides an additional concrete support condition in the area most likely to experience higher total settlement. If the approach slab is designed with enough structural rigidity to span any voids or settlement that may occur between the abutment and the sleeper slab, then deflection and transverse cracking will theoretically be mitigated. However, in their field study of several approach slab panels in Wisconsin, Phares and Dahlberg (2015) hypothesized that not all slabs were being adequately designed to span this settlement ditch between the sleeper slab and abutment. Moreover, a sleeper slab does not always perform as

intended. Should the approach slab be built on weak, settlement-prone soil, then it will vertically displace along with the rest of the approach slab system. Recommendations typically include proper compaction and use of geogrid layers for reinforcement beneath the sleeper slab (Chen and Abu-Farsakh 2016).

2.8.2. Structural Rigidity

While increasing soil stiffness and ensuring proper drainage are key factors in a successful tied moveable abutment design, several of these soil considerations are difficult to guarantee, and it is for this reason that many researchers recommend designing the approach slab with enough stiffness to span any voiding or settlement that may occur (Phares and Dahlberg 2015).

The factors generally studied regarding structural rigidity for approach slabs are slab thickness, reinforcement ratio, slab length, and concrete strength.

In a study performed by the NJDOT (Nassif et al. 2002) to improve approach slab design details, a finite element model was created utilizing ABAQUS modeling software. The goal of the study was to correlate the failure patterns of the computer model with those observed in field bridges. The computer models featured a series of springs to represent the subgrade beneath the approach slab, and these springs were added and removed at various points to simulate voiding conditions. These conditions were coupled with a standard HS-20 service truck load to simulate likely field loading. As noted in earlier field investigations above, the results indicated that an increase in soil settlement led to a higher likelihood of premature slab failure in the form of transverse cracking. The model displayed a cracking pattern similar to that observed in the field bridges, showing cracks near the entrance and exit of the slab. A parametric analysis was performed on the computer model to investigate how possible design detail modifications could improve performance in future designs. The most significant factor for mitigating transverse cracking and slab settlement was determined to be slab thickness; as the slab depth was increased, the forces present in the extreme tensile regions of the slab were reduced. Further study revealed that a higher concrete strength had a positive effect on tension reduction, although it was much less effective than increasing slab depth. An increased steel reinforcement ratio and a higher steel yield strength had little to no impact on limiting failure.

The results of this study are substantiated by a field study performed on behalf of the LaDOTD (Chen and Abu-Farsakh 2016), which monitored two similar approach slabs with different design details based on previous research (Cai et al. 2005, Chen 2007, Abu-Farsakh et al. 2008). It was clearly observed that an increased slab thickness and higher reinforcement ratio in the west approach slab led to significantly less cracking and reduced tensile strain values.

A similar finite element modeling approach was taken by Oliva and Rajek (2011). In this case, the goal was to quantify the amount of rotation that could be present at the connection between the approach slab and the abutment. It was observed that decreased soil stiffness led to higher amounts of settlement, connection rotation, and risk of transverse cracking. The transverse cracking observed in approach slabs with “loose” soil conditions and standard strength (4 ksi) concrete was mitigated by utilizing concrete with a higher compressive strength (8 ksi). It was

also noted that, based on the standard amount of rotation observed, the expansion joint or ductile concrete between the abutment and approach slab should be designed for a rotation of 0.002 radians. Further, voiding conditions adjacent to the abutment were modeled, and it was determined that slab performance was affected when voids were greater than 4 ft in length, with much higher levels of tensile forces becoming present once the voids became 6 ft or longer. Slab length was determined to have little effect on reducing transverse cracking beyond 10 ft.

2.9. Inventory of Iowa Approach Slab Performance

2.9.1. Approach Slab Inventory Background and Process

As a supplement to the studies performed above, the Iowa DOT, through the ISU Bridge Engineering Center, decided to perform an inventory quantifying the performance of Iowa DOT approach slabs constructed since 2009, as a number of design changes were made during that time. The motivation behind this review of approach slab performance in Iowa was to verify whether these design updates are working to mitigate common approach slab issues. It was the goal of this venture to gain a more complete idea of approach slab performance throughout the state to identify which design details and methods produce the best performance during field operation. As this investigation directly relates to the content and scope of the research presented in this report, it was determined that summarizing the results of this venture here would be beneficial to characterizing typical approach slab performance throughout the state.

As stated above, the goal of this inventory was to investigate and compare the performance of different approach slab details and conditions throughout the state of Iowa. Per the Iowa DOT, the key areas of concern for this review were identified as bump presence, slab settlement, slab cracking, joint issues, and paving notch issues. For the approach slabs investigated, these performance indicators were correlated based on their prevalence among bridges with similar designs and operational conditions, including bridge type, abutment type, approach type, and traffic data. By noting which bridges are susceptible to higher amounts of performance issues, specific designs can be investigated in more detail.

In most cases, the performance and design details of each approach slab were determined via Iowa's Structure Inventory and Inspection Management System (SIIMS), which contains original design documents and a record of all routine state inspections. Using this system, we were able to find plans, photographs, and inspection reports of bridges constructed from 2009 to 2020. From these files, we were able to compile relevant information on Iowa bridge structures.

It was noted that images of approach slab performance were often difficult to ascertain from the inspection reports and images, and Google Earth was utilized when necessary. Due to this lack of documentation, it was often surmised that a given issue was nonexistent for the approach slab if it was not explicitly stated in the inspection report and not clearly seen in the available images. In addition, several of the plan sets did not include the exact type of approach slab used. This was again surmised based on the thickness of the bridge deck, the type of the bridge, and the approach slab type used on similar structures.

To begin, we transferred the bridges from the large Excel file provided by the Iowa DOT to a new file that included the following columns: Parent Asset, Bridge ID, Year, FHWA [Federal Highway Administration] Number, NBI 007 Facility Carried, AADT [Annual Average Daily Traffic], Design Number, and Bridge Type. We also updated the hyperlinks in the new Excel file to allow easy access to the SIIMS webpage for each bridge. Next, we filled in the information for each bridge's design using the available plan sheets, which provided data for the following columns: Abutment Type, Approach Type, Approach Notes, and Paving Notch Width. After this basic information was filled in, we moved on to the photographs and inspection reports to find the current condition of each bridge and fill in the remainder of the columns, which documented any bridge issues. These columns included Bump Presence, Settlement, Approach Slab Crack Presence, Paving Notch Issues, and Joint Issues, each of which was followed by a column for related comments and notes.

For the Bump Presence column, we focused on the condition of the approach and expansion joint to determine whether a label of "Likely," "Possible," or "Not Likely" should be recorded in the column. This determination was based on the photographs in the inspection report for the most recent year along with the judgement of the individual observing the photographs. A note regarding differential settlement at the barriers and/or joint was recorded in the Bump Comments column when observable differential settlement was present at either or both the barriers and/or expansion joint (Figure 2.28 and Figure 2.29). This differential settlement was usually accompanied by a "Possible" label in the Bump Presence column. Occasionally, if the differential settlement appeared to be substantial, it would result in a label of "Likely" in the Bump Presence column. An additional description in the Bump Comments column of "Significant" or "Slight" occasionally accompanied the "Likely" or "Possible" label in Bump Presence.

Figure 2.28. Differential settlement at barrier

Figure 2.29. Differential settlement at joint

Spalling is another description recorded in the Bump Comments column. Figure 2.30 shows some common examples we saw and labeled as “Spalling.” This cracking of the pavement almost always resulted in a label of “Likely” in Bump Presence, as it appears to most likely cause a bump when a vehicle travels over it. Similar to spalling is the label “Abrasion at Joint.”

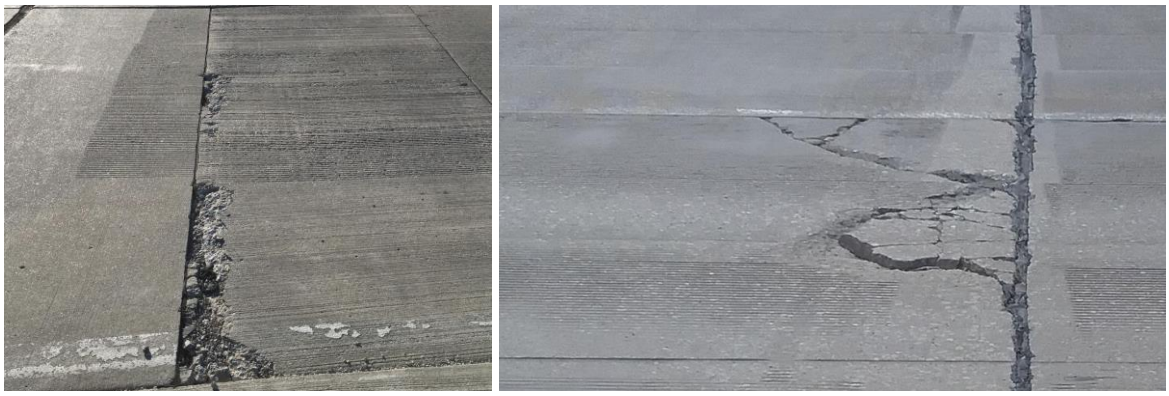

Figure 2.30. Examples of spalling

Another common description in the Bump Comments column is “Transverse Cracking.” This typically resulted in a label of “Likely” in the Bump Presence column. A transverse crack in the approach slab (Figure 2.31) usually appears to be significant enough to create a bump when a vehicle drives over it.

Figure 2.31. Transverse cracking

Large asphalt patches were observed a few times. Though this issue was rare, it would likely cause a bump in the bridge (Figure 2.32).

Figure 2.32. Asphalt patch

For the Settlement column, we looked for clear indications of settlement in the bridge structure and recorded a label of “No,” “Possible,” or “Likely” in the column. Cracking near or on the barriers was also an indicator of whether settlement had occurred. This can be seen in Figure 2.33 and Figure 2.34. Based on the clarity of the settlement, the terms “Slight” or “Clear” were also stated in the description.

Figure 2.33. Cracking/Differential settlement at barrier

Figure 2.34. Cracking at barrier

For the Approach Slab Crack Presence column, we looked at the photographs of the approach slabs and simply checked whether there were any cracks present. Transverse cracking was a common form of cracking on the bridges investigated. In the comments, we also stated whether cracking was seen on the near approach, far approach, or both approaches.

A label of either “Possible” or “Not Likely” was recorded in the Paving Notch Issues column based on inspection sheets and photographs found in the inspection report for the most recent year. If any cracking was found along the roadway at the expansion joint, a label of “Cracking at Abutment” was recorded in the comments. It was difficult to tell based on the photographs how significant the cracking was, so we assumed that any cracking was an indication of possible paving notch issues.

The label recorded in the Joint Issues column was based entirely on the inspection sheet comments. If “poor seal,” “debris present,” or “expansion joint was measured greater than 2 in.” was stated on the inspection sheet, it was added to our comments. This, along with the

photographs, helped to determine whether a label of “No,” “Possible,” or “Likely” should be recorded in the Joint Issues column.

Some examples are provided hereunder to show how we collected data and filled in the spreadsheet columns.

For the first example, the data collection process for an integral abutment bridge in good condition is provided along with some plans and photographs for explanation. To begin, we copied the relevant bridge information from the “All Bridges” Excel sheet to the “Slab Inspections” sheet, as seen in Figure 2.35.

Parent Asset	Bridge ID	Year	FHWA Number	NBI 007 Facility Carrie	AADT	Design Number	Bridge Type
State Bridges > District 3	1396.6R020	2012	609735	US 20 EB	1820	510	5 - Prestressed Concrete 02 - Stringer/Multi-beam or Girder

Figure 2.35. General information about the bridge

Next, the bridge webpage was found using the FHWA number of the bridge on the SIIMS website, and the bridge plan sheets were downloaded (Figure 2.36).

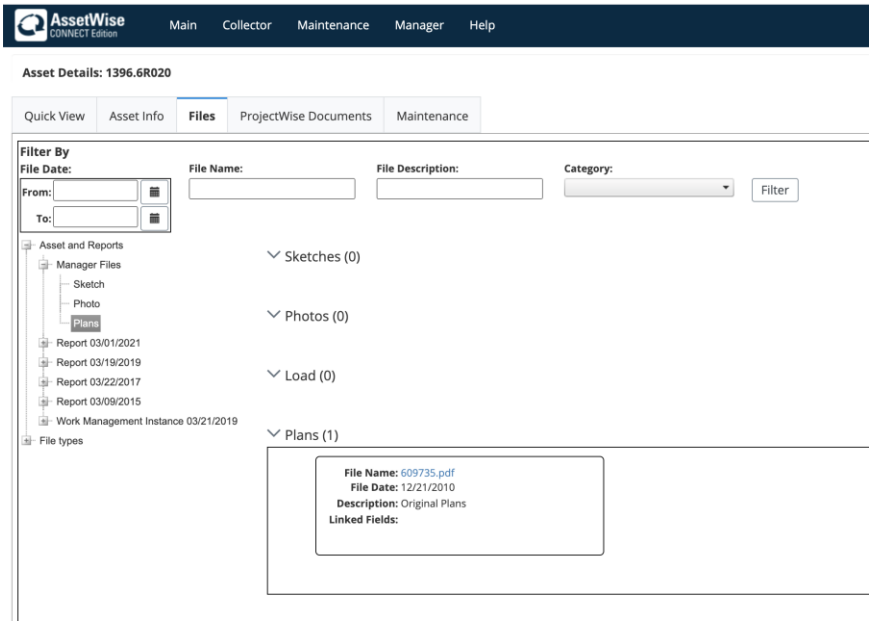

Figure 2.36. Bridge plan sheet location

From the plan sheets, we looked for five pieces of information: Design Number, Abutment Type, Approach Type, Approach Notes, and Paving Notch Width. The design number is found on the first page of the plan sheets, as seen in Figure 2.37. In this case, the design number is 510.

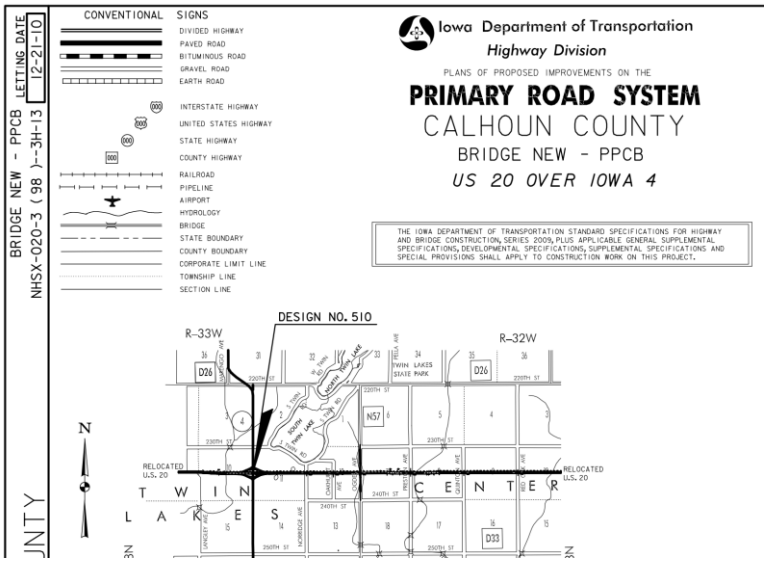

Figure 2.37. Bridge plan sheet—design number

Next, we looked for the Abutment Type and Paving Notch Width. On the plan sheet, integral abutments most often appeared as they do in Figure 2.38. This is typically found midway through the plan sheets. In this example, the paving notch width is equal to 1 ft 3 in.

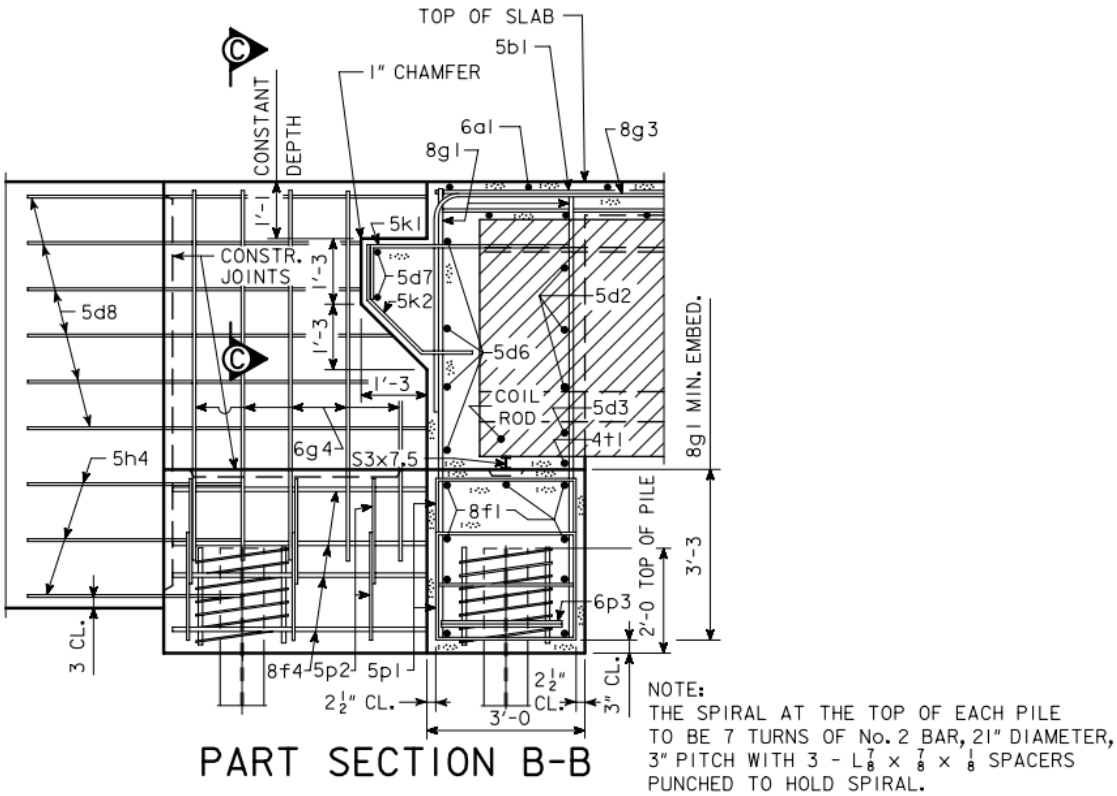

Figure 2.38. Bridge plan sheet—abutment type

The final two pieces, Approach Type and Approach Notes, can be found near the end of the plan sheets in the “Standard Road Plans” box. In this case, the approach type is RK-20, and the approach note is “Double Reinforced 12 in. Approach” (Figure 2.39).

STANDARD ROAD PLANS 105-4 10-16-07

The following Standard Road Plans shall be considered applicable to construction work on this project.

Number	Date	Sheets	Title
PV-1	10-19-10		Joints
RF-19E	10-20-09		Outlets for Longitudinal, Transverse and Backslope Subdrains
RF-39	04-20-10		Scour Protection for Bridge End Drain
RF-40	10-19-10		Rock Flume for Bridge End Drain
RK-20	10-19-10		Double Reinforced 12" Approach
RK-30	04-20-10		Bridge Approach (Abutting Pavement)
RM-37	10-21-08		Junction Box (Cast Iron)
TC-1	10-17-06		Work Not Affecting Traffic
TC-202	04-20-10		Shoulder Closure (One Lane)
TC-213	10-21-08		Lane Closure with Flaggers
TC-251	10-16-07		Temporary Road Closure

Figure 2.39. Bridge plan sheet—approach slab details

For the next step, we looked at photographs (Figure 2.40) from the most recent bridge inspection report to fill in information in the following columns: Bump Presence, Bump Comments, Settlement, Settlement Comments, Approach Slab Crack Presence, Cracking Location, Paving Notch Issues, Paving Notch Comments, Joint Issues, Joint Notes, and Additional Notes.

Approach Slab

Expansion Joints

Figure 2.40. Bridge inspection photographs—approach slabs

Looking at Figure 2.40, there is no clear evidence of transverse cracking, spalling, settlement, joint damage, or any other issues. This bridge appears to be in good condition. Looking at the photographs of the near and far expansion joints in the right-hand side of the figure, there is further evidence of good joint condition, no spalling, no settlement, and no cracking. The photographs of the barriers were also investigated to check for settlement or cracking at the barriers as well as erosion and any other issues (Figure 2.41). The four barrier photographs indicate that the barriers appear to be in good condition, with no signs of any issues.

Figure 2.41. Bridge inspection photographs—barriers

Lastly, we checked the inspection sheets (Figure 2.42) provided in the most recent inspection report to fill in any other relevant information. These sheets usually provided information for the Paving Notch Issues, Paving Notch Comments, Joint Issues, and Joint Notes columns.

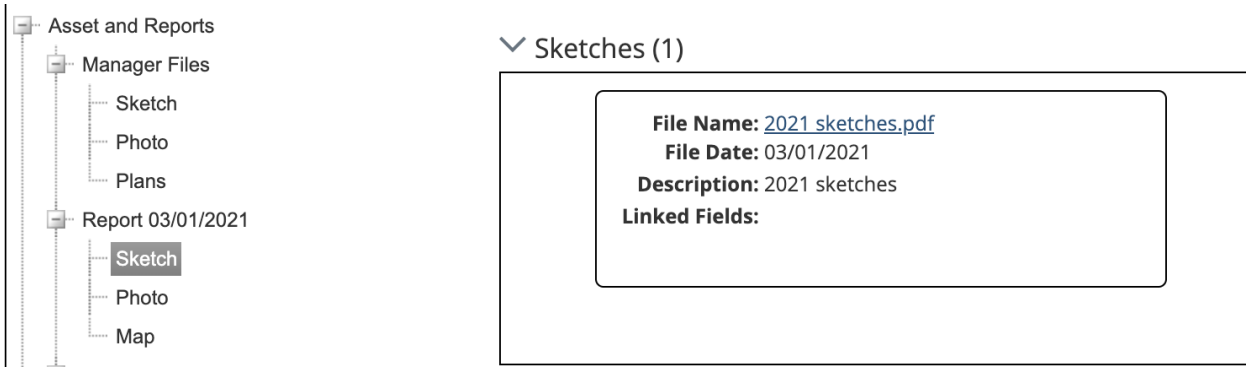

Figure 2.42. Bridge inspection sheet location

Sketches of the bridge deck as well as joint notes were used to determine whether there were any issues with the joint or paving notch. Some inspection sheets were more thoroughly filled in than others, but this one appeared to indicate no issues. Since there were no observable issues with

this bridge across the areas of concern, we filled out the rest of the information as seen in Figure 2.43.

Bump Presence	Bump Comments	Settlement	Settlement Comments	Approach Slab Crack Prese	Cracking Location	Paving Notch Issues	Paving Notch Comments	Joint Issues	Joint Notes	Additional Notes
Not likely		No		No		Not likely		No		

Figure 2.43. Bridge issues entries

The other type of bridge abutment investigated was a stub abutment with either a strip seal or finger joint for the expansion joint. The same process described above was used to collect the general data and download the bridge plan sheets for the next two example bridges: a stub abutment bridge with a strip seal and a stub abutment bridge with a finger joint. For this type of abutment, the plan sheets show a design similar to the two plans presented in Figure 2.44.

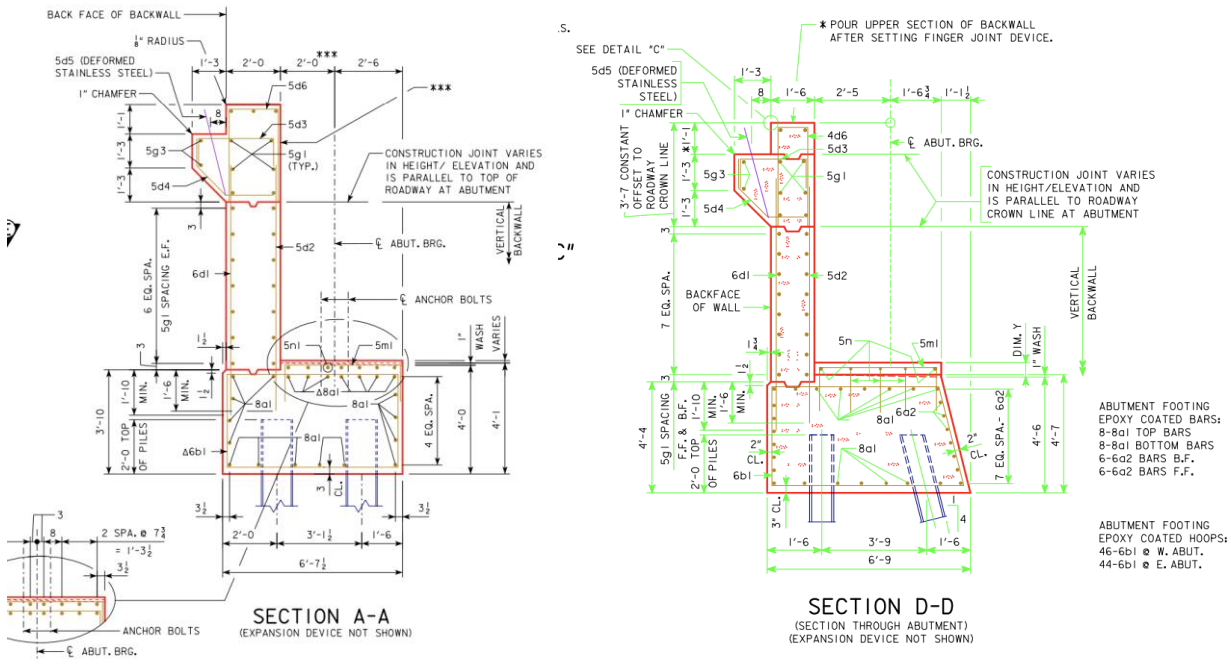

Figure 2.44. Bridges with stub abutments

To determine whether the expansion joint is a strip seal or finger joint, we looked at photographs from the most recent inspection report. Figure 2.45 shows a strip seal expansion joint on the left and a finger joint on the right. These are both examples of expansion joints in very good condition. Neither appears to cause a bump when a vehicle passes over the joint. There is no apparent cracking, abrasion, or spalling, and the joint material looks to be in good condition with no debris.

Strip Seal Finger Joint

Figure 2.45. Different types of joints in stub abutments

The approach type was extracted from the "Standard Road Plans" box. In the case of the strip seal bridge, the approach type was not provided in the plan sheets. Since it was not available, we recorded "Not in Plans" in the Approach Type column. For the finger joint bridge, as with many other stub abutment bridges, the approach type is BR-203, as seen in Figure 2.46. The Approach Type comment was "Double Reinforced 12 in. Approach."

105-4
10-18-11

STANDARD ROAD PLANS

The following Standard Road Plans apply to construction work on this project.

Number	Date	Title
BA-100	04-20-10	44" Concrete Median Barrier (Full Section)
BA-200	10-18-11	Steel Beam Guardrail Components
BA-201	10-20-15	Steel Beam Guardrail Barrier Transition Section
BA-202	10-20-15	Steel Beam Guardrail Bolted End Anchor
BA-205	10-18-11	Steel Beam Guardrail End Terminal
BA-250	10-20-15	Steel Beam Guardrail Installation at Concrete Barrier or Bridge End Post
BA-401	04-16-13	Temporary Barrier Rail (Precast Concrete)
BA-500	04-20-10	Temporary Crash Cushions Sand Barrel
BR-101	04-21-15	Bridge Approach Section (General Details)
BR-203	04-21-15	Double Reinforced 12" Approach
BR-212	04-21-15	Bridge Approach (Abutting HMA Pavement)

Figure 2.46. Bridge plan sheet—approach slab information

For the next step, we looked at more photographs of the bridges as well as the inspection sketches to see whether there are any issues with the bridges. As shown in Figure 2.47 for the

finger joint bridge, the barriers all look good, and there are no signs of settlement or cracking. The finger joint, as stated earlier, appears to be in good condition, and the inspection sheets provide no comments indicating otherwise. No photographs of the approach slab were provided, so we assumed that there is no transverse cracking or other issues with the approach.

Figure 2.47. Bridge inspection photographs

Figure 2.48 depicts how the spreadsheet columns were filled out to indicate that no issues were observed for the finger joint bridge.

Bump Presence	Bump Comments	Settlement	Settlement Comments	Approach Slab Crack Prese	Cracking Location	Paving Notch Issues	Paving Notch Comments	Joint Issues	Joint Notes	Additional Notes
Not likely		No		No		Not likely		No		

Figure 2.48. Table of bridge issues

For the strip seal bridge, we carried out the same process of looking at photographs and the inspection sheets in order to determine whether any issues are present on the bridge (Figure 2.49). Looking at the barriers, there is no clear sign of cracking or settlement. As stated earlier, the joint appears to be in good condition, and there are no signs of cracking at the abutment. The inspection sheets confirm this good condition. The approach slabs show no signs of transverse cracking. Note that this bridge is a good example of an instance when we could not get entirely clear information from the photographs. The barriers in this example are covered in snow, and there were no past reports available.

Bump Presence	Bump Comments	Settlement	Settlement Comments	Approach Slab Crack Prese	Cracking Location	Paving Notch Issues	Paving Notch Comments	Joint Issues	Joint Notes	Additional Notes
Not likely		No		No		Not likely		No		

Figure 2.49. Bridge issues table and bridge inspection photographs

The Excel sheet resulting from this investigation contained 344 bridges with their properties and issues, providing a source to study patterns in bridge issues.

2.9.2. Results and Discussion

The issues observed through this analysis were compiled to form three different charts (Figure 2.50). The three charts represent each of the three main abutment types in the analysis: Integral Abutment, Stub Abutment (Strip Seal), and Stub Abutment (Finger Joint). Each graph has four circular rings representing the four major issues observed: from the center out, the rings represent Bump Presence, Settlement, Paving Notch Issues, and Joint Issues. The charts provide a simple visual that can be used to easily understand the relationships between abutment type and the various issues observed.

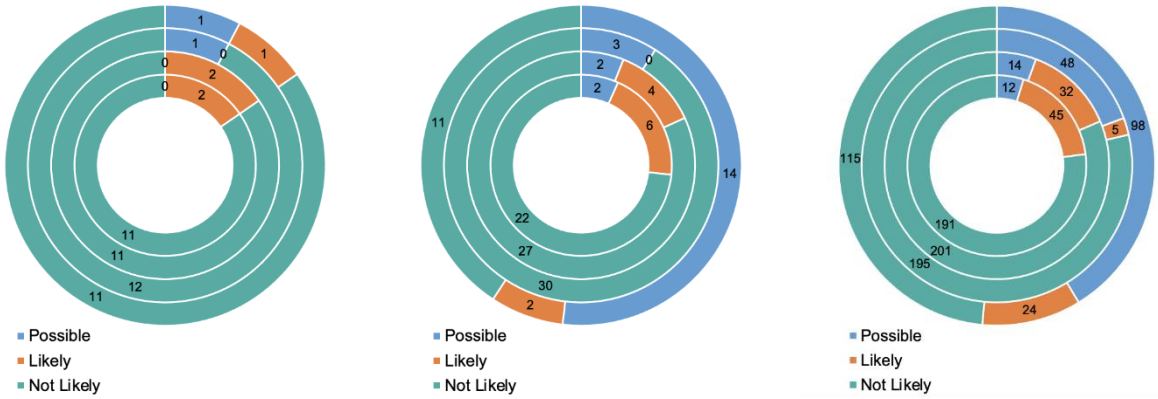

Stub Abutment (Finger Joint) Stub Abutment (Strip Seal) Integral Abutment

Figure 2.50. Bridge issues according to abutment type

The center ring, as stated, represents Bump Presence. All three of the abutment types appear to have similar results for this issue. Finger joint abutments appear to have an advantage over the integral and strip seal abutment types. One of the reasons for this was that many more integral and strip seal abutments had approach slab cracking than did finger joint abutments. This transverse cracking was often determined to be likely to cause a bump in the roadway. Also, many more integral and strip seal abutments had a “Likely” or “Possible” categorization in the Joint Issues column. Many of these joint issues that were observed could also create a bump. Finger joint abutments had very few noted issues with expansion joints in comparison to the other two abutment types, as seen in the outermost ring of the graphs.

The second ring from the center representing Settlement is pretty consistent across the three abutment types. We do not believe that abutment type plays a significant role in the amount of settlement observed. One ring out from there is the Paving Notch Issues ring. This clearly shows that integral abutments were much more likely to have paving notch issues. A very small percentage of the other two abutment types had observed paving notch issues.

The majority of the bridges can be described as prestressed concrete bridges with an integral abutment and an RK-20 approach type, as seen in Figure 2.51. As shown in previous figures, integral abutment bridges were found to have more issues in general than the other types of bridges. This may cause integral abutments to appear inferior, but some notes should be taken into consideration. During the analysis, it was noticed that finger joint and strip seal abutments have become more common in recent years. Many of the integral abutment bridges are older and more commonly show performance issues. The more recently constructed bridges may not show issues yet, but they may in the future. Also, with more integral abutment bridges constructed overall, this would lead to more mistakes during construction. Lastly, we noticed that prestressed concrete bridges usually use integral abutments, whereas continuous steel bridges use either finger joint or strip seal abutments. The larger number of issues seen with integral abutments may be related to the prestressed concrete bridges they are paired with rather than the abutment type itself.

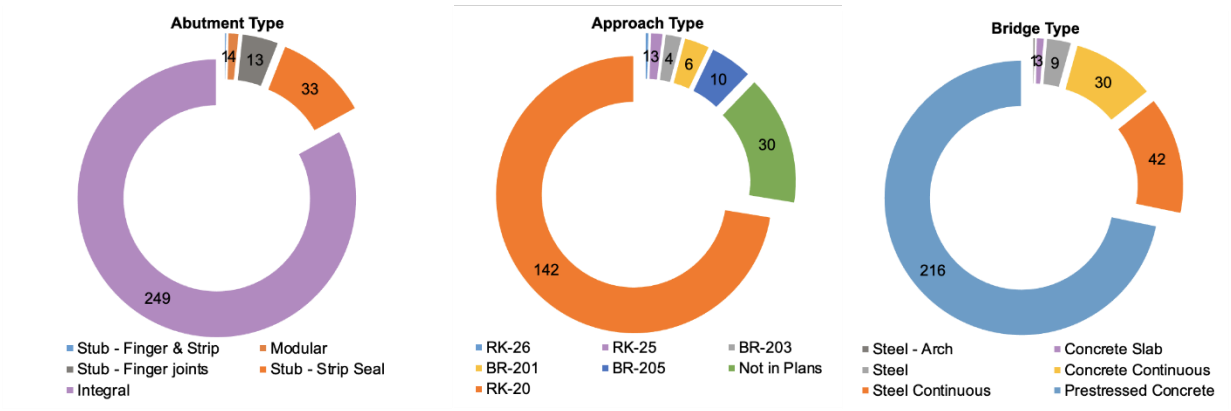

Figure 2.51. General properties of the investigated bridges

Table 2.2 provides the results of a thorough investigation of the number of specific issues that occur with another issue at the same time. For each state of the issue, the presence, possibility, and absence of the other issues are presented to show whether the issues are interrelated. The table indicates that bump presence does not show a good relationship with settlement. In 273 cases where bump presence is not likely, 253 cases did not show signs of settlement. However, in cases where bump presence is likely or possible, many cases did not show settlement, meaning that in some cases settlement could be the reason for bump presence, but in most cases other issues contribute to bump presence. In cases where settlement is not responsible for bump presence, approach slab cracking and joint issues could be the reasons for bump presence. Approach slab cracking shows a clearer relationship with bump presence, in that the absence of a bump is associated with no approach slab cracks, while many cases featuring cracks are likely to show signs of a bump. When cracking does not lead to bump presence, joint issues show a greater number of likely and possible instances associated with bump presence than settlement. On the other hand, paving notch issues show a weak relationship with bump presence, suggesting that paving notch issues are less likely to cause a bump. Also, there are many examples of joint issues that are not associated with bump presence, which suggests that joint issues often might not cause a bump. Therefore, crack propagation on the approach slab is one of the main reasons for bump presence, followed by settlement and joint issues in some cases. However, paving notch issues are not usually reflected in bump presence.

Table 2.2. Relationships among different bridge issues

	Issue	**Bump Presence**			**Settlement**				**Approach Slab Crack Presence**			**Paving Notch Issues**			**Joint Issues**		
	Status	*Not likely*	*Possible*	*Likely*	*No*	*Possible*	*Yes*	*Likely*	*Yes*	*No*	*Possible*	*Possible*	*Not likely*	*Likely*	*No*	*Possible*	*Likely*
	Total No. of Bridges	273	15	55	288	16	1	38	54	287	2	55	283	5	191	124	28
Bump Presence	*Not likely*				253	10	0	10	21	251	1	41	230	2	163	95	15
	Possible				8	3	0	4	4	11	0	3	10	1	5	8	3
	Likely				27	3	1	24	29	25	1	10	43	2	22	24	9
Settlement	*No*								36	251	1	44	239	5	166	104	18
	Possible								3	13	0	3	13	0	8	7	1
	Yes								0	1	0	0	1	0	0	1	0
	Likely								17	22	1	8	30	0	18	12	8
Approach Slab Crack Presence	*Yes*											11	42	1	27	20	7
	No											43	240	4	165	102	20
	Possible											1	1	0	0	2	0
Paving Notch Issues	*Possible*														21	29	5
	Not likely														170	95	20
	Likely														1	2	2

The table also shows the relationship between different phases of settlement and cracking presence, paving notch issues, and joint issues. According to the table, settlement could sometimes be associated with approach slab cracking, but in many cases where settlement was likely, no crack development was observed in the slab. Also, 36 out of the 54 reported instances of crack presence occurred when no settlement was detected. Thus, settlement might not be the primary reason for approach slab cracking. Twenty percent of all investigated stub abutment (strip seal) bridges showed cracks on their approach slabs, while this value was 15% and 11% for integral abutment bridges and stub abutment (finger joint) bridges, respectively. Settlement and paving notch issues also do not seem to be directly related, as likely settlement instances do not coincide with likely paving notch issues. Moreover, all of the likely and most of the possible instances of paving notch issues are associated with cases in which no settlement was observed. Regarding joint issues, the table clearly shows that settlement could cause joint issues in some cases, while other parameters contributing to joint issues could be considerable when there is no settlement. Paving notch issues were more common in integral abutment bridges, with 20% of all integral abutment bridges showing this issue, while only 6% of stub abutment bridges showed deficiencies related to the paving notch. It is also worth noting that integral abutments and stub abutments with finger joints were less likely to show paving notch issues and approach slab cracking at the same time, while stub abutments with strip seals showed these two issues together in most cases.

Approach slab crack presence shows a minimal relationship with paving notch issues, with 47 out of 60 possible and likely instances of paving notch issues occurring when no cracking was observed on the approach slab. Thus, paving notch issues played only a slight role in crack development in the approach slab. A comparison of crack presence versus joint issues also shows that cracking was more likely to be seen when joint issues were observed than when no joint issues were observed and that joint issues were less likely when there was no cracking on the approach slab. Moreover, while the instances of possible paving notch issues were associated with an increased possibility of joint issues, most of the likely joint issues occurred when paving notch issues were not likely to have occurred. Thus, paving notch issues might not contribute directly to joint issues. The table shows that a high number of both integral abutment bridges and stub abutment (strip seal) bridges showed joint issues (47%). However, only 11% of the stub abutment (finger joint) bridges showed joint issues.

Table 2.3 shows the common issues in bridges with different abutment types. According to the table, expansion joints that measured greater than 2 in. were common in integral abutment bridges, featuring in 36% of these bridges. Also, poor sealing, cracking at the abutments, and differential settlement at the barriers were other common damages observed in integral abutment bridges. Stub abutments (finger joints) performed better than the other bridge abutment types in this study, as they showed a lower number of issues compared to the other two abutment types. As such, differential settlement at the barriers was seen in only two of these bridges, while some cracking and joint issues were detected in only one of these bridges. The predominant types of damage in bridges with stub abutments (strip seals) were wide joint opening and presence of debris.

Table 2.3. Common issues in bridges with different abutment types

	Integral Abutment	Stub Abutment	
	277	*Finger Joint 17*	*Strip Seal 45*
Cracking at abutment	54	1	3
Poor Seal	46	0	3
Opening >2"	101	1	15
Debris presence	19	1	13
Clear settlement cracks	3	0	0
Cracking/diff. settlement at barrier	38	2	6
Cracking/diff. settlement at approach slab and abutment	5	0	0
Transverse cracking	14	1	1
Spalling	14	0	3
Abrasion at joint	4	0	0
Cracking at near and far expansion joint	3	0	1

In Table 2.4, the three abutment types are grouped according to bridge category (concrete slab, steel girders, or prestressed concrete girders), and the instances of various types of reported damage are shown for each bridge category and abutment type.

Table 2.4. Common issues in bridges with different slab types

	Concrete Slab	Steel Girders			Prestressed Concrete Girders		
	Integral 40	*Integral 30*	*Finger Joint 9*	*Strip Seal 19*	*Integral 207*	*Finger Joint 6*	*Strip Seal 25*
Cracking at abutment	2	7	0	0	44	1	3
Poor Seal	1	4	0	2	41	0	1
Opening >2"	10	12	1	4	79	0	11
Debris presence	0	0	0	4	19	0	9
Clear settlement cracks	0	0	0	0	3	0	0
Cracking/diff. settlement at barrier	2	2	0	2	34	2	4
Cracking/diff. settlement at approach slab and abutment	0	0	0	0	5	0	0
Transverse cracking	1	6	0	1	7	1	0
Spalling	0	2	0	1	12	0	2
Abrasion at joint	1	0	0	0	3	0	0
Cracking at near and far expansion joint	0	0	0	0	3	0	1

All of the bridges with a concrete slab had integral abutments. Wide joint opening was the main issue in these bridges, with 25% of all of the investigated abutments showing wide joint opening issues.

Regarding bridges with steel girders, 40% of all bridges with steel girders and integral abutments showed wide joint opening issues, followed by cracking at the abutments and transverse cracking as the other main issues. Steel girder bridges with stub abutments (finger joints) showed the best performance compared to the other abutment types, with only 1 out of 9 of these bridges exhibiting wide joint opening. Joint issues were also the most prevalent problem in steel girder bridges with stub abutments (strip seals), while differential settlement at the barriers was observed in some cases.

Joint issues, especially wide joint opening, was the most frequently reported issue in bridges with prestressed concrete girders and integral abutments, with 38% of these bridges showing this issue. Poor sealing, cracking at the abutments, and differential settlement were other common issues observed in these bridges. Of the 44 bridges with cracking at the abutment, 30 bridges showed joint issues too. Moreover, 19 out of the 34 bridges with settlement and cracking at the barriers showed joint issues, while settlement was not usually associated with cracking at the abutment. Bridges with prestressed girders and stub abutments (finger joints) showed more issues, particularly with settlement and cracking, in comparison with their steel girder counterparts. Of the 6 bridges with prestressed girders and stub abutments (finger joints), 3 showed likely settlement or possible paving notch issues. However, the prestressed bridges in this comparison were slightly older than the steel girder bridges and had higher AADT values, which could be contributing factors to the better performance of the steel girder bridges with stub abutments (finger joints).

In the case of bridges with steel girders and stub abutments (strip seals), wide joint opening and presence of debris were very common, as more than 40% of the bridges showed such joint issues. Differential settlement and crack development were also observed in some cases.

CHAPTER 3. BRIDGE VISUAL INSPECTIONS

Inspection of both semi-integral abutment bridges and bridges with tied approach slabs was used to examine details in practice to see possible deficiencies in real-world use. Nine bridges were chosen for inspection, with two locations having identical structures for a split roadway, resulting in a total of nine structures inspected on September 21 and 24, 2019. Bridges were chosen based on many factors, including length, width, skew, abutment type, use of a tied approach, and availability for inspection. Since inspections were done without the use of extensive traffic control and did not involve closing traffic lanes, certain bridges like those on I-35 at the I-80 interchange were eliminated from consideration. Otherwise, bridges with the most extreme lengths were chosen. The following bridges were inspected:

- 1215 Polk
- 310 Jasper (Northbound and Southbound)
- 208 Bremer (Northbound and Southbound)
- 108 Blackhawk
- 213 Cass
- 111 Pottawattamie
- 113 Cass

The plan for each bridge was to examine the entire bridge end, including sleeper slabs (if present), approach slabs, deck joints, embankments, abutment faces, and bearings (if possible). The focus included looking for any signs of poor performance, including cracking in any visible concrete surfaces, settlement of any structural members, erosion or voids in the soil, expansion joint damage, and impediments to drainage.

3.1. 1215 Polk

1215 Polk is a 330 ft long semi-integral abutment bridge located in Urbandale, Iowa, on 100th street at I-35/I-80. It has two identical spans and unique approach slabs at both ends due to its proximity to stoplight intersections. The bridge is 101 ft wide and accommodates sidewalks along its length. The bridge also has a small skew angle of 2.3 degrees.

The inspection began at the north end at the approach slab to the sleeper slab CF-3 joint. Joint filler appeared to be missing along part of the length, with debris filling the space. The north approach slab appeared to be in good condition, with no visible settlement; however, a large amount of joint sealant was missing in the approach to the abutment E joint. The embankment appeared intact, with no serious erosion aside from areas with no plant cover a distance away from the bridge due to construction for an added interchange.

The south approach-slab-to-sleeper-slab joint also had joint sealant missing and some expanding onto the roadway surface. The approach slab was in good condition along the south abutment-to-approach-slab joint except for excess sealant expanding out of the joint (Figure 3.1, left). This sealant has the possibility of being caught by a snowplow or other vehicle and being torn from

the joint. The south embankment appeared to be in adequate condition apart from a large void at the southwest corner of the bridge at the end of the wingwall. The void measured 22 in. deep and was estimated to be about 2 ft square in size. The embankment was not landscaped due to the interchange project and earthwork under construction, so it was unclear if that was a reason for the area not being filled with soil or if it was created by erosion.

Figure 3.1. South bridge-deck-to-approach-slab joint with excess sealant (left) and water and abutment staining at the outermost girder (right)

Both the north and south abutments had a large amount of rust-colored staining present below the bearings (Figure 3.2). At the corners, some water was still visible on the concrete surface (Figure 3.1, right). The source of the water was not readily apparent, but it was assumed it came through the abutment. Another possible source for the abutment staining could be that it happened during bridge construction if beams were placed and rain occurred before the bridge deck was placed to cover the beams. In that case, the water present at the corners could have been left over from a rain event before the time of inspection.

Figure 3.2. North abutment face

3.2. 111 Pottawattamie

111 Pottawattamie is located in Pottawattamie County, Iowa, on US 6 over Keg Creek. The 204.5 ft long and 44 ft wide bridge with a 0 degree skew has semi-integral abutments. A CF-2 joint lies between the 20 ft precast approach slab and abutment, with a precast sleeper slab supporting the other end of the approach.

Beginning at the sleeper slab, the joints were in adequate condition. The approach slabs and the entire bridge deck were covered in a polymer overlay consistent with available plans. The west approach slab was badly cracked across its entire width (Figure 3.3, left). The joints at the abutments on both ends of the bridge were in poor condition, with large amounts of sealant missing and debris filling the voids (Figure 3.3, right). A 6 in. deep void was discovered at the abutment-to-approach-slab joint where it met the barrier in the southwest corner (Figure 3.4). Bridge surface water likely drains through the gap in the barrier instead of following the curb. The abutment faces did not have any staining, indicating that there does not appear to be any water leaking through the abutment. The embankment condition was good, with no obvious erosion except near the bridge piers.

Figure 3.3. Transverse approach slab crack (left) and bridge-deck-to-approach-slab joint (right)

Figure 3.4. Void at the intersection of bridge-deck-to-approach-slab joint and barrier

3.3. 113 Cass

113 Cass is located west of Massena, Iowa, on IA 92 over a small creek. The semi-integral abutment bridge was constructed in 2013 and is 120 ft long and 44 ft wide with a skew of 0 degrees.

The pavement approaching the bridge from either direction and along the shoulder of the concrete panels was in poor condition and showed obvious settlement relative to the concrete. The joints at the end of the first approach slab section were in good condition, since there is no movement accommodated at that location. The east approach slab had a transverse crack near its eastern end. The abutment-to-approach-slab joints were in adequate or poor condition, with sealant missing and debris filling some of the joints. The curb joints between the approach slab and wingwall were in extremely poor condition, with sealant missing and large voids visible at each of the four corners of the bridge (Figure 3.5, left). The north wingwall at the east end of the bridge appeared to be moving away from the approach slab based on the gap present at the joint and misalignment of the barriers (Figure 3.5, right). The curb detail showing the E joint can be seen in Figure 3.6. The embankments were in good condition, and there was no staining on the abutment face. The bearings appeared to be working as intended.

Figure 3.5. Approach-slab-to-wingwall joint showing separation (left) and misaligned wingwall and barrier (right)

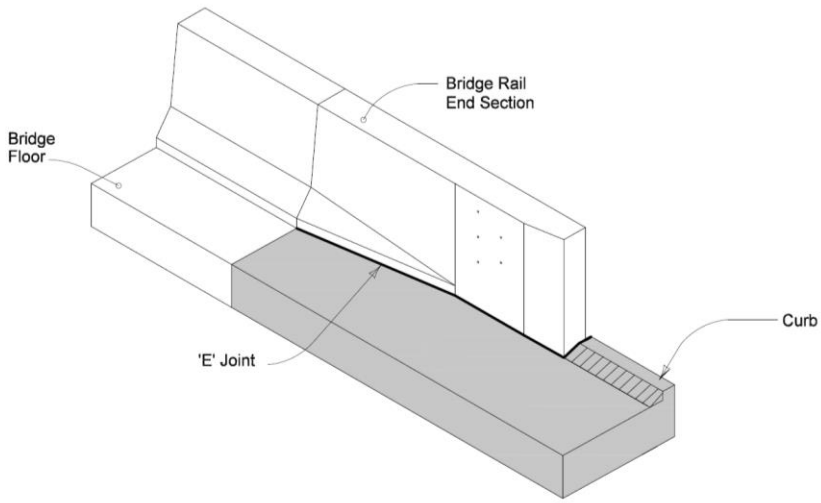

Iowa DOT

Figure 3.6. Iowa DOT curb E joint detail

3.4. 213 Cass

213 Cass is in Cass County, Iowa, on M56 over I-80. The bridge is 223.75 ft long and 30 ft wide with a skew of 7.75 degrees. Past rehabilitation work included conversion to a semi-integral abutment and a 20 ft tied approach slab with a 1/4 in. preformed joint at the abutment and a CF-2 joint at the sleeper slab.

The sleeper-slab-to-approach-slab joints at both ends were in adequate condition, with some sealant missing and minor spalling. The approach slabs did not have any obvious cracking or settlement. The approach-slab-to-abutment joints were in good condition, with minor spalling at the north joint. The embankments and curbs were working as intended. Staining was visible on both the north and south abutment faces at each bearing location, but this appeared to be left over from before the rehabilitation and conversion to semi-integral abutments (Figure 3.7).

Figure 3.7. Abutment face showing the new backwall on top of the old footing

3.5. 310 Jasper (Northbound and Southbound)

310 Jasper is located in Newton, Iowa, on US 6 over I-80. There are two identical northbound and southbound bridges, and both were included as part of the inspection. The bridges are 232 ft long and 32 ft wide with a skew of 6.25 degrees. A 2010 project saw the conversion to semi-integral abutments with tied approach slabs and 1/4 in. joints at the abutments. The approach uses a 20 ft doubly reinforced slab connected to a 4 ft transition slab by an EF joint.

3.5.1. Northbound

The northbound bridge was in generally good condition. Beginning at the ends, there was some joint sealant missing, and the joint between the transition slab and pavement was open on the north end. The approach-slab-to-transition-slab joints were all in good condition. The approach slabs had no major cracking or settlement and appeared to be performing well. At the south end, there was settlement of approximately 1 in. in the pavement meeting the concrete slabs in the shoulder. The drains exiting in the north embankment appeared shorter than they should be for proper drainage, as they are partially obscured by the embankment. The abutment was in good condition, with no visible staining. Minor cracking and spalling of the concrete were present at the wingwalls and the wingwall-to-approach-slab joints at the beginning of the curbs (Figure 3.8).

Figure 3.8. Concrete cracking at the end of the wingwall (left) and additional cracking at the end of the wingwall (right)

3.5.2. Southbound

The southbound bridge's condition was, unsurprisingly, very similar to that of the first. The joints between the transition slab and pavement were in very poor condition and open with sealant missing. The abutment-to-approach-slab joints appeared to be in good condition, apart from debris accumulating at the sides where the curb begins. Once again, the wingwalls showed some minor, seemingly random vertical cracking and minor spalling. The drains on the north end

were very close to becoming blocked, with debris piling up at the outlet and the northwest drain completely closed (Figure 3.9). In areas with pavement shoulders, there was visible settlement relative to the concrete panels.

Figure 3.9. Blocked embankment drainage (left) and additional blocked embankment drainage (right)

3.6. 208 Bremer (Northbound and Southbound)

208 Bremer is located in Denver, Iowa, on US 63 over 260th Street. There are two identical northbound and southbound bridges constructed in 1994. Both have three spans and are 161 ft long and 40 ft wide with a skew of 2.25 degrees. The bridge approaches have been redone, with plans dated 2008 to use 20 ft precast concrete panels. Slightly inclined rebar ties were embedded 1 ft into the abutments, and 4 ft transition slabs were used between the approach slabs and the pavement. Quarter-inch joints exist at the abutments, and EF joints exist between the abutment and transition slab.

3.6.1. Northbound

The EF joints between the approach slab and transition slab appeared to be in adequate condition, except for vegetation growing in the joints outside the traffic lanes. The approach slabs were also performing well except for some spalling on the north end (Figure 3.10).

Figure 3.10. Deck-to-approach-slab joint showing severe spalling (left) and additional deck-to-approach-slab joint showing severe spalling (right)

The embankments used concrete slope protection under the bridge. On the north end, there was a large gap between the inclined portion and flat section at the top of the embankment as if the entire concrete slope was sliding (Figure 3.11, left). The slope portion was otherwise intact. The south end was performing even worse, with a larger gap between the concrete slabs, broken sections around the pier columns, and vertical settlement based on markings on the abutment. Repair work had attempted to fill the joints, but the material was cracked into pieces and joints have continued to open.

Figure 3.11. Typical embankment condition (left) and embankment condition at the abutment (right)

At the west corner of the south abutment, there was a large void at the corner of the abutment that measured 23 in. deep (Figure 3.12, Figure 3.13). The end of the tape measure used to assess the void was able to hook onto the underside of the concrete abutment.

Figure 3.12. Horizontal void created by the embankment pulling away from the abutment

Figure 3.13. Measuring tape showing the vertical depth of the void

3.6.2. Southbound

The condition of the southbound bridge was very similar to that of the northbound bridge, including reasonable joint condition with some spalling of the approach slab at the abutment joint. The embankments and slope protection were just as poor as on the northbound bridge, with another large void located at the west side of the south abutment. The concrete slope protection was broken, and there were large voids around the pier column bases (Figure 3.11, right). It was surmised that the curb and joint between the approach slab and barrier must not be effective in draining surface water for large voids to appear. There were also large amounts of settlement in the embankment that could have been caused by water infiltration.

3.7. 108 Blackhawk

108 Blackhawk is a single-span, 130 ft long, 40 ft wide bridge with a skew angle of 0 degrees. It is located west of Cedar Falls, Iowa, on IA 57 over a small stream. The bridge uses a 1/4 in. preformed joint at the abutment, a 20 ft approach slab, and a CF-3 joint at the sleeper slab. The joints were in good condition, with no large amounts of sealant missing or other common issues. The embankments were in good condition. The stream water levels were very high at the time of inspection, but the embankment did not appear to be experiencing erosion at the abutment face.

3.8. Joint Condition

The joints at both ends of each bridge were measured, and Table 3.1 shows the recorded values, with air temperatures ranging from 60°F to 80°F. Joint widths at the time of construction were taken from the bridge plans for comparison. Joint 1 is at the deck-to-approach-slab joint, and Joint 2 is the next joint moving away from the bridge either between the approach slab and sleeper slab or between the approach slab and transition slab.

Table 3.1. Joint measurements and design plan values

Bridge Name	Joint Location			Joint 1		Joint 2	
				Design (in.)	Measured (in.)	Design (in.)	Measured (in.)
208 Bremer	Tied Approach	NB	North	0.25	1.5	3.5	2.5
			South	0.25	1.625	3.5	2.5
		SB	North	0.25	1	3.5	2.5
			South	0.25	1	3.5	1.75
108 Blackhawk	Tied Approach		East	0.25	1	3	2.875
			West	0.25	0.875	3	2.875
310 Jasper	Tied Approach	NB	North	0.25	0.875	3.5	2.75
			South	0.25	0.625	3.5	2.5
		SB	North	0.25	0.75	3.5	1.875
			South	0.25	0.625	3.5	2.125
213 Cass	Tied Approach		North	0.25	0.375	2.5	1.625
			South	0.25	0.5	2.5	2
111 Pottawattamie	Semi-Integral		East	2	1.5	N/A	N/A
			West	2	1.5	N/A	N/A
113 Cass	Semi-Integral		East	No Plans	1.875	No Plans	0.25
			West	No Plans	1.75	No Plans	0.375
1215 Polk	Semi-Integral		North	1	1.625	3	2
			South	1	2	3	1.5

The tied approach joint values show that the tied connections are not performing well. Over time, a design value of 1/4 in. has become, in some cases, up to a 1 5/8 in. opening. The decrease in joint width at the opposite end of the slabs clearly shows the movement of the approach slabs away from the deck. Ideally there would be no movement at the tied approach, and the approach slab would move with the abutment and deck, allowing all movement to occur only at the sleeper or transition slab joint. The tied connection details show, for the most part, vertical bars that, after an initially good outlook in previous studies (Greimann et al. 2008), have performed poorly in the long term. The semi-integral abutment joints appeared to function as expected. Without any rebar to tie the approach slab to the bridge, the approach slabs would be pushed away from the bridge during expansion due to increasing temperatures. Then, as temperatures decrease, the bridge would contract, and without a tied connection to pull the slab with it, the joint would widen.

CHAPTER 4. BRIDGE INSTRUMENTATION AND DATA

The instrumentation of four Iowa bridges was completed to further understand the behavior of integral and semi-integral abutment bridges in the real world. Multiple different types of sensors were used to obtain different measurements for each bridge. Strain gauges, earth pressure cells, crackmeters, and displacement meters were all used to gain important information over time.

4.1. Sensor Descriptions

All measurements were taken by Geokon vibrating wire (VW) gauges intended for long-term use. Since the monitoring period for each of the bridges was at least one year, VW gauges were ideal for periodic data recording since continuous data collection was not necessary.

The VW gauges are very resilient and must withstand the installation and construction process along with exposure to the elements. The VW technology uses a steel wire located in each gauge tensioned at its two ends. When a measurement is taken, the wire is plucked and vibrates at a certain frequency depending on the tension. The vibration is measured by an electromagnetic coil and can be converted to the applicable measurement of strain, pressure, or displacement. Each sensor contains an internal thermistor in order to measure the temperature inside the concrete if it is embedded or external temperatures if it is attached to the exterior of the bridge.

The wires for each sensor were run to a central location at each end of the bridge to either a multiplexer or datalogger. An additional wire was run the length of the bridge between the multiplexer location and the datalogger and attached to the exterior of the barrier wall.

4.1.1. Earth Pressure Cells

The Geokon Model 4810 “Fat Back” Pressure Cell was chosen for use since it is designed to measure earth pressures on the surface of concrete structures. Each cell consists of two circular metal plates with a fluid trapped between them. As earth pressure on the exterior increases, so does the interior fluid pressure. The thicker back plate is designed to minimize any point loading effects. Pressure cells with a range of 700 KPa were chosen for use on Jasper County 118 based on an examination of previous research for earth pressures recorded on similar bridges. The cells provide a resolution of 0.175 KPa with an accuracy of 7 KPa.

4.1.2. Strain Gauges

The Geokon Model 4200 Strain Gauge was used for its intended purpose of being embedded inside concrete. The standard version was deemed satisfactory, since extremely large strains or extremely high temperatures were not expected. The gauges are designed for embedment and long-term stability, a key factor when monitoring periods are expected to exceed one year. The Model 4200 device provides a resolution of 1.0 $\mu\varepsilon$ and an accuracy of 15 $\mu\varepsilon$.

4.1.3. Crackmeters

The Geokon Model 4420 Crackmeter is designed for measuring movement across cracks or joints, making it ideal for bridge applications. The crackmeter has ball joints at either end and accommodates threaded concrete anchors. By attaching the crackmeter across a joint, the relative displacement between two objects can be measured.

The ranges of the crackmeters used for Jasper County 118 and Story County 118 were determined by calculating the theoretical free expansion of the bridges using Table 5.8.3.1.2 in the Iowa DOT *LRFD Bridge Design Manual*:

$$\Delta_T = \alpha L(T_{MaxDesign} - T_{MinDesign})$$

where

Δ_T = design thermal movement range
α = coefficient of thermal expansion
L = expansion length
$T_{MaxDesign}$ = maximum design temperature
$T_{MinDesign}$ = minimum design temperature

For example, the movement range of Story County 118 is computed as 30.5 mm for the total length, indicating that the 50 mm range of the crackmeter is capable of accommodating errors in placing the crackmeter at the correct extension length based on the expected movement after installation. The 50 mm range provides a resolution of 0.0125 mm with an accuracy of 0.05 mm.

$$(6E-6)[(375' + 40')/2](100°F) = 1.49 \text{ in.} = 37.9 \text{ mm}$$

4.1.4. Displacement Transducers

The Geokon 4427 Long Range Displacement Transducer is intended for measuring large displacements like those seen at an integral bridge abutment. The sensors consist of a spring drive motor connected to a lead screw. The rotation of the lead screw is converted to a linear displacement. The spring drive motor maintains a constant tension on the cable exiting the protective case.

In the case of Jasper County 118, four Geokon 4427s were reused from past ISU projects, and the calibration sheets were available from documentation kept by the ISU Structural Engineering Research Laboratory. The Geokon 4427 has a range of 1 m with a resolution of 0.25 mm and an accuracy of 10 mm.

4.2. Jasper County 118

Jasper County 118 is a bridge located near Kellogg, Iowa, and was chosen for monitoring due to its 45 degree skew, which matches the current maximum allowed by the Iowa DOT for semi-integral abutments. The bridge is 184 ft long by 28 ft wide and carries two lanes of traffic on US 6 over a railroad using three spans. The construction work included a deck overlay and conversion to semi-integral abutments with complete reconstruction of the bridge approaches. The bearings remained unchanged, so the west end of the bridge remains stationary while the east end moves to accommodate the thermal movements (Figure 4.1). The approach slab on the west end is tied to the abutment (Figure 4.2), while the east end is not tied. It would follow that neither approach slab should experience any movement due to thermal expansion of the deck.

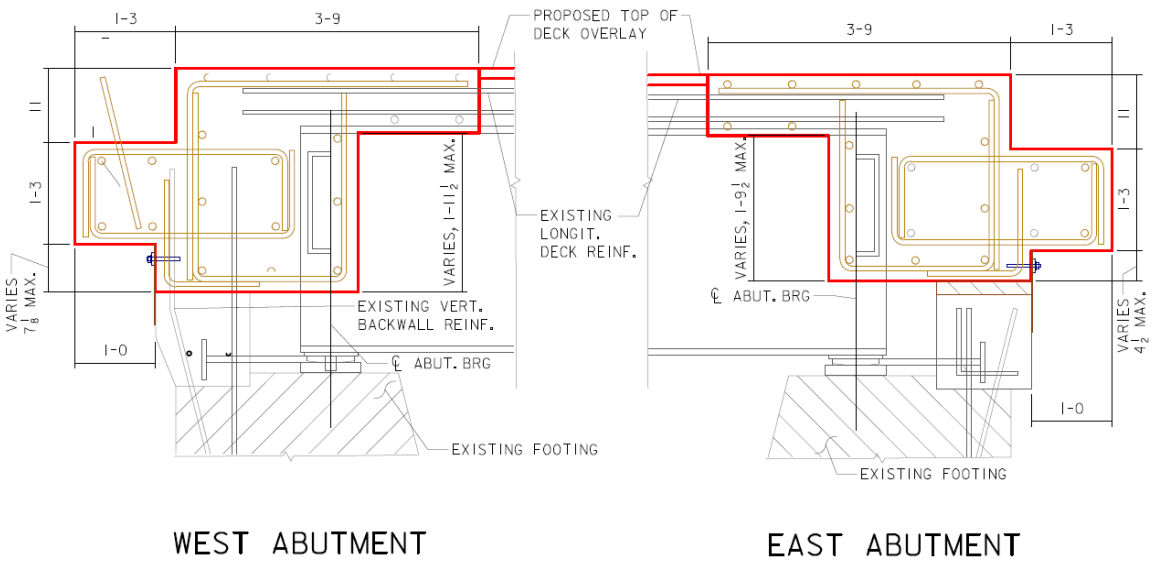

Iowa DOT

Figure 4.1. Jasper County 118—east and west abutments

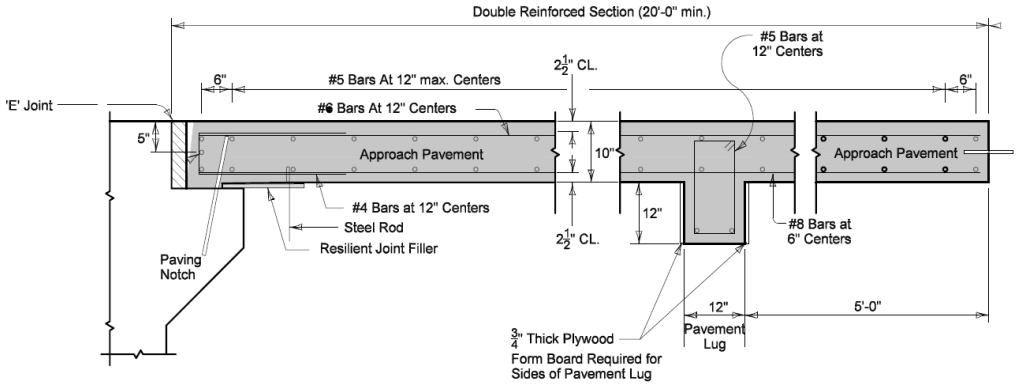

Iowa DOT

Figure 4.2. Jasper County 118—approach slab dimensions and section view

Both ends of the bridge were monitored to determine whether it behaves as intended, as a precaution for the possibility of corroded bearings or other performance issues. The instrumentation plan seen in Figure 4.3 shows the locations of the sensors, which are identical for each end of the bridge. Displacement meters were placed at the acute bridge corners in orthogonal directions to measure not only longitudinal movement but also transverse movement. The large skew angle is likely to cause transverse movement in opposite directions at either end, resulting in a slight rotation of the entire bridge. Crackmeters measured the relative longitudinal movement between the bridge deck and approach slab at each corner. Earth pressure sensors located on the abutment backwall were placed at each corner to measure active and passive earth pressures. It was anticipated that the pressure would differ between the gauges at the acute and obtuse corners of the bridge. Strain gauges were placed in the approach slab to measure any strains and forces that may occur. Should the bridge and bearings act as intended, strains in the approach slabs should be insignificant.

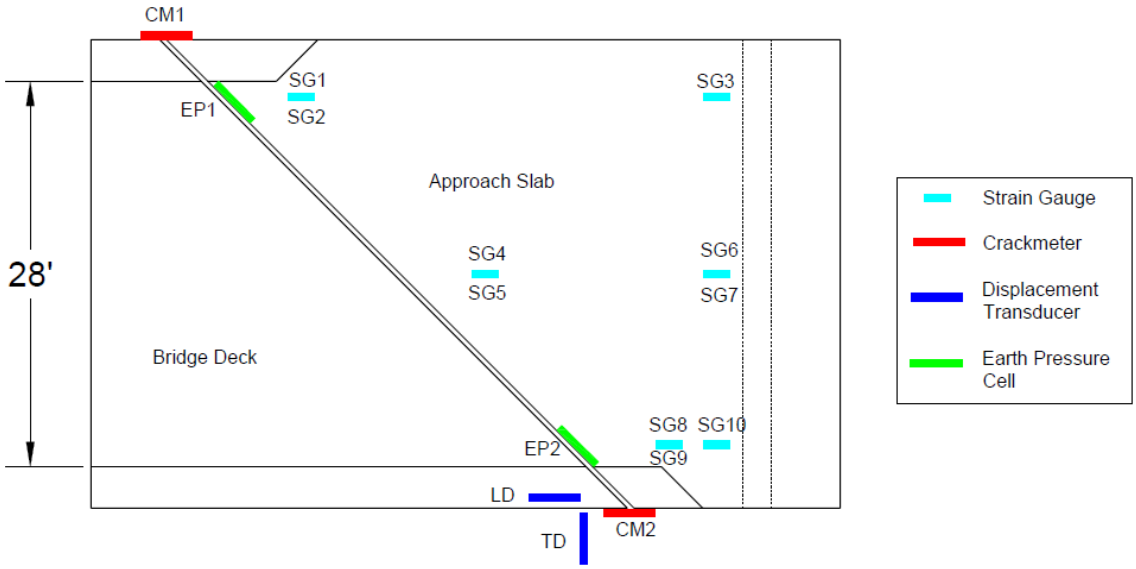

Figure 4.3. Jasper County 118—instrumentation plan (typical of east and west ends)

4.2.1. Jasper County 118 Earth Pressure Sensor Installation Process

Sensor installation at Jasper County 118 began with placement of earth pressure sensors at the west abutment out of necessity due to construction sequencing. The contractor completed the bridge deck replacement first before constructing and pouring the semi-integral abutments. The abutment backwall was left exposed for earth pressure sensor installation before backfilling (Figure 4.4). Initially, the sensors were intended to be placed on the same longitudinal axis as the outer bridge girders; however, due to the extreme 45 degree skew of the bridge and working space limitations, they were placed closer to the center, with the outside edge of the sensor on the girder axis. The decision was made to shift all other sensors to the same axis for the sake of consistency. The earth pressure sensors were intended to illustrate how earth pressure along the backwall can vary due to skew.

Figure 4.4. Jasper County 118—EP1-W earth pressure sensor after installation

Each sensor had been prepared by attaching an adhesive neoprene layer to the face to help distribute load for granular particles. A thick layer of mastic adhesive was applied to the back of each sensor, and the sensor was pressed against the concrete surface, causing mastic to flow out from behind. While the sensor was held in place, holes were drilled using a hammer drill for each of the four tabs for attachment. Concrete screws attached the sensor to the concrete, and the excess mastic was removed from the edges. The wires were run around the abutment and kept tight to the concrete surface using small tabs and additional concrete screws. The final step included taking initial digit and temperature readings using a Geokon GK-404 readout unit on position B. The contractor was advised to use smaller 3/8 in. aggregate from a pile located on site to fill against the sensors.

4.2.2. Jasper County 118 Strain Gauge Installation Process

Shortly after backfilling the area, the contractor prepared the first half of the west approach slab by completing formwork and tying the rebar. Ten strain gauges were placed, including three along the same axis as the earth pressure sensors at the obtuse and acute corners and four as close to the centerline of the roadway as possible. Strain gauges were placed according to the plan in Figure 4.3, with gauges 1, 3, 4, and 6 on the top layer of bars and gauges 2, 5, and 7 on the lower layer of bars. Small 1/2 in. rubber spacers were used to position the gauges with sufficient clearance to the bars with zip ties to hold them in place (Figure 4.5). The strain gauges were checked previously for proper function and set to the middle of their range of measurement per recommendation from the Geokon manual. Wires were zip-tied periodically along their lengths to keep them tight to the bars. After the contractor poured the first half of the approach slab and tied the rebar for the second, the last three strain gauges were installed in the same manner as the first along the axis of the acute bridge corner earth pressure sensor.

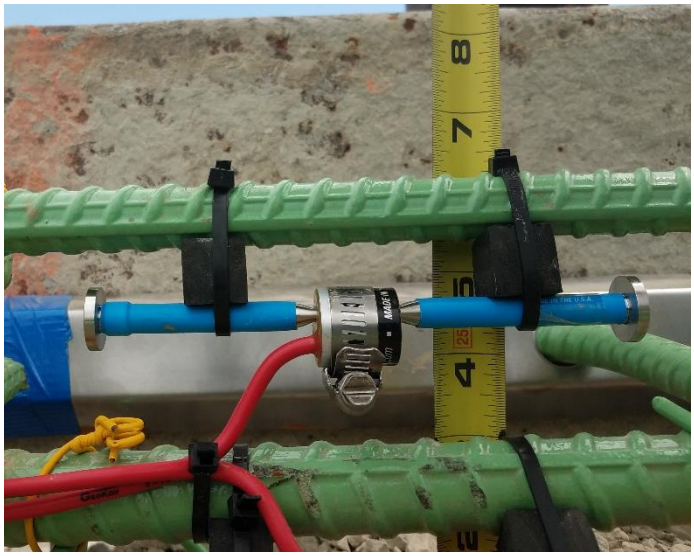

Figure 4.5. Jasper County 118—typical strain gauge installation

All wiring exited the slab on the north side and was bundled together for connection to a multiplexer. The earth pressure sensors and strain gauges on the east end of the bridge were installed one week later in the same manner as the west end.

4.2.3. Jasper County 118 Crackmeter Installation Process

Crackmeters were installed at the approach slab surface with the approval of the Iowa DOT, and protective covers were fabricated using a steel angle to prevent damage by snowplows (Figure 4.6). Since the crackmeters were placed under the barrier, they would not be hit by traffic or snowplows. Crackmeters were installed per the Geokon manual and set at 25% of maximum extension. Since installation occurred in the summer, it was anticipated that the bridge would experience almost entirely contraction, thus opening the joints between the abutment and approach slabs.

Figure 4.6. Jasper County 118—crackmeter without protective cover (left) and crackmeter with protective cover installed (right)

The crackmeter located in the northeast corner of the bridge was placed in a different location than the rest due to the different construction process used at that corner of the bridge. A large crash barrier prevented the crackmeter from attaching to the approach slab, so it was located across the joint between the bridge and stationary wingwall. Since the approach slab is not designed to move with the bridge, the crackmeter should theoretically measure the same joint movement. Since the railings were being installed by the contractor on the same day as the crackmeters, the northwest crackmeter cover was impacted by a large wooden post, causing a shear failure of the concrete screws and allowing the metal cover to impact the sensor and shear the anchor. The crackmeter was removed and sent to Geokon for a calibration check before being reinstalled at a later date.

4.2.4. Jasper County 118 Displacement Transducer Installation Process

Measuring the abutment displacement of integral or semi-integral abutment bridges is difficult due to the requirement of a stationary reference post somewhat near the abutment itself. Both settlement of the embankment and movement of the abutment itself can affect the reference post and skew the results. A discussion between the principal investigators of the project and the manager of the ISU Structural Engineering Research Laboratory yielded no definitive preferred method. Using a reference post can be unreliable, but using surveying equipment only provides periodic results, unlike displacement sensors that can provide hourly or daily results. Data taken by total station may also miss seasonal extremes of movement since it is impossible to predict the coldest or warmest days of the year.

Since Jasper County 118 was only being partially reconstructed with no effect on the substructure, it was determined that a reference post should yield satisfactory results. During construction, a layer of embankment was removed and replaced to improve erosion protection, but the depth was limited. The method used a 1 1/2 in. steel pipe driven 5 ft into the ground to reach frost depth and act as a reference post (Figure 4.7, left). The Geokon 4427 sensor was attached to the bridge abutment using concrete screws and a coupler attached to a cable that spanned the distance to the reference post. At each acute bridge corner, two displacement meters measure in orthogonal directions to measure longitudinal and transverse displacement (Figure 4.7, right).

Figure 4.7. Jasper County 118—displacement transducer with reference post (left) and longitudinal and transverse displacement transducers attached at the acute bridge corner (right)

4.2.5. Jasper County 118 Datalogger Installation

The datalogger used to record measurements was installed with the last of the bridge sensors one day before the bridge was opened to traffic. The 16 wires on the west end of the bridge converge on a central location on the west abutment face to a multiplexer, which condenses the data to be run through a single wire the length of the bridge. The single wire runs to the opposite corner of the bridge to a datalogger placed on the east abutment face, allowing for connection to a solar panel on the south face of the structure to provide power. Initial readings from all sensors were taken to verify proper function. All sensors provided readings indicating that damage resulting in failure had been avoided during construction.

4.2.6. Jasper County 118 Data Collection and Processing

Data were collected from the datalogger by traveling to the bridge site and downloading the data to a .DAT file. The data recording began on August 30, 2018, and data were retrieved on January 4 and May 8, 2019, providing over 8 months of data. The datalogger recorded measurements every hour, resulting in over 6,000 data recordings for each of the 32 sensors in the bridge.

4.2.6.1. Jasper County 118 Instrumentation Results

Data processing began by examining trends in the data for each sensor type to verify proper operation. As mentioned previously, each sensor contains a thermistor to measure temperature. Measurements taken by the sensors are much more valuable when compared with temperature than time due to the long-term nature of the project and the relatively long time between measurements. In order to determine the ambient air temperature at the bridge location, the temperature data from each sensor not embedded in concrete or soil nor exposed to the sun were averaged for the entire time history. For example, the displacement transducers on the east end of the bridge were not included since they receive direct sunlight from the south, especially during the winter. Air temperatures for the monitoring period ranged between 88.2°F in September and -19.4°F in January. The largest difference between the minimum and maximum temperatures on a single day was 24.2°F and occurred on October 3, when the maximum and minimum temperatures reached 62.1°F and 37.9°F, respectively.

The week of September 9 through 15 was chosen for in-depth analysis to narrow the amount of data used in plots and further examine trends. The plot of daily maximum and minimum air temperatures (Figure 4.8) shows a large discrepancy in the minimum temperature compared with the maximum temperature. This means that there was a large daily temperature range during the entire week, with the high temperatures more than 10°F higher than the low temperatures. This time period also shows a general increasing trend over the course of the week, with both the high and low temperatures increasing steadily by 15°F. This seven-day period captures both the daily cyclic loading and long-term trends in seasonal temperature.

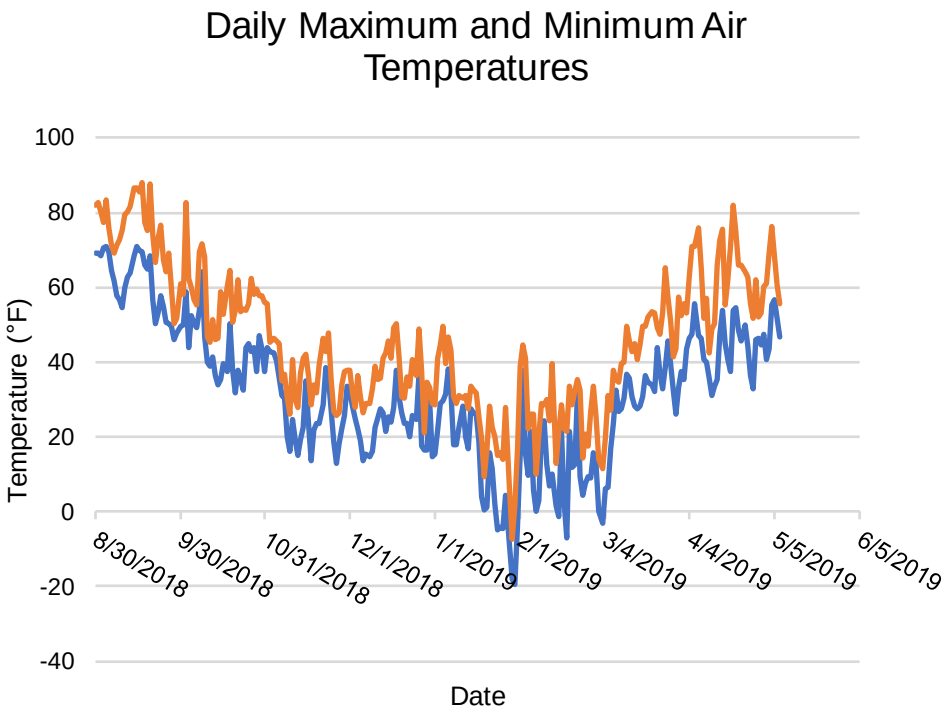

Figure 4.8. Jasper County 118—daily maximum and minimum air temperatures, August 30, 2018, to May 8, 2019

4.2.6.2. Jasper County 118 Bridge Longitudinal Expansion

Displacement transducers were installed on the bridge with the intent to measure expansion for comparison to theoretical calculations per Table 5.8.3.1.2 in the Iowa DOT *LRFD Bridge Design Manual*, illustrate changes in expansion over long time periods, and examine the effect of the 45 degree skew angle on transverse displacement. The displacement of the east and west ends of the bridge over the full monitoring period can be seen in Figure 4.9 and Figure 4.10, which show the cyclical nature of the displacement and its relationship with temperature.

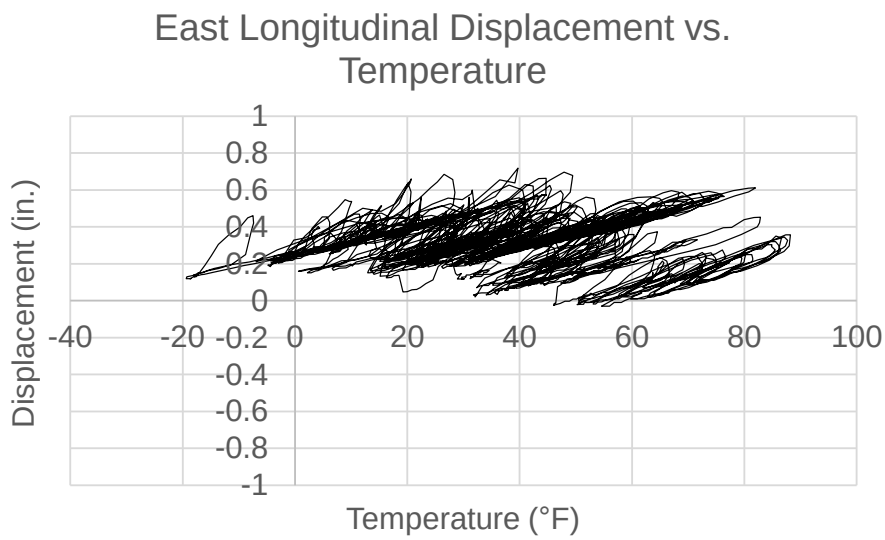

Figure 4.9. Jasper County 118—east longitudinal displacement

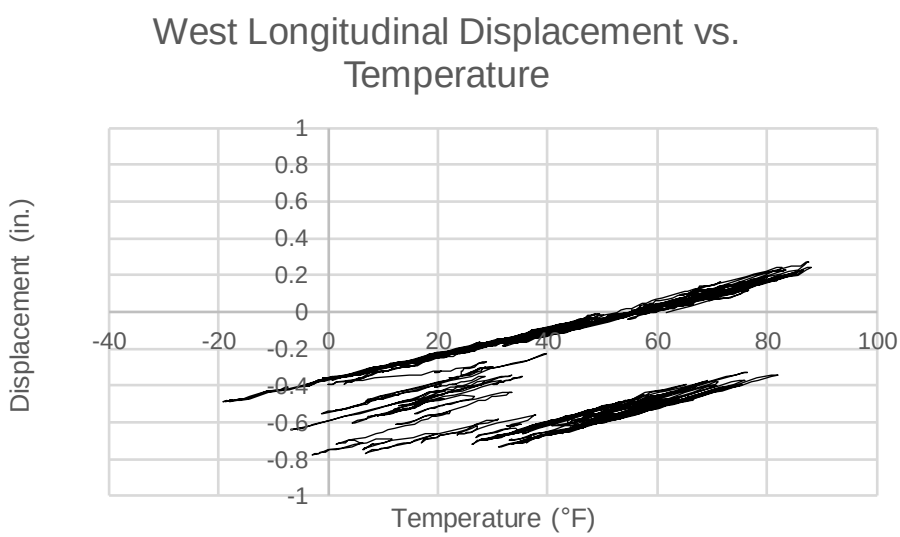

Figure 4.10. Jasper County 118—west longitudinal displacement

In order to compare the measured expansion to calculated values, the total longitudinal bridge expansion was plotted versus time, as shown in Figure 4.11. Total expansion includes both the east and west ends of the bridge corrected for the change in length of the steel cables attached to the transducers.

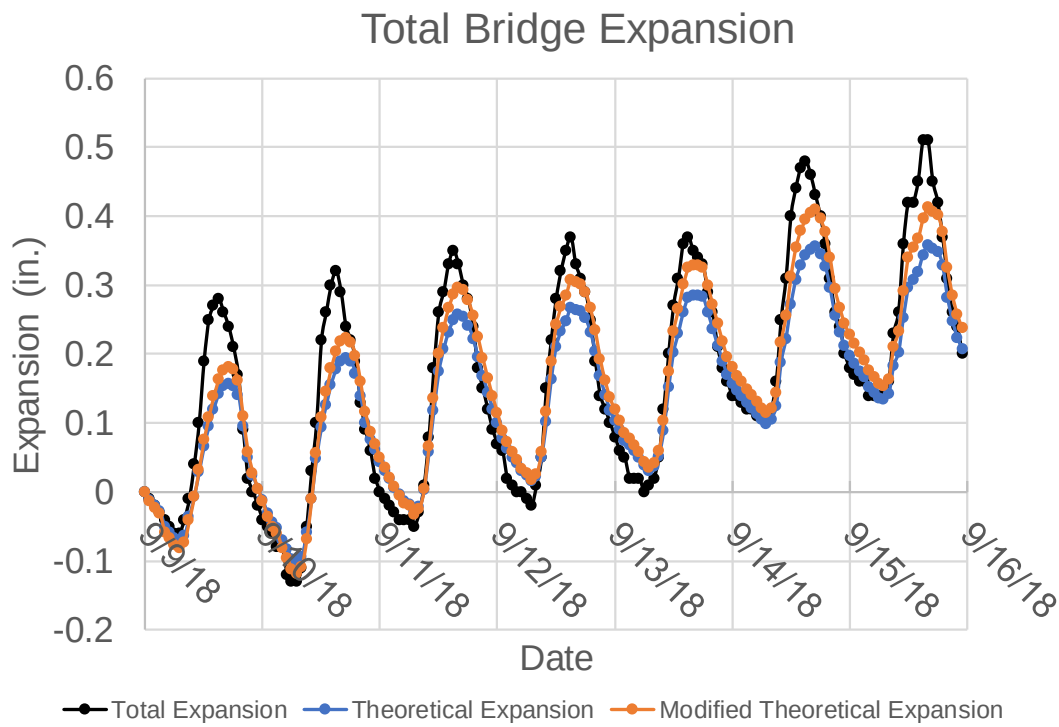

Figure 4.11. Jasper County 118—total measured, theoretical, and modified bridge expansion

The Jasper County 118 semi-integral abutment conversion was designed for zero displacement at the west end. However, the data show a significant amount of movement over the entire four-month period similar to the movement seen at the east end. A temperature range of 75°F produced a total displacement range of 0.66 in. A comparison of the total longitudinal expansion to the theoretical expansion shows nearly identical trends, with daily ranges for calculated values underestimating measured values by 52.7% on average (Table 4.1). The bridge is expanding and contracting more than expected. The discrepancy could be a result of many different factors, including the true coefficient of thermal expansion for the structure as a whole, the effect of skew angle on expansion, the limited accuracy of the sensor setup, or the temperature gradient through the depth of the structure due to sunlight.

Table 4.1. Peak total expansion values and range percent error

Measured Maximum (in.)	Measured Minimum (in.)	Measured Range (in.)	Theoretical Maximum (in.)	Theoretical Minimum (in.)	Theoretical Range (in.)	Range Percent Difference
0.28	-0.06	0.34	0.16	-0.07	0.23	49.2
0.34	-0.13	0.47	0.19	-0.10	0.30	58.2
0.35	-0.05	0.40	0.26	-0.03	0.29	40.2
0.37	-0.02	0.39	0.27	0.02	0.25	54.7
0.37	0.00	0.37	0.28	0.03	0.25	45.6
0.48	0.09	0.39	0.36	0.10	0.26	52.0
0.53	0.14	0.39	0.36	0.13	0.23	69.0

In order to better account for the effect of bridge skew, a new modified expansion was calculated using the principle that skewed bridges expand and contract along an axis between the two acute corners (Aktan and Attanayake 2011). The modified theoretical expansion, which was calculated using the longitudinal component of expansion considering a modified bridge length of 212.5 ft, is also included in Figure 4.11. The modified theoretical expansion is 15% larger than the standard calculated value, which more closely resembles the measured values.

The calculated longitudinal expansion underestimates expansion more as time increases, shown especially from September 14, 2018, onward, when minimum expansion values begin to show a gap between calculated and theoretical values, whereas previously only positive peaks showed a similar gap. The displacement data show no lag between the measured values and the theoretical values based on air temperature. This illustrates that the expansion of the bridge reacts to changes in temperature within one hour, which is the time between data points. The steel girders of the Jasper County 118 bridge do not show any thermal inertia comparable to the thermal expansion exhibited by concrete girder bridges. Concrete girders take time for heat to transfer through the entire cross section, so expansion lags behind air temperature changes.

This concept can be observed by comparing the temperatures in the concrete approach slab with air temperatures. Figure 4.12 shows the temperatures in both the east and west approach slabs along with air temperatures over the seven-day period from September 9 through 15, 2018. The concrete temperatures show peaks roughly three hours after the air temperatures, and daily air temperature ranges are 50% larger than those of the 10 in. concrete slab. The temperatures within the slabs reach a higher peak value on September 9, 2018, when weather records show sunny conditions without cloud cover. The roadway's exposure to sunlight resulted in a temperature higher than the air temperature, not only on the road surface but also through the depth of the slab.

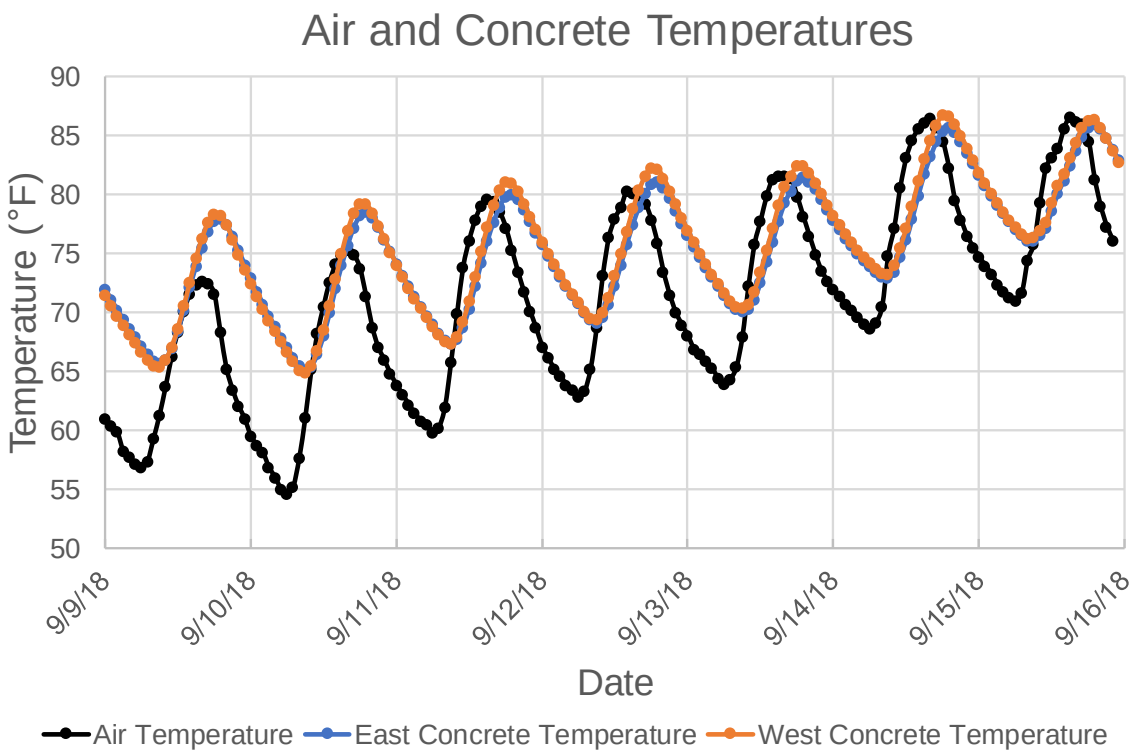

Figure 4.12. Jasper County 118—air and concrete temperatures over time

The crackmeters installed on the Jasper County 118 bridge were intended to measure the relative movement between the bridge and the approach slabs. The data taken from all four crackmeters are similar to each other but do not match the expected trends. The west end joints show minimal movement (Figure 4.13, Figure 4.14), with ranges of 0.08 in. and 0.061 in., respectively. This is reasonable given the expectation that the west approach slab is tied to the abutment. Zero expansion corresponds to the joint condition at the time datalogger began recording. Even if the abutment moves despite its intended design, the approach slab would be pulled with it and the crackmeters would measure limited opening of the tied joint.

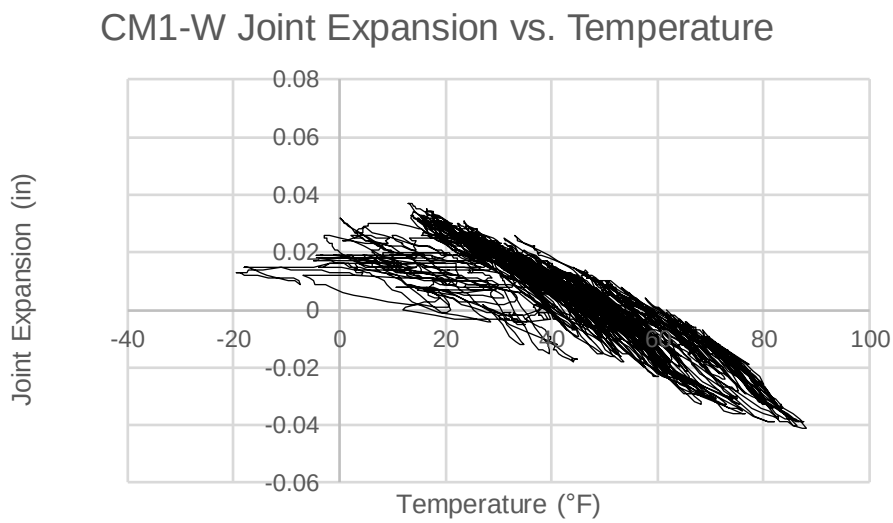

Figure 4.13. Jasper County 118—west end joint expansion (southwest bridge corner)

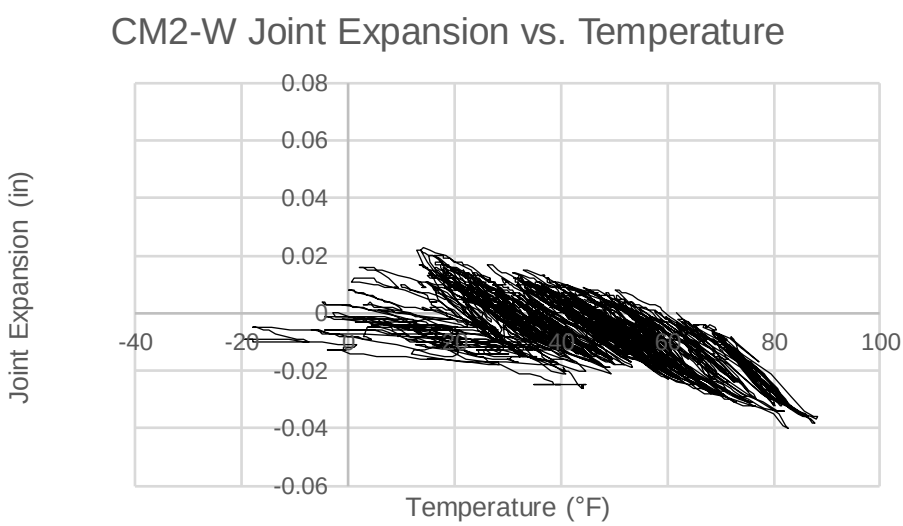

Figure 4.14. Jasper County 118—west end joint expansion (northwest bridge corner)

The movements recorded by the east crackmeters (Figure 4.15, Figure 4.16) are on the same magnitude as those recorded by the west crackmeters, but they should be an order of magnitude higher and more in line with the displacement data. Ideally, the east crackmeters would match the east displacement data due to the abutment moving independently of the separated approach slab. Two possible explanations for this discrepancy include malfunctions in the crackmeters or incomplete separation of the approach slab from the abutment.

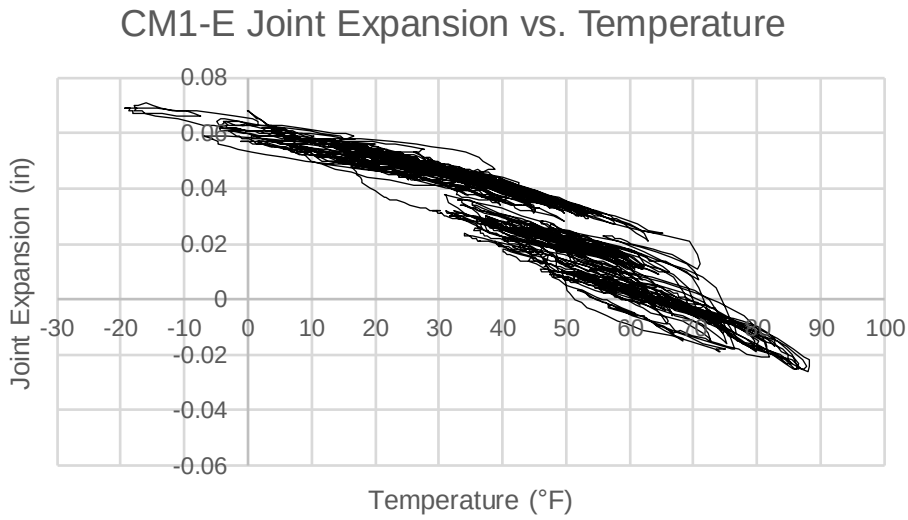

Figure 4.15. Jasper County 118—east end joint expansion (northeast bridge corner)

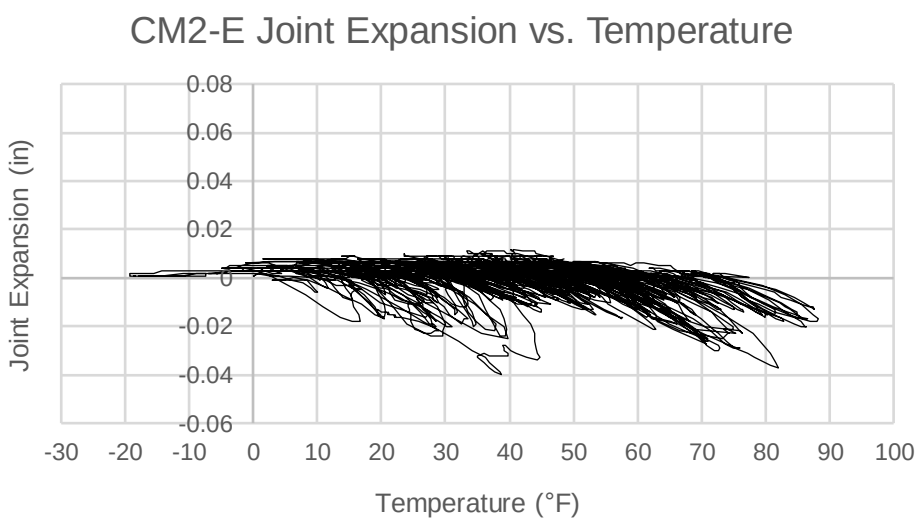

Figure 4.16. Jasper County 118—east end joint expansion (southeast bridge corner)

4.2.6.3. Jasper County 118 Bridge Transverse Expansion

One of the reasons skew is so problematic for moveable abutment bridges is the transverse displacement that arises as a result of earth pressures normal to the skewed abutment backwall. Longitudinal expansion leads to a rotation of the entire bridge structure as both ends tend to move perpendicular to the bridge centerline in the direction of the acute bridge corners. Transverse displacement can be on the same magnitude as longitudinal displacement (Arenas et al. 2013).

Transverse displacement values for the east and west ends of the Jasper County 118 bridge are plotted against temperature in Figure 4.17 and Figure 4.18, respectively.

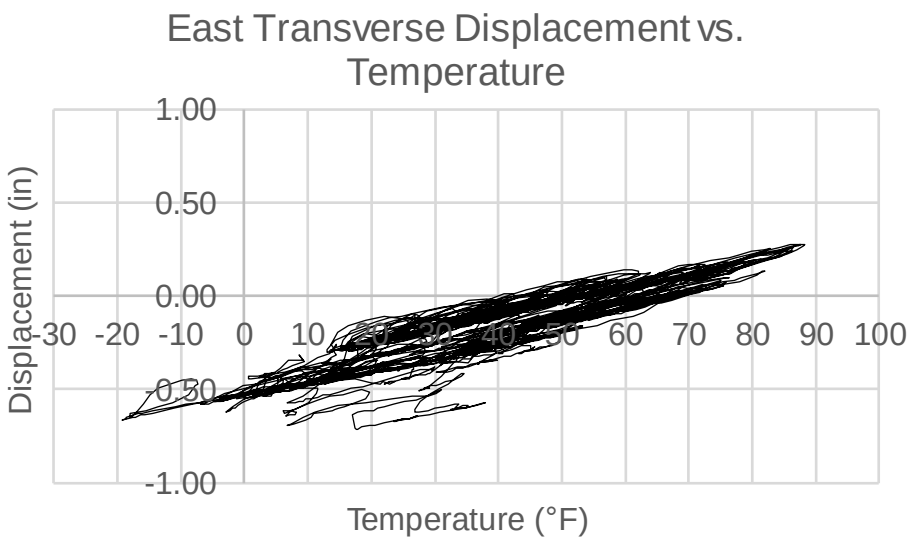

Figure 4.17. Jasper County 118—east abutment transverse displacement

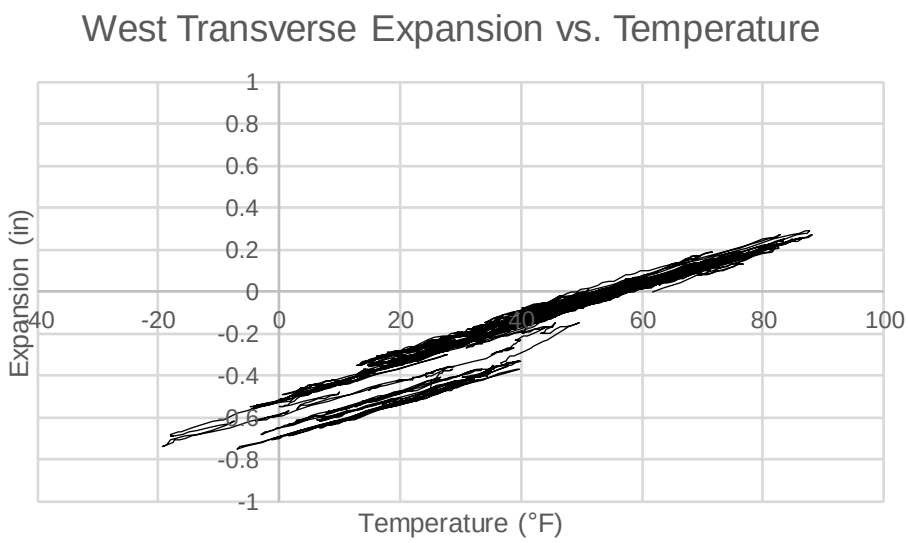

Figure 4.18. Jasper County 118—west abutment transverse displacement

The two directions of displacement for the east end of the bridge during the period of September 9 through 15, 2019 are plotted against each other in Figure 4.19 to see their relationship. Through seven daily temperature cycles, the two variables show a linear relationship, with the line of best fit shown on the plot with an R^2 value of 0.95. The relationship shows that for the east end of the Jasper County 118 bridge, the transverse displacement is equal to 81% of the longitudinal displacement. This value is in line with expectations considering the 45 degree

skew. At lower skew angles, earth pressures are more aligned with the bridge centerline and do not result in a large rotational force.

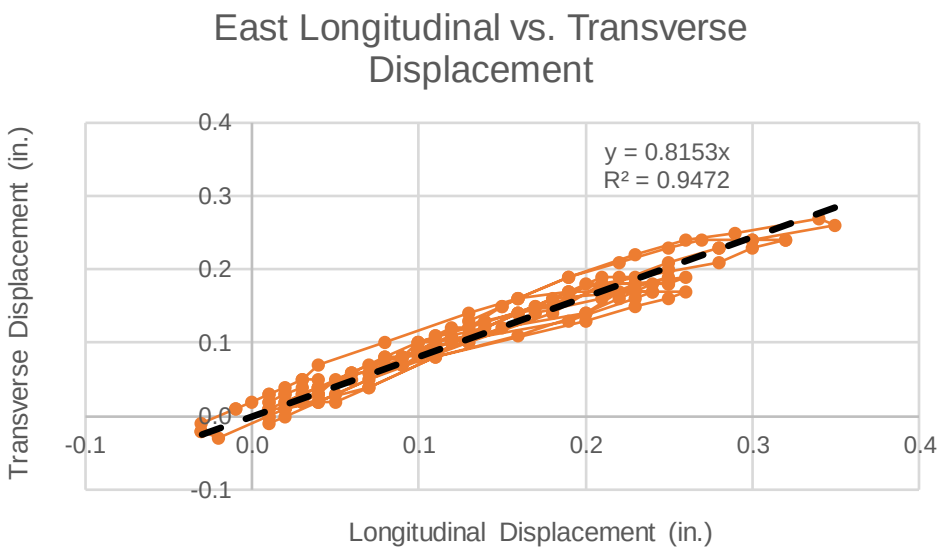

Figure 4.19. Jasper County 118—east longitudinal and transverse displacement relationship

A similar relationship exists for the west end of the bridge, with transverse displacement equaling approximately 120% of the longitudinal displacement (Figure 4.20).

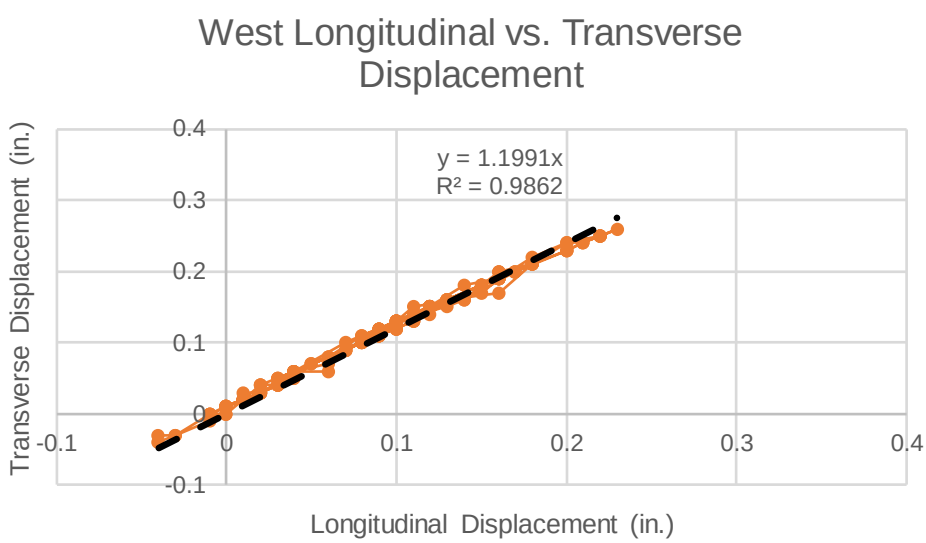

Figure 4.20. Jasper County 118—west longitudinal and transverse displacement relationship

4.2.6.4. Jasper County 118 Abutment Backwall Earth Pressures

Two earth pressure sensors were installed on each abutment backwall directly below the approach slab. One of the four sensors, EP1-E, was not functioning correctly, as evidenced by the extreme results it produced. The other three sensors show pressures on the magnitude of 100 psf, but EP1-E shows pressures averaging 19 ksf. Given the depth of the sensor and the surcharge loading above it, it can be concluded that the sensor is not functioning correctly. The discussion in this section will cover the remaining sensors: EP2-E, EP1-W, and EP2-W. Immediately after construction and before any abutment movement, earth pressures should match the at-rest earth pressure given below (Das 2016):

$$\sigma_h = K_o \sigma_o' + u$$

$$\sigma_h = K_o (q + \gamma H_1) + u$$

$$K_0 \approx 1 - \sin \varphi'$$

In the case of the Jasper County 118 bridge, the pore water pressure (u) is assumed to be zero due to the porous backfill used and the design of the bridge drainage. The surcharge loading is equal to 125 psf based on the approach slab weight, and the sensor is located at a depth of 0.625 ft. The active earth pressure coefficient is calculated to be 0.357 using an assumed friction angle of 40 degrees based on correspondence with the Iowa DOT. The at-rest earth pressure is calculated to be 75.9 psf for the given conditions. Another value of note is Coulomb's passive earth pressure (Das 2016):

$$\sigma_p' = \gamma z K_p$$

The passive pressure is calculated to be 402.5 psf using the same soil depth as the previous calculation and using K_p equal to 4.6 for a friction angle equal to 40 degrees, a wall angle equal to 90 degrees, and a backfill angle equal to 0 degrees since the approach slab lies on a flat surface. The earth pressure data for each of the three sensors for the entire eight-month monitoring period is shown in Figure 4.21, Figure 4.22, and Figure 4.23. The Geokon earth pressure sensors used provide a resolution of 0.025% of their maximum pressure of 14.6 ksf, which is why the data appear discretized, especially for the west end. These sensors are more suitable for measuring large bearing pressures under foundations. However, they can still provide useful data for low pressure ranges such as the ones seen below the Jasper County 118 approach slab.

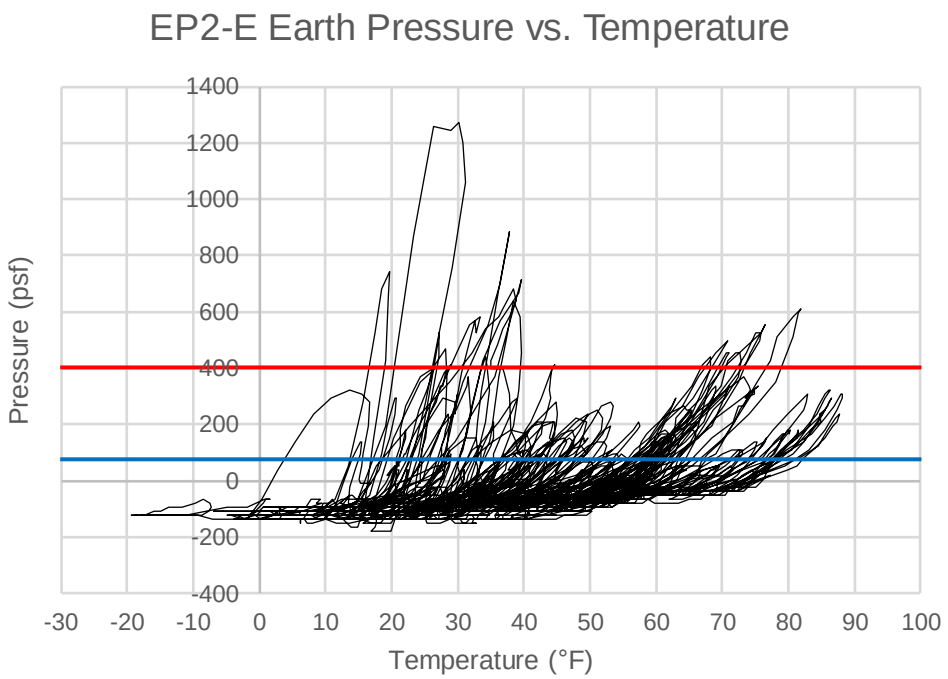

Figure 4.21. Jasper County 118—EP2-E earth pressure for full monitoring period

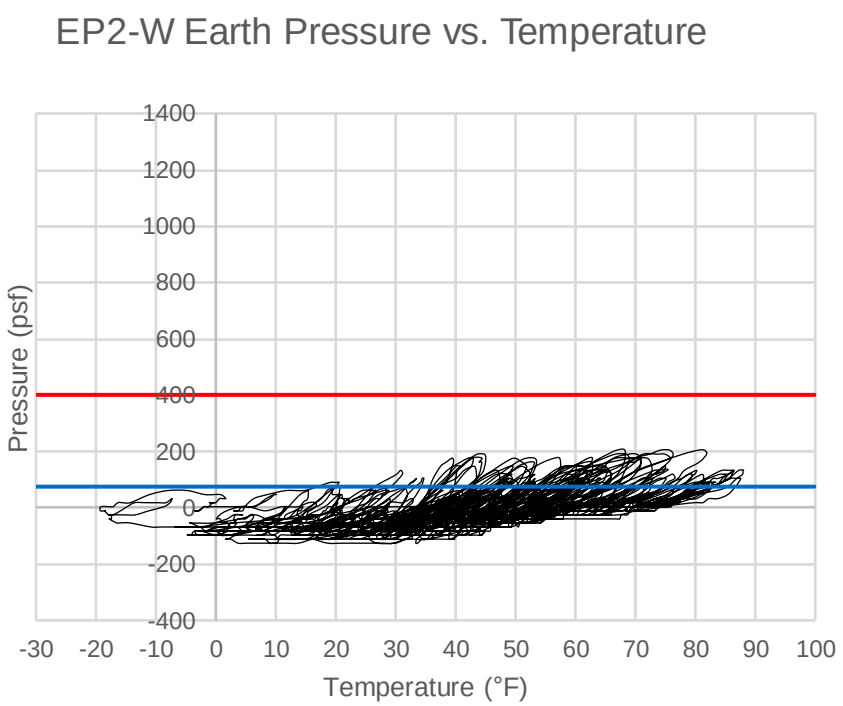

Figure 4.22. Jasper County 118—EP2-W earth pressure for full monitoring period

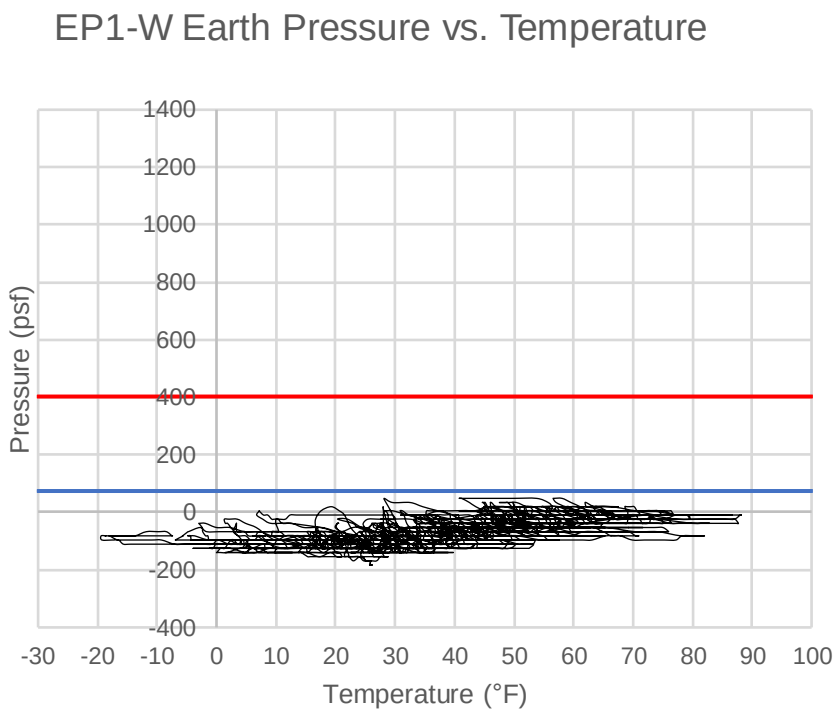

Figure 4.23. Jasper County 118—EP1-W earth pressure for full monitoring period

EP1-W, located at the bridge's obtuse corner, shows lower magnitudes of pressure compared to the two sensors located at the bridge's acute corners (EP2-W, EP2-E). This is the opposite of the findings of Hassiotis et al. (2006), which state that pressures are higher in the obtuse corner for skewed bridges. One possible explanation may be the difficulty of compaction in the obtuse corner, which corresponds to the acute approach slab corner. Space to install the sensors was limited due to the high skew, and it was anticipated that compaction would be difficult around the sensors. Zero pressure corresponds to the sensor's initial condition before any backfill was placed against the face of the sensor. A large portion of measurements are for a negative pressure, indicating the abutment pulling away from the soil.

Over the first four months from September to January during a period of generally decreasing temperatures, EP2-E and EP2-W show maximum pressures of 324 and 134 psf, respectively. A higher pressure at the east end of the bridge where expansion is designed for is expected, since the abutment should push farther into the soil due to a larger displacement, resulting in a larger pressure. Both sets of data show interesting trends related to temperature. On a small scale, for a temperature change of around 10°F pressures increase greatly and decrease with approximately the same slope. If this relationship were consistent over time, all data would fall in a single line. This is not the case, since there are multiple peaks visible at different temperatures. For example, EP2-E shows a peak pressure of 324 psf at 88°F during September after initial construction and a maximum pressure of 1,274.4 psf at 30.2°F. This peak value is a spike almost twice the magnitude of all other data recorded, so it may be the result of point loading by a piece of aggregate. However, there are many consistent spikes in pressure at temperatures lower than the highest recorded value of 88°F. One possible explanation for this behavior is a ratcheting effect

on the abutment. As the abutment pulls away from the soil when the temperature decreases, soil falls into the void left by the abutment. When the abutment expands into the soil during a temperature increase, the resulting pressure is larger at a lower temperature than before.

Overall, the general shape of the curves suggests that higher temperatures are associated with higher pressures, which matches the expected trend. Half of the Jasper County 118 data set that was analyzed covered a period in the fall and winter, which generally coincided with bridge contraction. The second half shows significant bridge expansion, with increasing temperatures and generally higher pressures than those recorded at the same temperatures during the cooling period. The peak pressures for EP2-E did surpass the calculated passive pressure value multiple times over a single daily cycle before pressures decreased drastically during bridge cooling overnight.

4.3. Story County 118

Story County 118 is a new construction bridge located near Ames, Iowa, and was chosen for monitoring due to its tied approach slabs. The bridge is 374.5 ft long by 60 ft wide with a skew angle of 15 degrees and carries two lanes of northbound traffic on I-35 over the Skunk River using four spans. The bridge uses integral abutments at both ends, with approach slabs attached using inclined tie bars. The approach slabs are supported by inverted-T sleeper slabs at the other end (Figure 4.24). Sleeper slabs exist to support the end of the approach slab away from the deck and minimize the effects of settlement of fill below the slab.

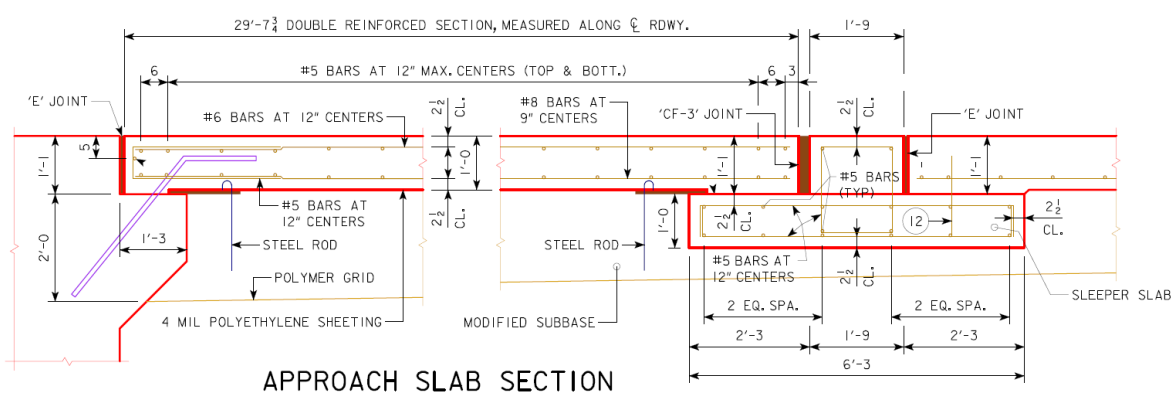

Iowa DOT

Figure 4.24. Story County 118—approach slab section and dimensions

The instrumentation plan can be seen in Figure 4.25. Both the north and south ends of the bridge were outfitted with identical sensors. Due to the symmetric nature of the bridge, it was expected that the behavior observed at both ends would be identical. In the event of any sensor malfunctions, there would be no loss of critical data. Strain gauges were placed throughout the slab across the width and at both ends near the abutment and the sleeper slab. These gauges were expected to capture axial strain and force in the slab due to temperature effects, along with any bending. Three strain gauges were also placed on the tie bars connecting the approach slab to the

abutment in an attempt to capture the axial forces in those bars. A total of twelve strain gauges were placed in each approach slab. Four crackmeters were installed at each bridge end to measure joint movement in both the abutment-to-approach-slab joint and the approach-slab-to-sleeper-slab joint.

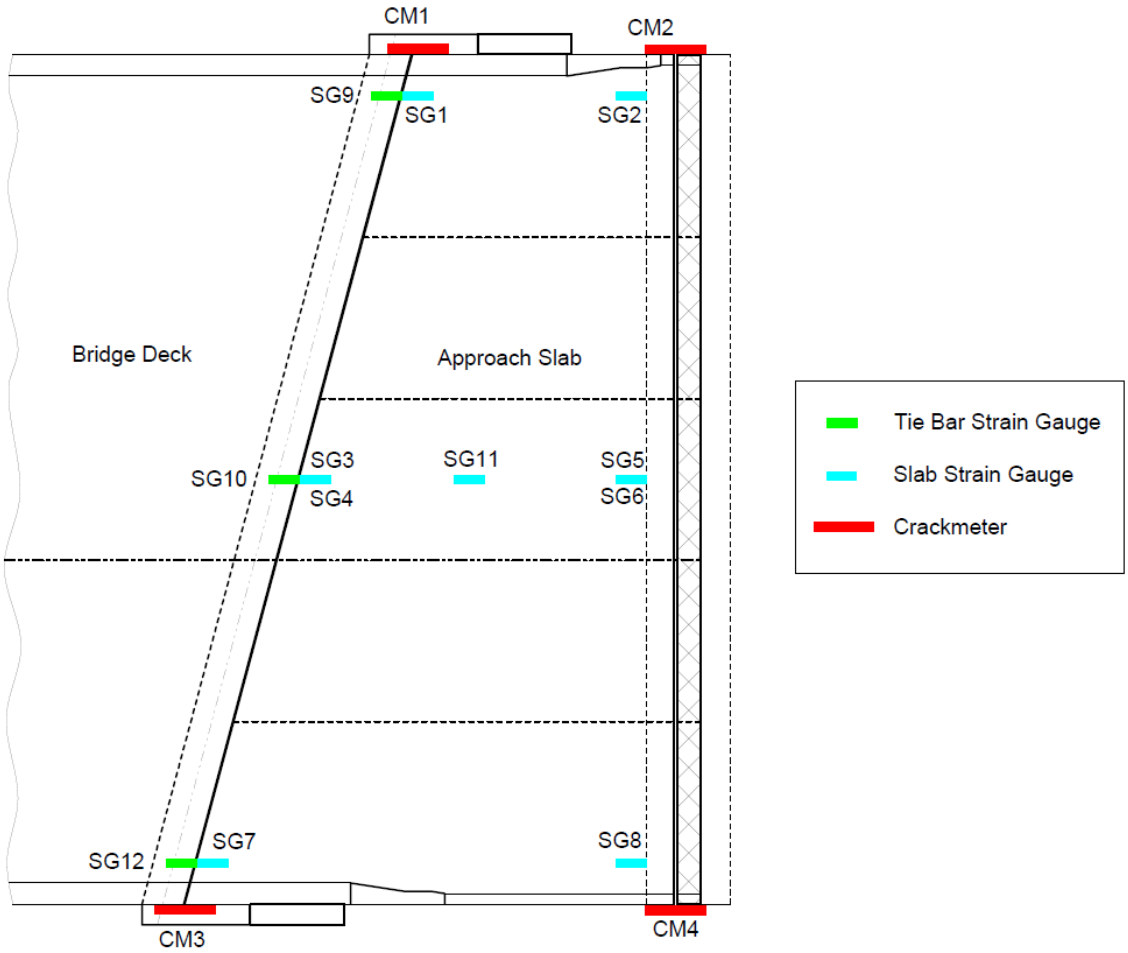

Figure 4.25. Story County 118—approach slab instrumentation plan

4.3.1. Story County 118 Strain Gauge Installation Process

Strain gauges were installed in a layout similar to that used for Jasper County 118. Nine strain gauges were zip-tied to the longitudinal bars to measure strains in the longitudinal direction. Three gauges were placed on the bars tying the approach slab to the bridge abutment. The tie bars are inclined where they exit the abutment, and strain gauges were attached as close to the joint as possible to measure axial strains in the bars (Figure 4.26). The approach slabs were poured in two sections, and wires were run to a single location before exiting the slab.

Figure 4.26. Story County 118—strain gauges installed on the longitudinal rebar and tie bars

4.3.2. Story County 118 Crackmeter Installation Process

Four crackmeters were placed over joints in the concrete barrier rail (Figure 4.27). The majority of the barrier is continuous with the bridge deck, while the end portion rests on the approach slab. Any movement at the roadway joint was expected to match the movement between the barrier segments. The crackmeters were placed on the exterior to protect them from any potential impacts or debris. One crackmeter was placed at each of the four corners of the bridge. Joint measurements on either side were expected to be extremely similar if not identical; however, due to the 15 degree skew of the bridge, both sides were measured to monitor any variations.

Figure 4.27. Story County 118—crackmeter installation across the barrier rail joint

The installation process consisted of placing one anchor, determining the location of the other anchor by reading the sensor output using a VW reader, placing the second anchor, installing the sensor, and installing a metal cover. The crackmeters were installed at 25% of their total 2 in. range, since temperatures during installation were between 25°F and 30°F. Since the maximum expected movement at any one joint is only 1.2 in., there was adequate room for movement during both expansion and contraction of the joint.

Four additional crackmeters were placed to measure the approach-slab-to-sleeper-slab joints. For the crackmeters to avoid interfering with the road surface, they were placed on the sides of the approach slabs (Figure 4.28). Wooden blocks were placed at the corners of the approach slabs where they overlapped with the sleeper slabs before the concrete was poured so the blocks could be pried out after curing to provide a space for the crackmeters. This location and method allowed for the crackmeters to be flush with the side of the slab and avoid interference with any posts driven into the soil to support the metal barrier railing. Accessing the blockout locations required digging large holes in two locations and breaking through a large amount of excess concrete in another. This excess concrete was left over as a result of the placement of the concrete barrier rail and had buried a bundle of strain gauge wires at one corner of the bridge. Fortunately, the concrete was broken up with no visible damage to the wires.

Figure 4.28. Story County 118—crackmeter approach slab side blockout location

4.3.3. Story County 118 Datalogger Installation

Delays in the construction of the Story County 118 bridge on I-35 resulted in the final crackmeters being installed in January. The winter temperatures in Iowa during the month of January rarely reach above freezing, making installation of a datalogger all but impossible due to the fine motor skills necessary to strip and attach the sensor wires to the datalogger itself. The wires from all sensors were tacked to the bridge to organize them, and lengths were cut at a central location that would be the future location of the datalogger. Temperatures through the winter remained too low for the installation of the datalogger, since fine motor skills are required to correctly organize and connect the tiny wires. The datalogger was installed on March 21, 2019, in reasonable temperatures and without any precipitation.

4.3.4. Story County 118 Data Collection and Processing

Data were retrieved from the datalogger on May 7, 2019, 46 days after installation. The datalogger recorded measurements every hour, providing 942 data points for 32 different sensors. The records for crackmeter CM4-S were deemed unusable even after the wiring was checked after initial problems were discovered with the datalogger installation. The data from this sensor, which included temperatures over 190°F and expansion readings over 4 in., are not consistent with the data from the other sensors of the same type. All other sensors appeared to be functioning correctly.

Analysis of the Story County 118 bridge instrumentation data began with an examination of the temperatures experienced by the bridge over the weeklong time period from March 22 to 30,

2019. Air temperatures were taken by the datalogger itself, which was placed on the abutment face, protected from sunlight. The crackmeters may be exposed to sunlight depending on the time of day and season due to their locations at each of the four corners; however, each crackmeter was installed with a steel angle cover that blocks any direct sunlight. Even though the ends of the covers were left open, the sensors may experience minimal amounts of indirect heating from sunlight on the cover. The minimum air temperature reached was 25.8°F on March 31, 2019, and the maximum air temperature of 85.2°F was reached on April 21, 2019 (Figure 4.29). Concrete temperatures were taken by averaging the strain gauge temperatures and are included in the plot with the air temperatures.

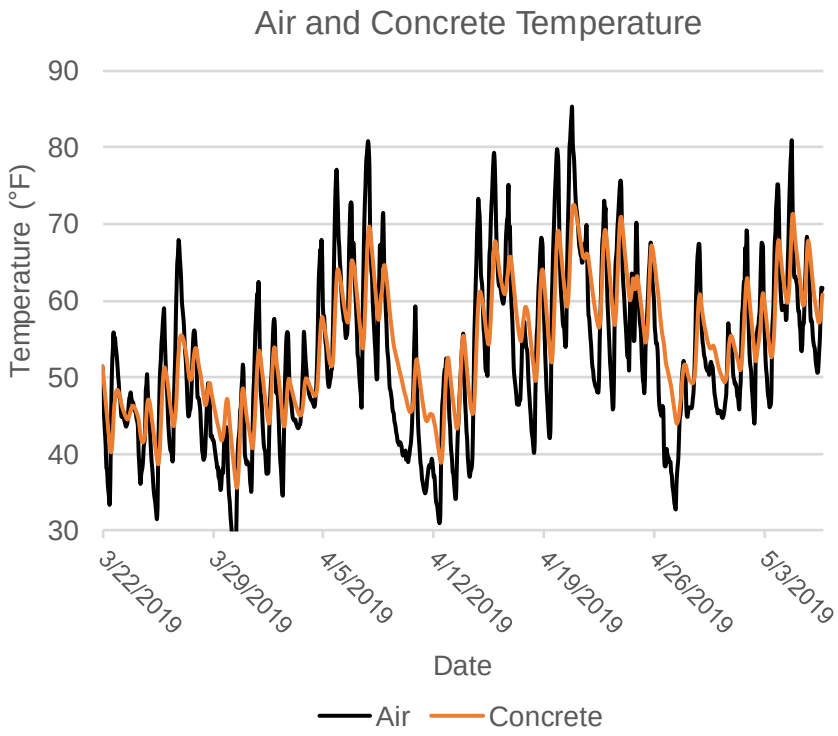

Figure 4.29. Story County 118—air and concrete slab temperatures

The same relationship between the two as observed in the Jasper County 118 bridge can be seen. Concrete has a thermal inertia due to its insulation properties and does not react to changes in air temperature immediately. The maximum and minimum concrete temperatures also are smaller in magnitude. The maximum concrete temperature was 72.6°F, 12.6°F less than the maximum air temperature. The minimum concrete temperature of 35.6°F was 9.8°F higher than the minimum air temperature. Relatively cloudy weather during the monitoring period prevented the concrete temperatures from reaching higher peaks due to direct sunlight.

Placement of crackmeters on both joints at either end of the bridge approach slabs allowed for calculation of the relative and absolute displacement of the bridge superstructure and both approach slabs. The sleeper slabs at either end of the bridge were assumed to be stationary. Using the displacement measurements and theoretical expansion of the approach slab, the total

expansion of the superstructure could be determined. Expansion is plotted in Figure 4.30 using the start of the monitoring period as zero displacement. Crackmeter data from the east side of the bridge (CM3-N, CM4-N, CM1-S, CM2-S) were used since CM4-S did not function correctly.

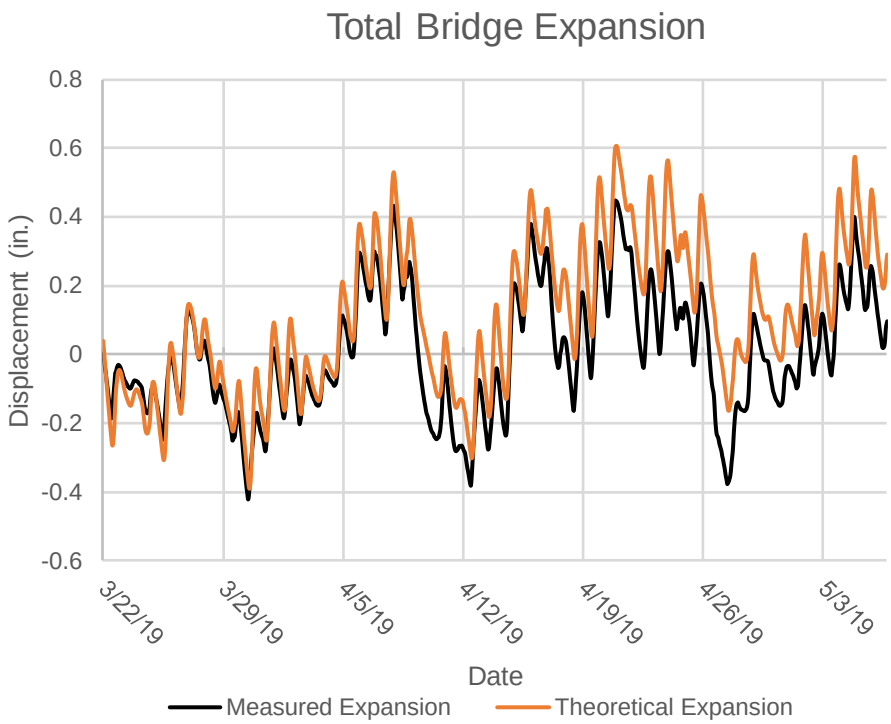

Figure 4.30. Story County 118—measured and theoretical longitudinal bridge expansion

Approach slab expansion was calculated in the same manner as bridge expansion using a coefficient of thermal expansion of 6e-06/°F. Due to the 15 degree skew of the Story County 118 bridge, the total approach slab length on each side of the bridge is 56 ft 11 in. The sum of expansion measured by the crackmeters minus the theoretical expansion of approach slabs leaves the amount of expansion that can be attributed to the superstructure. The theoretical bridge expansion was calculated in the same manner as for the Jasper County 118 bridge using a length of 375 ft. The temperatures for the expansion calculations used the average concrete temperatures from the slabs instead of the air temperature. The temperatures of the precast prestressed concrete girders used in the construction of the Story County 118 bridge more closely match the temperatures of the slab for the same reason that a lower temperature range is used for calculating maximum expansion. The relationship between the temperatures within the concrete members and the air temperature was discussed previously.

Analysis of the crackmeter data began with an analysis of the data from the three operational crackmeters placed between the approach slab and sleeper slab (CM2-N, CM4-N, CM2-S). Figure 4.31, Figure 4.32, and Figure 4.33 show joint expansion versus concrete temperatures to visualize joint movement with expansion and contraction of the bridge. Positive values correspond to bridge contraction, in which the approach slab pulls away from the sleeper slab.

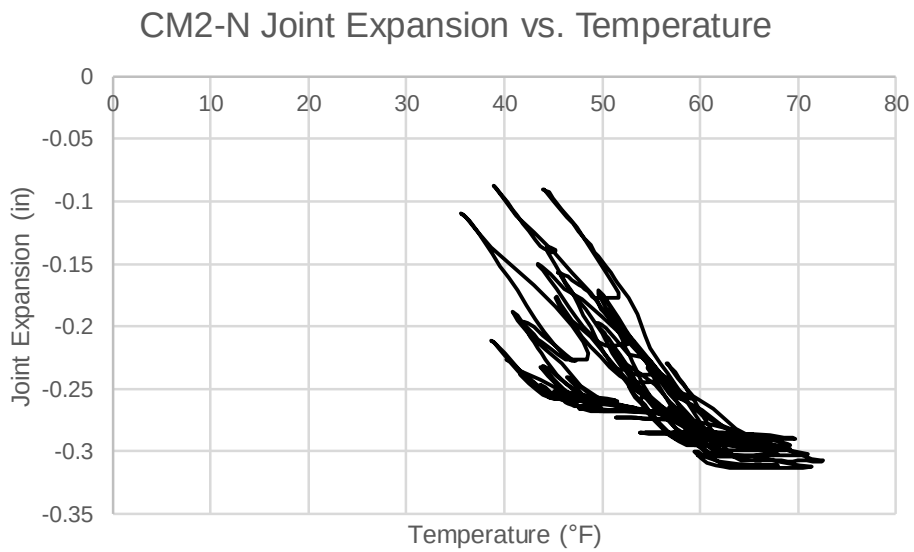

Figure 4.31. Story County 118—approach-slab-to-sleeper-slab joint expansion

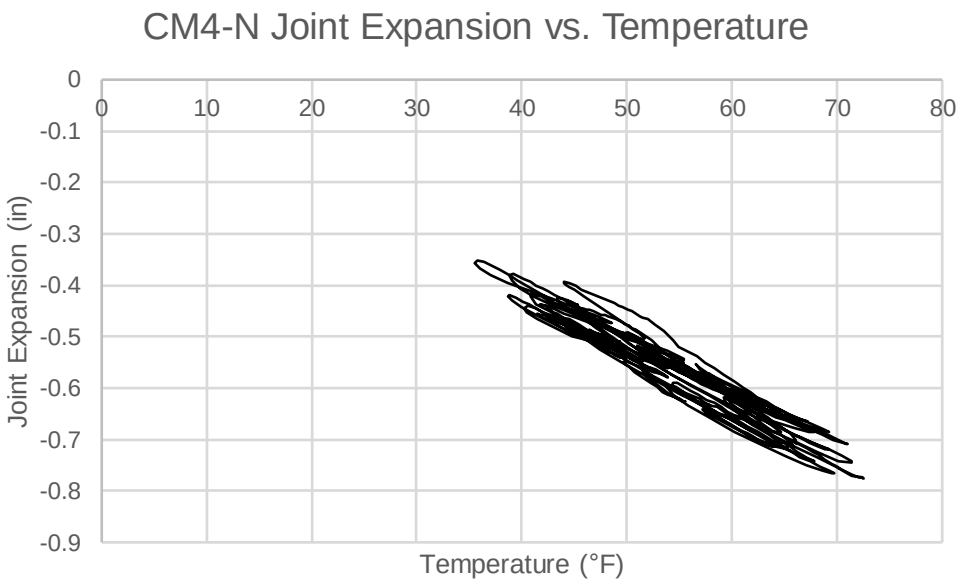

Figure 4.32. Story County 118—approach-slab-to-sleeper-slab joint expansion

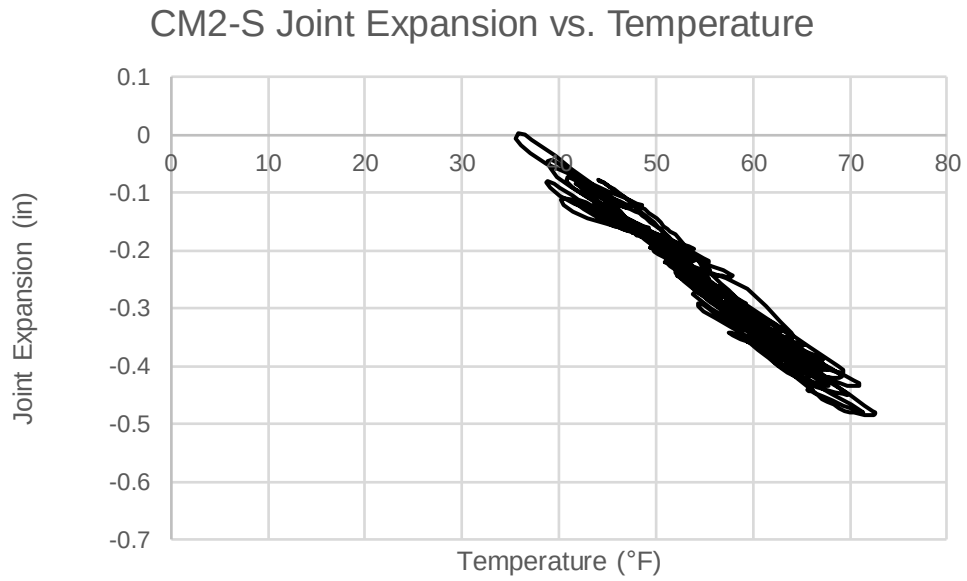

Figure 4.33. Story County 118—approach-slab-to-sleeper-slab joint expansion

Generally, negative values were expected since the crackmeters were installed during temperatures lower than those observed during the monitoring period, so the bridge would have expanded during the monitoring period and pushed the approach slab towards the sleeper slab. CM2-N and CM4-N show a strong linear relationship with temperature, indicating that the joint opens and closes depending on the expansion of the bridge. CM3-N shows similar behavior minus a flat portion at its most negative expansion. It is possible that the sensor bottomed out at a lower limit due to installation issues, with the slab pushing the anchorage hardware used to attach the sensor to the sleeper slab. CM3-N was not used for calculation of bridge expansion. Overall, the joints between the approach slabs and sleeper slabs appear to be functioning correctly in terms of the movement that is supposed to be accommodated at those locations. The physical condition of the CF-3 joints at those locations should be monitored for performance and for the joints' ability to prevent surface water intrusion.

The crackmeters placed between the main bridge barrier rail and approach slab rail section will continually provide extremely valuable data on the tied approach slab joint over the entire long-term monitoring period of the bridge. These crackmeters directly measure an aspect of the bridge that contributes greatly to overall service life by preventing or allowing infiltration of water from the bridge surface into the embankment behind the bridge abutment. In a perfect scenario, the tie bars would not allow any relative movement between the approach slab and the abutment. The data recorded by each of the four crackmeters show that this is not the case (Figure 4.34, Figure 4.35, Figure 4.36, and Figure 4.37). All four crackmeter plots for CM1-N, CM3-N, CM1-S, and CM3-S have been corrected to use zero expansion for the joint condition at the time of installation and are plotted with the average concrete temperatures on the X-axis.

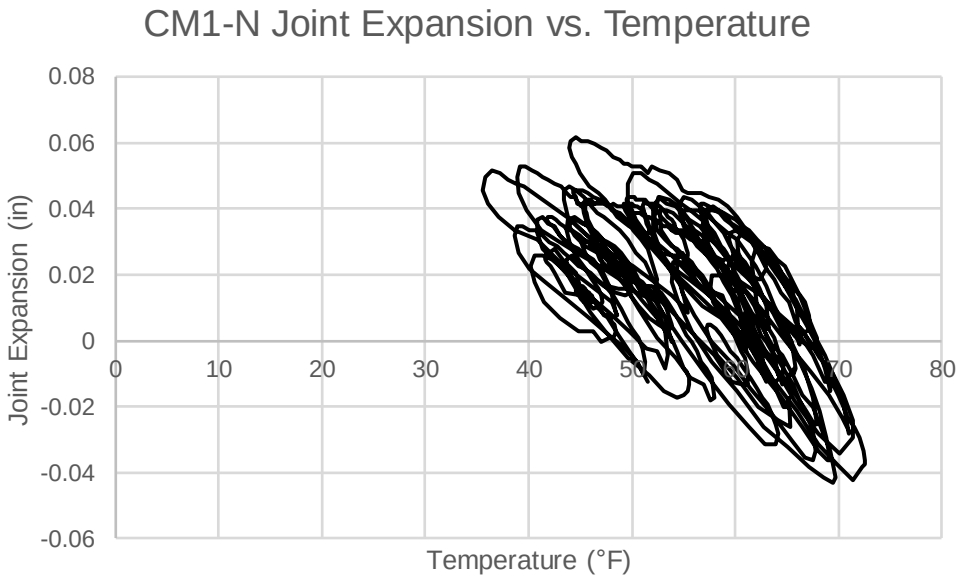

Figure 4.34. Story County 118—bridge-barrier-to-approach-slab-barrier joint expansion

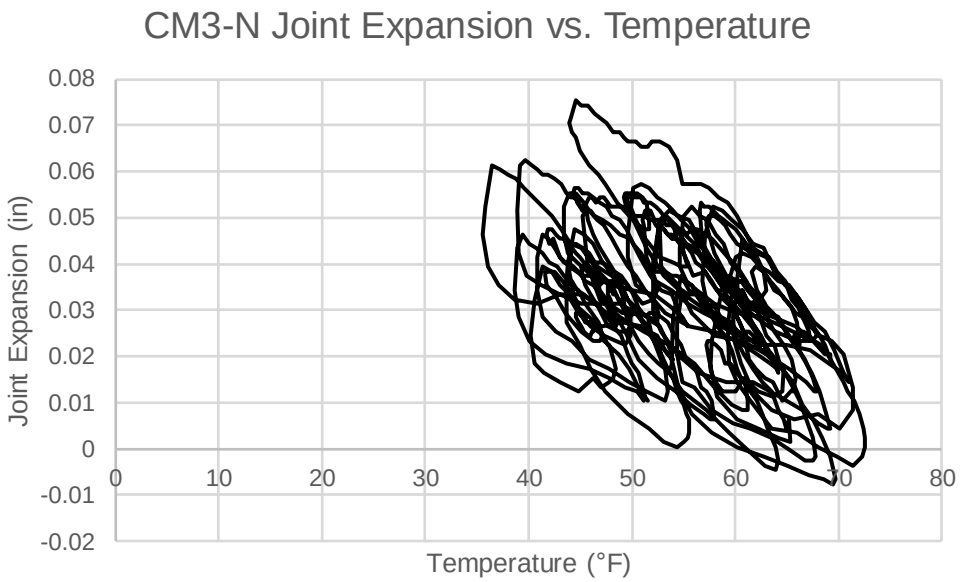

Figure 4.35. Story County 118—bridge-barrier-to-approach-slab-barrier joint expansion

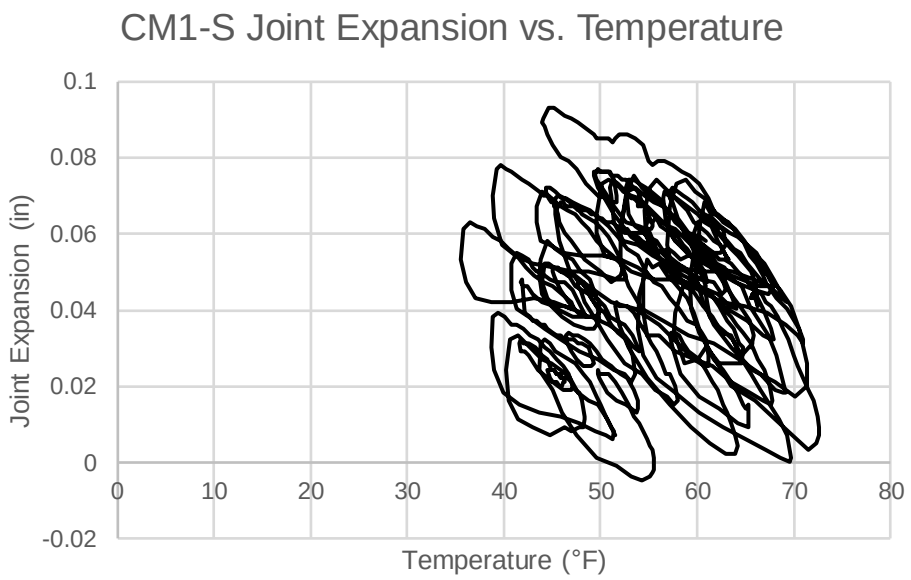

Figure 4.36. Story County 118—bridge-barrier-to-approach-slab-barrier joint expansion

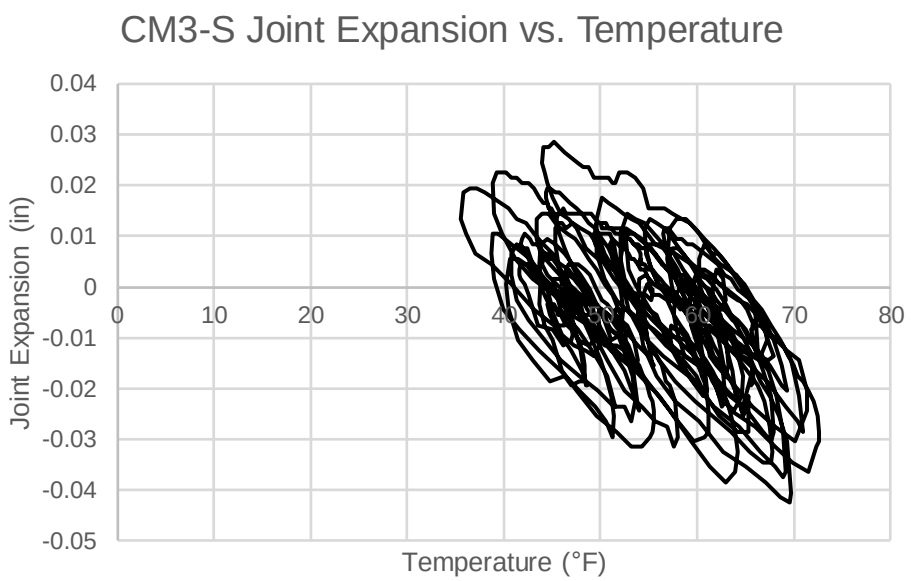

Figure 4.37. Story County 118—bridge-barrier-to-approach-slab-barrier joint expansion

CM3-N and CM1-S were installed on December 13, 2018, when temperatures reached a high of 38°F. CM1-N and CM3-S were installed on January 17, 2019, when temperatures reached a high of 29°F. All four crackmeters share two common trends and show similar behaviors and shapes in the curves where temperatures reached a maximum of over 72.6°F within the concrete approach slabs.

The first trend is that joint expansion appears to be related to temperature, which is apparent from the general negative slope of each of the four curves. As temperature decreases, the bridge contracts and pulls on the approach slab, inducing tension. This behavior is not unexpected and should not cause a problem for the joint as long as the stresses in the bars are not high enough to cause yielding and permanent deformation. Generally, the joints close when temperatures increase, and bridge expansion releases the force on the joint created by contraction. If the joints acted in a purely elastic fashion, the curves would only cross the X-axis at the temperature at which the crackmeters were installed. This is not the case, and a zero reading at a higher temperature may indicate the fact that the 1/4 in. joints may reach a limit where increasing the temperature only serves to push the approach slab and further closure of the joint is not possible. Further monitoring through the summer would shed more light on long-term behavior.

The second trend shared by all crackmeters is that in the short period of data collection, all four crackmeter curves show a looping behavior in contrast with the linear behavior of the other set of four crackmeters. As the bridge switches from expansion to contraction or vice versa, the joint will open or close before the slab begins to slide in either direction. If repeated cycles result in increasing measurements at the joint, this indicates a gradual opening of the joint over time. CM1-S especially seems to be exhibiting increasing joint widths over time as the looping behavior creeps in the positive direction with increasing temperatures. A year of joint expansion data would prove very valuable in examining trends such as this.

The initial slab strains show similar behavior for almost all of the gauges embedded in the Story County 118 bridge approach slabs. The gauges show an expected response to temperature changes, in that they show a linear relationship. The slopes of the trendlines vary from -1.5με/°F to -4.5με/°F depending on the gauge location. The plots of data from each gauge are not included here for the sake of brevity, but a representative set of data from SG3-N can be seen in Figure 4.38. A large set of strain data over a longer time period would prove beneficial and allow for more in-depth analysis.

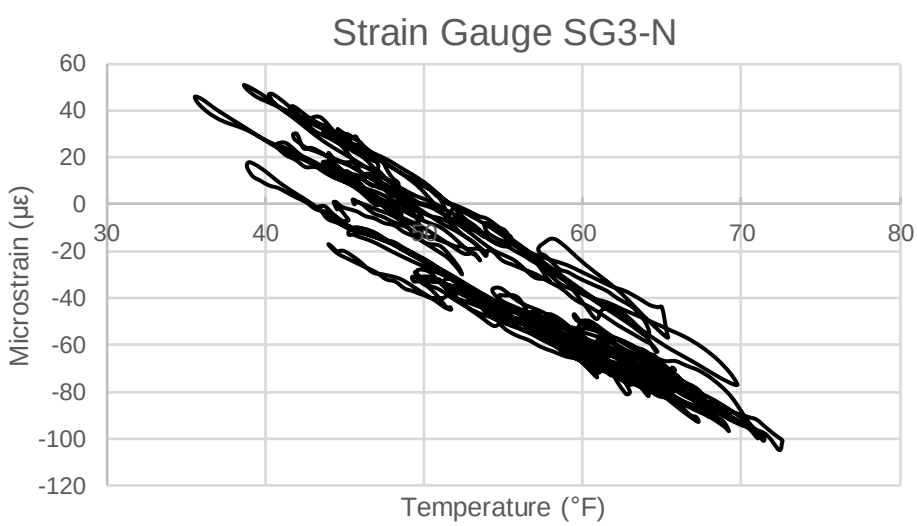

Figure 4.38. Story County 118—representative slab strain gauge behavior

SG10-S is the gauge located on the center tie bar of the south approach slab. The plot of strains in SG10-S versus temperature in Figure 4.39 shows a curve very similar in shape to the one produced by the crackmeter joint measurements seen previously. A comparison with the strain data taken from the finite element modeling activities is available in Chapter 5.

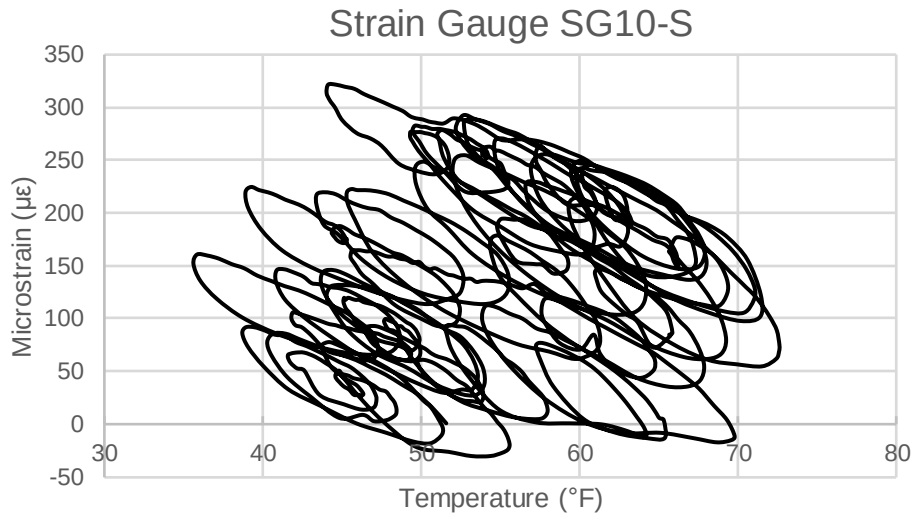

Figure 4.39. Story County 118—SG10-S measured strains

4.3.5. Story County 118 Construction Issues

Several issues arose during the construction of the Story County 118 bridge that were observed while installing sensors both during construction and after opening of the bridge. The many issues apparent during construction of the bridge give credence to claims that poor approach slab performance in terms of settlement is commonly due to poor construction (Yasrobi et al. 2016, Dupont and Allen 2002). Improperly constructed bridge elements do not develop problems over time; rather, the problems are present from the very beginning and can impact service life immediately.

In the case of Story County 118, a section of the concrete barrier rail was placed on the approach slab to allow for drainage continuity and to direct water away from the bridge abutments and deck joints. The plans show the concrete curb formed up to the end of the barrier to create a continuous vertical surface. However, it appears that the formwork used for the barrier end has left a gap in the curb where it meets the barrier at each of the four corners of the bridge (Figure 4.40). Water will run through this gap into the embankment closer to the abutment than desired and avoid erosion control measures.

Figure 4.40. Story County 118—curb gap at the barrier end (typical)

The Story County 118 bridge was opened to traffic with an open joint lacking joint filler at each end of both barriers, as shown in Figure 4.41. However, the bridge plans indicate an E joint in the concrete barrier wall between the main section and the approach slab section (Figure 4.42). Crackmeters were installed at these locations since it was apparent that no further work would be completed. The open joints will allow snow and ice to fill the gaps, possibly expanding and damaging the surrounding concrete. The longitudinal rebar in the barrier appeared to be continuous across the joint in multiple locations, likely due to shifting during formation of the barrier. Vertical cracking appeared one month after bridge opening in the barrier near the joint location.

Figure 4.41. Story County 118—open barrier joint (typical)

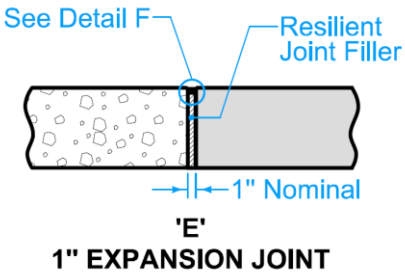

Iowa DOT

Figure 4.42. Iowa DOT E joint

The approach slabs were poured directly onto the modified subbase fill without the use of the 4 mil polyethylene sheeting specified in the approach plans (Figure 4.43). Due to the large aggregate used for the modified subbase, there is a concern the concrete has penetrated the voids around the individual pieces and will cause an interlocking effect when the slab attempts to slide. This potential issue will become more apparent as time goes on and the tied approach connection is forced open by a slab that will not move as it was designed.

Figure 4.43. Story County 118—approach slab modified subbase condition immediately before concrete pouring

The cause for most concern was a large void under the south abutment discovered in January 2019 while attaching wires to the bridge exterior (Figure 4.44). A large portion of soil support under the northwest corner of the south abutment had eroded, leaving a large space many feet deep in the abutment footprint and at least 1 ft tall.

Figure 4.44. Story County 118—large void under the south abutment corner

Rebar was clearly visible protruding from the bottom of the abutment, along with one of the foundation piles (Figure 4.45). A ribbed drainpipe ended directly at the void location, but it was unclear where it came from or if it was the reason for the erosion. The Iowa DOT was notified of the issue and inspected the area of concern.

Figure 4.45. Story County 118—visible exposed rebar and foundation pile

4.4. Polk County 120

Polk County 120 is a reconstruction bridge located in Polk County, Iowa, and was chosen for monitoring due to its tied approach slabs. The improvement work was for outside widening and repairs to the westbound of existing twin 710 ft 6 in. long by 62 ft 4 in. wide prestressed concrete bridges on I-80/I-35 over the Des Moines River. The skew angle of the bridge is 15 degrees. Also, the bridge uses semi-integral abutments at both ends, with approach slabs attached using tie bars. Each approach slab is supported by an inverted-T sleeper slab at the other end (Figure 4.46). The sleeper slabs exist to support the end of the approach slab away from the deck and minimize the effects of settlement of fill below the slab.

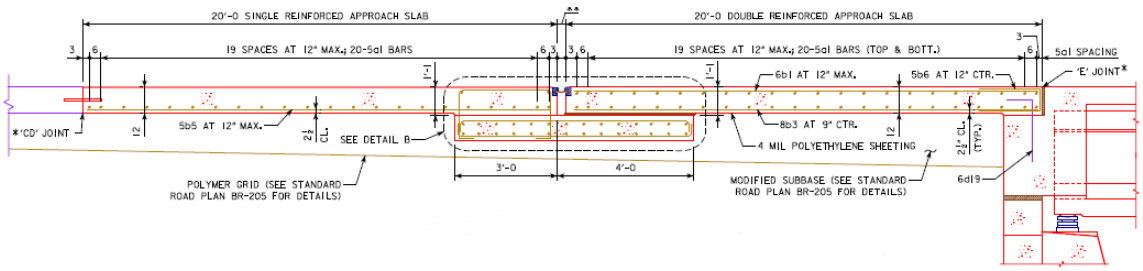

Iowa DOT

Figure 4.46. Polk County 120—approach slab section and dimensions

The instrumentation plan can be seen in Figure 4.47. Both the west and east end of the bridge were outfitted with identical sensors. Due to the symmetric nature of the bridge, it was expected that the behavior at both ends would be identical. Strain gauges were placed throughout the slab across the width and at both ends near the abutment. These gauges were expected to capture axial strain and force in the slab due to temperature effects, along with any bending.

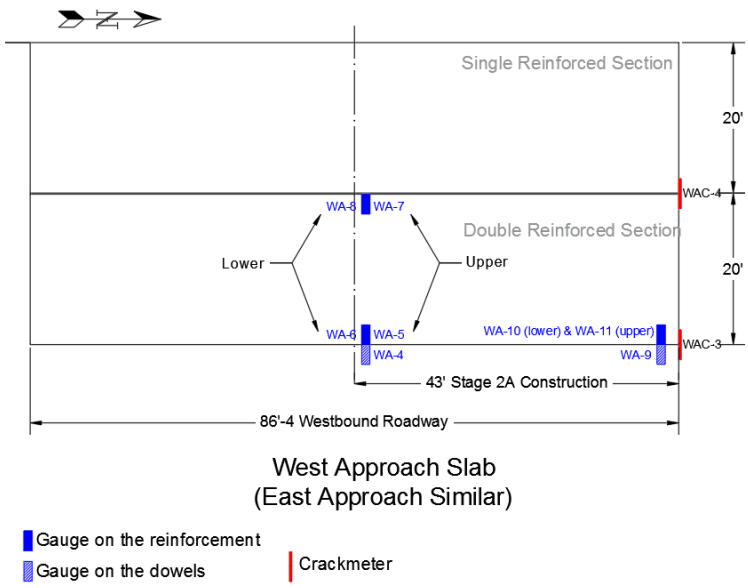

Figure 4.47. Polk County 120—approach slab instrumentation plan

Two strain gauges were also placed on the tie bars connecting the approach slab to the abutment in an attempt to capture the axial forces in those bars, as shown in Figure 4.48. A total of eight strain gauges were placed in each approach slab. Two crackmeters were installed at each bridge end to measure joint movement of both the abutment-to-approach-slab joint and the approach-slab-to-sleeper-slab joint.

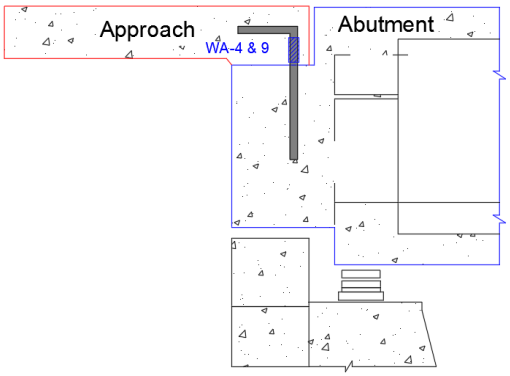

Figure 4.48. Polk County 120—strain gauges in tie

4.4.1. Polk County 120 Strain Gauge Installation Process

Strain gauges were installed in a layout similar to that of the previous bridges. Eight strain gauges were zip-tied to longitudinal bars to measure strains in the longitudinal direction. Two gauges were placed on the bars tying the approach slab to the bridge abutment. The tie bars are bent where they exit the abutment, and strain gauges were attached as close to the joint as possible to measure axial strains in the bars (Figure 4.49).

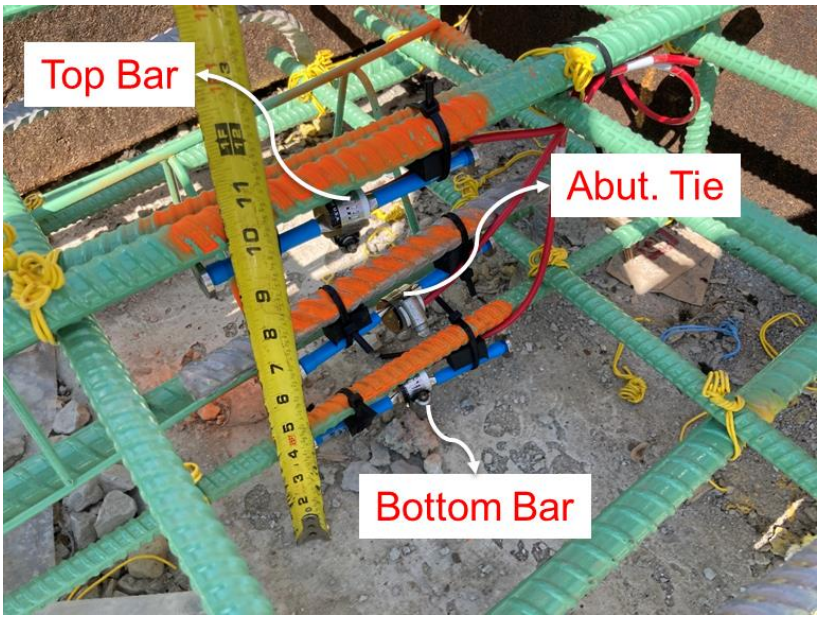

Figure 4.49. Polk County 120—strain gauges installed on the longitudinal rebar and tie bars

4.4.2. Polk County 120 Crackmeter Installation Process

Four crackmeters were placed over the joints between the approach slab and the abutment (Figure 4.50). The installation process consisted of placing a foam block prior to the concrete

pour to create a pocket so that the crackmeter could be placed later. A metal cover was used to close the pocket and protect the crackmeter after installation.

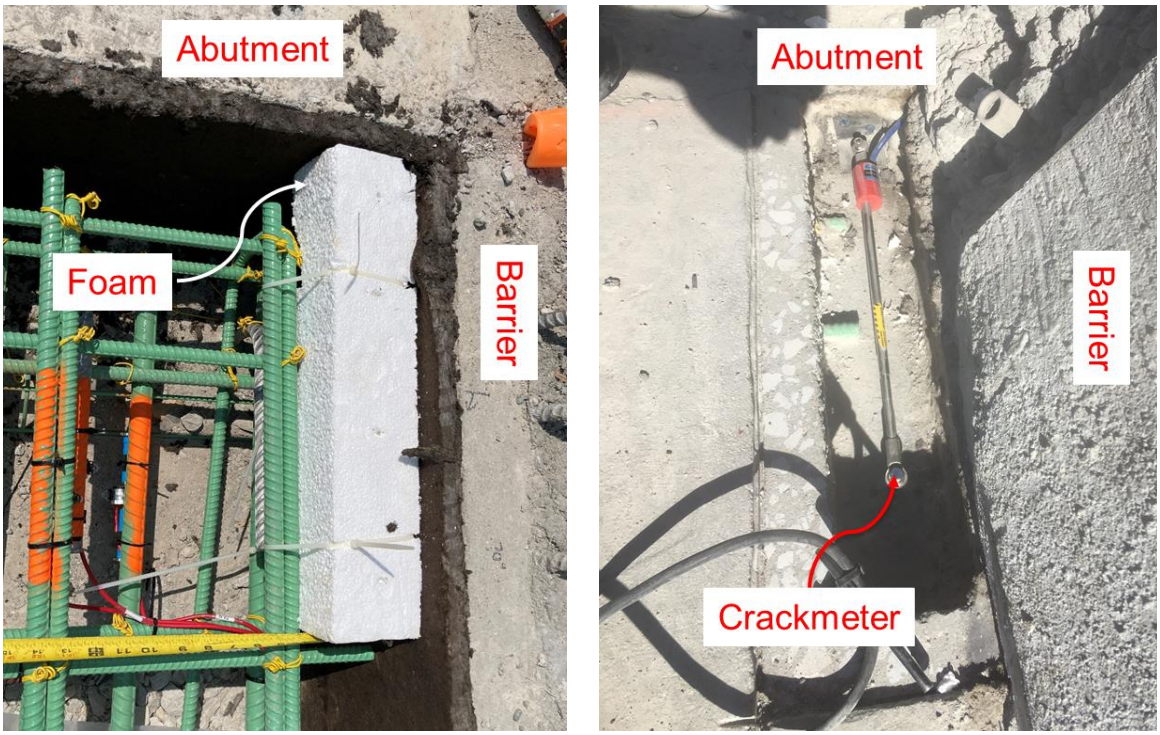

(a) Foam placed for crackmeter installation (b) Crackmeter installation

Figure 4.50. Polk County 120—crackmeter installation across the abutment-to-approach-slab joint

4.4.3. Polk County 120 Datalogger Installation

After all of the instrumentation was installed, the wires from all sensors were tacked to the bridge to organize them, and the lengths were cut at a central location that would be the future location of the datalogger. The datalogger was installed on November 19, 2020, in reasonable temperatures and without any precipitation.

4.4.4. Polk County 120 Data Collection and Processing

Data were retrieved from the datalogger on March 19, 2023. Air temperatures were taken by the datalogger itself, which was placed on the abutment face, protected from sunlight. The minimum air temperature reached was -8°F on February 16, 2021, and the maximum air temperature of 91°F was reached on July 23, 2022 (Figure 4.51). Concrete temperatures in the east and west ends were taken by averaging the strain gauge temperatures and are included in the plot with the air temperatures. Concrete has a thermal lag due to its insulation properties and does not react to changes in air temperature immediately. The maximum temperature in the approach slab was 97°F, 6°F higher than the maximum air temperature; the minimum temperature in the approach slab was 10.5°F, 18.5°F higher than the minimum air temperature.

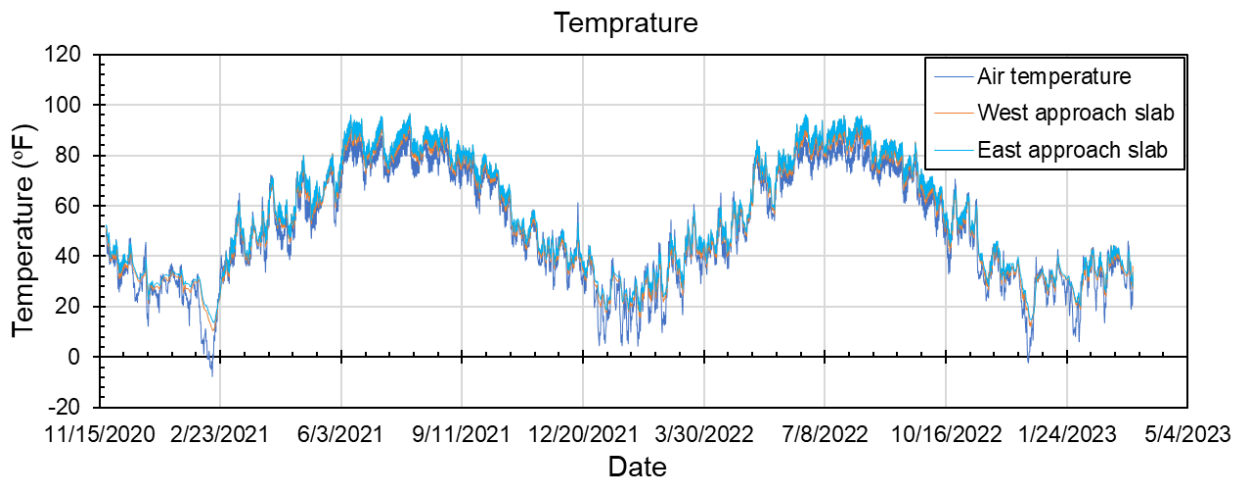

Figure 4.51. Polk County 120—air and concrete slab temperatures

Figure 4.52 and Figure 4.53 show joint expansion versus concrete temperatures to visualize joint movement with expansion and contraction of the bridge. Positive values correspond to bridge contraction, in which the approach slab pulls away from the sleeper slab. As can be seen in the figures, overall the joints between the approach slabs and sleeper slabs appear to be functioning correctly in terms of the movement that is supposed to be accommodated at those locations. The movement between the approach slab and the abutment was found to be significantly low, indicating a good connection. A strong linear relationship with temperature for gauges EAC4 and WAC4 indicates that the joint opens and closes depending on expansion and contraction of the bridge. As the temperature decreases, the bridge contracts and pulls on the approach slab, inducing tension.

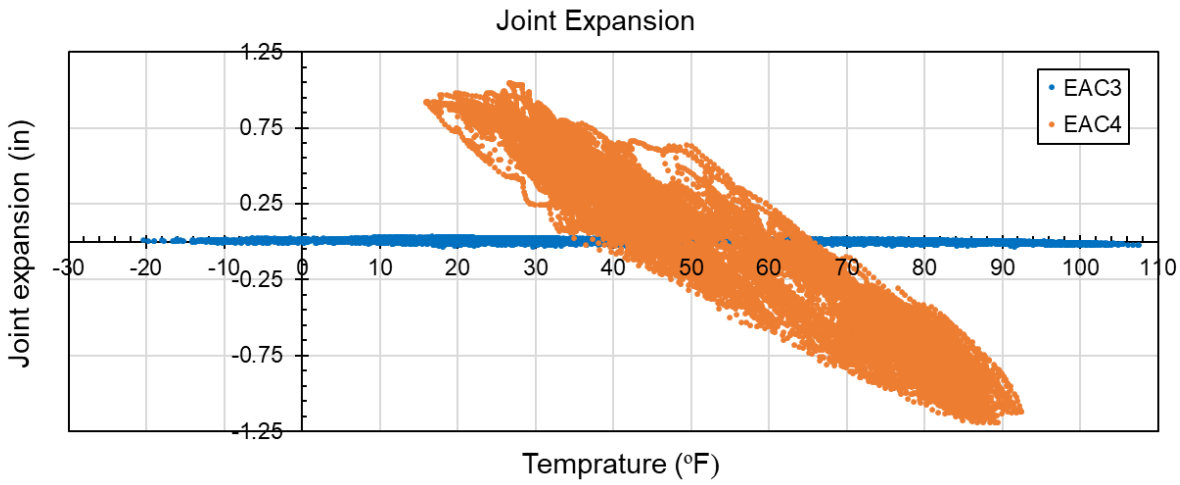

Figure 4.52. Polk County 120—measured longitudinal bridge expansion at east end

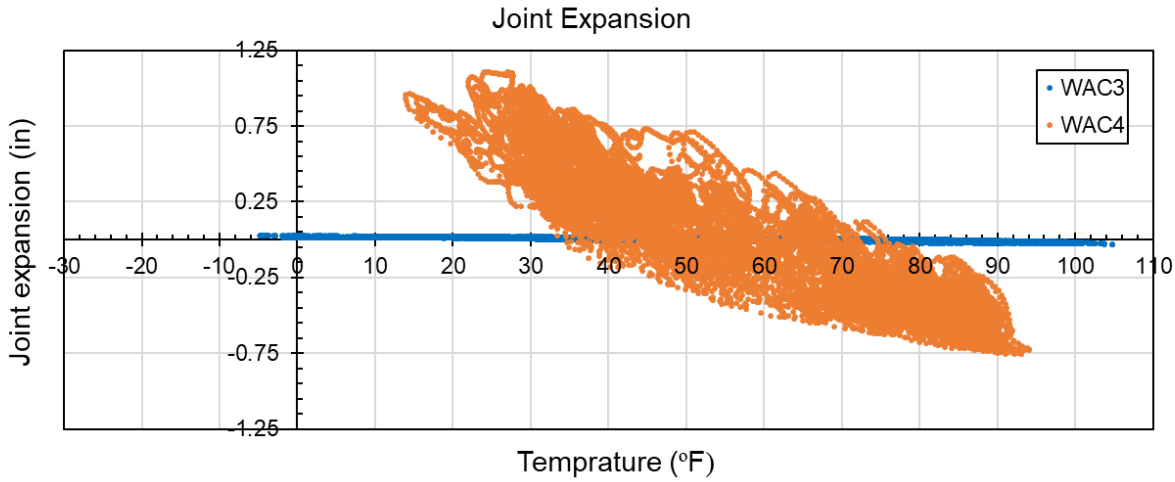

Figure 4.53. Polk County 120—measured longitudinal bridge expansion at west end

Plots of data from each gauge are not included here for the sake of brevity, but a representative set of data from gauges EA5 and EA6 at the east and west abutments can be seen in Figure 4.54 and Figure 4.55. It was found that the recorded strains ranged from -150 to 160 με.

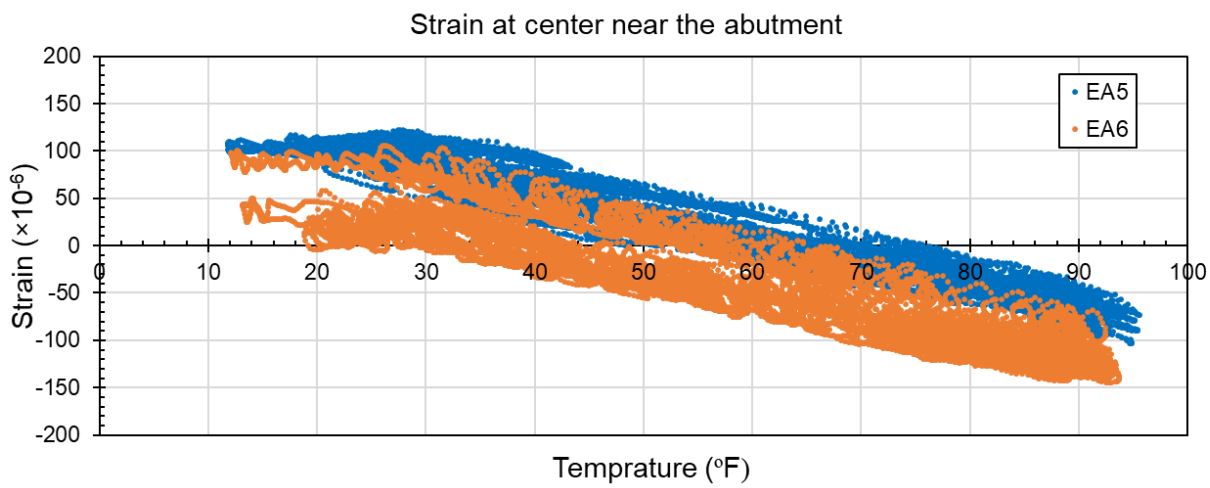

Figure 4.54. Polk County 120—measured strains, EA5 and EA6

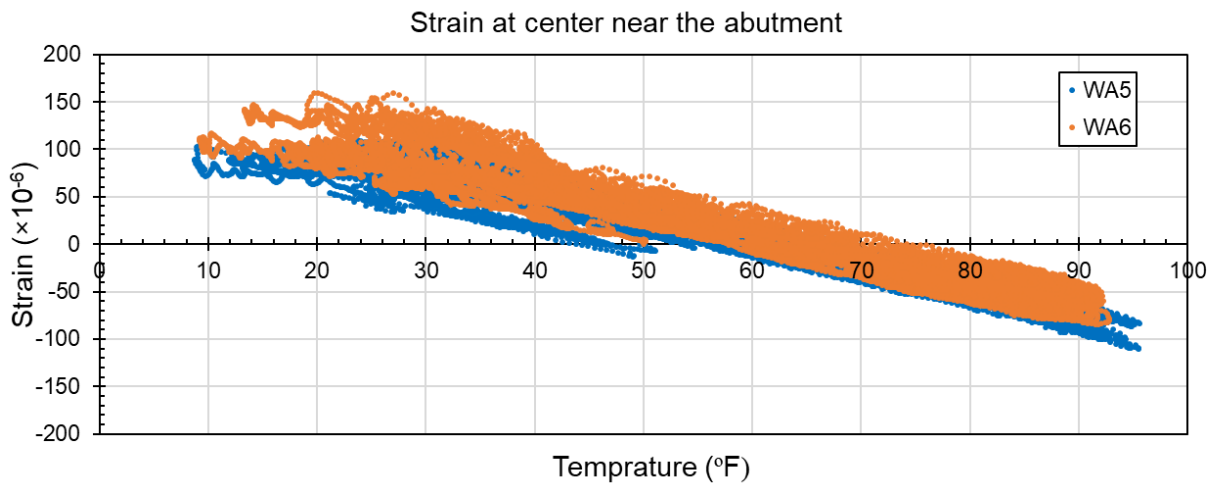

Figure 4.55. Polk County 120—measured strains, WA5 and WA6

A linear trend was found between strains and temperatures, which was also observed for the gauges in other locations (Figure 4.56 through Figure 4.59).

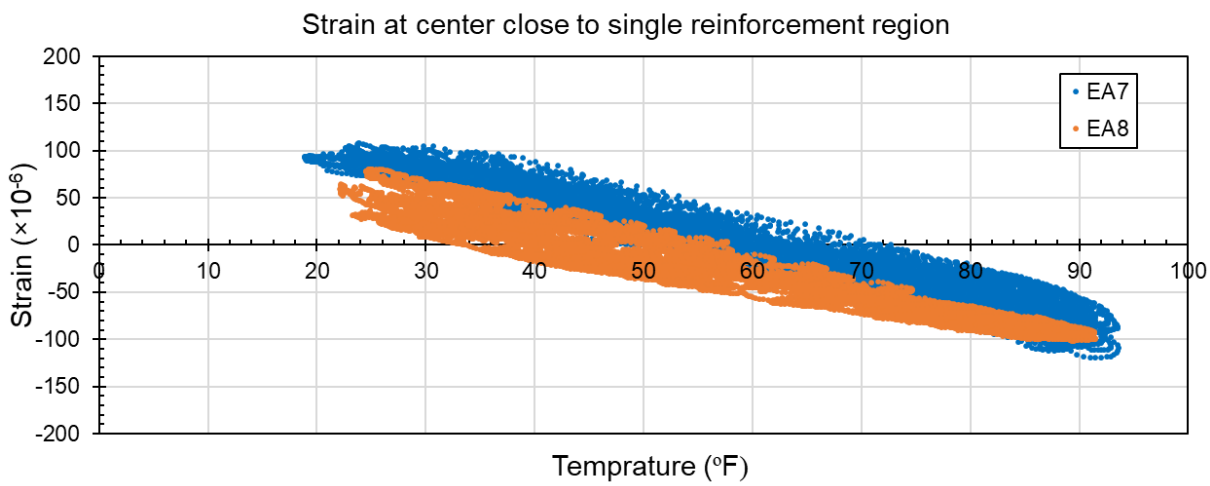

Figure 4.56. Polk County 120—measured strains, EA7 and EA8

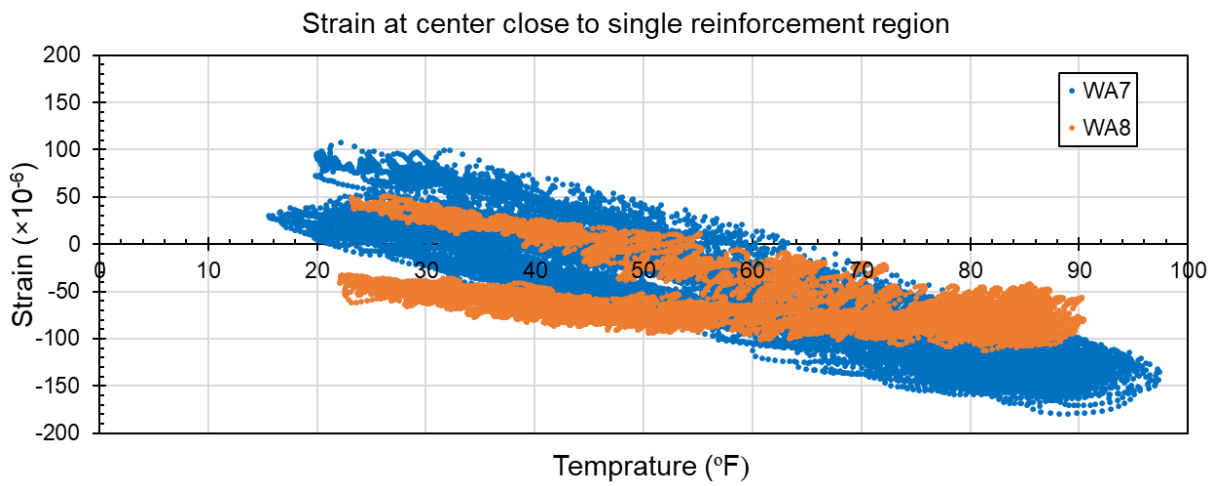

Figure 4.57. Polk County 120—measured strains, WA7 and WA8

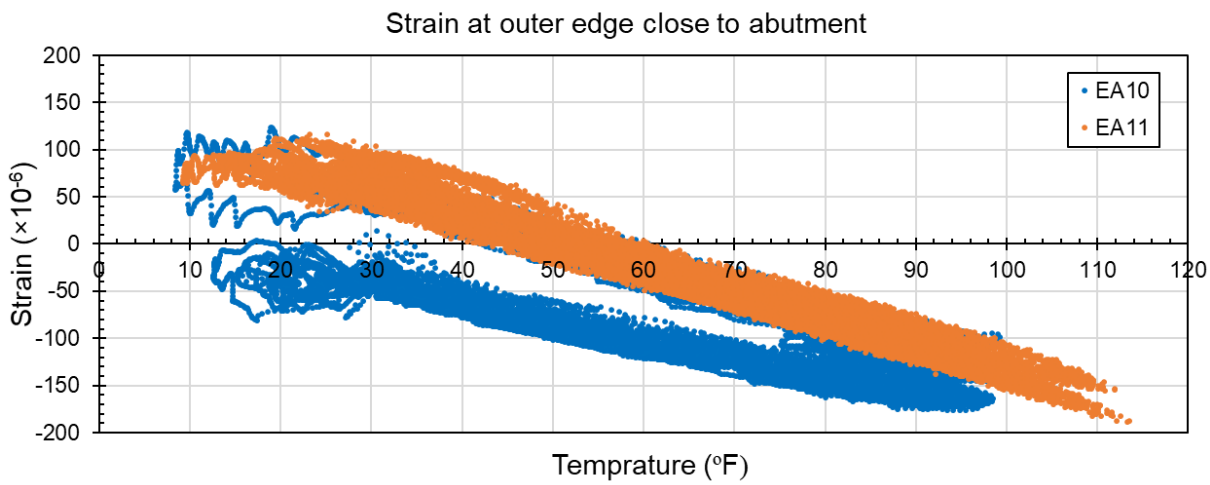

Figure 4.58. Polk County 120—measured strains, EA10 and EA11

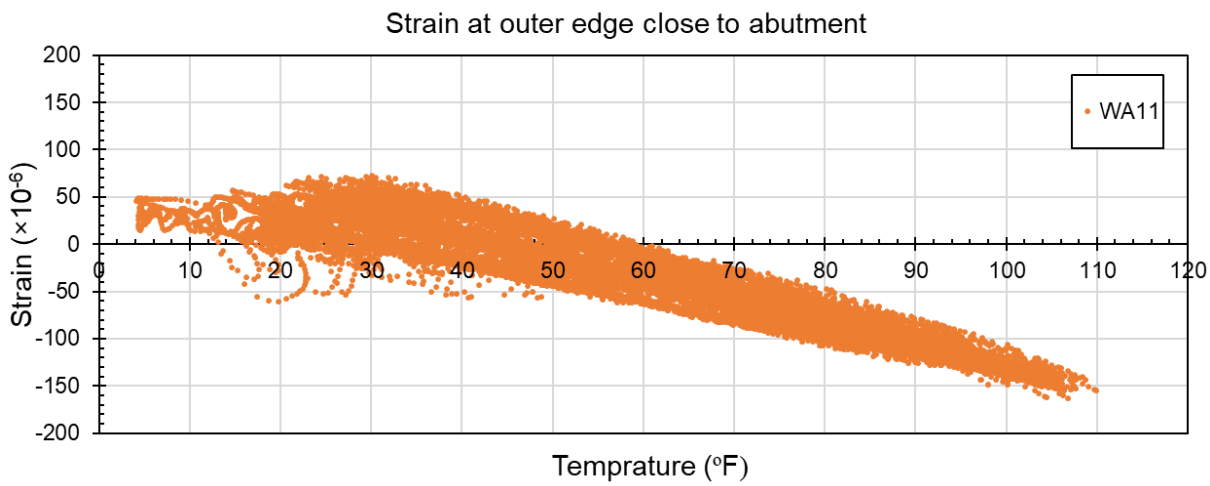

Figure 4.59. Polk County 120—measured strains, WA10 and WA11

The plots of strains versus temperatures in the abutment ties can be seen in Figure 4.60 and Figure 4.61. As can be observed in the figures, the strains ranged from -135 to 155 με, indicating a good connection between the abutment and the approach.

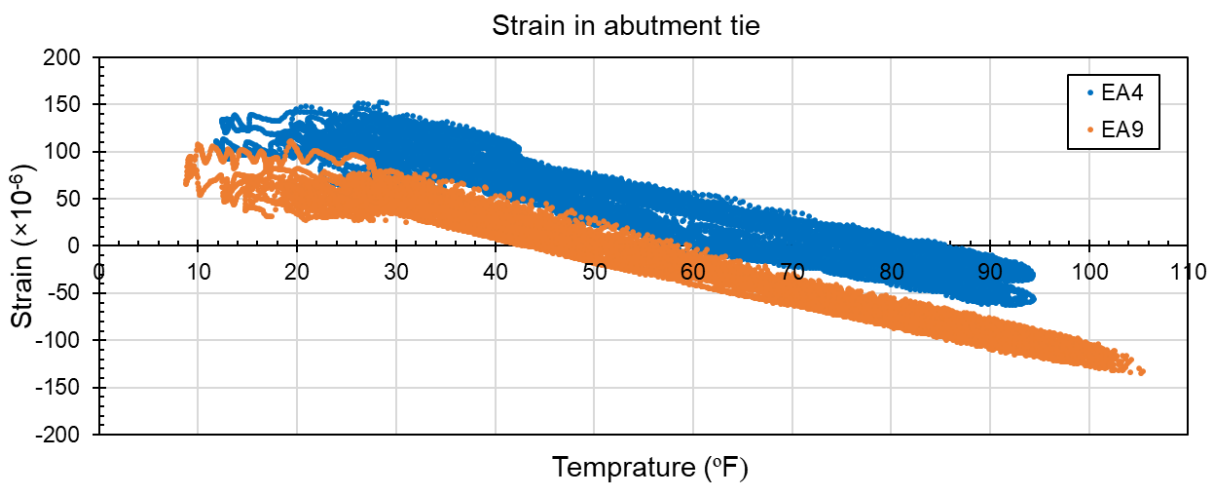

Figure 4.60. Polk County 120—measured strains in the ties, EA4 and EA9

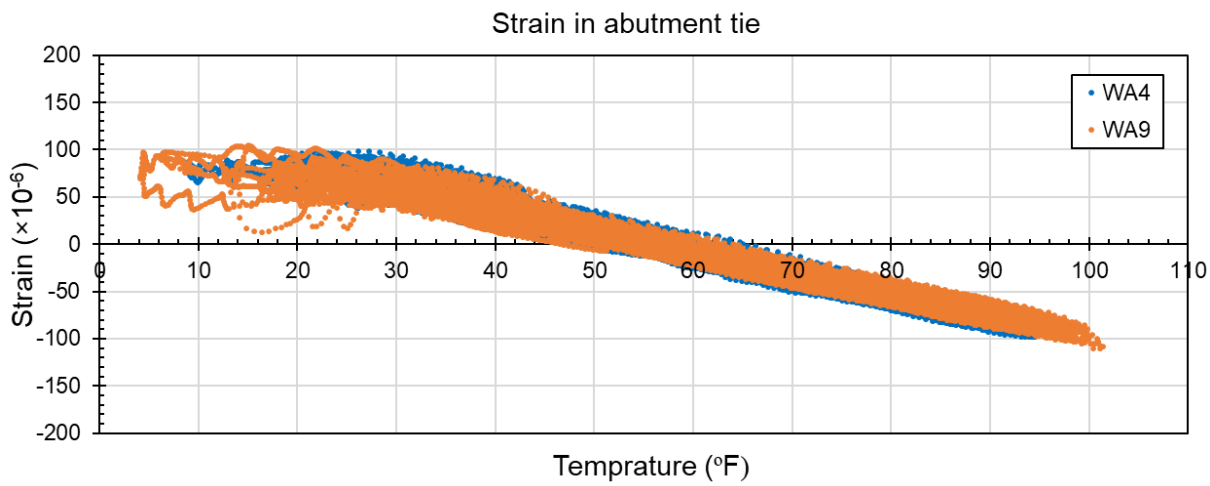

Figure 4.61. Polk County 120—measured strains in the ties, WA4 and WA9

4.5. Butler County 118

Butler County 118 is a new construction bridge located on IA 3 over the West Fork Cedar River in Butler County, Iowa. The bridge is 498 ft long and 44 ft wide with five spans and a skew angle of 15 degrees. It was selected for monitoring due to the adjusted design used for one of the abutments.

In this bridge, the west abutment was designed as an integral abutment, while the east abutment was constructed as a semi-stub abutment. In the design process, the second pier was fixed such that the presumed thermal expansion length to the east abutment was 325 ft. If this bridge were symmetrical with respect to the fixed pier/east abutment, the bridge length would equal 2 × 325 ft = 650 ft, which, according to current practice, would require stub abutments. However, the design team wanted to choose an abutment type for the east side of the Butler County 118 bridge that had the potential to replace stub abutments for even longer structures (e.g., +1,000 ft bridge lengths). Therefore, they developed the semi-stub abutment for this purpose featuring the following details:

- The approach slab is tied.
- An inverted-T sleeper slab is used similar to that used in Road Design Standard BR-205. The sleeper slab has a spread footing with no pile support.
- The expansion joint at the sleeper slab is a preformed, precompressed, self-expanding sealant system with a silicone precoated surface.
- The abutment wings are pushed out, and the barrier rail is mounted on the approach slab rather than the wings.
- The gap between the abutment diaphragm and backwall is 7 in. to provide some working room for the contractor, considering the total estimated thermal movement of 2.5 in.
- The approach slab was designed not to bear on the backwall. This should help to prevent a pivot point that would be detrimental to the approach slab tie bar and would likely open the gap between the approach slab and the bridge deck, creating more leakage. Two layers of 1

in. by 2 ft wide resilient joint filler for the full width of the approach slab are incorporated to maintain the gap between the top of the backwall and the approach slab.

- The backwall is simply designed to keep earth pressure off of the superstructure, which should help prevent ratcheting for skewed bridges.
- At a minimum, the backwall is designed for at-rest horizontal earth pressure and a horizontal live load surcharge (even though it is unlikely that a live load surcharge would ever be present).
- To prevent fill from spilling from between the top of the backwall and the approach slab onto the beam seat, a butyl rubber membrane was fastened with waterproof adhesives to the soil surface of the backwall all the way to the bottom of the resilient joint filler.
- Hooked bars in the joint filler and butyl membrane were used to attach those components to the embankment fill so they would not be displaced when the approach slab concrete was poured.

The overall configuration of the east approach slab as well as the east and west abutment sections are provided in Figure 4.62.

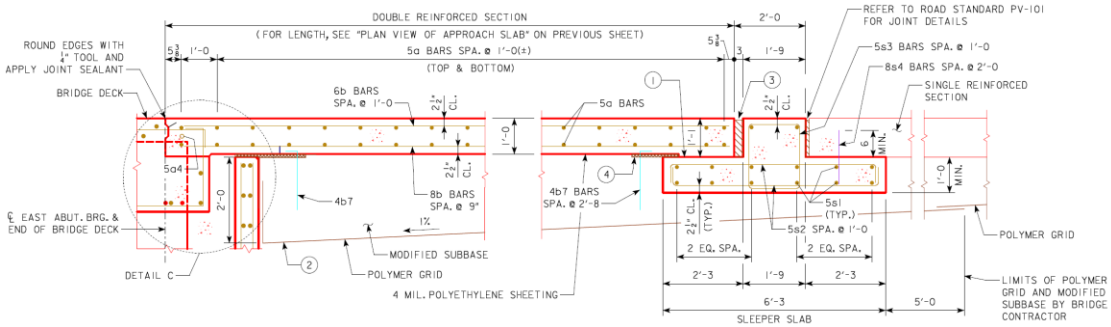

East approach slab section

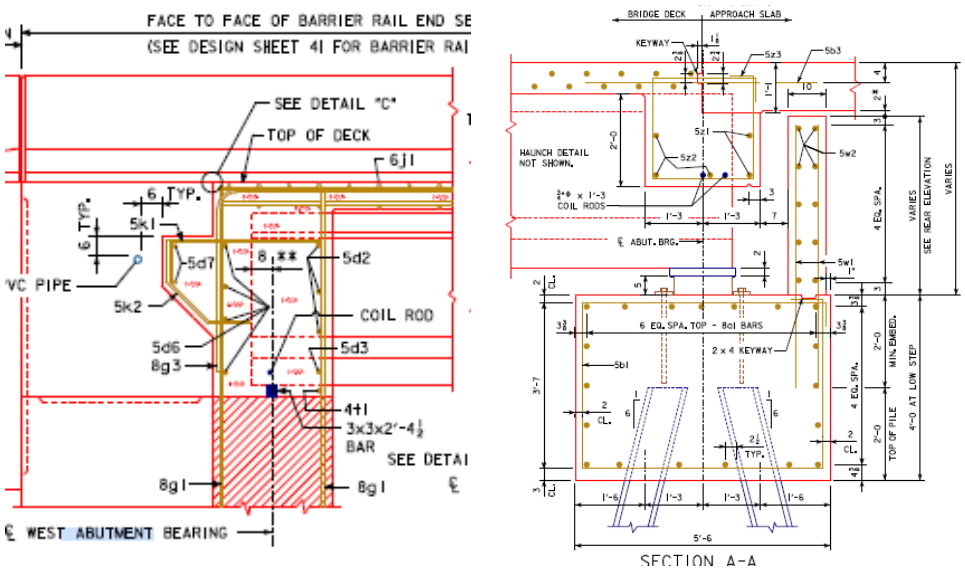

West abutment East abutment

Iowa DOT

Figure 4.62. Butler County 118—approach slab section and dimensions

The instrumentation plan can be seen in Figure 4.63. Both the west and east ends of the bridge were outfitted with identical sensors. Six strain gauges were placed throughout the slab across the width and at each end near the abutment. Another four strain gauges were placed close to the approach-slab-to-sleeper-slab joint at each end. These gauges were expected to capture axial strain and force in the slab due to temperature effects, along with any bending. A total of ten strain gauges were placed in each approach slab. Two crackmeters were also installed at each bridge end to measure movement in the approach-slab-to-abutment joint.

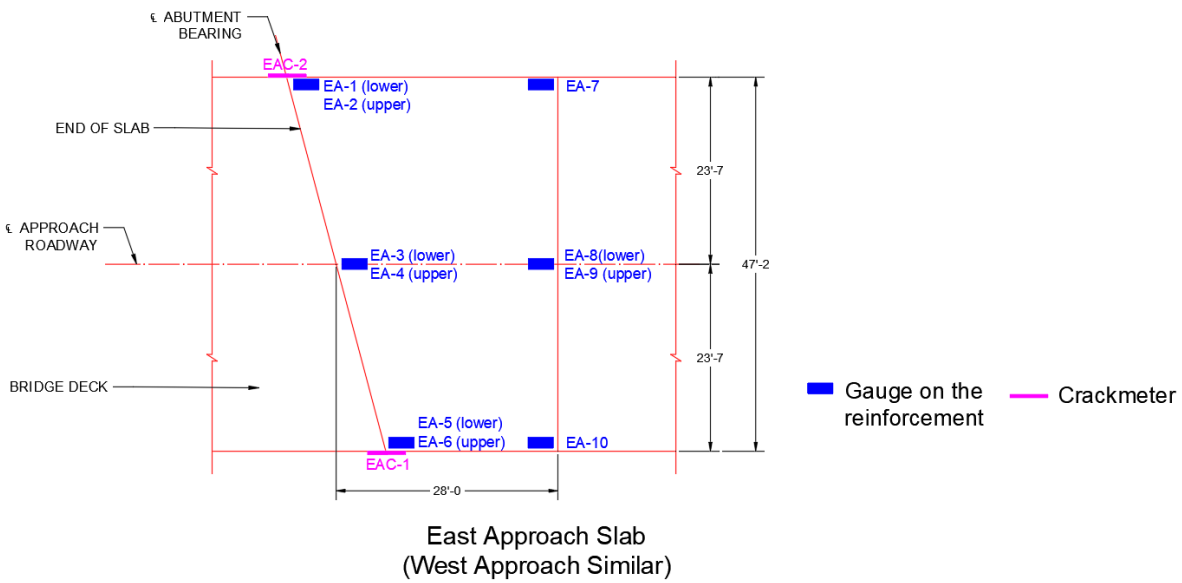

Figure 4.63. Butler County 118—approach slab instrumentation plan

4.5.1. Butler County 118 Strain Gauge Installation Process

Strain gauges were installed in a layout similar to that used for the previous bridges. Ten strain gauges were zip-tied to the top and bottom longitudinal bars to measure strains in the longitudinal direction. Figure 4.64 shows some photographs from the strain gauge installation process on the Butler County 118 bridge.

East side West side

Figure 4.64. Butler County 118—strain gauges installed on the longitudinal rebars

4.5.2. Butler County 118 Crackmeter Installation Process

Two crackmeters were placed over the joints between the approach slab and the abutment (Figure 4.65). The installation process consisted of placing a foam block prior to concrete placement to create a pocket so that the crackmeter could be placed later. A wooden cover was used to close the pocket and protect the crackmeter after installation.

Foam placed for crackmeter installation Crackmeter installation

Figure 4.65. Butler County 118—crackmeter installation across the abutment-to-approach-slab joint

4.5.3. Butler County 118 Datalogger Installation

After all of the instrumentation was installed, the wires were run though the bridge ends to dataloggers placed at west and east ends. The dataloggers were installed on October 21, 2021, in reasonable temperatures and without any precipitation.

4.5.4. Butler County 118 Data Collection and Processing

Data were retrieved from the datalogger on May 30, 2023. Air temperatures were taken by the dataloggers, which were placed on the abutment faces, protected from sunlight. The minimum air temperature reached was -10°F on January 26, 2022, and the maximum air temperature of 88°F was reached on May 12, 2022 (Figure 4.66). Concrete temperatures in the east and west ends were taken by averaging the strain gauge temperatures and are included in the plot with the air temperatures. Concrete has a thermal lag due to its insulation properties and does not react to changes in air temperature immediately. The maximum temperature in the approach slab was 98°F, 10°F higher than the maximum air temperature; the minimum temperature in the approach slab was 2.8°F, 12.8°F higher than the minimum air temperature.

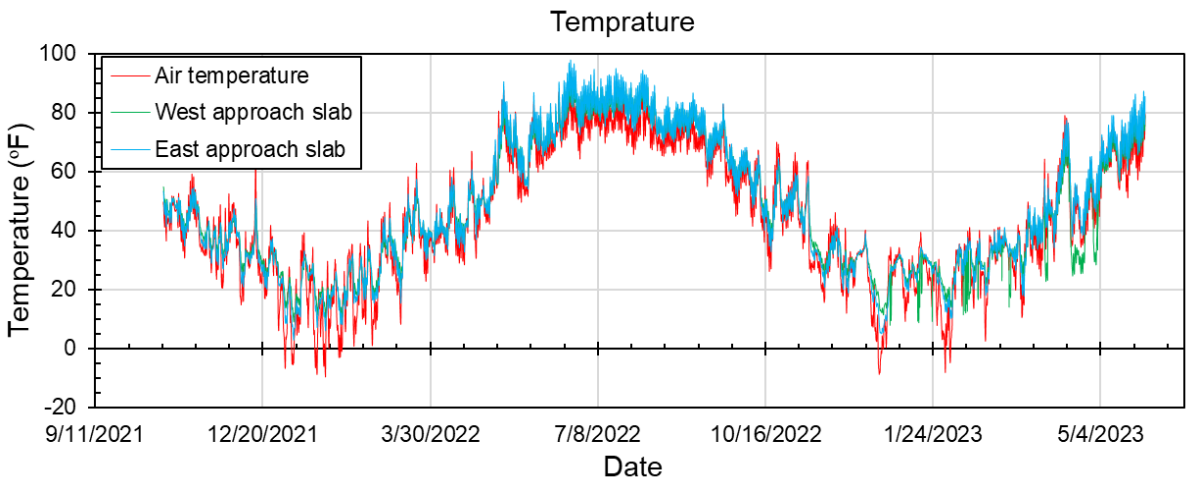

Figure 4.66. Butler County 118—air and concrete slab temperatures

Figure 4.67 and Figure 4.68 show approach-slab-to-bridge-deck joint expansion versus concrete temperatures to visualize joint movement with expansion and contraction of the bridge. Positive values correspond to bridge contraction, in which the approach slab pulls away from the sleeper slab. The movement between the approach slab and the abutment is between -1.2 to 1.0 in. at the east side and between -0.3 to 0.8 in. at the west side. A strong linear relationship with temperature indicates that the joint opens and closes with the movement of the bridge.

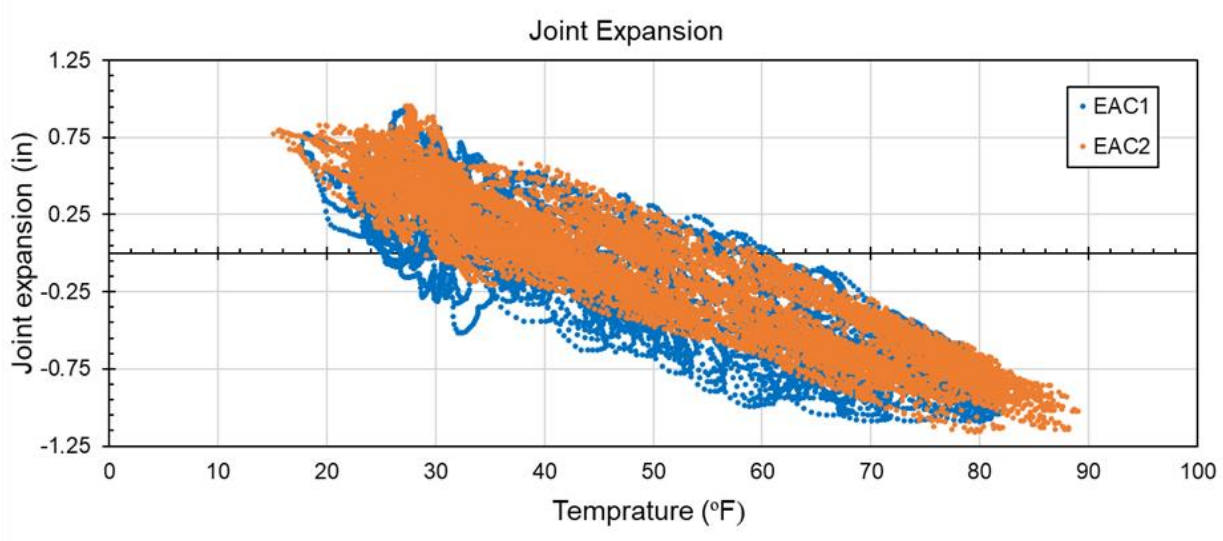

Figure 4.67. Butler County 118—measured longitudinal bridge expansion at east end

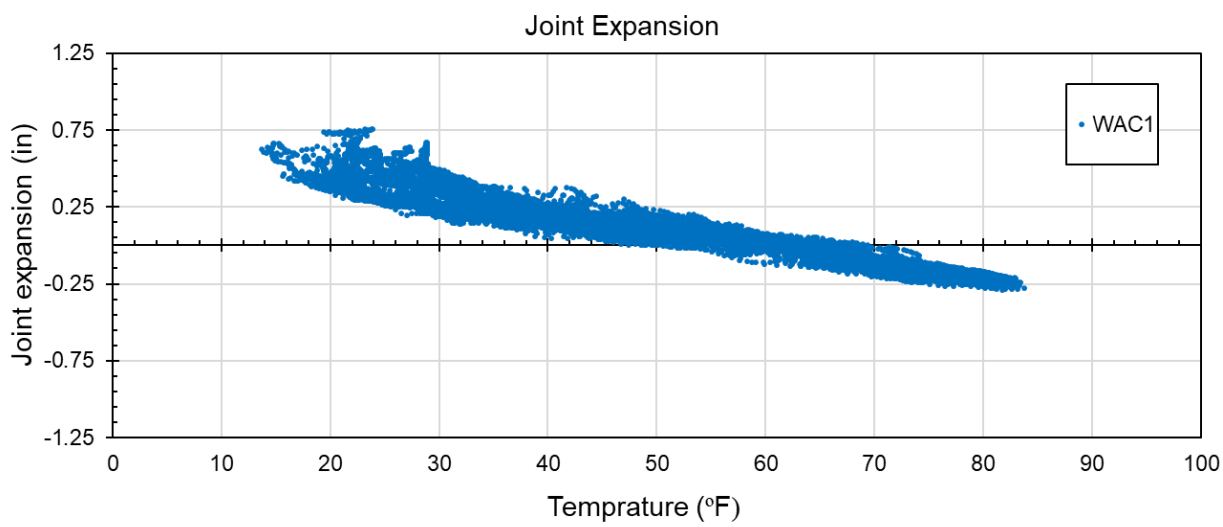

Figure 4.68. Butler County 118—measured longitudinal bridge expansion at west end

Figure 4.69 shows the strain versus temperature plots of the sensors close to the approach-slab-to-sleeper-slab joints. All of the graphs follow an almost linear trend, indicating high tensile strains corresponding to low temperatures and high compressive strains corresponding to high temperatures. The strain recordings in the middle part of the joint and the corners cover similar ranges from -160 με to 130 με.

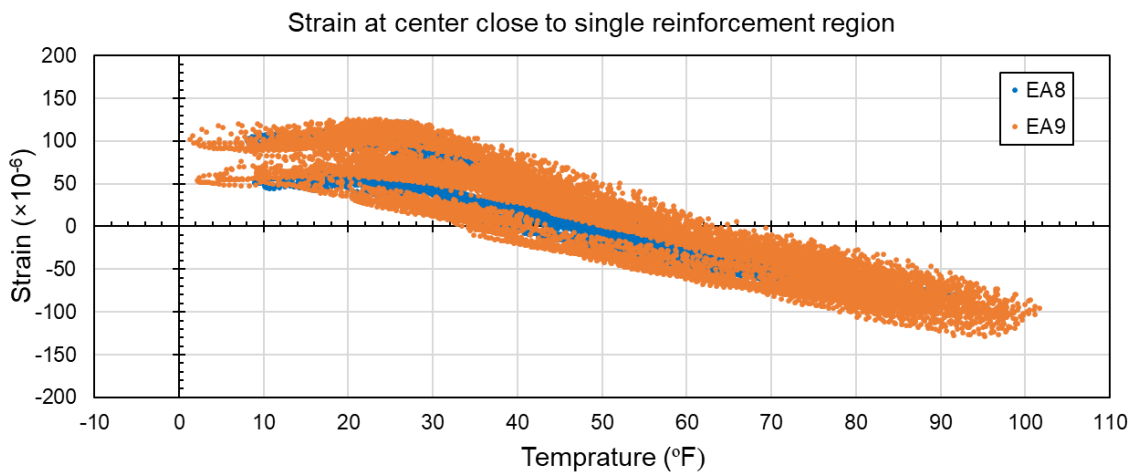

East Approach Slab Middle Part

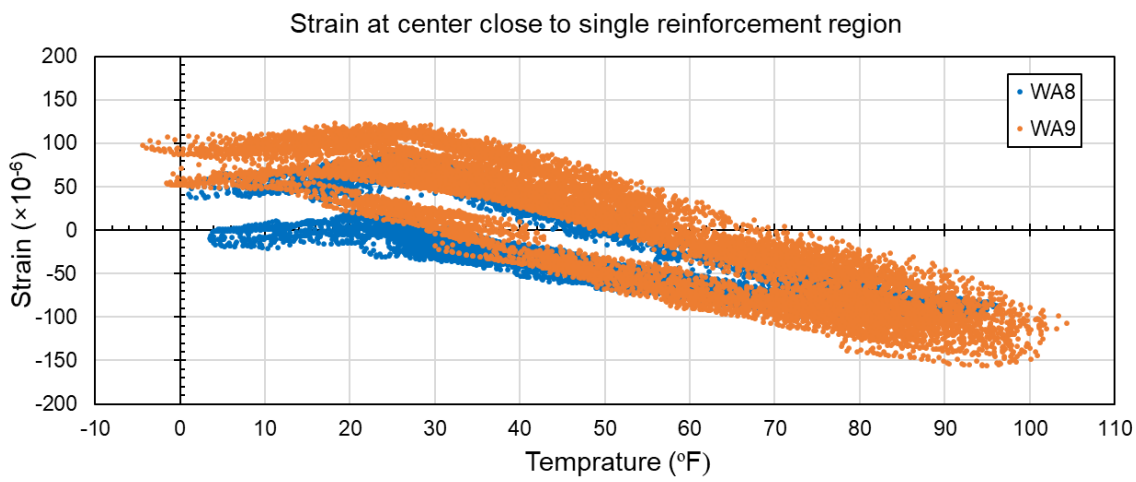

West Approach Slab Middle Part

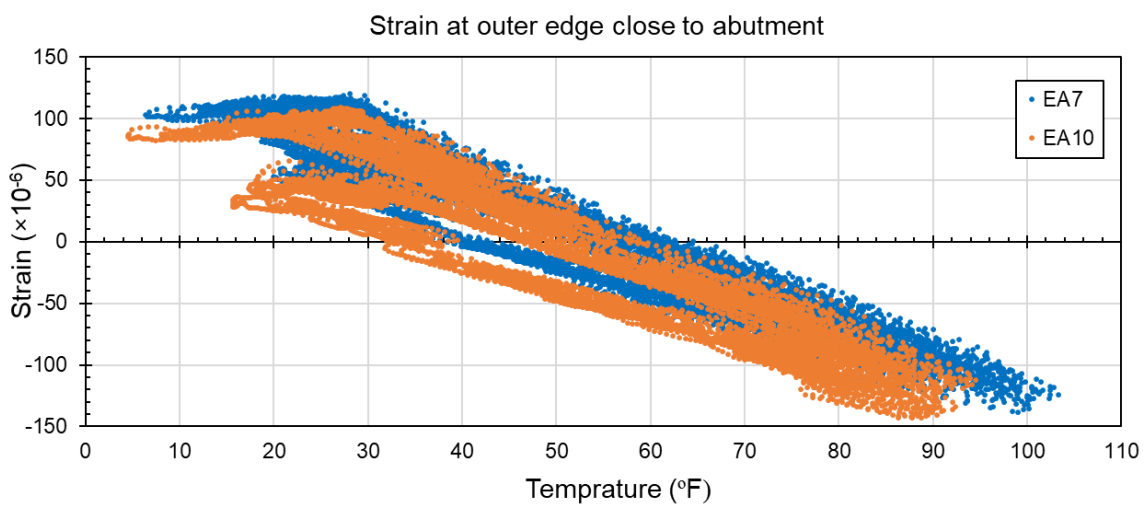

East Approach Slab Corners

Figure 4.69. Butler County 118—measured strains at the approach-slab-to-sleeper-slab joint

The strain data versus temperature plots at the joints between the approach slab and the bridge deck for the middle part of the approach slabs are shown in Figure 4.70. The bottom bars at both ends show normal behavior, with linear trends that correspond reasonably to high and low temperatures. The east side bottom bars show strains ranging from -80 με to 180 με, which is a slightly larger range compared to the west side bottom bars.

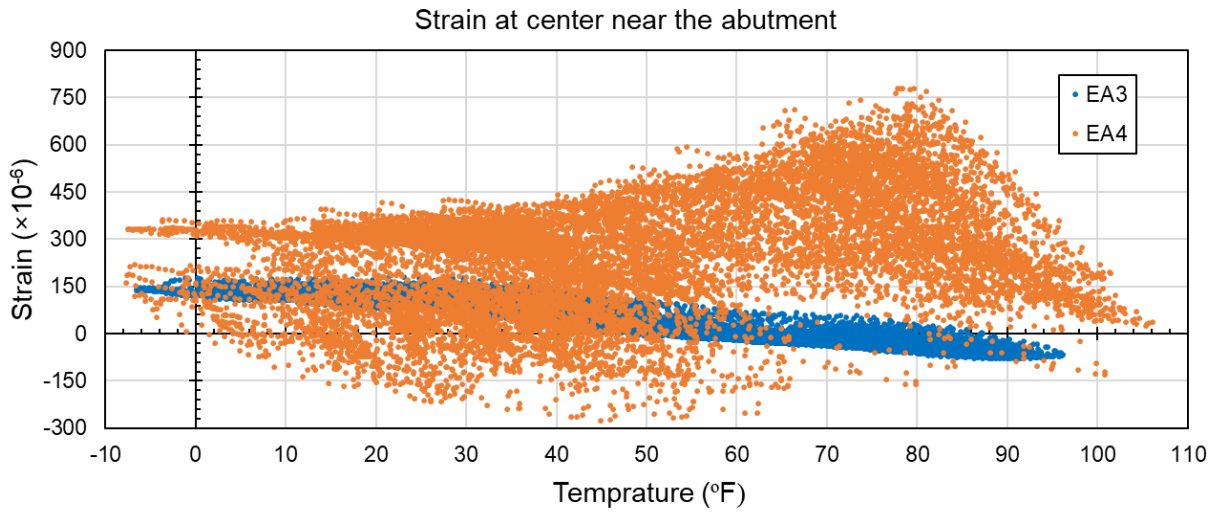

East Approach Slab

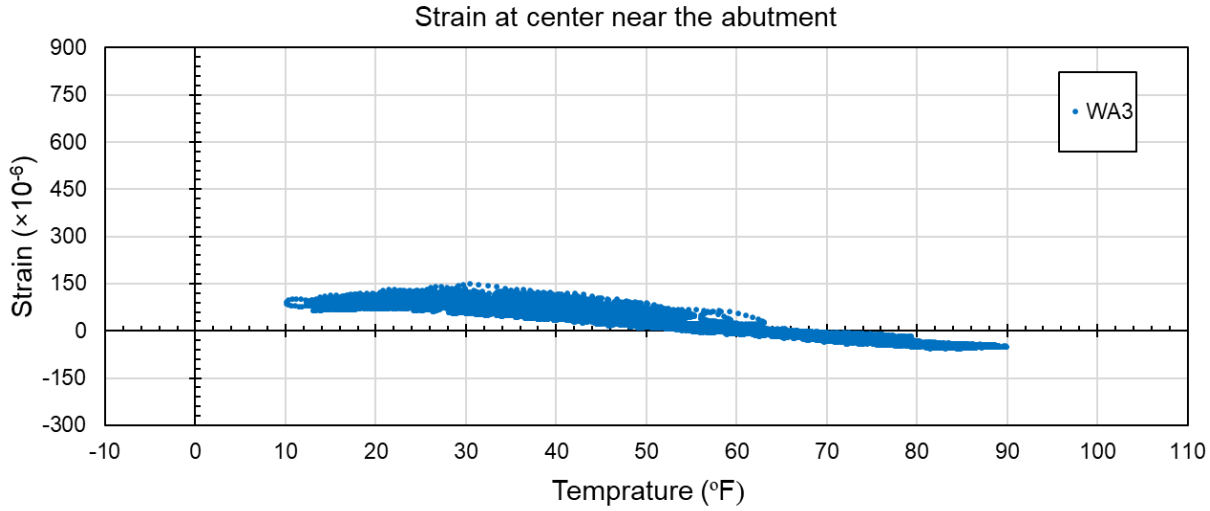

West Approach Slab

Figure 4.70. Butler County 118—measured strains at the approach-slab-to-bridge-deck joint, middle

Figure 4.71 presents the same plots for the acute and obtuse corners of the approach slabs. The east side corners show different patterns with respect to temperature. The top and bottom bars at the acute corners show almost linear behavior. The bottom bars mainly show compressive strains after the first cycle of cold and warm temperatures, while the top bars are mainly in tension even at high temperatures. As such, the strains in the bottom and top bars of the acute corners range

from -215 με to 165 με and from -90 με to 210 με, respectively. However, the behavior of the approach slab is different in the obtuse corners. The bottom bars show normal linear behavior, with strains approaching zero values after the first cycle of cold and warm temperatures, ranging from -130 με to 130 με. On the other hand, the top bars are mainly in tension and do not show any particular trend against large temperature changes. The strains range from small compressive strains of -60 με to large tensile strains of 460 με.

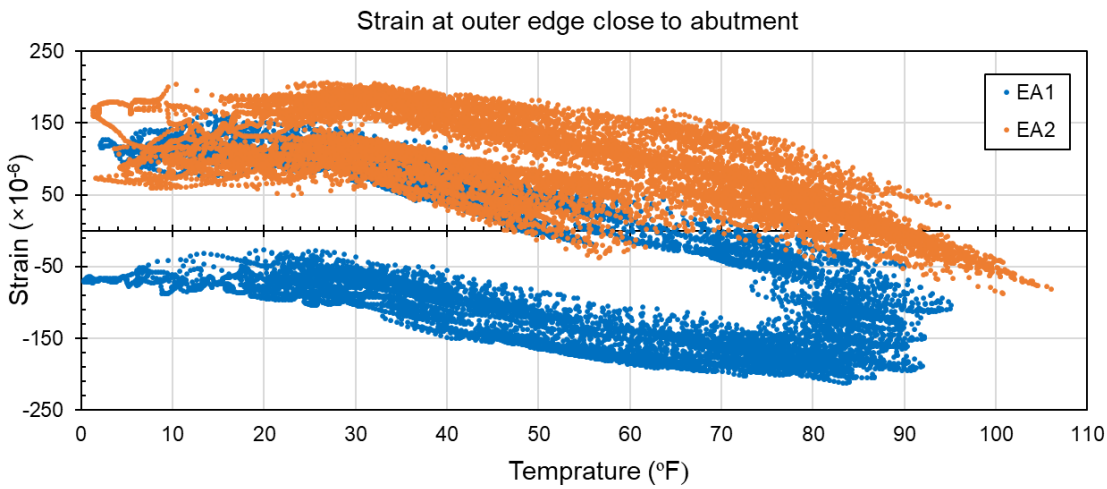

East Approach Slab Acute Corner

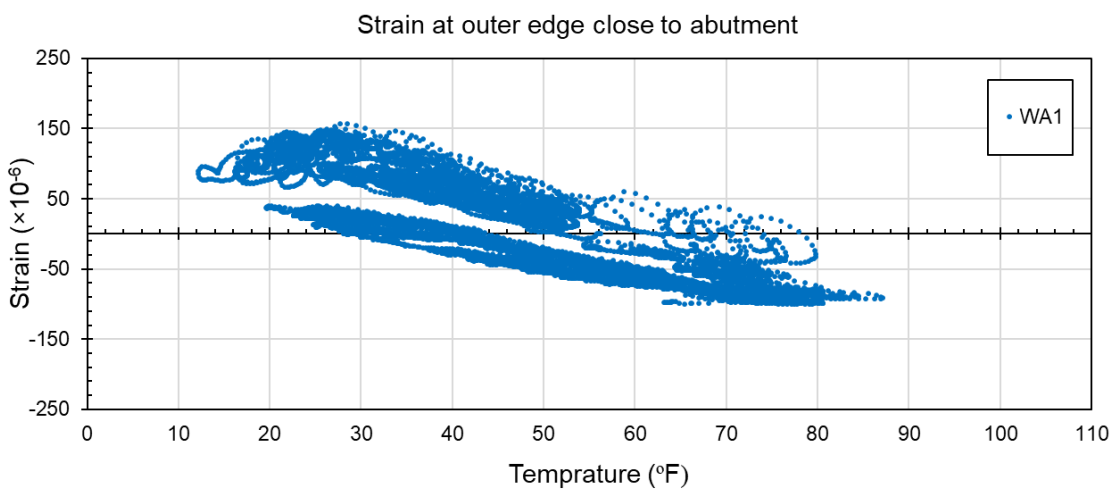

West Approach Slab Acute Corner

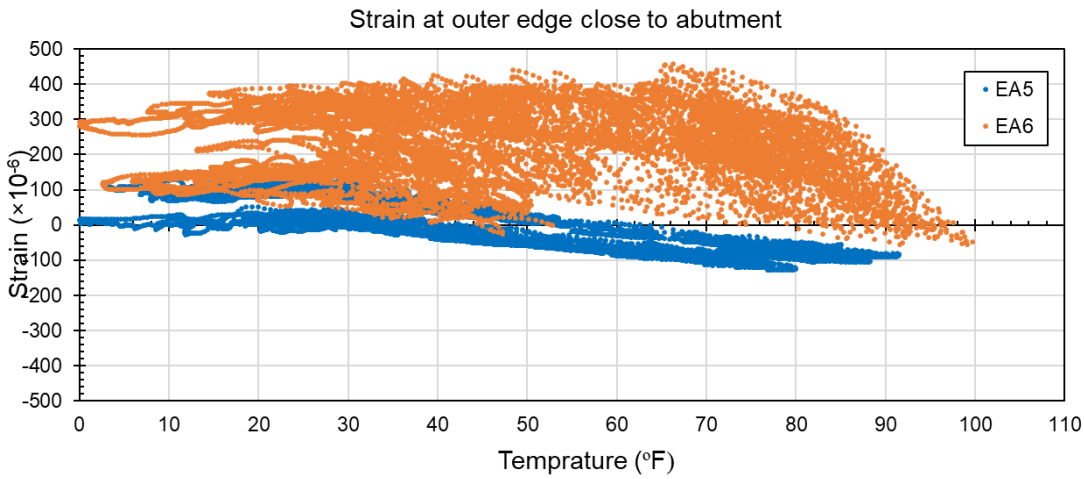

East Approach Slab Obtuse Corner

Figure 4.71. Butler County 118—measured strains at the approach-slab-to-bridge-deck joint, corners

Figure 4.72 presents the strain versus temperature plots as well as the time series of the top and bottom bars of the east approach slabs. For the bottom bars, the strain gauges show similar behavior from the start of data recording all the way through June 2022. After this date, the strain data drift apart, with the middle sensor data showing normal behavior, the acute corner sensor data decreasing to show only compressive strains, and the obtuse corner sensor data approaching close to zero values. For the top bars, the acute corner shows normal behavior; however, the tensile strains of the second year are larger than those of the first year.

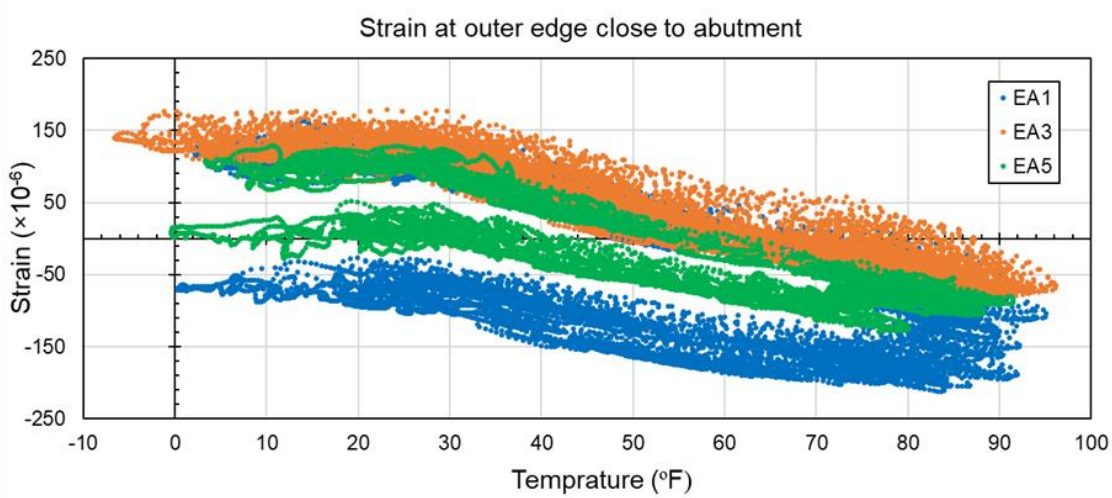

East Approach Slab Bottom Bars – Strain Versus Temperature

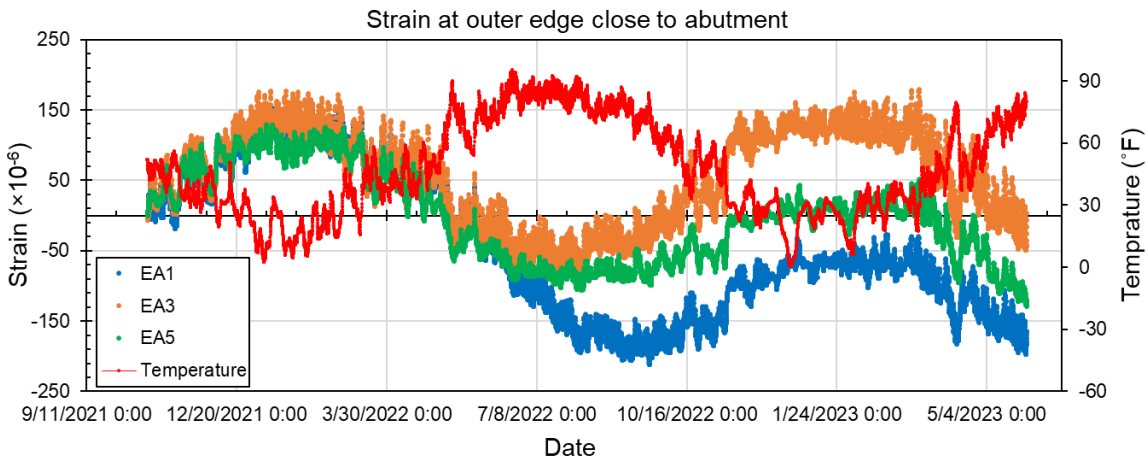

East Approach Slab Bottom Bars – Time Series

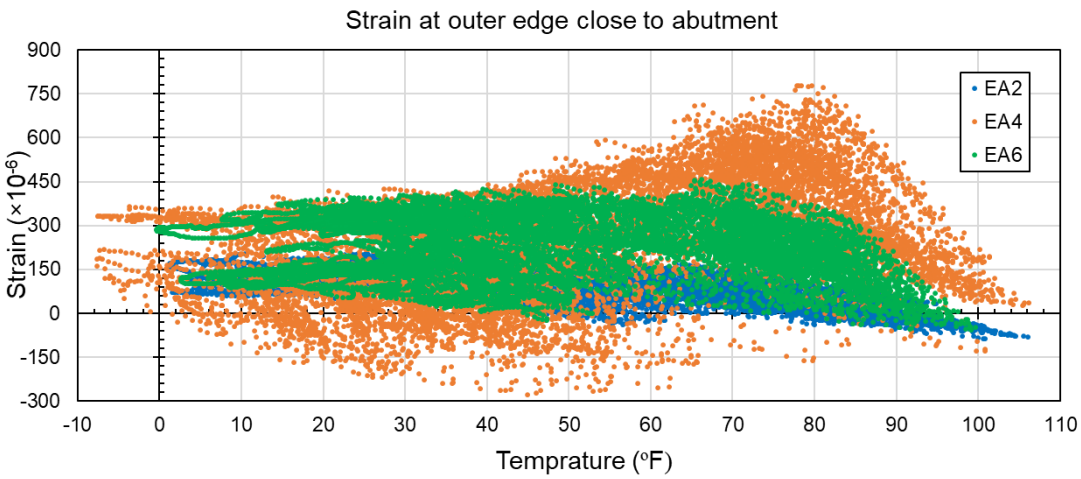

East Approach Slab Top Bars – Strain Versus Temperature

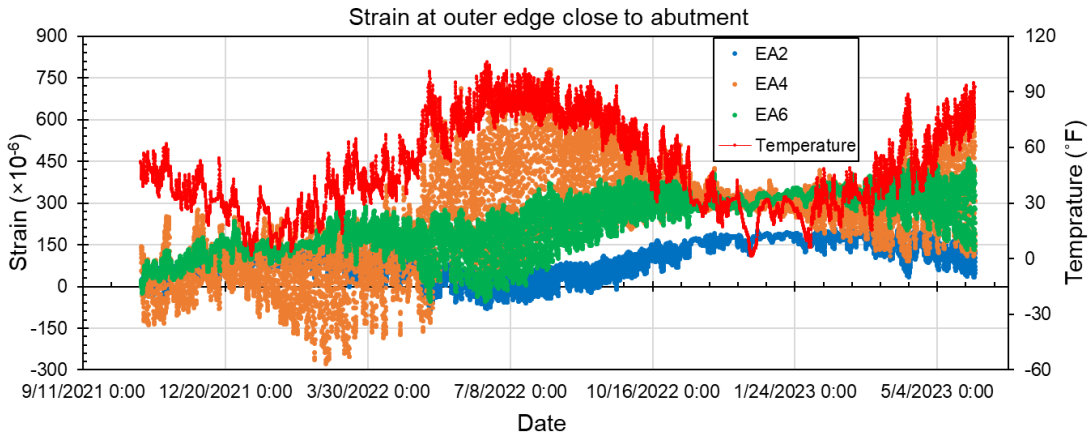

East Approach Slab Top Bars – Time Series

Figure 4.72. Butler County 118—measured strains at the east approach-slab-to-bridge-deck joint

The high tensile strains of the top bars could be attributed to the minor transverse crack observed on the east approach slab along the joint between the approach slab and the abutment during the last visit to the bridge on May 30, 2023 (Figure 4.73). The connection's rigidity could also play a role in the crack's development. Additionally, the working room gap between the abutment diaphragm and the backwall pushes the backwall toward the middle part of the approach slab, which could make a detrimental pivot point if the approach slab ends up bearing on the backwall. The additional effects from the live loads and the settlement of the initial approach slab might increase the chance of forming a pivot point that could finally result in crack development.

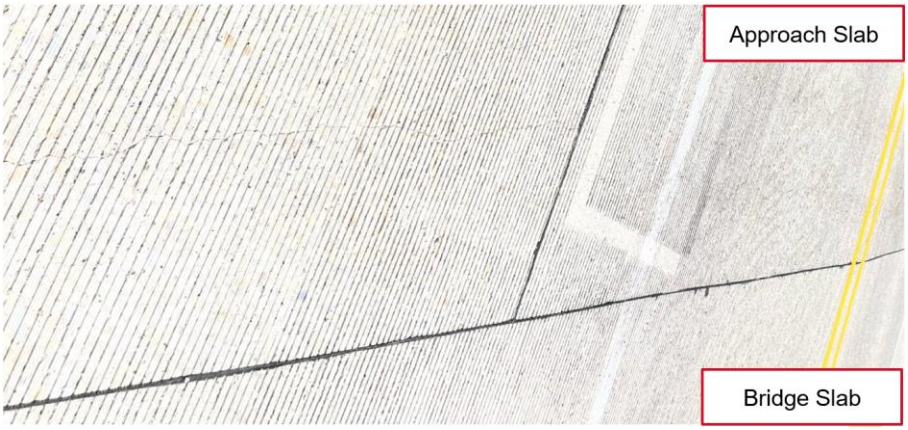

Figure 4.73. Butler County 118—transverse crack on the east approach slab

CHAPTER 5. FINITE ELEMENT MODELING

FE models of various bridge ends were created using ABAQUS finite element analysis (FEA) software. The purpose of the models was to represent the behavior of the bridge approach slabs and their response to bridge thermal movement and thus to allow for a parametric study through changes to different model attributes. The models were limited to only the first section of the approach slab, the soil beneath the slab, and a portion of the abutment. The study did not aim to accurately model the thermal expansion of the bridge deck but rather sought to apply the displacement caused by the theoretical expansion of the bridge to the abutment, simulating the bridge pushing/pulling on the approach slab while simultaneously including the appropriate temperature change that corresponds to the maximum bridge movement. The results are focused on the behavior of the approach slab itself and the steel tie bars in response to thermal movement. Ideally, an FE model would be able to capture every aspect of approach slab behavior, but simplifications must be made due to computational requirements and idealized material models.

In response to concerns about the performance of approach slabs used with skewed bridges (or other bridges not currently allowed to use tied approaches), it is clear that, when performing properly, tied approach joints act less like a joint and more like a continuation of the deck. They can prevent water and deicing solution from leaking into the bridge embankment and help to avoid the associated issues. The FE models were intended to help illustrate how friction force is carried by the tie bars and give some insight into how tie bar type and bridge skew affect behavior. Improvement in the performance of tied approach joints is anticipated to improve bridge service life.

A 3D model was chosen to allow for skew of the approach slab. 3D solid C3D8R elements were used for both the concrete approach slab and the soil below to allow for frictional contact between the two surfaces. A 2D model would have allowed for modeling of a deeper depth of soil under the approach slab and a more accurate representation of soil behavior and the interaction between the soil and the abutment. However, a 2D model does not in any way allow for bridge skew other than 0 degrees. It was also determined that replacing the soil with properly calibrated spring elements would not provide the same effects as a solid element with frictional contact, since friction is a nonconservative force.

Further to the base models of the Jasper County 118 and Story County 118 bridges, additional models were developed to investigate the settlement and erosion noted during the inspections. Another FE model was developed to numerically study the approach slab behavior of a highly skewed bridge (Shelby County 188) in order to evaluate the effects of a theoretical tied approach connection in the context of an overly high skew. A final FE model was created of a bridge in Washington County to study the effects of settlement on the damage observed at the tied connection between the abutment and the approach slabs.

5.1. Jasper County 118 FE Model

Model formation began with geometry taken from the Jasper County 118 plans. The approach slab and abutment are 28 ft wide to match the lane width of the bridge. A 10 in. thick trapezoidal shape approximates the geometry of the approach slab. A large soil block was created with the same shape, and the cut geometry function removed any overlapping volumes between the soil and both the approach slab and abutment to simulate good compaction against all surfaces with no voids. The model geometry can be seen in Figure 5.1. All models align the centerline of the bridge roadway with the X-axis, the vertical direction with the Y-axis, and the transverse direction with the Z-axis.

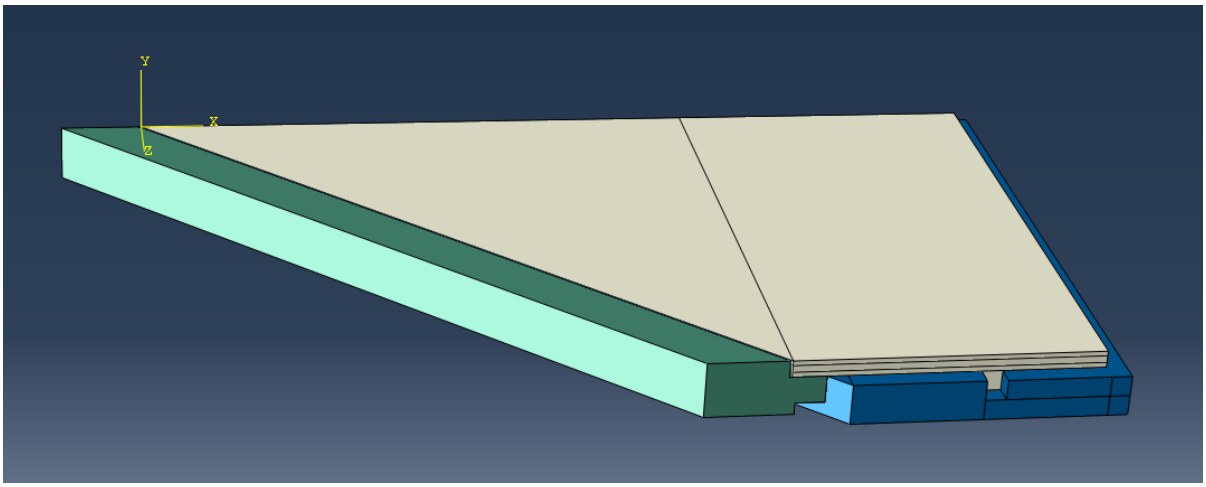

Figure 5.1. Jasper County 118—finite element model geometry

5.1.1. Material Properties

A standard 4 ksi compressive strength concrete was created per the Jasper County 118 bridge plans and applied to the approach slab and abutment. A Young's modulus of 3,605 ksi and a Poisson's ratio of 0.3 were used for linear-elastic behavior. Concrete stresses were expected to remain low, and given the scale of the model the use of a Concrete Damaged Plasticity model in ABAQUS was deemed unnecessary and unattainable.

The soil properties represented typical values for the "modified subbase" used by the Iowa DOT under approach slabs. Correspondence with the Iowa DOT provided a compacted unit weight of 140 pcf. A gradation table per Iowa DOT Article 4109.02 is provided in Table 5.1. Figure 5.2 shows the limits provided by the gradation table plotted on a grain size distribution chart. Classification using the Unified Soil Classification Chart (ASTM D2487) indicates that the modified subbase is a coarse-grained soil. Based on the fact that the curves provided fall mostly below the point included in red that corresponds to the #4 sieve and 50% passing, it is likely that most subbase material would be classified as a well-graded gravel (GW) or poorly graded gravel (GP). The modulus of elasticity was taken to be 20 ksi after finding a range of values from 14 to 30 ksi in the available literature for compacted gravel (Kaniraj 1988), and the gravel's Poisson's ratio was taken to be 0.35.

Table 5.1. Iowa DOT modified subbase gradation

Sieve	Size (in.)	Size (mm)	Percent Passing
1 ½”	1.5	38.1	100
¾”	0.75	19.1	70–90
#8	0.093	2.38	10–40
#200	0.0029	0.074	3–10

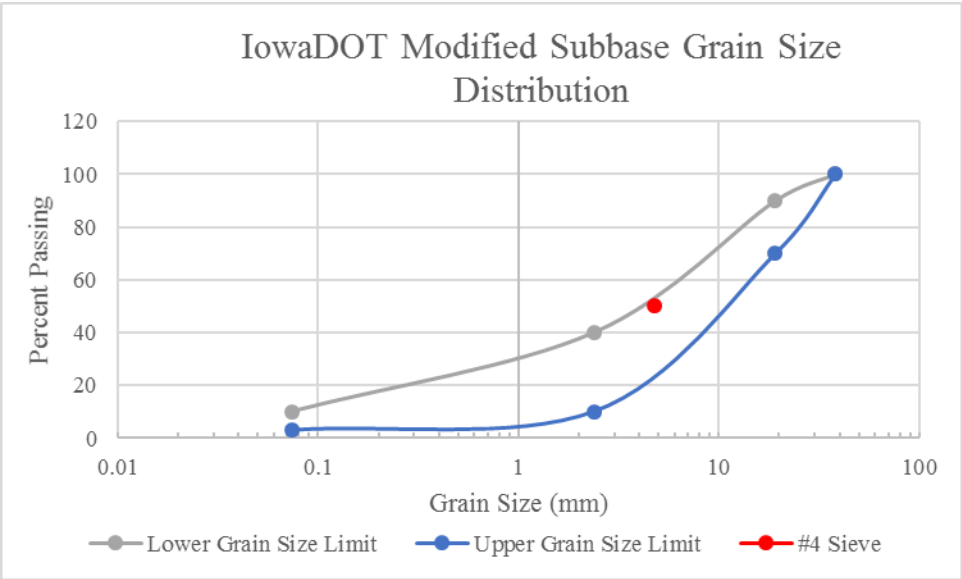

Figure 5.2. Iowa DOT modified subbase grain size distribution

Soil behavior was limited to linear-elastic behavior due to the nature of the analysis being performed and the desired results. The 3D soil elements are present only to provide a frictional surface to interact with the bottom of the approach slab simulating the friction between the approach slab and the soil beneath. The bearing capacity of the soil is of no concern, nor is the soil properties’ effect on the expansion of the bridge, since the expansion displacement is applied to the model as input. The vertical loading consists only of the self-weight of the slab, and the 3D solid elements chosen for representation of the soil provide minimal settlement of the approach slab.

5.1.2. Element Meshing

Element meshing was completed part by part (Figure 5.3). Due to the 45 degree skew, it was extremely difficult to maintain properly shaped elements and avoid poor element shapes. Meshing of the approach slab and soil proved to be more difficult than meshing of the abutment. Partition planes were used to divide the parts into segments. For the approach slab, partitions were used to split the part into a large triangular piece and several long rectangular pieces. The soil part was split up in a similar fashion. A size control applied after partitioning resulted in the desired mesh. Some elements produced warnings of poor shape; these elements occurred in the triangular portions of the parts, and an effort was made to adjust them. The approach slab and

soil mesh sizing were chosen to be the same size in order to provide better contact simulation results.

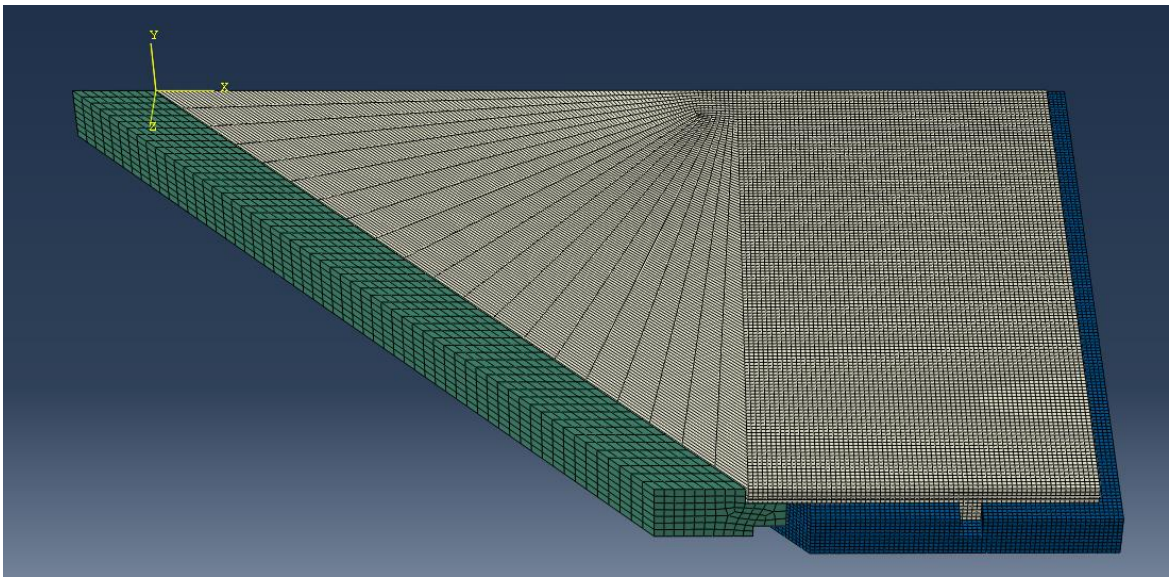

Figure 5.3. Jasper County 118—finite element model mesh

5.1.3. Boundary Conditions

The boundary conditions applied to the model aimed to replicate the real-life support conditions of the bridge (Figure 5.4). The base of the soil was fixed for all translation, and the sides of the soil not in contact with the abutment or footing were fixed in translation in the X and Y directions to contain the soil within an imaginary box. No boundary conditions were placed on the approach slab itself; however, the soil lug held the approach slab in place and prevented translation in the X direction.

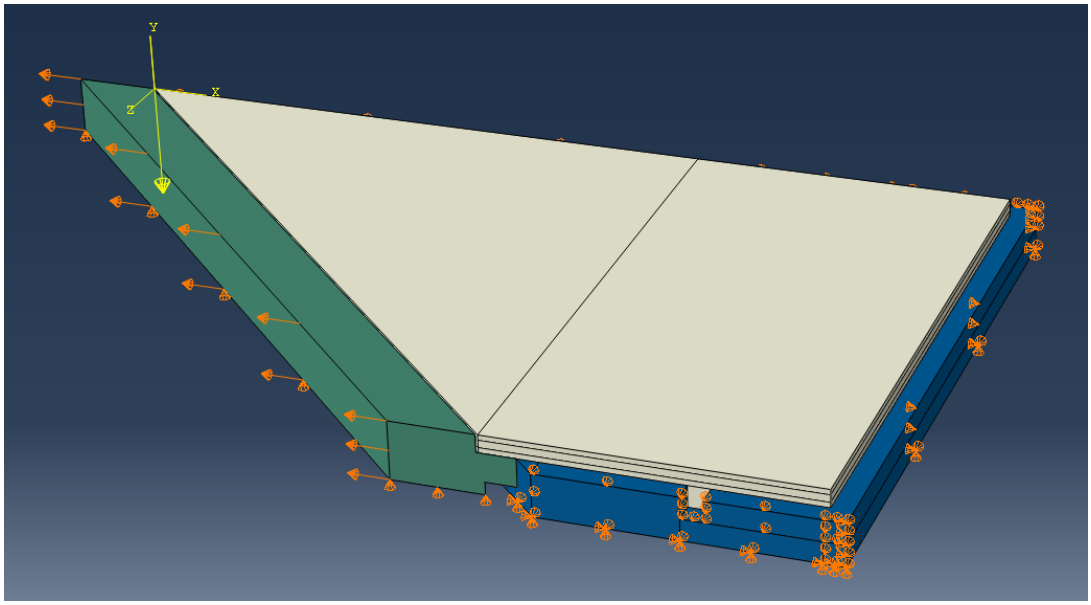

Figure 5.4. Jasper County 118—finite element model boundary conditions

5.1.4. Loading

The first loading step was to introduce gravity loads. Since ABAQUS is unitless, verification was required to check that gravity was working as intended. The material density of the concrete was set to 0.087 and the gravity was set to -1 in the negative Y direction, so that when multiplied together they would produce a unit weight of 0.87 psi, equaling 150 pcf. As a test, a nonskewed 10 in. thick concrete slab was simply supported along two edges with gravity loading applied. The support reactions at either end matched the expected values, and the deflection in the center of the slab matched the expected values for a beam to within 5%.

The second loading step applied was a temperature change applied to make the slab shrink or expand. The same test slab shrank as expected based on calculations using a concrete coefficient of thermal expansion of 6.0×10^{-6}/°F. Loading applied to the full-scale model included both contraction and expansion, with full temperature changes applied to the concrete elements. Negative temperature loading is applied with simulated bridge contraction, and positive thermal loading is applied with simulated bridge expansion. Full longitudinal movement was calculated as 2.16 in. per Table 5.8.3.1.2 of the Iowa DOT *LRFD Bridge Design Manual* for the Jasper County bridge using a 184.5 ft length. Typically only half the length would be used for a symmetrical bridge, but the Jasper County bridge is designed to accommodate all expansion at the east end. Spring elements were added in the Z direction to the ends of the abutment and were calibrated to provide the correct Z displacement per unit X displacement. The Jasper County bridge instrumentation data indicated that the transverse (Z) displacement equals 81% of the longitudinal (X) displacement for that bridge.

5.1.5. Surface Contact

Contact surface pairs were identified between the approach slab and soil, approach slab and abutment, abutment and soil, and abutment and footing. Two different contact properties were created, one for concrete-to-concrete friction and one for concrete-to-soil friction. The general contact function of ABAQUS provided a satisfactory method due to the simple geometry of the contact surfaces of the model. A coefficient of 0.6 was assigned for concrete-to-concrete contact per Table 22.9.4.2 in ACI 318-14, and a coefficient of 0.55 for concrete-to-soil contact was used to represent concrete on gravel or coarse sand (Potyondy 1961).

ABAQUS contact behavior was tested using a simple rectangular member placed onto another member of the same size. After gravity was applied to initiate contact between the two surfaces, the top member was displaced laterally by a distance of 1 in. The theoretical friction force was calculated as the weight of the member, 1,250 lbs, multiplied by the friction coefficient of 0.5. The load-displacement data for the incremented displacement showed a force nearly identical to the calculated value of 625 lbs after ramping up almost immediately from zero, which was maintained through the rest of the movement (Figure 5.5). This behavior shows that the ABAQUS "penalty" frictional behavior used works as intended by maintaining a constant force after slippage occurs.

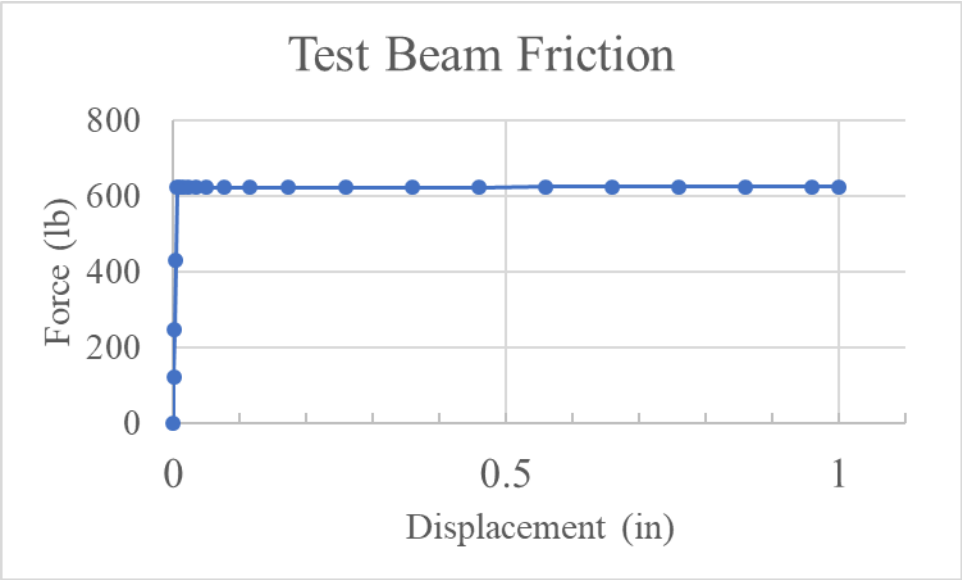

Figure 5.5. ABAQUS friction behavior verification

5.1.6. Slab Rebar

ABAQUS allows for the modeling of rebar using multiple different methods. Elements can be embedded within others to constrain their translational degrees of freedom. The embedded elements must lie completely within the host elements, as rebar does within concrete. The element type chosen for the slab was a SFM3D4 surface embedded within 3D solid elements. The surface section properties allow for input of the rebar material, area per bar, bar spacing, and

bar orientation. The bar inputs are converted into shell elements of an equivalent thickness of steel spread over the surface area. Using bar orientations of 0 and 90 degrees allows for the specification of longitudinal and transverse bar layers according to the local part coordinates. A simple test beam confirmed the effect of layer orientation, where the displacement and stress results matched plain concrete with a bar orientation set to 90 degrees while both stress and displacement decreased with an orientation set to 0 degrees.

Two different surfaces were used, one for the upper layers of bars and one for the lower layers of bars per the Jasper County 118 plan set. Surface depths within the set were determined by the clear cover given in the plans and the longitudinal bar diameter to result in surfaces placed at the centroid of the longitudinal bars.

5.1.7. Model Calibration

Strain gauge data were used to calibrate the FE models using temperature changes and corresponding strain values to determine appropriate coefficients of thermal expansion. The use of air temperature values was deemed inappropriate since the temperature of the slab does not match the air temperature due to thermal inertia. The temperature of the slab lags slightly behind the air temperature since it takes time for heat to transfer through the depth of the 10 in. approach slab where the strain gauges are located. For this reason, an average temperature for both the east and west approach slabs was calculated using an average of the thermistor values for all strain gauges embedded in the slabs.

Strain values in the X direction were extracted from the model results for the locations of the strain gauges placed in the instrumented Jasper County 118 bridge. The temperature ranges for each month of instrumentation along with the single daily highest temperature change were extracted from the thousands of data points available. Data for all ten strain gauges provided a corresponding strain value, and the temperature change was used to backcalculate an equivalent alpha (α) value for each strain gauge. The α values generally agreed with each other except for SG9-E, which exhibited extremely low strains no matter the time period or temperature change that was examined.

In general, the backcalculated α values were on the order of $2x10^{-6}$/°F for the day with the largest temperature change. These numbers did not match the initial model results, in which the strains corresponded to α values of $6x10^{-6}$/°F. The same backcalculation of α done for the model output results produced values very similar to the material property input value, indicating that the model slab expands and contracts freely, with no discernable impact from friction with soil. The instrumentation data show that there may be other factors influencing expansion that cannot be captured in the model, which is to be expected given the scope of the model and the simplifications made for modeling.

Different time periods for strain gauge data were examined by calculating a running α value based on the strains for the last 24 hours at each hourly data point. The α values for the strain gauges reached a maximum of $7.77x10^{-6}$ for SG5-E, with typical maximums around $6.0x10^{-6}$ for the other gauges apart from SG9-E, which did not appear to be performing correctly.

The FHWA provides a range of expected thermal coefficients of thermal expansion for different materials, including aggregate, cement, and concrete. Since concrete composition varies greatly between batches and even within a single slab, the FHWA gives a typical range of 4.1 to 7.3×10^{-6}/°F for concrete. An α value of 4.1×10^{-6} was adopted for use in the model since it was clear that the slab was expanding and contracting on the lower end of the FHWA range. A comparison of all measured and FE α values is available in Figure 5.6.

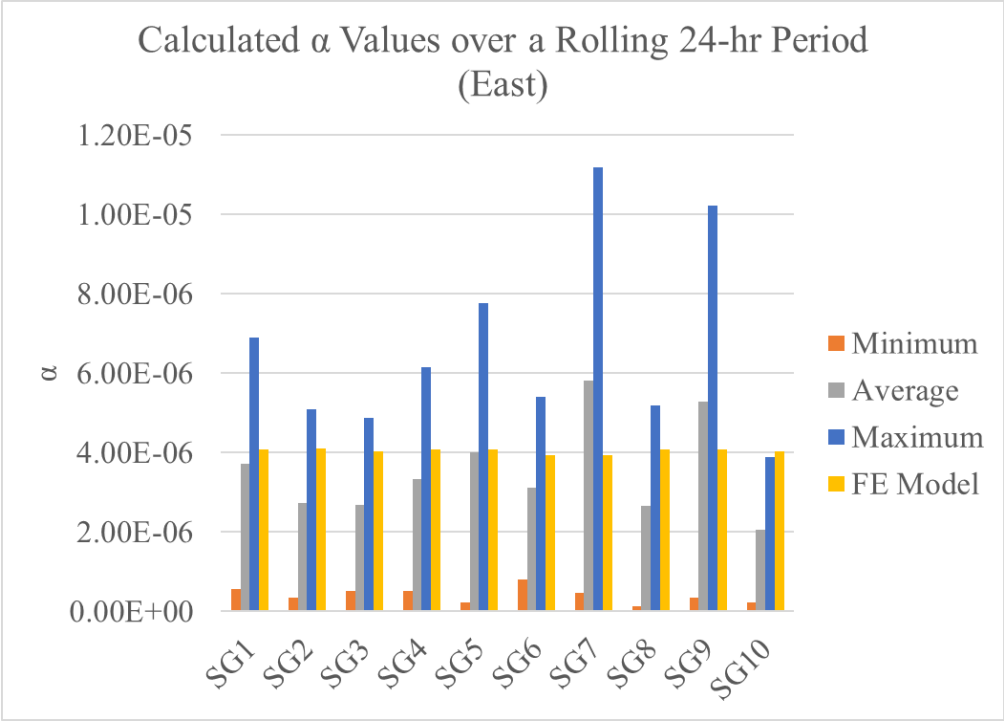

Figure 5.6. Jasper County 118—equivalent thermal coefficient of expansion

Other properties, such as surface friction coefficients, cannot be calibrated correctly with the data provided from the instrumentation, so they must be taken from the literature and can be varied as part of a parametric study.

5.1.8. FE Results

In order to study the effect of a tied connection on the slab in combination with a 45 degree skew, a second model was made to include a tied connection (Figure 5.7). The soil block dimensions were 1 ft wider than the slab on each side to allow for frictional sliding without loss of contact. The soil lug on the bottom of the slab was eliminated to create a smooth surface to allow sliding.

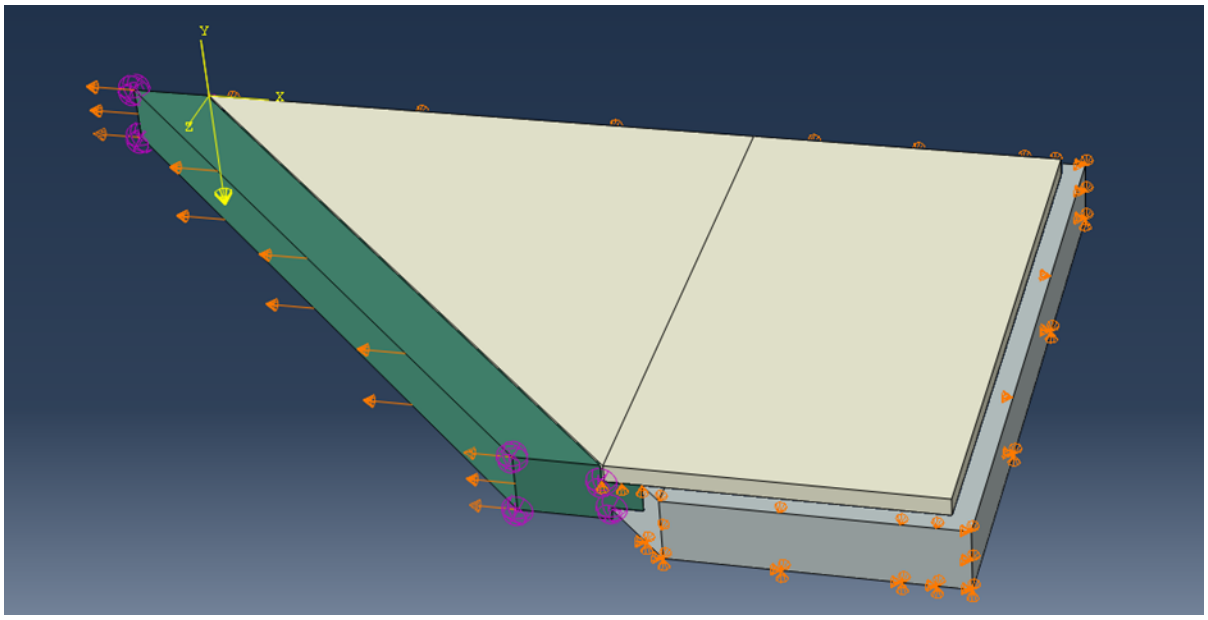

Figure 5.7. Jasper County 118—modified (tied) finite element model boundary conditions

In order to simulate a tied connection, the embedded element function was used again; in this case, wires meshed with beam elements approximated the individual bars. The tie bar size, shape, and spacing was adopted from the Story County 118 plans, resulting in angled #8 bars spaced 14.8 in. apart for a total of 23 bars across the joint width. The beam elements were embedded in both the abutment and approach slab host elements (Figure 5.8). Applying a displacement in the negative X direction to the abutment pulled the slab with it as expected, confirming that the bars were working as intended in tying the abutment and approach slab together.

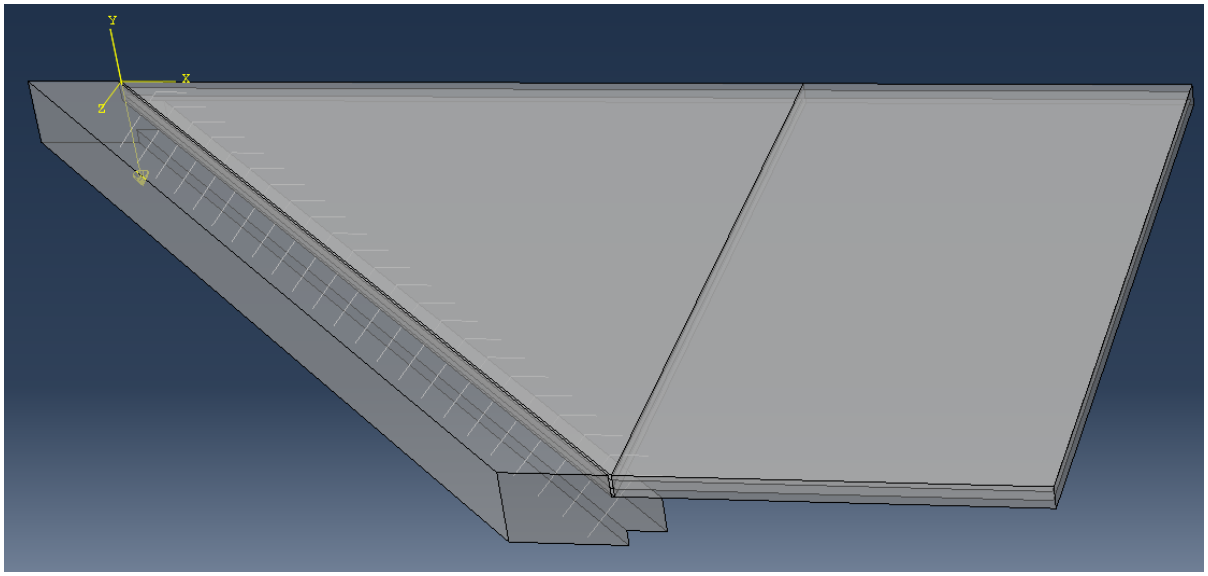

Figure 5.8. Jasper County 118—modified (tied) finite element model with tie bars

Since the tie bars and sleeper slab used in this modified model were not specifically designed for construction with the Jasper County approach slab, they are not suitable for examination of any stresses or forces. They exist solely for the investigation of the displacement of a tied approach slab with a 45 degree skew. The Jasper County slab itself, including its thickness and rebar, were not designed to be tied to a moveable abutment either; however, stress contours are extremely valuable for identifying critical locations and seeing trends that would not otherwise be present if not for the high skew.

Two different loading scenarios were applied to both the original (free) and modified (tied) models, for a total of four load cases (Table 5.2). The non-tied approach slab model was developed to verify the modeling assumptions and to serve as a baseline for a comparison of numerical studies. A positive thermal loading condition applied a temperature change of +100°F and a corresponding displacement of 2.16 in. in the positive X direction to simulate expansion of the bridge superstructure, which was calculated using a temperature change of +150°F for steel girders. The opposite loading was applied to simulate bridge superstructure contraction under negative thermal loading.

Table 5.2. Jasper County 118—finite element model load cases

Load Case	Model	Abutment Movement	Thermal Loading
1	Free	Expansion	Positive
2	Free	Contraction	Negative
3	Tied	Expansion	Positive
4	Tied	Contraction	Negative

The high skew angle of the Jasper County bridge results in the bridge displacements being of particular interest. The tied approach slab connection leads to the investigation of corresponding approach slab displacements. The same loading scenario and abutment movements for the two different models produced different approach slab movements. The free contraction loading in Case 2 shows that the slab's soil lug works as intended by holding the slab in place and pulling the outer edges of the slab to a centroid located roughly in the center of the slab width at the soil lug (Figure 5.9). The expansion in Case 1 mirrors this behavior, with the slab edges moving away from the same central location.

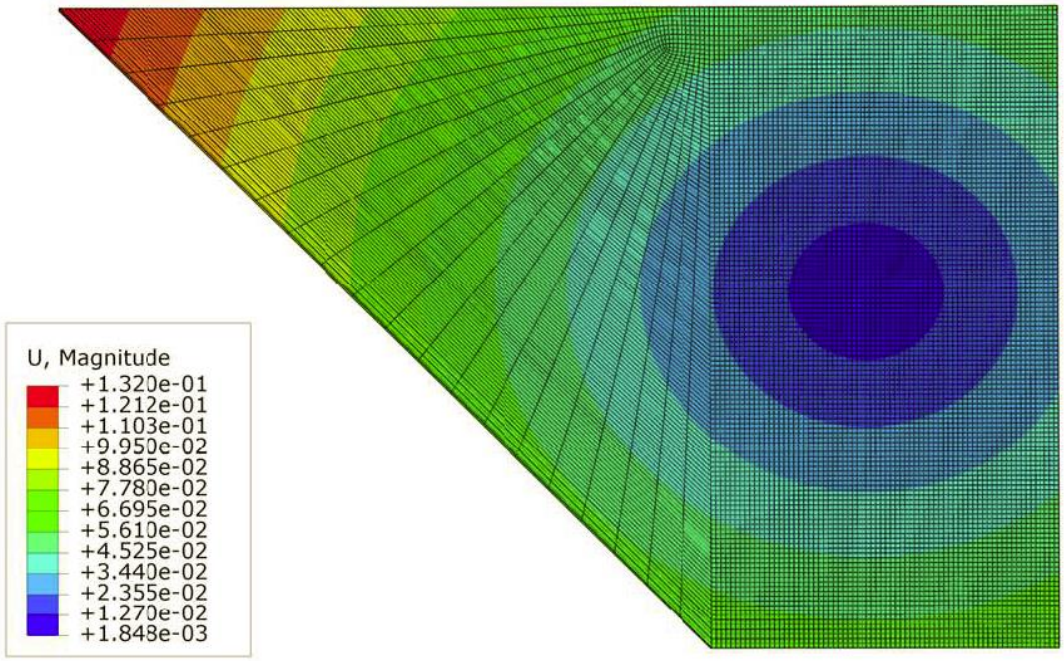

Figure 5.9. Jasper County 118—Case 2 displacement magnitude

Displacement contour plots help to illustrate how the slab moves in response to both an applied displacement to the abutment and a temperature change. The X displacement values for Case 3, shown in Figure 5.10, range from 2.103 to 2.257 in. The difference can be attributed to the expansion of the slab itself. The farther reaches of the slab are pushed away from the joint, as indicated by the maximum magnitude located in the corner.

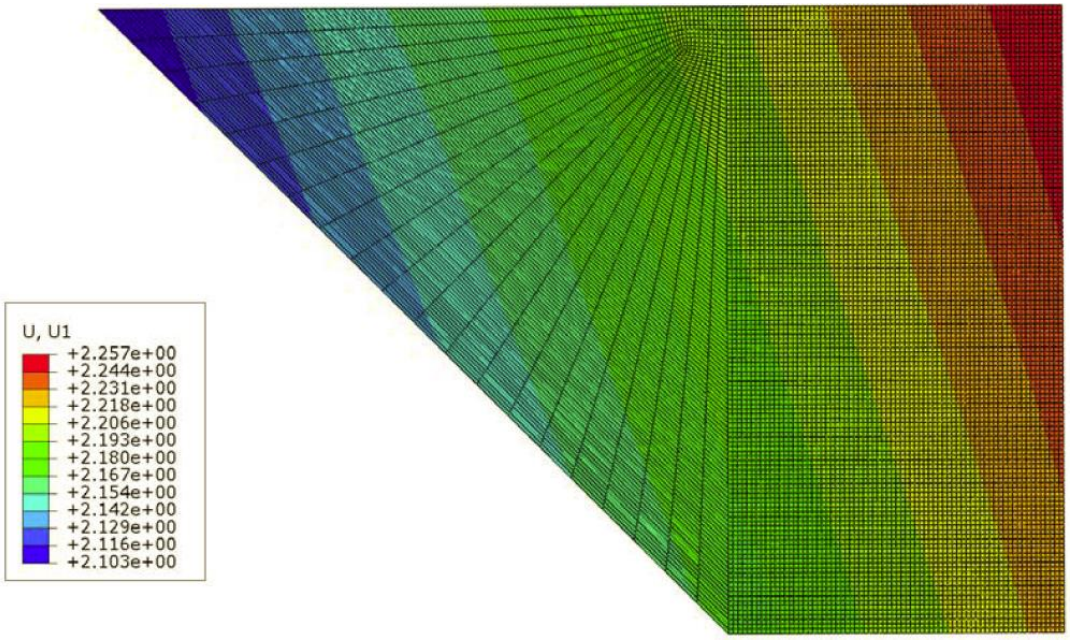

Figure 5.10. Jasper County 118—Case 3 X displacement

The X displacement values for Case 4 show a similar pattern (Figure 5.11), with values ranging from -2.159 in. to -2.325 in. The contours in Case 4 are angled differently to those in Case 3, since Case 4 does not include a large transverse displacement at the abutment.

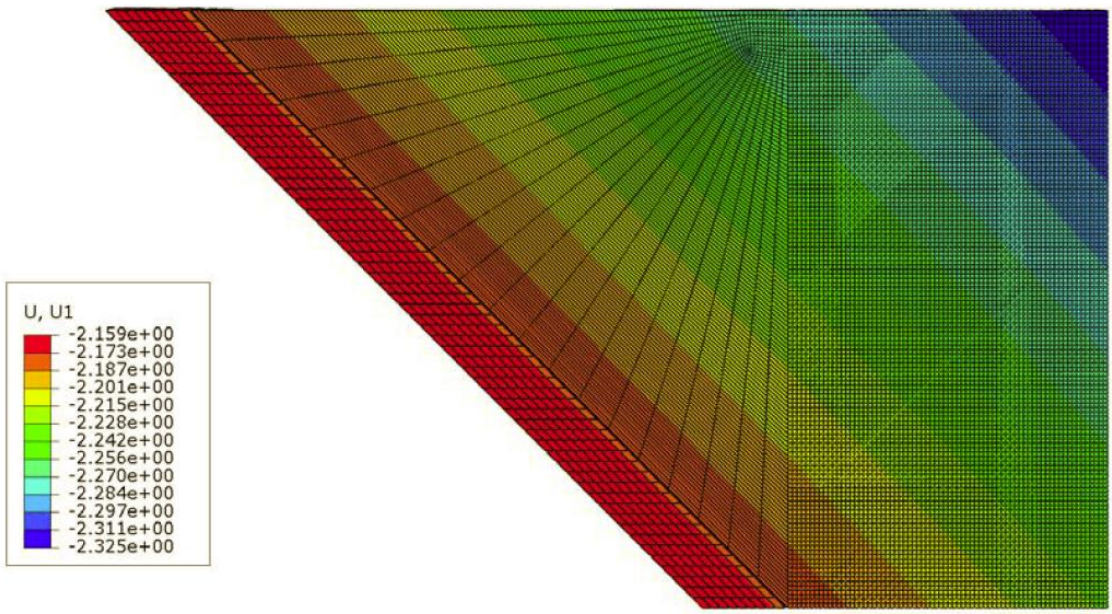

Figure 5.11. Jasper County 118—Case 4 X displacement

The displacements for all four load cases can be seen in Table 5.3.

Table 5.3. Jasper County 118—approach slab corner displacements

Point	Base Coordinates (in.)		Displacement (in.)							
			Tied				Non-Tied			
			Expansion		Contraction		Expansion		Contraction	
			Case 3		Case 4		Case 1		Case 2	
	X	Z	X	Z	X	Z	X	Z	X	Z
Pt 1	0	0	2.108	1.865	-2.175	0.105	-0.122	-0.052	0.120	0.052
Pt 2	516	0	2.256	1.916	-2.324	-0.041	0.028	-0.047	-0.030	0.048
Pt 3	516	336	2.224	2.026	-2.230	-0.150	0.026	0.062	-0.028	-0.061
Pt 4	336	336	2.170	2.010	-2.177	-0.101	-0.027	0.062	0.025	-0.061

Figure 5.12 shows the free expansion and contraction of the slab for Cases 1 and 2 with displacements amplified by a 100x scale for clarity. The deformed shapes are all concentric about the center.

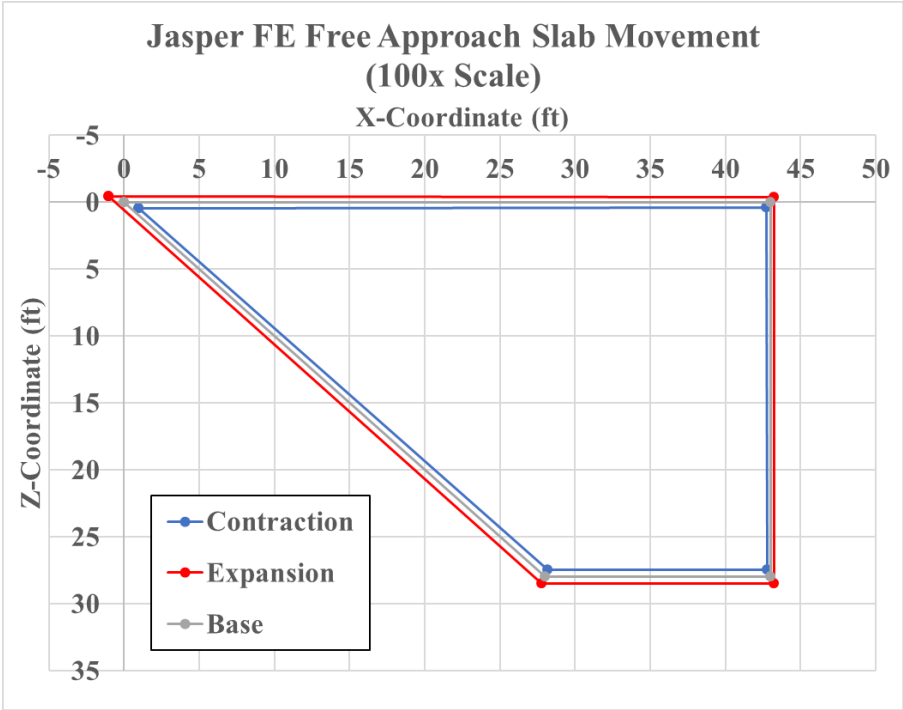

Figure 5.12. Jasper County 118—Cases 1 and 2 approach slab movement

Compare the displacements for Cases 1 and 2 with the displacements for Cases 3 and 4, which are shown in Figure 5.13 with a much lower 10x scale amplification. A similar shape change occurs due to temperature change, but global displacements are much larger.

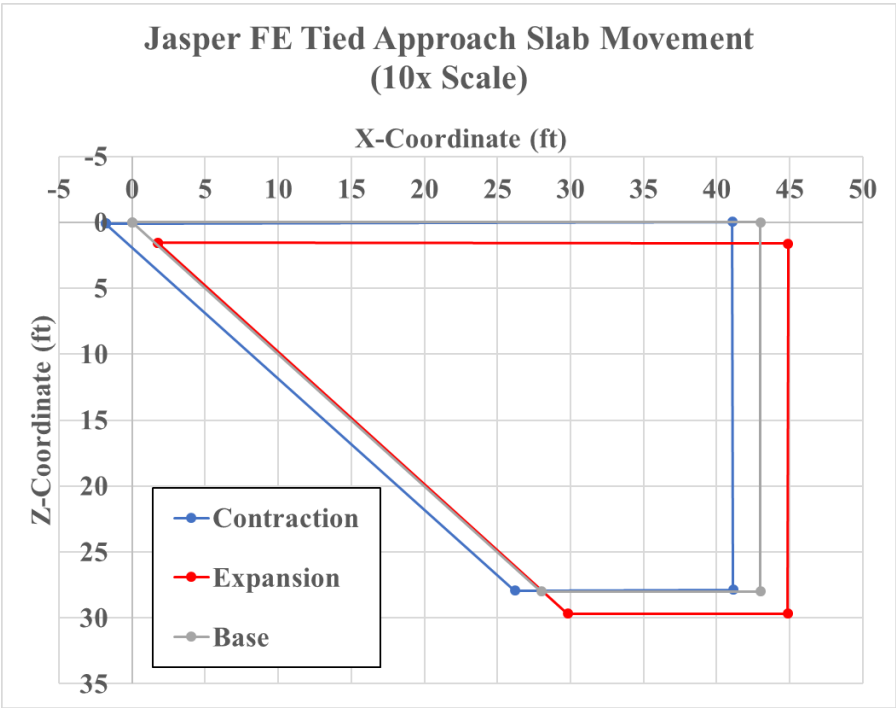

Figure 5.13. Jasper County 118—Cases 3 and 4 approach slab movements

Case 3, which captures the expansion of the slab, drags the slab transversely, while Case 4 does not have nearly as much transverse deflection. Slab rotations were calculated using the position of the two points located on the slab edges along the road centerline and at the joint itself using two points at either end of the joint. Rotation for Case 3 is -0.0071 degrees about the Y-axis at the abutment-to-approach-slab joint and only -0.0055 degrees along the slab centerline. A frictional force located at the centroid of the slab acting in the opposite direction of transverse displacement would cause a positive rotation about the joint end of the slab, possibly accounting for the discrepancy. Similarly, rotation at the abutment-to-approach-slab joint is 0.0161 degrees for Case 4 and 0.0174 degrees measured at the slab centerline. Using the same logic described previously, it follows that the slab rotation would be lower than at the joint.

The friction force (F) between the approach slab and soil is determined by the normal force between the two surfaces (N) and a coefficient of friction (μ) given a fiction model of $F = \mu N$. The contact pressures calculated in ABAQUS are shown in Figure 5.14 and Figure 5.15 for Cases 3 and 4, respectively.

Figure 5.14. Jasper County 118—Case 3 soil contact pressure contour plot

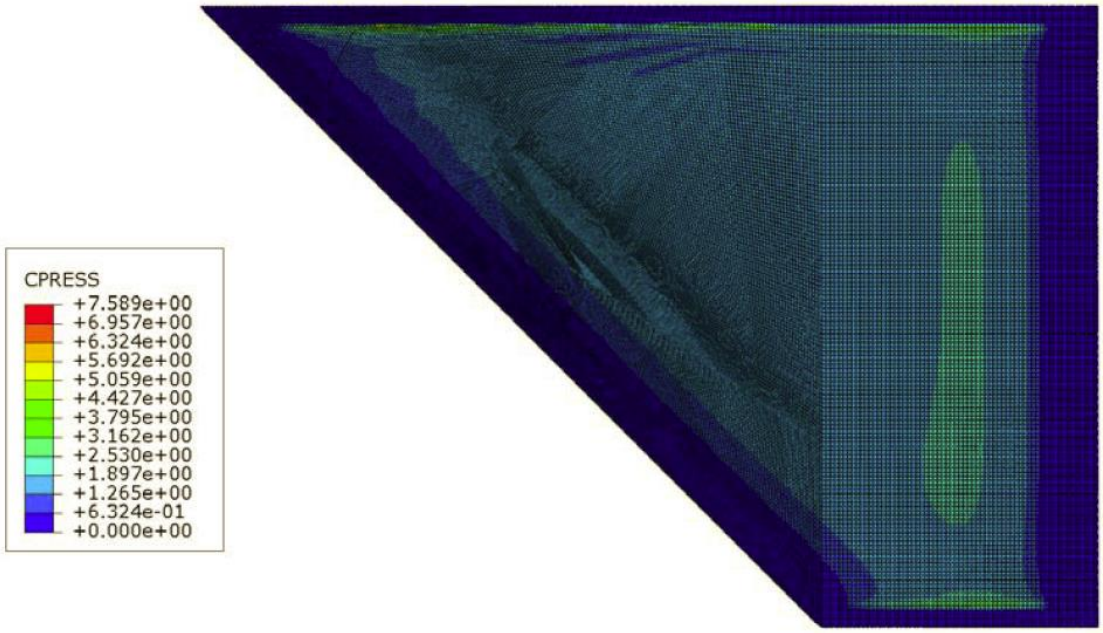

Figure 5.15. Jasper County 118—Case 4 soil contact pressure contact plot

The two profiles show very different behavior due to the effect of the abutment movement. Case 4 shows a contact shape similar to the approach slab shape, indicating that the slab generally has a low, even contact pressure across its entire surface. The contact shape for Case 3 is extremely high near the abutment-to-approach-slab joint and comparatively low enough elsewhere that it becomes difficult to distinguish due to the contour colors used. The abutment movement pushes into the soil, creating a small upward deflection due to the Poisson effect. The upward movement of the soil is resisted by the slab and results in high contact pressure and thus a high contact shear that resists slab sliding. This behavior is not unexpected given the boundary conditions applied to the soil; however, it represents a worst case scenario that is unlikely to occur. Settlement of the soil beneath approach slabs would likely mean that even with bridge expansion, the soil would not result in a net upward deflection of the approach slab of the magnitude seen in this analysis.

True loading also occurs in many small cycles due to daily temperature swings, alternating between expansion and contraction. Ratcheting of the soil or erosion occurring near the abutment would create a void and space for the soil to deflect upwards at the abutment backwall without creating additional upward pressure on the approach slab. Both Case 3 and 4 showed a peak soil pressure at the acute approach slab corner that corresponds to the obtuse bridge corner.

Soil pressures translate directly to shear forces, given the frictional behavior chosen for modeling. The contact shear profiles match the contact pressure profiles shown above. Summing all contact shear force on the surface of the slab gives the total force required to move the slab. The same results can be reached by extracting the forces from the tie bars connecting the abutment and approach slabs.

Expansion and contraction show two different behaviors, as seen in the load-displacement plot for the Jasper County bridge (Figure 5.16). Case 4 (negative displacement) shows an ideal friction curve similar to that of the test beam. Once the peak friction force is reached, the slab slides with a constant force value of around 78 kips. Case 3 (positive displacement) shows a slight dip in force before increasing steadily to a maximum value of 99 kips. The changing force value can be attributed to the changing contact surface shape. The positive slope in force may be a result of the upward deflection of the soil near the abutment-to-approach-slab joint. The lateral movement of the abutment creates the upward deflection of the soil. The approach slab is tied to the abutment and resists the upward deflection, increasing contact pressure and contact shear. As the abutment moves farther, the effect is amplified and the overall friction force increases.

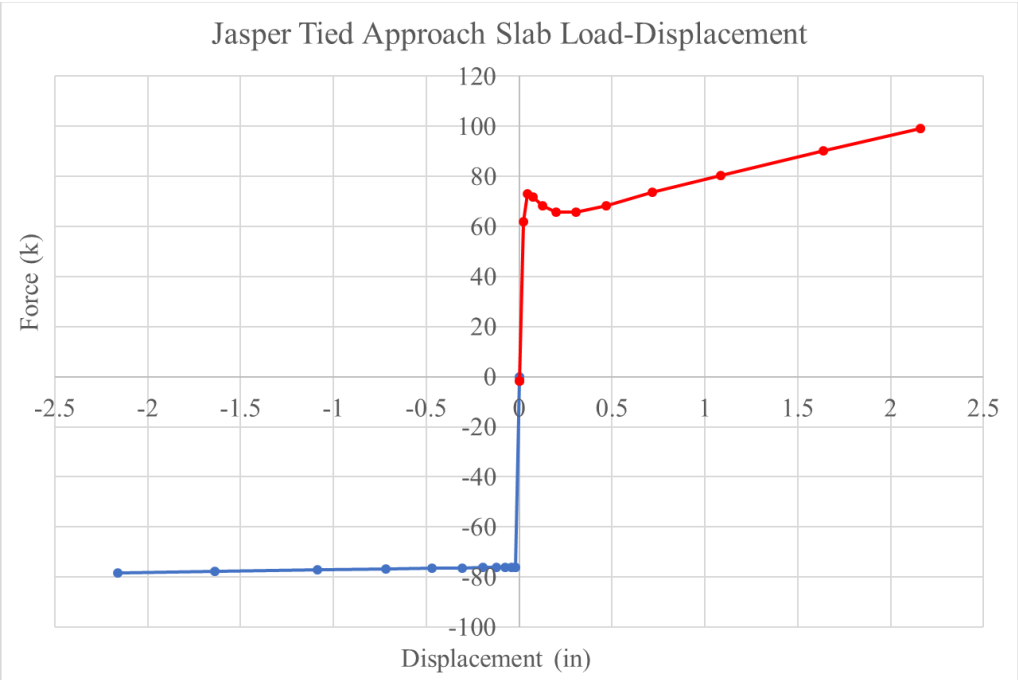

Figure 5.16. Jasper County 118—tied approach slab load-displacement (X direction)

A load-displacement curve for longitudinal and transverse force is shown in Figure 5.17. Recall that during bridge expansion, the Jasper County bridge experiences a transverse displacement equal to 81% of the longitudinal displacement. The plot shows the total transverse shear force taken from the tie bars during bridge expansion compared with the longitudinal force. The forces are of similar magnitudes since the approach slab is moving in both directions and is resisted by a contact shear force in both directions.

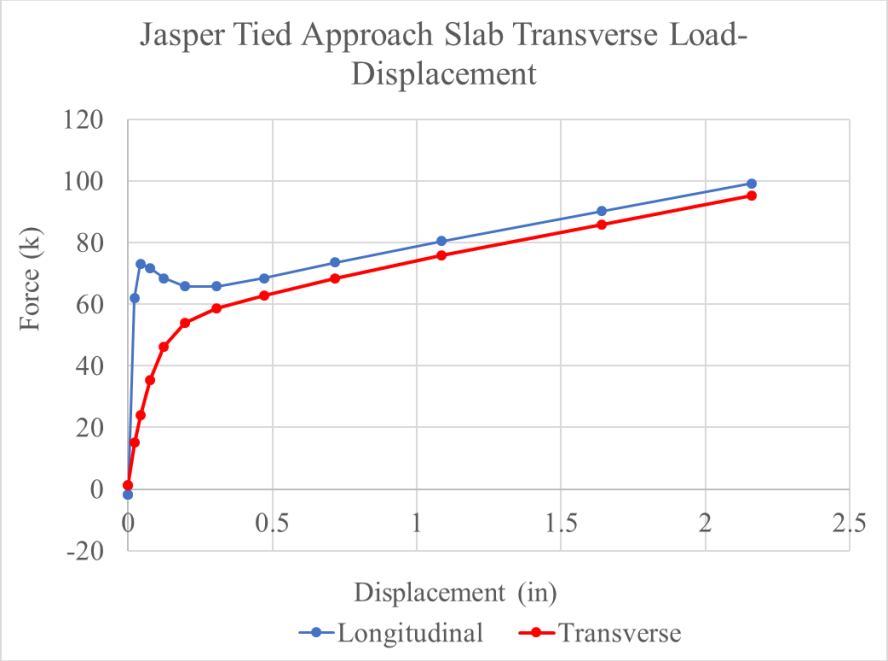

Figure 5.17. Jasper County 118—tied approach slab transverse load-displacement (expansion)

5.2. Story County 118 FE Model

A finite element model was created to replicate the Story County 118 bridge that was instrumented with sensors similarly to the Jasper County 118 bridge. Model formulation began with the same techniques employed for the Jasper County model. The model consists of a 2 ft deep soil block matching the depth of the modified subbase. An equal-depth portion of the abutment is tied to the approach slab using 53 inclined paving notch dowels placed per the Story County 118 bridge plans. The approach slab is 63.2 ft wide to accommodate a 60 ft roadway and has a length at the longer edge of 36.5 ft. The soil and sleeper slab extend 1 ft beyond the edges of the approach slab to provide a continuous surface for sliding. The dowels are Grade 75 stainless steel to match those installed per Iowa DOT standards. The stainless steel material is modeled with plastic behavior at 75,000 psi. Other material properties match those seen in the previous analysis for the Jasper County 118 FE model.

The boundary conditions are similar to those of the Jasper County model as well. Z direction restraint is only present on the sides of the soil for a 12 ft length extending away from the abutment to simulate confinement due to the wingwalls. Concrete barrier loading was placed on the approach slab using an equivalent pressure and a 14 in. width for a length of 19 ft on each side. The pressure loading was applied to a partitioned section of the approach slab matching the footprint of the barriers.

Soil boundary conditions vary slightly from those used in the previous analysis. Since the Story County 118 bridge utilizes integral abutments, the backwall deforms the soil at all depths, so modeling a thicker depth of soil than the abutment to allow for a pinned condition is not possible.

Therefore, a roller condition supports the soil. A loss of relative displacement between the slab and soil occurs but is extremely minimal and occurs after full friction is realized.

5.2.1. Mesh Density Study

A study was completed on the mesh sizing of both the approach slab and the soil beneath it. Mesh sizes were applied using a size control for both parts, since it is recommended to maintain similar sizes between surfaces for optimal contact simulation. Sizes began with 12 in., which allowed for one element through the full depth of the slab, and decreased to 3 in. The axial stress in the X direction of the approach slab after application of only gravity loads is shown in Table 5.4 and is plotted versus mesh size in Figure 5.18. The time taken for computation of the gravity step is also displayed in Table 5.4. A mesh size of 4 in. was chosen to provide proper result accuracy and minimize run time.

Table 5.4. Story County 118—approach slab mesh sensitivity results

Mesh Size (in.)	Axial Stress (X-Direction)	Gravity Step Analysis Time
12	0.109	4:59
8	0.327	16:54
6	0.314	12:54
5	0.342	33:37
4.5	0.506	53:58
4	0.508	36:36
3.5	0.513	1:05:12
3	0.508	1:42:17

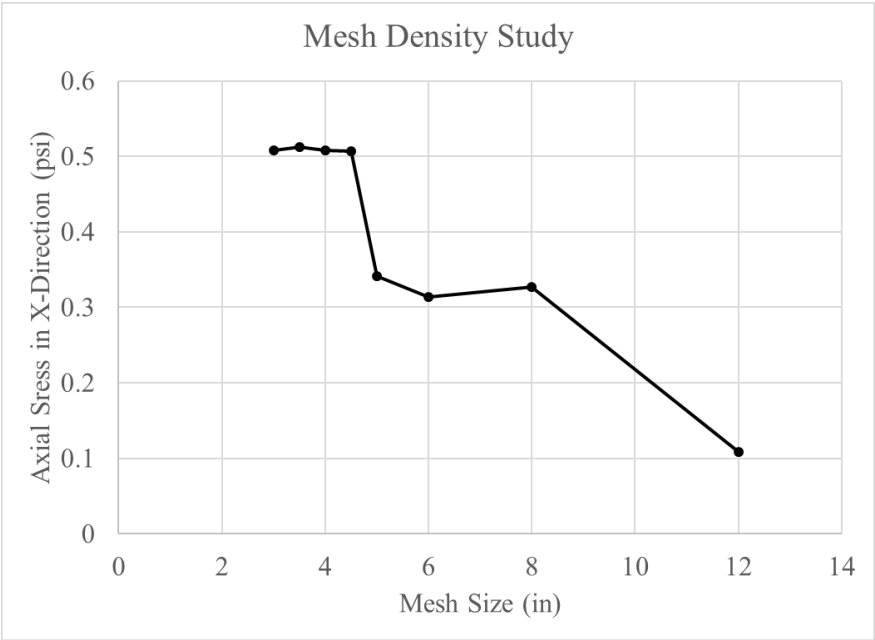

Figure 5.18. Story County 118—approach slab mesh density sensitivity

5.2.2. Comparison with Field Results

The FE results were compared with field monitoring data to examine how accurately the FE model captures the true performance of the bridge. A short period of bridge contraction and negative thermal loading was chosen for study. Beginning on March 25 at 7:00 p.m., the bridge underwent a temperature decrease until March 26 at 8:00 a.m. The associated 8.1°F drop in temperature and 0.074 in. abutment displacement were applied to the Story County 118 bridge base model.

Figure 5.19 shows the measured strains of all nine slab strain gauges for both the north and south approach slabs. Also included in the plot is the measured strains from the same locations in the FE model slab. The strains from the north and south slabs are consistent with each other but show much more variation between gauges than the FE model results. Overall, the strains are all in the correct direction and on the same magnitude. A longer time scale and larger temperature range would provide a better comparison, especially for extremely high temperatures during maximum bridge expansion, since the FE results for the expansion case are anticipated to be highly conservative.

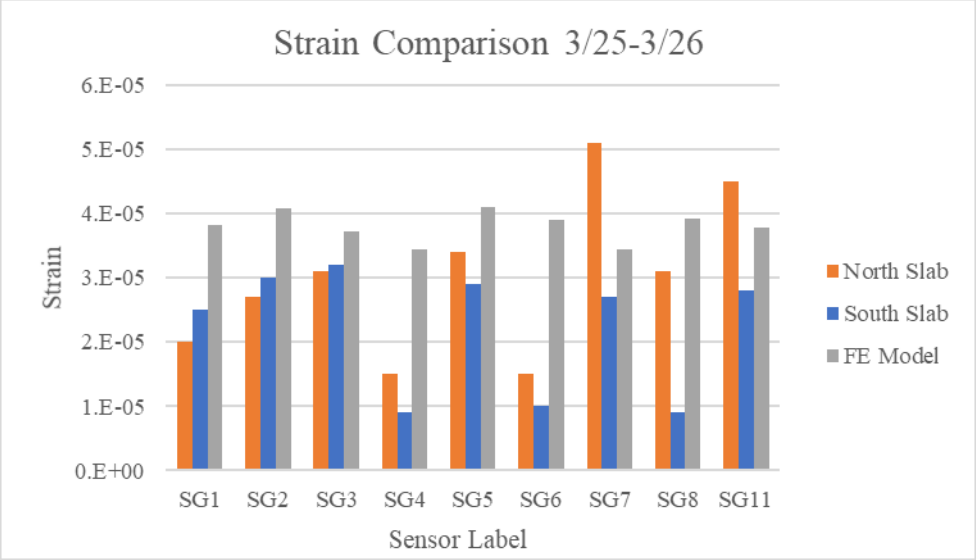

Figure 5.19. Story County 118—approach slab strain comparison

Figure 5.20 shows the strain measured by gauge SG10-S for the same 13-hour period plotted with the strain extracted from the FE model from the center tie bar at the location of SG10-S. The strain measured by SG10-S is the only recorded strain included in the comparison since SG10-S was the only tie bar strain gauge determined to be capturing strain in the bar to which it was connected. The final results were 62 με and 60 με for the field results and FE model, respectively. The shapes of the two curves differ, with the model showing a linear increase in strain initially with a plateau after the slab begins to slide. The data from SG10-S show a consistent increase in strain throughout the temperature change.

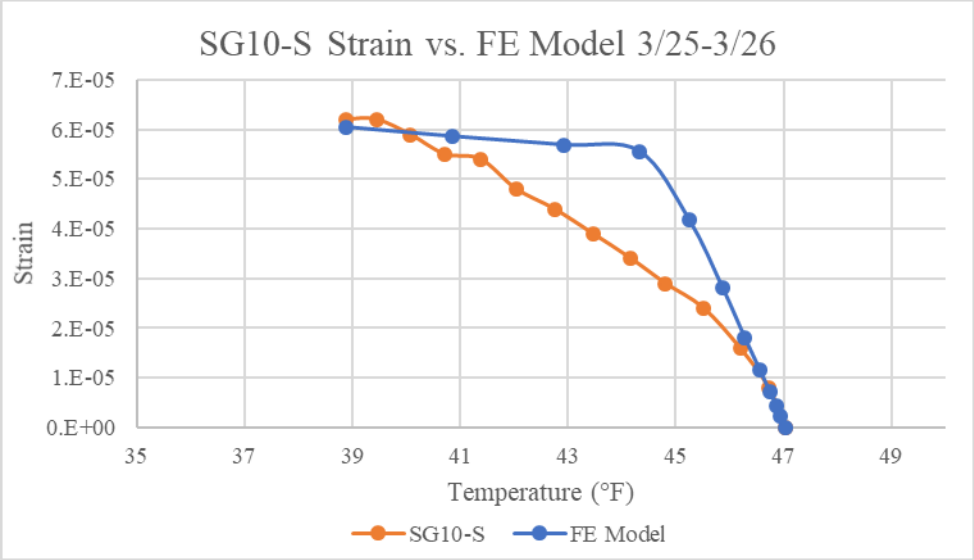

Figure 5.20. Story County 118—tie bar strain comparison

Comparisons of approach slab displacement at the sleeper slab and tied approach slab expansion are provided in Figure 5.21 and Figure 5.22, respectively.

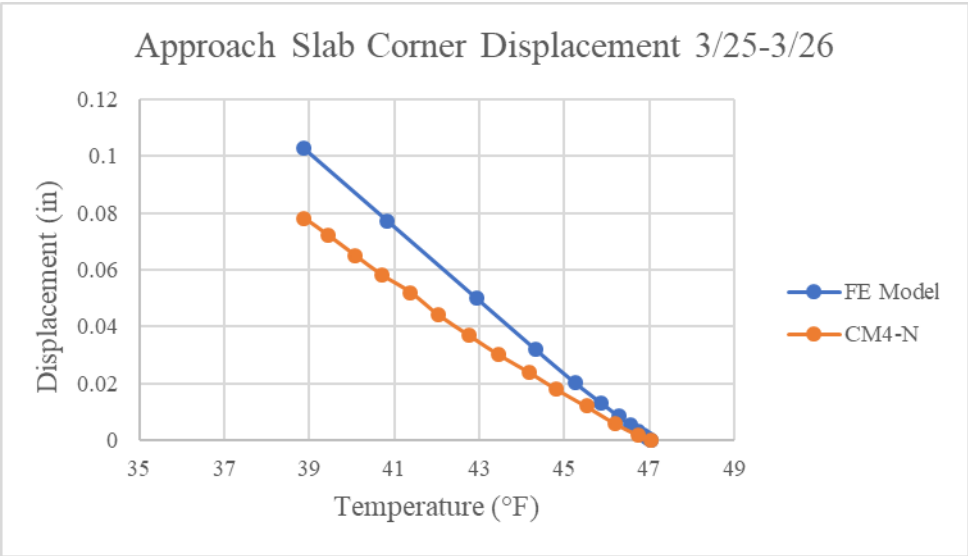

Figure 5.21. Story County 118—approach slab corner displacement comparison

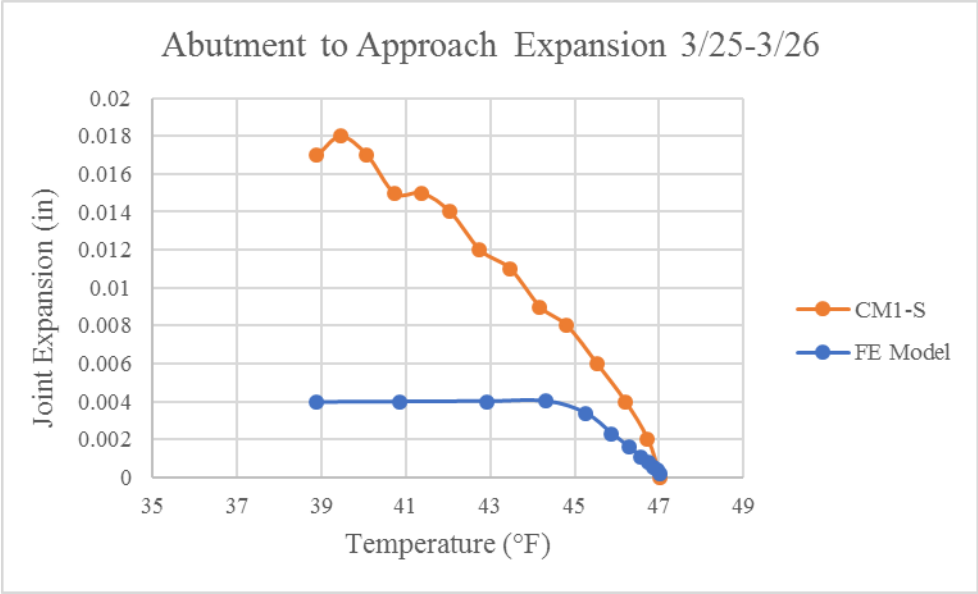

Figure 5.22. Story County 118—tied approach expansion comparison

Both the FE model and field results show the same increasing displacement with decreasing temperature. However, the model overestimates displacement by 30%. Peak model displacement is 0.10 in. compared to the field results of 0.08 in. The only two factors contributing to the displacement at the approach slab end are the tied approach slab joint and the change in length of the approach slab itself.

Joint expansion was determined from the FE model results by subtracting the approach slab edge displacement from the abutment edge displacement to find the relative displacement between the two parts. The comparison of the joint behavior exhibited by the FE model and the field data in Figure 5.22 shows two different pictures. In the model results, expansion increases slowly and reaches a maximum plateau of 0.004 in. The crackmeter data, in contrast, show that the joint expansion increases steadily to a maximum value of 0.018 in., over four times the model value. The difference between the two values, 0.014 in., is similar in magnitude to the difference between the approach slab displacement results shown in Figure 5.21. An underestimation of joint expansion by the model would be reflected in an overestimation of approach slab displacement at the sleeper slab.

Overall, the model generally captures the thermal behavior of the approach slab. However, it does have limitations and does not appear to capture the continuous opening of the approach-slab-to-abutment joint. According to the field data, the joint does not seem to be limited by a plateauing frictional force. Possible explanations include a force present at the approach-slab-to-sleeper-slab joint or a more complicated frictional behavior that cannot be represented with the frictional behavior used in this model.

5.2.3. Parametric Studies

In order to study the effect of different input parameters on the model's behavior, parametric studies were completed on the coefficient of friction between the concrete and the soil, the approach slab tie bar type, and bridge skew. The base model parameters and variations made in each study are seen in Table 5.5.

Table 5.5. Parametric study model variations

	Friction Coefficient	Soil Stiffness	Tie Bar Angle	Skew
Base	0.55	20 ksi	40°	15°
Friction Study	**0.4**	20 ksi	40°	15°
	0.55	20 ksi	40°	15°
	0.7	20 ksi	40°	15°
	1	20 ksi	40°	15°
Soil Study	0.55	**13.9 ksi**	40°	15°
	0.55	**20 ksi**	40°	15°
	0.55	**27.8 ksi**	40°	15°
Tie Bar Study	0.55	20 ksi	**40°**	15°
	0.55	20 ksi	**20°**	15°
	0.55	20 ksi	**0°**	15°
Skew Study	0.55	20 ksi	40°	**0°**
	0.55	20 ksi	40°	**15°**
	0.55	20 ksi	40°	**30°**

Each study was completed independent of each other and included one full cycle of expansion and contraction. Loading included a temperature change of positive or negative 100°F, along with an abutment movement of 1.35 in. in either direction. Expansion and contraction were run as separate analyses, simulating a worst-case scenario in which the bridge experiences full expansion or full contraction. As discussed previously, true temperature cycles induce expansion and contraction daily accompanied by general seasonal trends. However, simulation of these numerous reversing cycles would prove to be computationally unreasonable. Important results obtained from the parametric studies include load-displacement plots, contact pressure distributions, tie bar stresses, and slab stresses.

5.2.3.1. Parametric Study of Soil to Concrete Coefficient of Friction

The coefficient of friction will vary from bridge to bridge, depending greatly on the materials used, the condition of the soil, and the construction of the slab. The amount of friction between the slab and soil beneath it is difficult to measure due to the large contact surface of the slab and the fact that it must be indirectly measured through strains in the slab. Placing instrumentation on each tie bar is simply not reasonable due to the cost and effort it would require. Predicting the amount of friction a slab will experience is therefore difficult, and this study aimed to assess slab and tie bar behavior as a result of varying amounts of friction. If force is distributed in the same

manner no matter the magnitude, a design can be completed under the expectation that the locations of maximum tie bar or concrete stresses will not shift.

Four different values were used for the coefficient of friction to determine what effect, if any, a changing coefficient of friction has on the slab and tie bar behavior other than simply increasing the force required to pull the approach slab. Increasing the coefficient of friction will directly increase friction force, but a more in-depth look is required to determine if the increased force is carried in different ways or if the contact surface is affected. Values of 0.4, 0.55, 0.7 and 1.0 were input in the Story County 118 bridge base model, as described above.

Load-displacement curves for each case are visible in Figure 5.23. Increasing the coefficient of friction increases the total amount of force necessary to pull the slab, as expected. Maximum contraction forces are 172, 236, 299, and 452 kips for coefficients of friction equal to 0.4, 0.55, 0.7, and 1.0, respectively. The shape of the curves is maintained across the different values, and the forces are amplified.

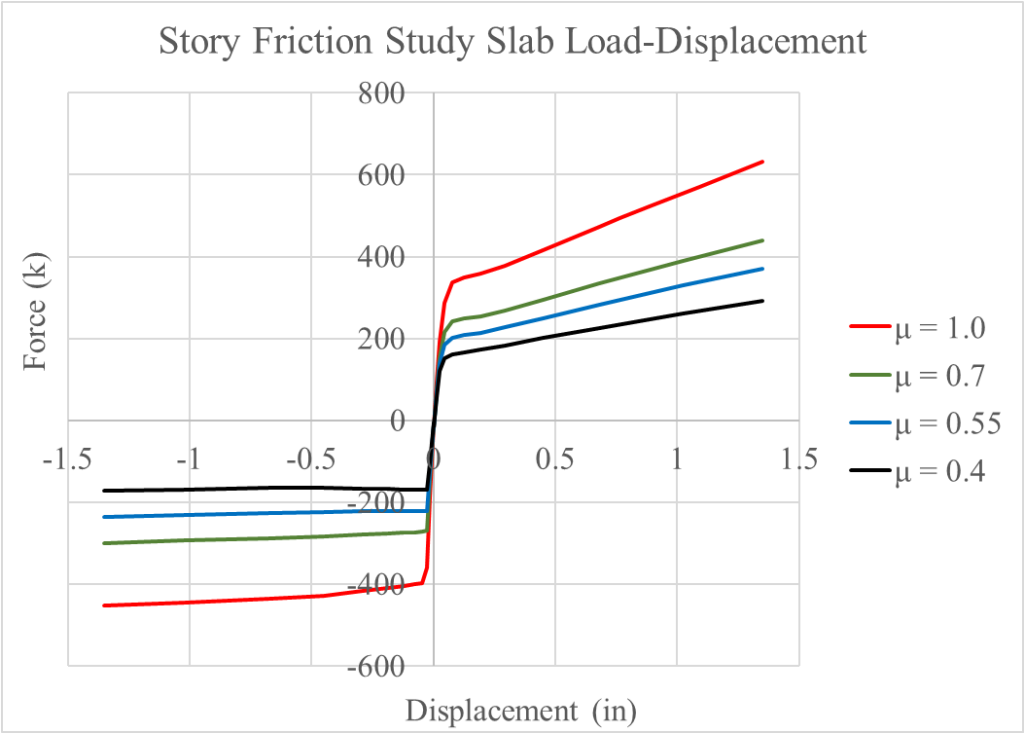

Figure 5.23. Story County 118—soil friction load-displacement comparison

Table 5.6 provides the von Mises stresses and maximum principal stresses in the approach slab surface. Overall, the stresses in the tie bars and concrete are larger during bridge expansion due to the compression of the soil and subsequent vertical displacement of the approach slab. Both of these stresses for all four cases show increasing magnitudes with increasing friction, which is an expected result. The incremental increases in von Mises stress for contraction and expansion are similar in magnitude. The maximum principal concrete stress in the approach slab increases only 25 psi from the lowest friction to the highest friction.

Table 5.6. Story County 118—friction study tie bar and concrete stress results

Friction (μ)	Tie Bar von Mises Stress (ksi)		Concrete Maximum Principal Stress (psi)	
	Contraction	Expansion	Contraction	Expansion
0.4	8.4	41.4	191	468
0.55	13.1	43.0	197	482
0.7	16.3	43.2	203	474
1	22.7	42.7	216	442

A visual representation of tie bar stresses during bridge contraction is provided in Figure 5.24. Stresses increase linearly with increasing friction, but a coefficient of friction between the soil and concrete equal to 0 would not eliminate all stress in the tie bars, since some friction remains between the approach slab and sleeper slab. If more data points were available for μ between 0 and 0.4, the curve would show a small amount of stress, similar to the stress after only gravity loading.

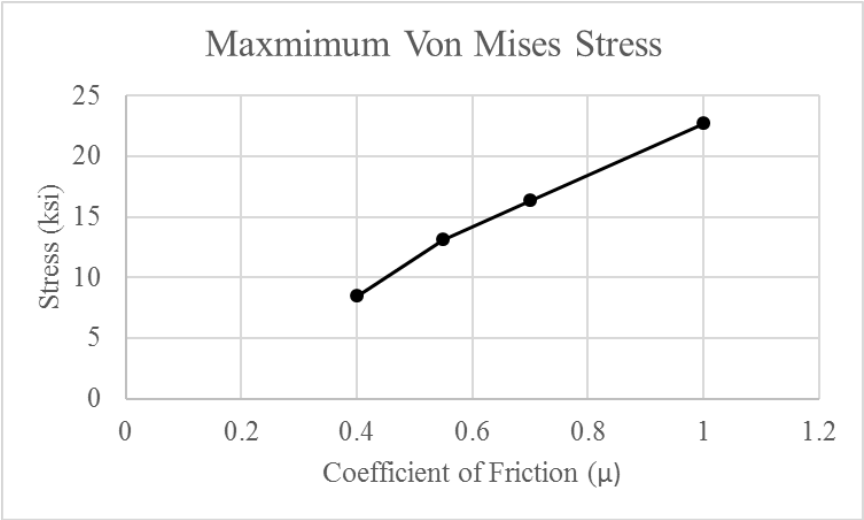

Figure 5.24. Story County 118—von Mises stress for varying coefficients of friction (contraction)

5.2.3.2. Parametric Study of Soil Stiffness

Three different soil stiffness values were used to determine the sensitivity of the model to changing soil stiffness and its effects on important results. The Story County 118 base model uses a modulus of elasticity of 20 ksi for the soil material. This value was taken from the literature as an average for dense gravel, since no material testing was completed on modified subbase material. The modulus of elasticity values for loose and stiff soil were taken as 13.9 and 27.8 ksi, respectively, the typical upper and lower limits for the same soil.

The variations in soil stiffness had an extremely small effect on both approach slab stress and tie bar stress when considering the bridge contraction load case. This is an expected result, since the approach slab is being pulled over the surface of the soil, which remains relatively flat. The maximum principal stress in the approach slab increased only 2 psi for the contraction case (Table 5.7). The concrete stresses for both contraction and expansion are compared in Figure 5.25. The trends for the two loading cases are different, in that soil stiffness had a minimal effect during bridge contraction, while concrete stresses increased by 140 psi over the range of soil stiffness values during bridge expansion. Upward deflection of the soil at the obtuse corner of the approach slab creates an upward pressure underneath the approach slab and induces a negative bending moment in the slab. This results in a greater positive principal stress in the approach slab surface. A stiffer soil provides a larger upward pressure and thus a larger maximum principal stress.

Table 5.7. Story County 118—soil stiffness study approach slab concrete stresses

Approach Slab Maximum Principal Stress (psi)		
Soil	**Contraction**	**Expansion**
Loose	197	358
Medium	198	431
Stiff	199	498

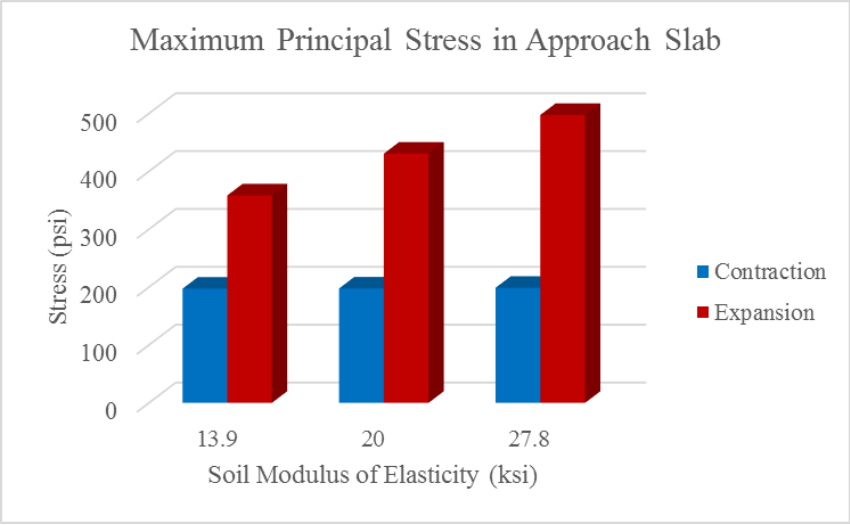

Figure 5.25. Story County 118—soil stiffness study approach slab concrete stresses

The maximum von Mises stress in the tie bars increased only 0.2 ksi, and the range between the minimum and maximum stresses in any one bar increased only 0.5 ksi (Table 5.8). This is also an expected result for the same reasons that concrete stresses were expected to undergo minimal changes in response to soil stiffness during bridge contraction. In the same way that soil stiffness affects concrete stress during bridge expansion, tie bar stresses are also increased. Both behaviors result from the same upward deflection of the soil.

Table 5.8. Story County 118—soil stiffness study tie bar von Mises stresses

Tie Bar Von Mises Stress at Joint (ksi)					
Soil		**Contraction**	**Range**	**Expansion**	**Range**
Loose	Maximum	12.9	10.2	31.9	30.4
	Minimum	2.7		1.4	
Medium	Maximum	12.8	9.9	38.0	37.7
	Minimum	2.9		0.3	
Stiff	Maximum	12.7	9.7	43.9	42.6
	Minimum	3.0		1.3	

5.2.3.3. Parametric Study of Tie Bar Orientation

Variation exists in the types of dowels used to connect approach slabs to abutments and bridge decks. For example, the Iowa DOT uses vertical bars in the BR-205 standard approach slab (Figure 5.26). Alternatively, the dowels used in the construction of Story County 118 are inclined at approximately a 40 degree angle from vertical. Inclined bars are recommended for semi-integral abutments (Aktan et al. 2008), and abutment-to-approach-slab connections should be designed to allow rotation (Hassiotis et al. 2006, Weakley 2005). A continuous connection using horizontal bars can be redesigned as a deck-over-backwall concept, in which the deck is made continuous and a backwall exists only to hold back the soil embankment. In this configuration, the design is made to accommodate a connection that transfers moment.

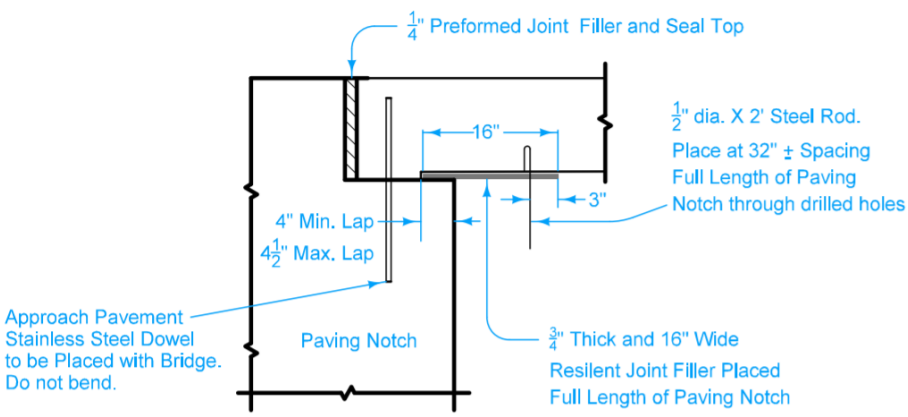

Iowa DOT

Figure 5.26 Iowa DOT BR-205 standard tied connection

Three different bar orientations were analyzed to compare their responses to identical loading cases. A vertical orientation, an inclined orientation per the Story County 118 plans, and a third orientation with an inclination angle of 20 degrees, which can be considered the median between the other two cases, were modeled in ABAQUS. All three bars were the same #8 size and grade 75 stainless steel. The bars were placed exiting the abutment at the same location, 8 in. from the vertical face of the paving notch. Bar orientation was the only change applied to the base model,

with the loading case being identical to that used for the base model. Load-displacement plots are not included here since all three cases show the same behavior, which is to be expected.

Table 5.9 shows the maximum principal concrete stress in the approach slab surface for each load case and bar orientation. During contraction loading, vertical bars result in the lowest concrete stress of 176 psi, and bars with a 40 degree orientation produce a stress of 197 psi. Bars with a median orientation produce a concrete stress only 2 psi less than the more inclined bars. There does not appear to be any clear trend in the resulting concrete stress. Expansion loading also does not show a clear increasing or decreasing trend in stresses with changing bar orientations (Figure 5.27). The maximum stress of 530 psi occurs with the median-orientation bars. The maximum principal stresses in the approach slab surface occur in locations not coinciding with the bars and seem to be more dependent on friction force and soil stiffness in the case of bridge expansion.

Table 5.9. Story County 118—tie bar study approach slab concrete stresses

Approach Slab Maximum Principal Stress (psi)		
Bar Angle (°)	**Contraction**	**Expansion**
40	197	482
20	195	530
0	176	455

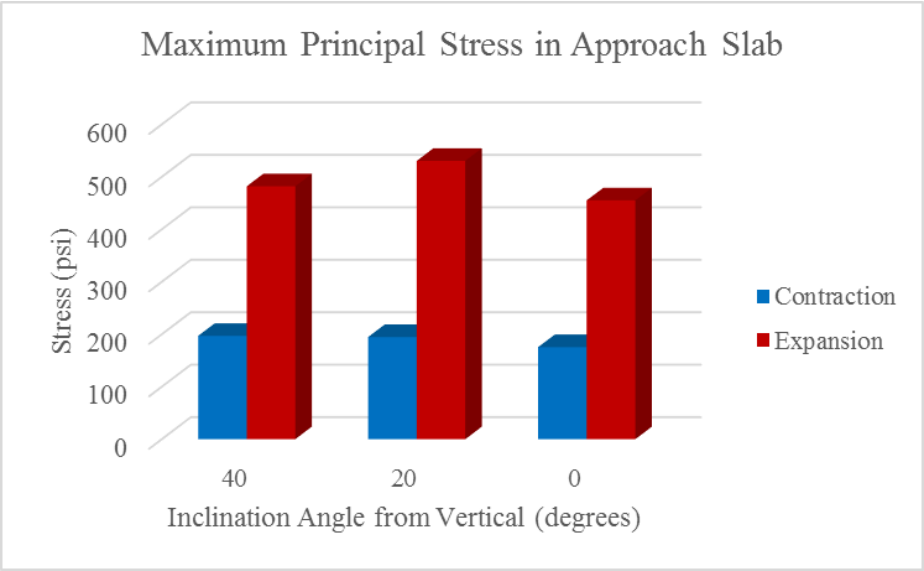

Figure 5.27. Story County 118—tie bar study approach slab stresses

The maximum and minimum von Mises stresses for any single bar across the tied approach joint are listed in Table 5.10.

Table 5.10. Story County 118—tie bar study tie bar von Mises stresses

Tie Bar Von Mises Stress at Joint (ksi)					
Bar Angle (°)		**Contraction**	**Range**	**Expansion**	**Range**
40	Maximum	13.1	10.1	43.0	42.3
	Minimum	3.0		0.6	
20	Maximum	18.7	11.9	44.6	44.5
	Minimum	6.7		0.0	
0	Maximum	22.6	15.8	59.5	19.6
	Minimum	6.8		39.9	

The lowest maximum and minimum stresses during bridge contraction of 13.1 and 3.0 ksi, respectively, both occur for the most inclined bars, the orientation used in the Story County 118 bridge. Stresses increase as the bars are made more vertical until the highest stresses are seen in the vertical tie bars (Figure 5.28).

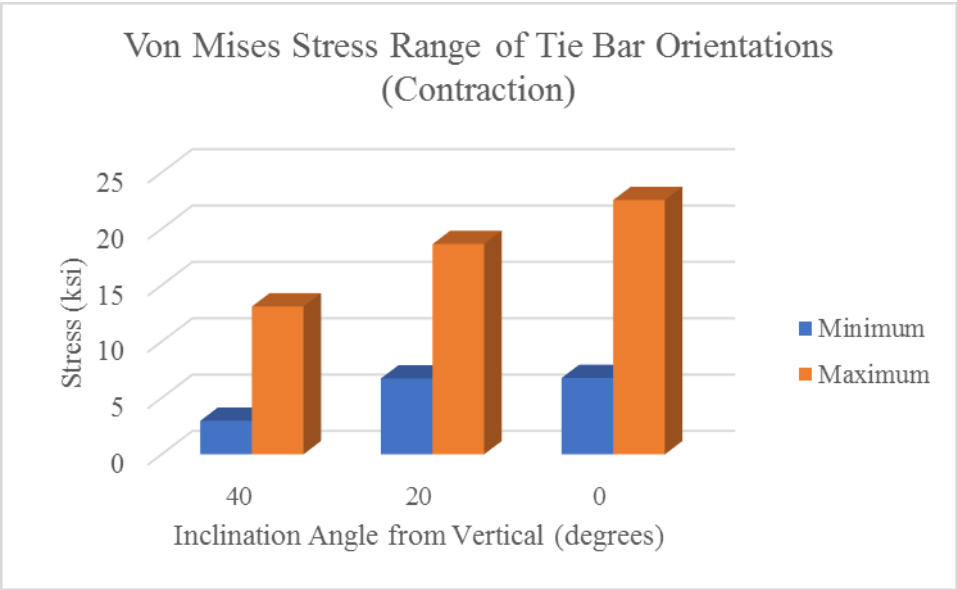

Figure 5.28. Story County 118—tie bar study von Mises stresses (contraction)

Bridge expansion does not show a similar trend, as stresses are almost identical for the two inclined bar orientations and increase for the vertical bars. The minimum Von Mises stresses in the two inclined bar cases were extremely low, reaching less than 100 psi in one case. This behavior was seen in individual tie bars as loading progressed and as the vertical slab movement reversed the axial force in the bars from compression to tension. Bridge expansion pushes the slab and induces compression in the inclined tie bars, but as the abutment moves, the soil pushes the approach slab upwards, inducing tension in the tie bars. No clear trend can be identified in the expansion load case with regard to a reduction in stress resulting from a change in tie bar orientation (Figure 5.29).

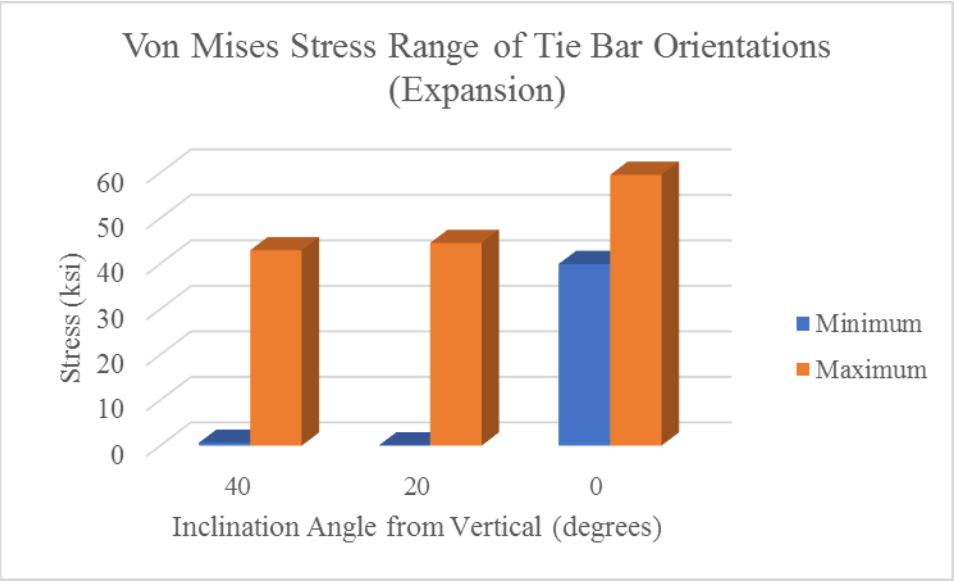

Figure 5.29. Story County 118—tie bar study von Mises stresses (expansion)

Rotation at the abutment occurs due to settlement of the approach slab and creates an upward displacement of the approach slab due to the paving notch edge acting like a fulcrum for the slab. As noted previously, horizontal tie bars that resist this movement only result in cracking of the slab, and an inclined connection is preferred to accommodate rotation. It follows that when examining the connection's response to a horizontal movement, as in this analysis, a more horizontal orientation would perform better. The maximum von Mises stresses decreased with an increasing inclination angle from vertical.

5.2.3.4. Parametric Study of Skew Angle

The most important aspect of the finite element analysis of these bridge approach slabs is the effects of bridge skew on the stresses in the approach slabs and tie bars. Currently there are limitations placed on the use of different types of bridges and details, including integral abutments, semi-integral abutments, and tied approach slabs. Increasing the skew angle creates unknown consequences in many cases that must be investigated through the use of finite element analysis to avoid the risks associated with constructing new details that may perform extremely poorly.

A bridge with 0 degrees of skew will have the entire force of the approach slab carried by the tie bars in one direction, and bridge movement should be limited to one axis aligned with the bridge centerline. The approach slab will have a constant length across the width of the bridge, and it can be assumed that the tie bars can be spread across the joint with regular spacing to carry an equal amount of force by attributing a tributary width. Increasing the bridge skew angle not only changes the shape of the approach slab, making it longer at one side than the other, but also changes the stress distribution across the abutment-to-approach-slab joint.

Three different skew angles were used for analysis, including 0, 15, and 30 degrees (Figure 5.30).

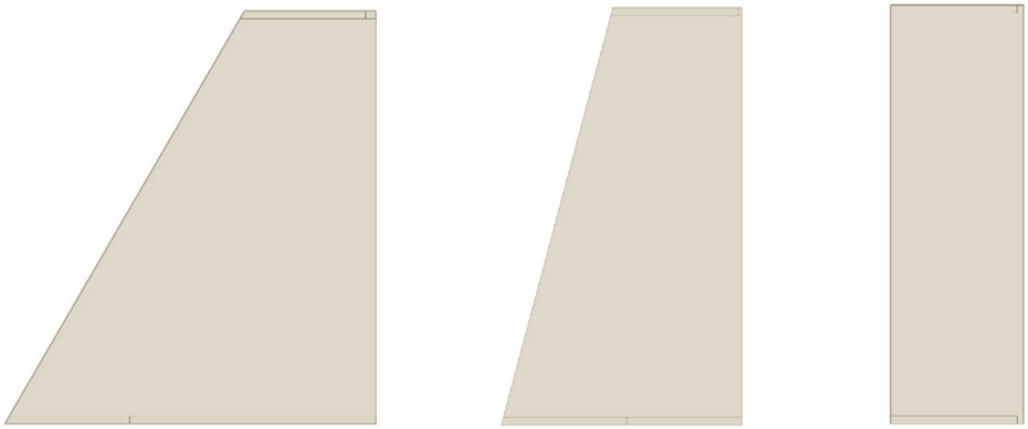

Figure 5.30. Story County 118—approach slab plan view for changing skew angle from 30 to 0 degrees (left to right)

The slab length at the short side was kept at 20 ft to accommodate the barrier rail used for Story County 118, which has a length of 19 ft. Increasing the slab size results in an increased slab weight (Table 5.11) and friction force (Figure 5.31). It would follow that the forces and stresses in the tie bars, along with the stress in the approach slab, would generally increase. These values are discussed in more detail in this section.

Table 5.11. Story County 118—skew angle study slab weights

Skew (°)	Obtuse Side Length (ft)	Acute Side Length (ft)	Slab Area (ft^2)	Slab Weight (k)
0	20.0	20.0	1263.4	189.5
15	20.0	36.9	1798.0	269.7
30	20.0	56.5	2415.3	362.3
45	20.0	83.2	3258.6	488.8

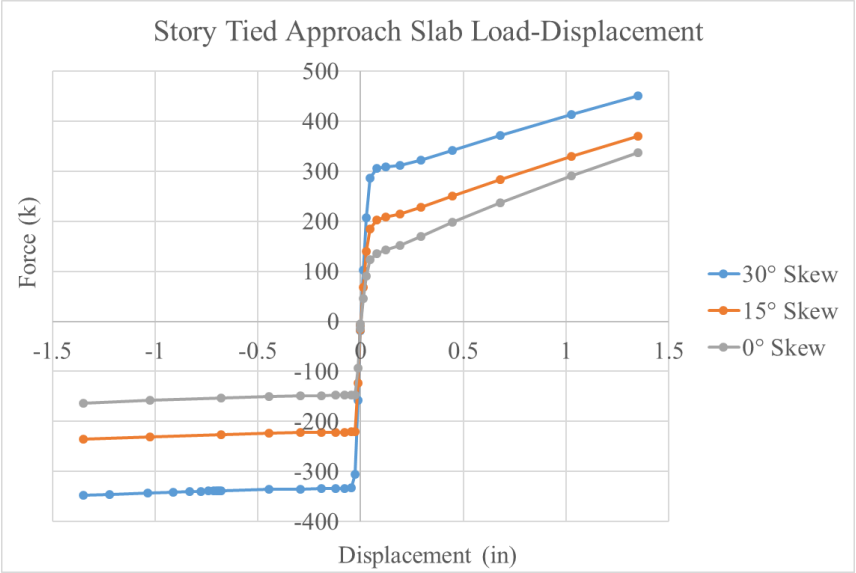

Figure 5.31. Story County 118—skew angle study load-displacement

Identical loading was applied to each model that consisted of an abutment movement of positive or negative 1.35 in. and a temperature change of positive or negative 100°F. The maximum principal stresses in the concrete in the top surface of the approach slab are shown in Figure 5.32. The concrete stresses during bridge contraction increase by a relatively small amount of 27 psi between 0 degrees of skew and 30 degrees of skew.

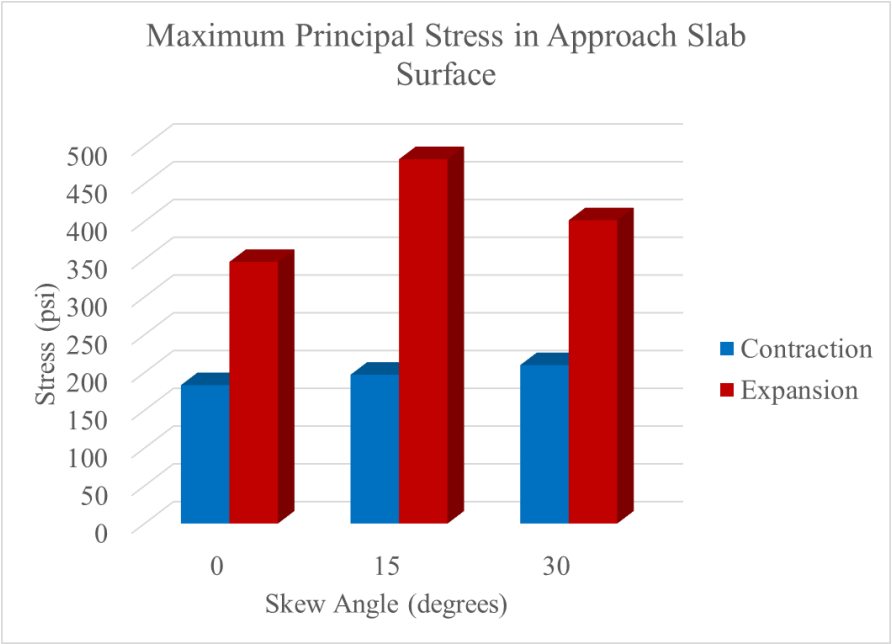

Figure 5.32. Story County 118—skew angle study concrete stresses

The maximum values are located near the acute slab corner (Figure 5.33), which corresponds to the longer side of the slab. This location is expected, since there is a larger amount of contact

surface between the slab and soil and thus a larger total friction force. All stresses during contraction, including the maximum of 210 psi for the slab with 30 degrees of skew, remain below the modulus of rupture of 480 psi per Section 5.4.2.6 of the AASHTO *LRFD Bridge Design Specifications*. For every case during bridge expansion, the approach slab surface stresses are higher than even the maximum value during contraction. The maximum approach slab principal stress of 482 psi occurs in the slab with 15 degrees of skew. The maximum stress during expansion occurs on the side opposite the maximum stress during contraction, on the short slab slide near the obtuse approach slab corner (Figure 5.33). Contraction forces the soil under the slab upwards, creating a tension force in the top of the slab. As discussed previously, the expansion load case is conservative, assuming no soil settlement, no void formation near the abutment, and a rigid boundary condition at a reasonably shallow depth.

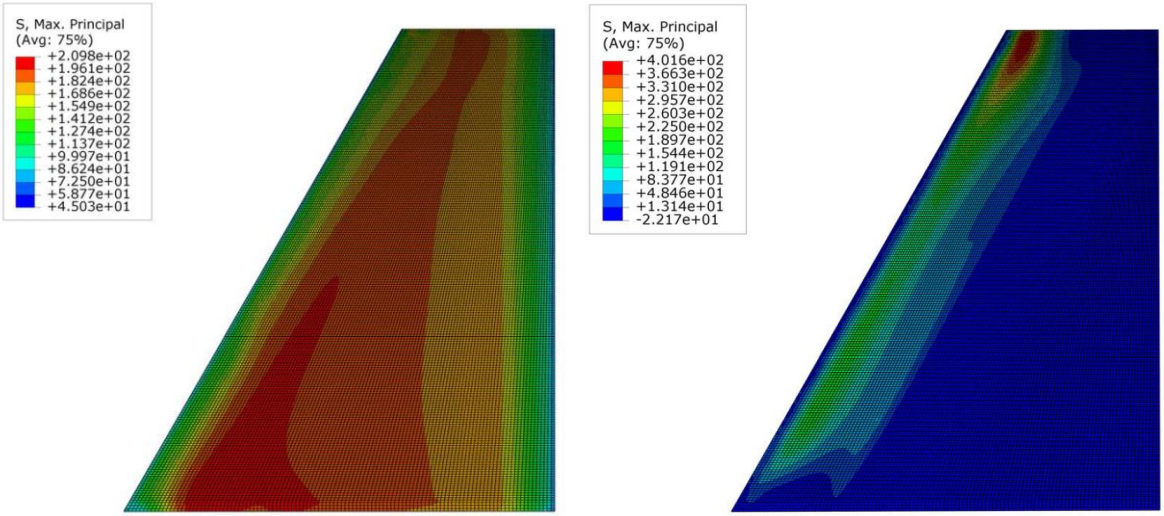

Figure 5.33. Story County 118—concrete stress contours for 30 degree skew for contraction (left) and expansion (right)

Tie bar stresses, much like concrete stresses, also vary with bridge skew angle. As seen previously, increasing the skew angle increases the total size of the slab and the force required to move it. However, tie bar stresses do not increase evenly in response. Figure 5.34 shows the maximum and minimum von Mises stresses in the set of 53 tie bars across the joint. The maximum values increase from 5.4 ksi to 17.3 ksi as the skew increases from 0 to 30 degrees. The minimum von Mises stress values decrease from 3.8 ksi to 0.3 ksi. The range increases from 1.6 ksi to 17.0 ksi. The stress distribution in the bars across the joint changes greatly due to the changing skew angle.

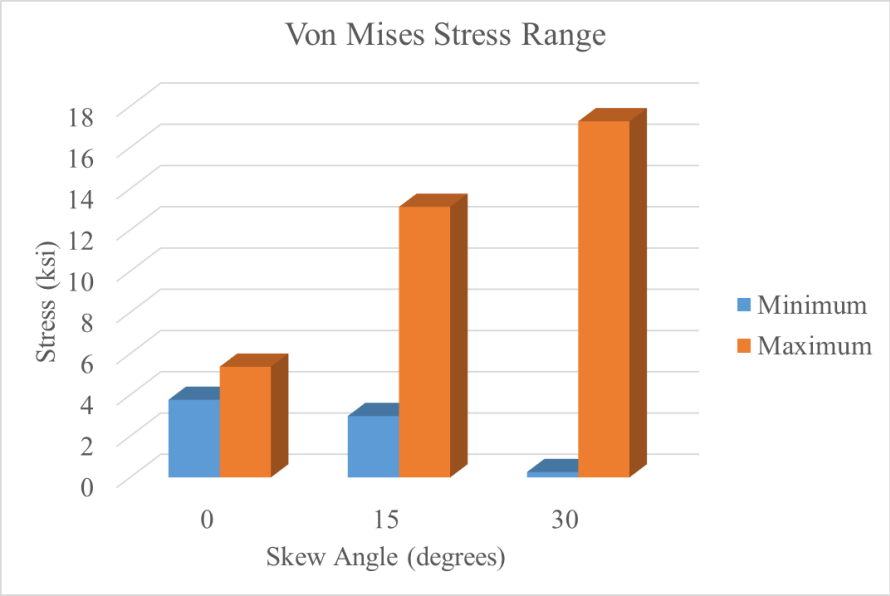

Figure 5.34. Story County 118—skew angle study von Mises stress range (contraction)

The distribution in stresses for all 53 tie bars can be seen for each skew case in Figure 5.35, Figure 5.36, and Figure 5.37. Stresses increase slowly over the course of the first step as gravity is applied, then increase greatly at the beginning of the second step as the slab begins to slide. The increase in the stress range as skew increases and the maximum values increase accordingly is very apparent in the changing scale of the Y-axis between the plots. Using the ABAQUS visualization module, a clear gradient can be seen across the joint, where the highest stresses occur in bars closer to the acute slab corner and the lowest stresses occur in the obtuse approach slab corner. The same behavior is present in the contraction case, minus the two or three highest stresses in the bars at the obtuse corner, where approach slab uplift is highest.

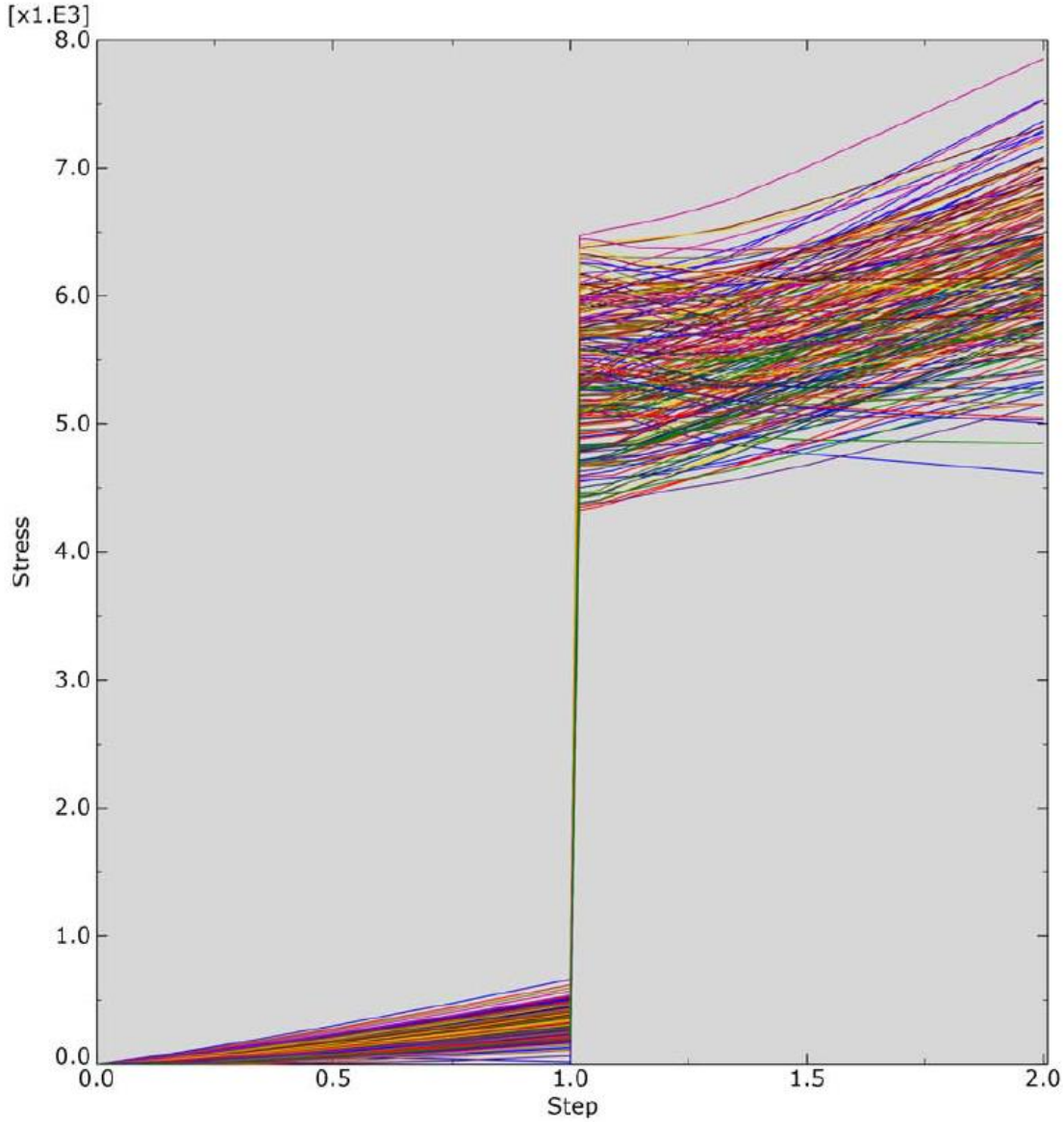

Figure 5.35. Story County 118—von Mises distribution for 0 degree skew

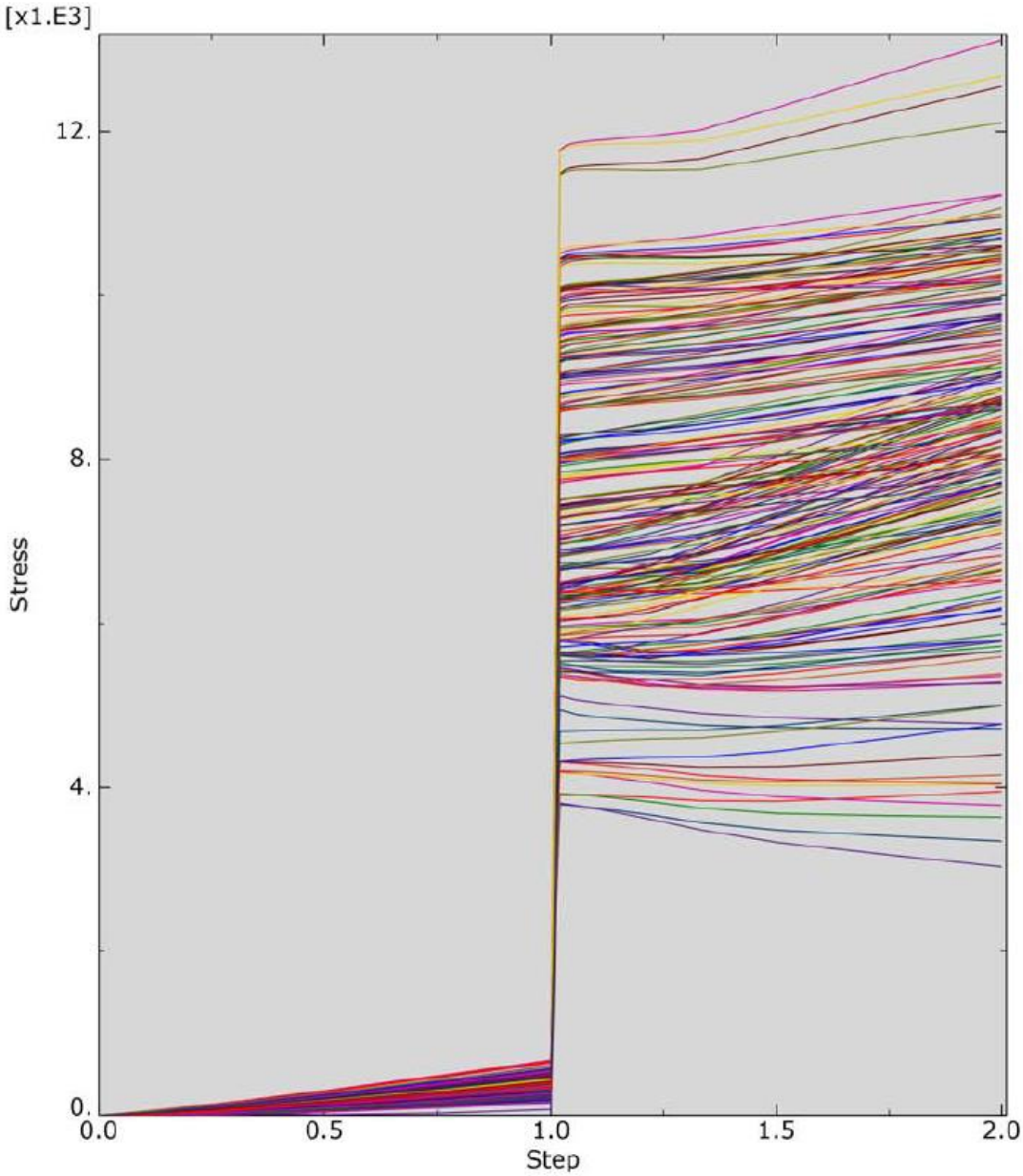

Figure 5.36. Story County 118—von Mises distribution for 15 degree skew

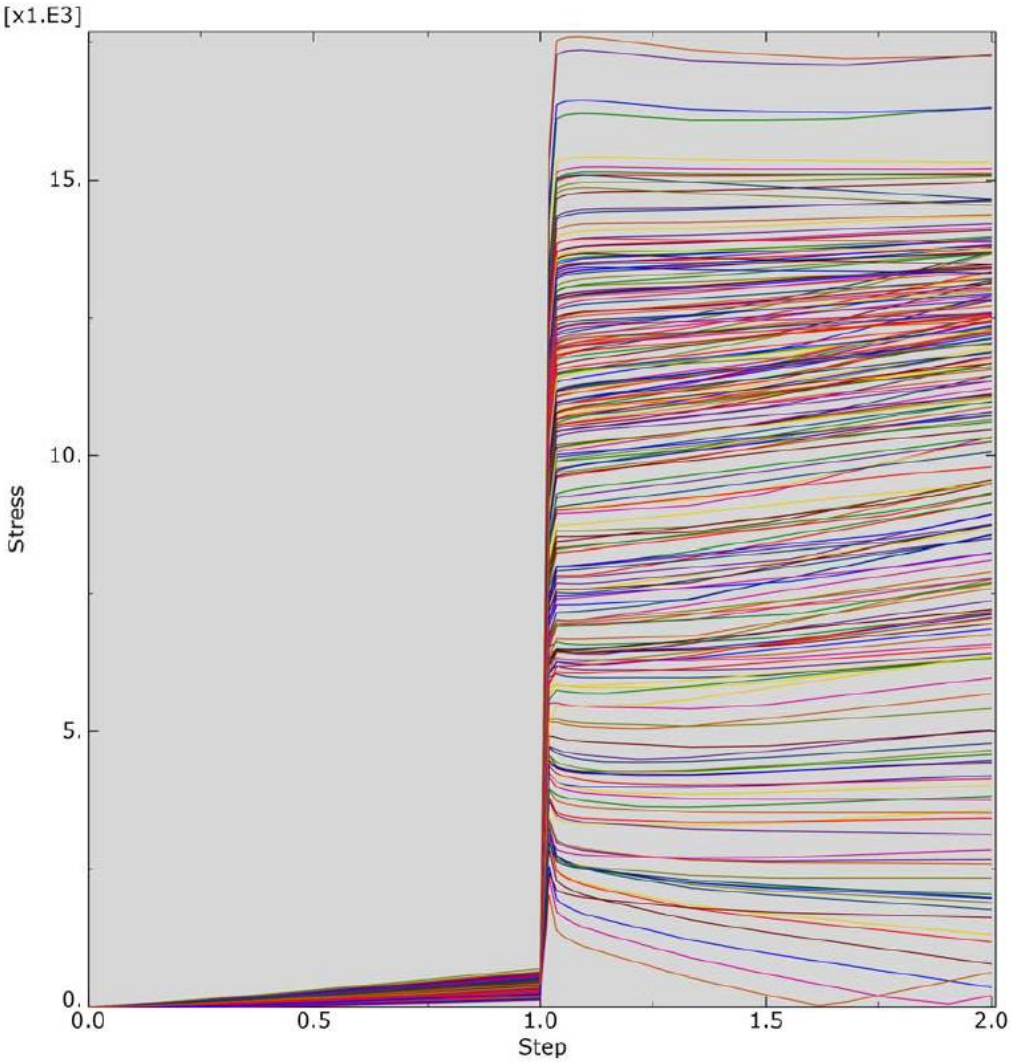

Figure 5.37. Story County 118—von Mises distribution for 30 degree skew

The increase in stresses in the bars is not a direct result of the increase in slab size. If that were the case, the stresses in the bars near the obtuse slab corner would remain the same instead of decreasing. The change in slab shape due to the increased skew angle is shifting the force towards the acute slab corner. This result is especially important considering that tie bars are currently distributed evenly across the tied approach slab joint no matter the skew in Iowa DOT's J40 standard bridge plans. The standards are available for bridges with skew angles of 0, 15, 30, and 45 degrees, and all abutment plans indicate that ties use the same spacing.

5.3. Additional Models for Investigation of Settlement and Erosion

Acting as an extension of the studies described in Sections 5.1 and 5.2, the analyses run on the two models included in this section were intended to refine and expand upon those initially observed to account for settlement and erosion. Each of the initial models was originally constructed to model the effects of thermal movement on the tied connection joint between the

approach slab and the moveable abutment connected to the bridge superstructure. However, given the issues with settlement and voiding erosion noted in the inspections of approach slabs throughout the state, it was determined that additional parameters should be added to these models to gain a more accurate picture of their behavior.

The two models were created to investigate the impact of thermal movement on two moveable abutment brides located in Jasper County and Story County, Iowa. Additionally, both of these bridges were instrumented to correlate the FE models' behavior to that observed in the field bridges. The previous simulations run on these models sought to investigate how friction force from the slab was carried by the tied bars connecting the approach slab to the abutment.

The investigations described in this section focus on the effects of settlement on the approach slab in a tied moveable abutment configuration. By applying the settlement and voiding conditions observed in field bridges to these previously established models, an understanding of their structural response to these conditions can be observed.

5.3.1. Model Parts and Assembly

Several of the model components remained the same or similar to those of the original models described in the previous section, including the abutment section, the approach slab adjacent to the abutment, the tied connection dowels, the slab rebar, and, in the case of the Story County model, the sleeper slab. However, due to this set of studies' focus on the behavior of concrete when subjected to soil settlement and voiding, it was important to determine an appropriate way of modeling soil-structure interaction.

A set of linear springs was used to model the settlement of the soil beneath the approach slab as it was loaded. As it was deemed important to maintain the soil-to-concrete interaction present in the previous study, the set of soil springs was set beneath a modified version of the soil block included in the previous models. In order to minimize the impact that this added soil weight would provide, the thickness of the soil block was adjusted to be as thin as possible without creating convergence issues with each model—the final thickness used was 1/2 in. thick. For these two models, the longitudinal and transverse rebar were modeled as planar shell elements with a spacing and bar orientation taken from the plan sets for each bridge. The dowel placement and angle of the paving notch connection were taken from a combination of the plan sets and Iowa DOT design standards. The FE model for the Story County 118 bridge is shown in Figure 5.38.

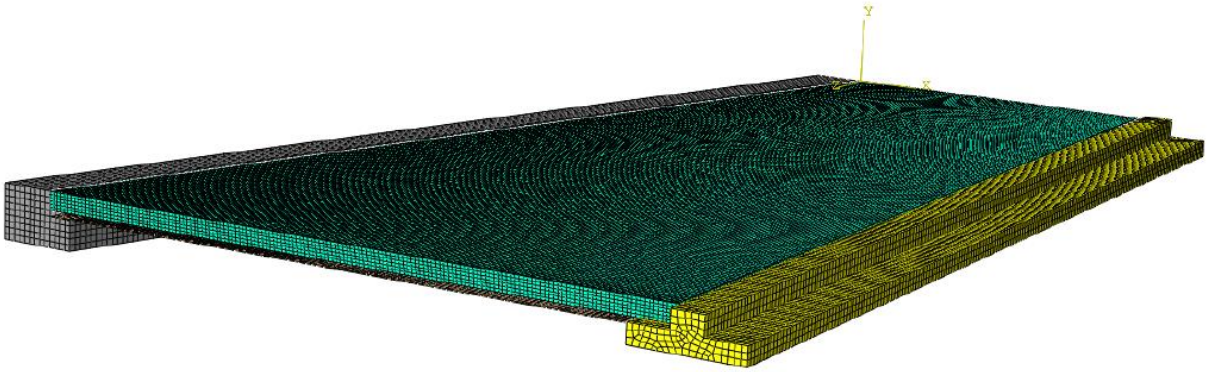

Figure 5.38. Story County 118—FE assembly and mesh

5.3.2. Material Properties

The material properties for the models were generally kept similar to those utilized in the previous studies. Because this study was concerned with cracking and failure of the concrete in the approach slab as settlement and voiding is applied, the Concrete Damaged Plasticity and Concrete Compression Damage settings in ABAQUS were applied to each model to investigate concrete failure behavior. The concrete strength for each model was set as 4 ksi per the plan sets. The soil properties were taken from correspondence with the Iowa DOT and were intended to make the soil act as a shear layer between the approach slab and springs; this layer ties the springs together, preventing them from acting as completely independent elements. The steel properties for the longitudinal and transverse rebar, in addition to the tied dowels, were taken from the respective plan sets.

5.3.3. Boundary Conditions

The boundary conditions for the models were modified from the previous studies to allow for an accurate representation of approach slab settlement. The entirety of the abutment was not modeled, as it would needlessly increase the complexity and runtime of the models. Instead, the top portion of the abutment was modeled to provide support for the approach slab as it would in the field bridge. The portion of the abutment that was removed was replaced with a roller to represent the moveable abutment condition. Nonvertical movement of the soil condition was restricted to represent soil support surrounding the modeled soil block. No explicit boundary conditions were placed on the approach slab, but it was supported by the abutment, soil and springs, and, in the case of the Story County bridge, the sleeper slab.

5.3.4. Springs and Model Calibration

To model the void and settlement conditions present in the models, a series of linear-elastic springs coupled with a thin shear layer of soil were used to represent different soil scenarios. Several different modeling techniques were considered to model soil conditions. Initial models used a displacement-based approach, where the soil block beneath the approach slab was moved a specified distance as a boundary condition. However, it was noted that this produced settlement

patterns that were not indicative of situations observed in the field. A literature review of similar approach slab FE models led to the decision to use a layer of linear springs (Oliva and Rajek 2011). Initially, the springs were arranged on the bottom of the soil layer in a grid with 2 ft spacing. Uneven settlement patterns and convergence issues were eventually resolved via a finer spring grid with a higher number of spring elements. As the spring elements were linearly elastic, a spring stiffness constant, *K*, was required. The initial stiffness value for each spring was calculated by multiplying the anticipated modulus of subgrade reaction, *Ks*, for the soil by the tributary area acting on each spring.

To ensure that the loading and spring scenarios in each of the two models were accurate and would appropriately model the anticipated settlement once loading was applied, a calibration model was also created. Set in a simpler configuration than the two models mentioned previously, the parts for the test model consisted of a 10 ft by 10 ft by 10 in. concrete slab resting on a thin layer of soil and a linear spring grid. As this model was intended to verify the effects of gravity and settlement, no additional support conditions were applied, and no abutments or sleeper slabs were added. Accounting for the volume of concrete and the load applied to the slab, hand calculations were performed, and a theoretical settlement of 1 in. was calculated. The model analysis was run and correctly displaced 1 in. vertically in the negative Y direction, indicating that the slab had settled as expected. This verified that the material properties, load application, and linear springs were performing as intended with no unusual irregularities.

5.3.5. Loading

Loading for the models consisted of the self-weight of the slab coupled with expected loading from truck traffic. Per the normal strength concrete used in these approach slabs, the material density for the slab concrete was set as 0.087 with the gravity set to -1; this produced an end weight of 150 pcf of self-weight. The weight of HL-93 design trucks was used to simulate field loading, and the number of trucks simulated on each approach slab was determined by the number of available lanes. As the purpose of this study was to determine the effects of gradual settlement of the slab, it was deemed reasonable to model the total load of each truck as two distributed tire loads running in the direction of traffic. One truck's worth of load was applied for each traffic lane present on the approach slab. In the case of the Jasper County model, a maximum loading scenario consisted of two trucks crossing the bridge simultaneously. As the Story County bridge is expected to accommodate three traffic lanes in the future, it was modeled with the weight of three truck paths.

5.3.6. Model Analyses

The simulations performed on the Jasper County and Story County finite element models were meant to investigate the structural impact of common approach slab issues related to the underlying soil. As observed in the field inspections and literature review, there are two main soil-related issues that result in approach slab cracking. The first type of failure is related to general settlement, which occurs when soil with a less-than-optimal stiffness is utilized and results in vertical displacement of the entire approach slab. Because the slab is supported on one end by the abutment seat and connection joint, excessive rotation of the entire slab system about

the abutment connection occurs, creating a higher-than-anticipated tensile stress in the top of the approach slab. The second type of failure occurs when the soil erodes and a void forms underneath the approach slab, typically beginning adjacent to the abutment. In this case, the approach slab is required to span this void, as it is still supported on each end by the abutment and remaining soil. This second failure scenario introduces tensile stresses in the bottom of the approach slab. In each case, if the approach slab has not been designed to adequately resist these tensile forces, the slab is liable to crack and create an uneven riding surface.

The focus of the Jasper County FE analysis was to investigate the impact of general settlement and rotation on an approach slab designed without a sleeper slab. Upon establishing the expected structural response of the original field structure, the model was modified to feature a standard dowel-tied connection joint. By comparing these two analyses, the differences in their structural response to a settlement scenario could be compared. In the case of the Story County model, the inclusion of the sleeper slab would likely provide additional support against complete settlement of the slab. Based on the prevalence of voiding and erosion noted in Iowa approach slabs, the Story County FE analysis focused on determining whether the current approach slab is sufficiently rigid to span a standard settlement trench.

5.3.6.1. Jasper County FE Model Analysis

The purpose of the FE analysis of the Jasper County model was to investigate the impact of tied connection dowels on the stress distribution within an approach slab as it settles over time. The Jasper County models created for the previous study offer an ideal opportunity for investigating this effect, as two previously existing versions of the same slab exist. The first version—the base model that replicates the current field bridge—features a standard approach slab design without a tied connection. This model was used to investigate the initial stress distributions expected in the field bridge. After establishing these values, a similar set of conditions was applied to the modified version of the approach slab to investigate how the addition of connection dowels impact the stresses within the slab.

The base model for this study was adapted from the previous section. However, as noted earlier in the discussion of modeling techniques, it was modified to create a settlement condition as opposed to a thermal movement condition. This was accomplished by resting a thin layer of soil atop a grid of linear-elastic springs calibrated with a loading condition to approximate 1/2 in. of settlement. The Jasper County approach slab is 28 ft wide and 10 in. thick with a 45 degree skew and supports two traffic lanes. Therefore, loading consisted of two HL-93 truckloads placed as a total of four strip-loads of 36 kips each, approximating the load that would be applied by each wheel path. Meshing for the Jasper County model proved to be incredibly difficult given the combination of the high skew angle and the geometric issues required to partition surfaces for the wheel loads. Attempts were made to refine the mesh to prevent issues due to meshing.

Following the tests run on the base model, the same loading scenario was run on the modified Jasper County model, which features the addition of 23 #8 bars spaced 14.8 in. apart tying the approach slab to the abutment. Compared to the original model, significant issues arose with establishing convergence as the modified model attempted to run. Further investigation into this

issue revealed that the concrete in the connection joint was experiencing material failure at a very low level of settlement. Tensile forces in the connection reached the limit to induce cracking, and this led to premature model failure as the stiffness matrix was unable to establish stability. Unlike the peak stresses observed in the original model, the maximum stresses observed in the modified model occurred at the dowel connection points between the approach slab base and the abutment seat. These stress concentrations make sense given that the steel dowels are embedded in both the approach slab and the abutment; as the slab settles and begins to rotate about the abutment, the dowels are pulled from both ends and put in tension. This behavior also creates additional tension in the concrete in the top of the slab directly above the edge of the abutment seat. It is likely that as the general settlement of the approach slab increases, these areas of initial stress concentration would be the first to fail.

It is important to note, however, that this approach slab was not originally designed to accommodate the forces created by this type of connection joint. The purpose of this investigation was to theoretically investigate how the stresses within the slab are impacted by the addition of a tied connection condition. As a result, continuing to run the model utilizing the same damage parameters was unrealistic for the scope of this project. In order to allow the model to continue running past the point of theoretical concrete failure, the material properties of the concrete were adjusted to assume a linear-elastic model, ensuring that the stress concentrations would not lead to model instability prior to reaching the desired settlement. Due to the fact that the embedded tie bars in the FE model do not allow rotation of the approach slab at the connection joint, these forces result in high stress concentrations that may be unrealistic representations of what would occur in the field. As such, it was important to investigate other potential areas of failure.

Removing the damage parameters removed any convergence issues, and the model completed running without any additional errors. While this is a less accurate means of determining how and when the model would fail, it does provide a general view of how the stresses in the model would develop past the point of initial failure in the connection joint. Similar to the original Jasper County model, the area with the highest stress values occurs at the obtuse corner in the top of the slab (Figure 5.39). However, the stress value in this area at 1/2 in. of settlement was now recorded as 440 psi as opposed to the 287 psi noted in the original model. This indicates that the rotation restriction introduced by the connection dowels results in increased amounts of tensile stress along the top portion of the slab about the connection joint.

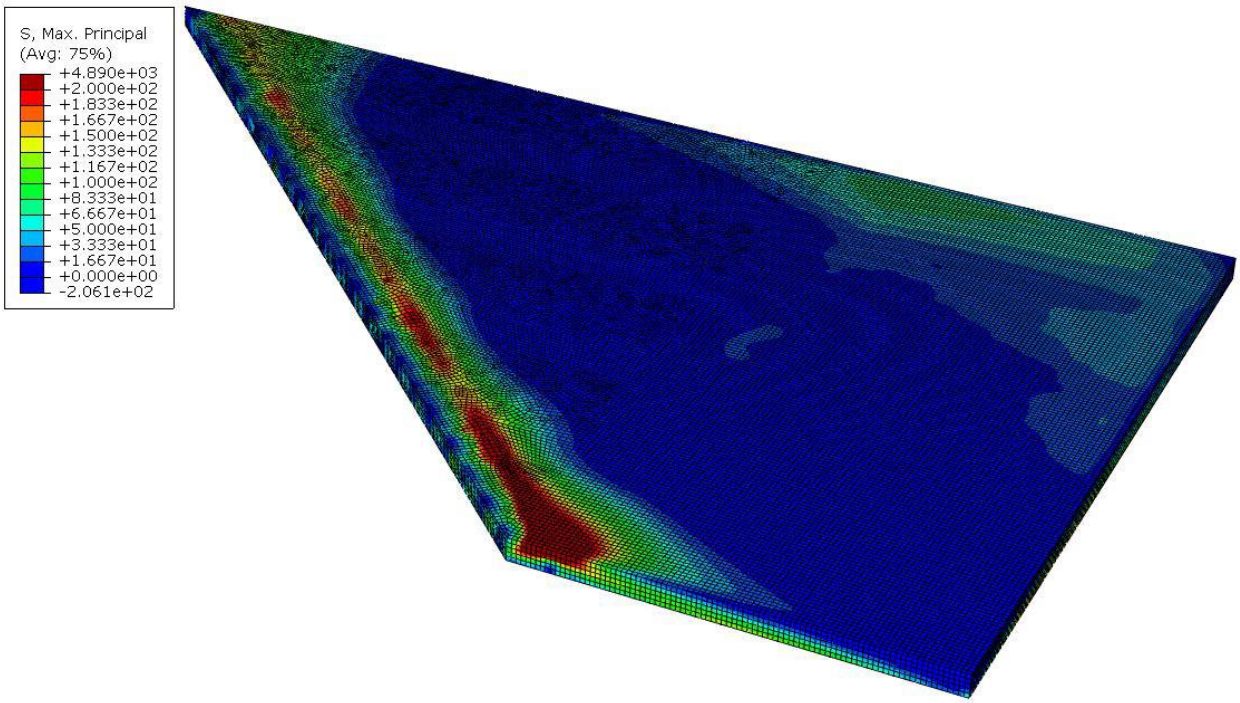

Figure 5.39. Jasper County model stress distribution

These results indicate that a consequence of utilizing tied connection dowels to accommodate thermal movement is additional stresses should the slab begin to settle over time. Due to the fact that settlement is not an uncommon occurrence in many of Iowa's approach slabs, it follows that approach slabs designed with tied approach slab connections should factor in the increased stress values that come with restricting the rotation of the approach slab about the abutment.

5.3.6.2. Story County FE Model Analysis

The analyses performed on the Story County approach slab models were performed to model the results observed from the WJE inspections from 2011 and 2018 (Rende and Donnelly 2011, WJE 2018), which indicated that a fair amount of Iowa DOT approach slabs suffered from erosion of the original subbase. However, these reports also noted that a majority of the approach slabs suffering from voiding were performing adequately with little structural damage. Following these conclusions, the FE models described in this section sought to investigate how the Story County approach slab would perform should it experience voiding and erosion in the future.

An initial model with no erosion or voiding was run to gain insight into how the approach slab would behave in a best-case scenario. Again, this version adapted the thermal movement models from the previous study to account for vertical displacement due to settlement. Initially, adequately stiff soil was used to create a base model with a minor amount of settlement (Figure 5.40). As expected, the slab was supported on each end by the abutment seat and sleeper slab, resulting in a maximum displacement 0.0673 in. roughly near the middle of the slab.

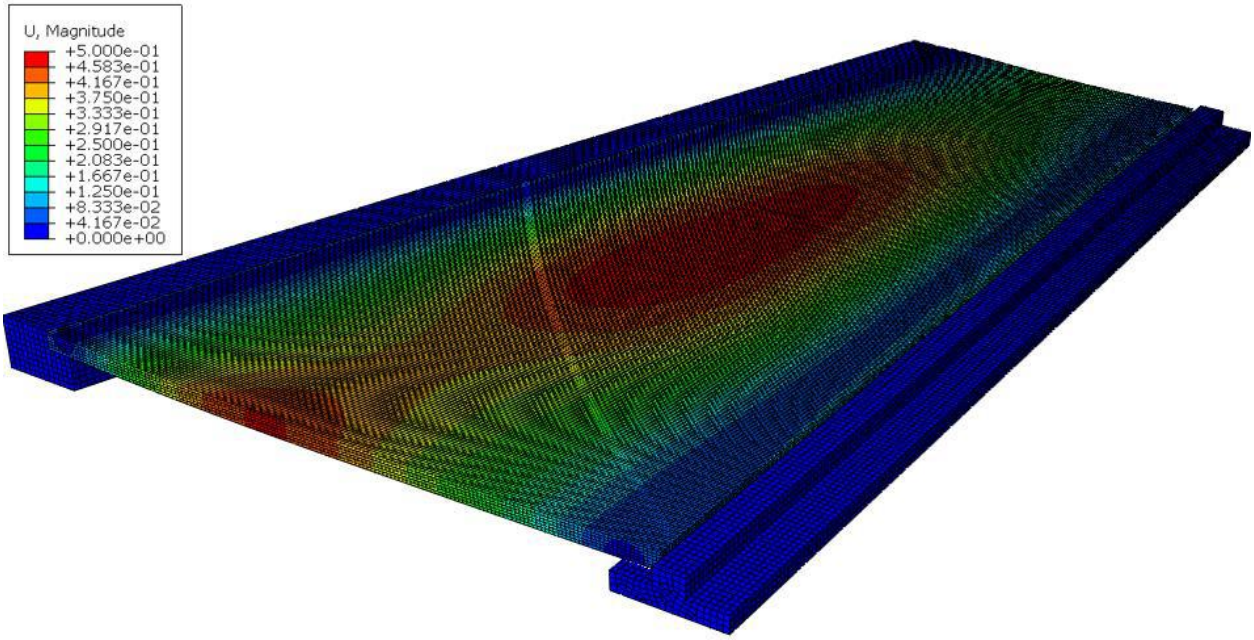

Figure 5.40. Initial vertical settlement for Story County approach slab

Based on this flexural behavior, it follows that the tensile stresses in the bottom of the slab were much higher than those in the top: 161 psi compared to 27 psi, respectively (Figure 5.41 and Figure 5.42).

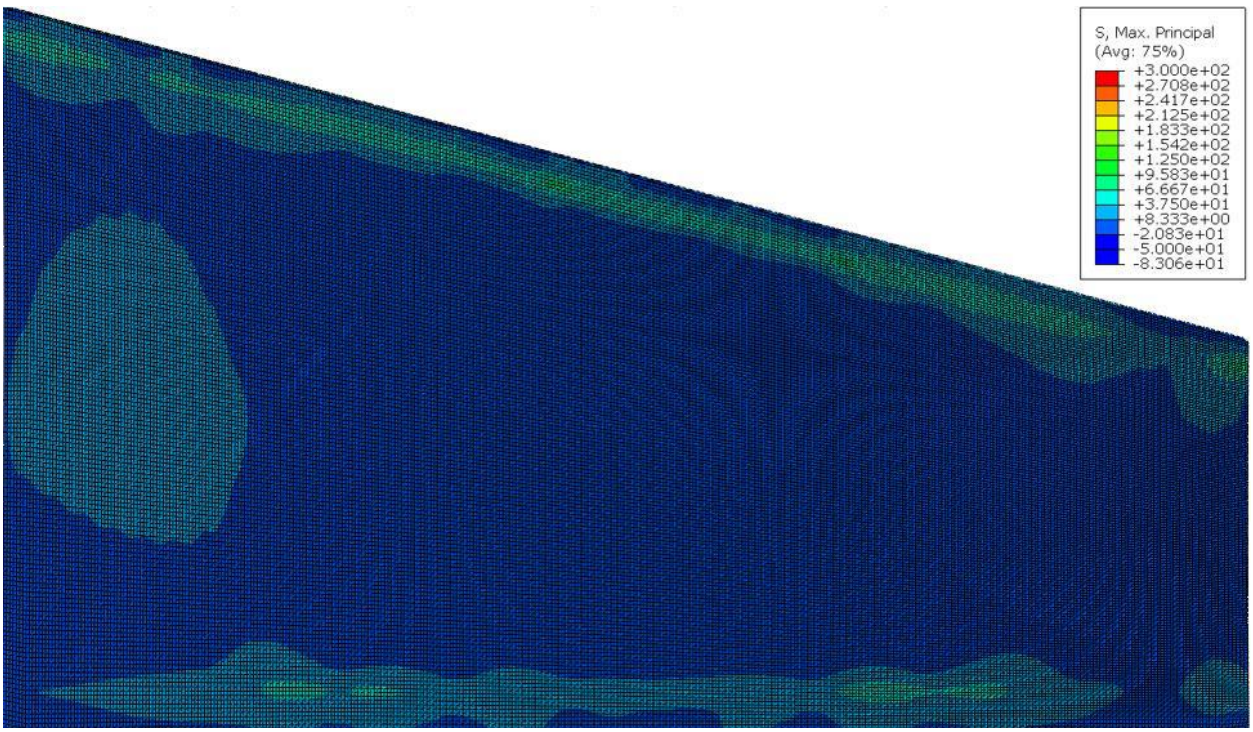

Figure 5.41. Initial stress values for Story County model (top)

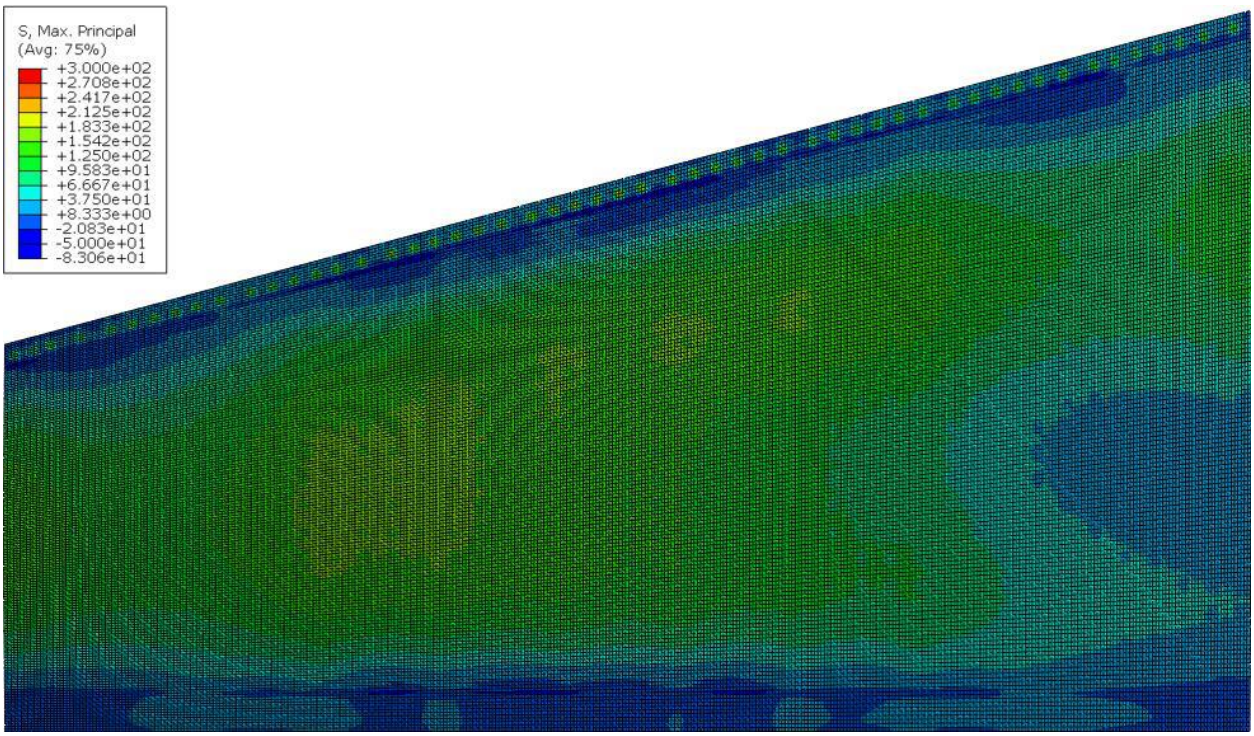

Figure 5.42. Initial stress values for Story County model (bottom)

The highest stress values were observed in the concrete surrounding the embedded connection dowels (Figure 5.43), with a peak value of 270 psi. This is likely a result of the dowel being pulled away from the abutment as the approach slab attempts to rotate at the abutment seat due to settlement.

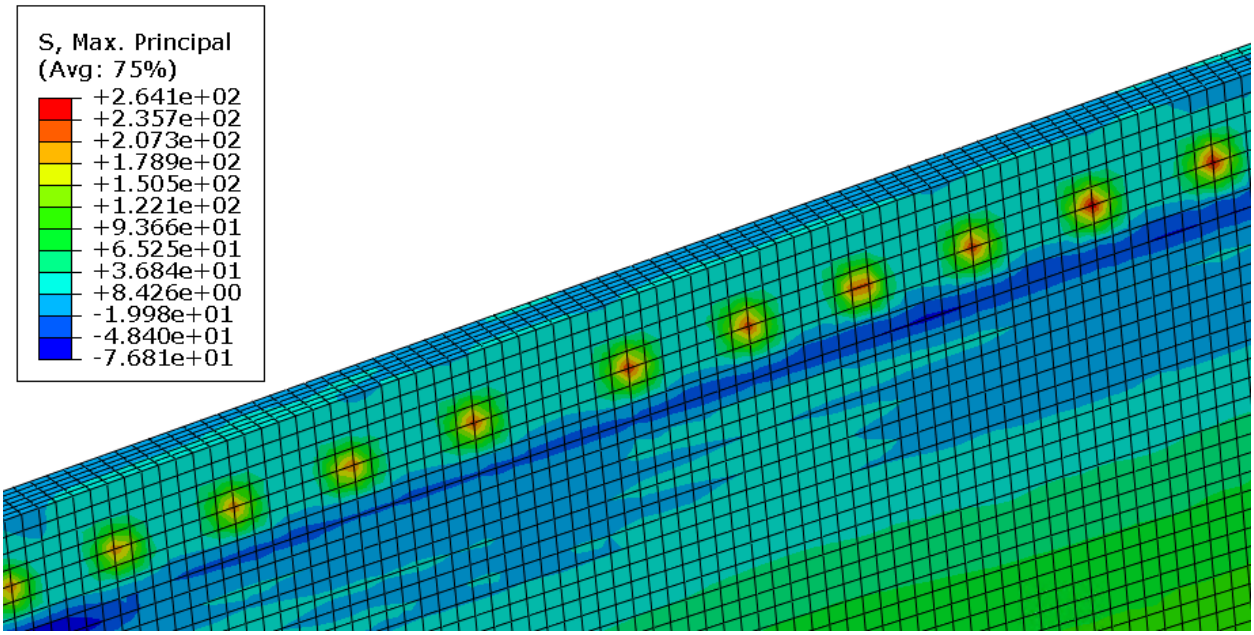

Figure 5.43. Stress concentrations at dowel connection

It is important to note that the boundary conditions of this model operate under the assumption that the sleeper slab undergoes no settlement. This is to ensure that the model's focus is on whether the approach slab has been designed to adequately span the distance between the abutment and sleeper slab should a full loss of soil support occur.

Following a similar approach to those performed by Nassif et al. (2002) and Oliva and Rajek (2011) on similar projects, voids due to erosion were modeled by removing the soil springs directly adjacent to the abutment at varying lengths. The lengths and patterns of the voiding scenarios were modeled based on those observed in the WJE research reports (Rende and Donnelly 2011), which indicated that voiding generally follows the same skew angle as the abutment. An example of the spring layout for an 8 ft simulated void is given in Figure 5.44.

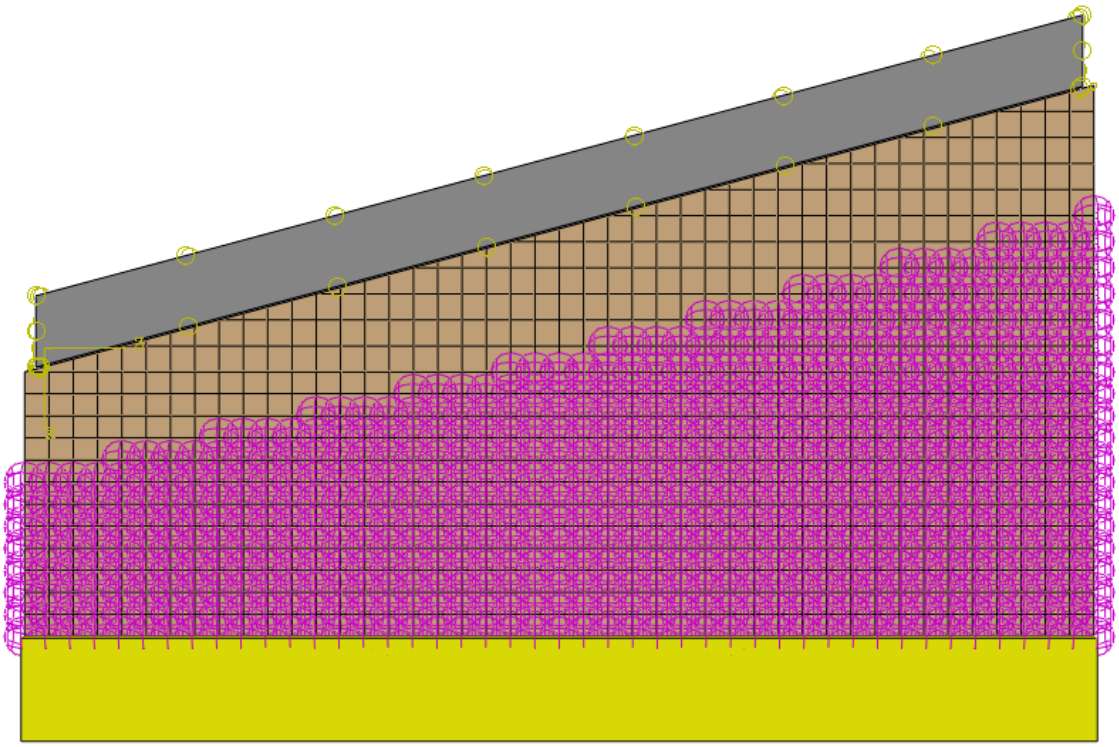

Figure 5.44. Story County 8 ft void scenario

Test models were run for voids of 5, 8, 10, 13, and 16 ft to determine the point where the structural rigidity of the approach slab would be compromised and the slab would begin to excessively deflect and show signs of cracking. The models exhibited expected behaviors. An increased void length resulted in higher peak deflections (Figure 5.45), stress concentrations at the tied connections (Figure 5.46), and tensile stresses in the bottom of the slab (Figure 5.47).

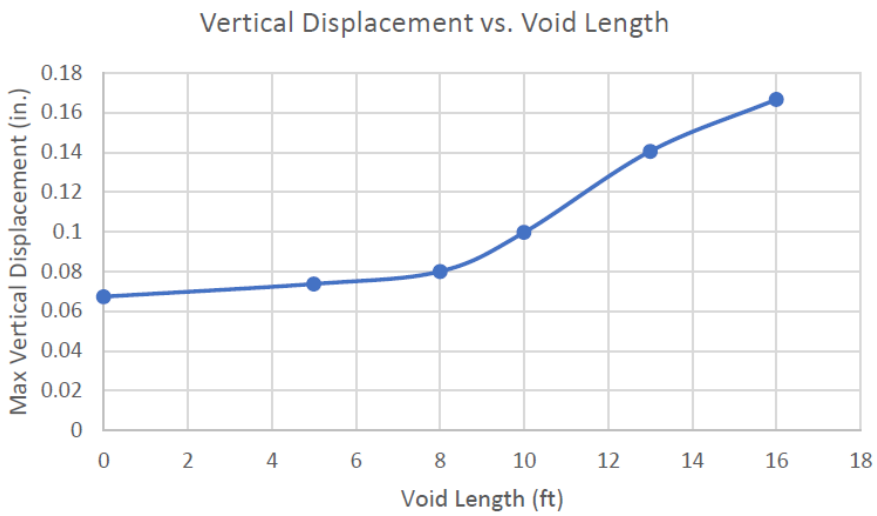

Figure 5.45. Maximum vertical displacement versus void length

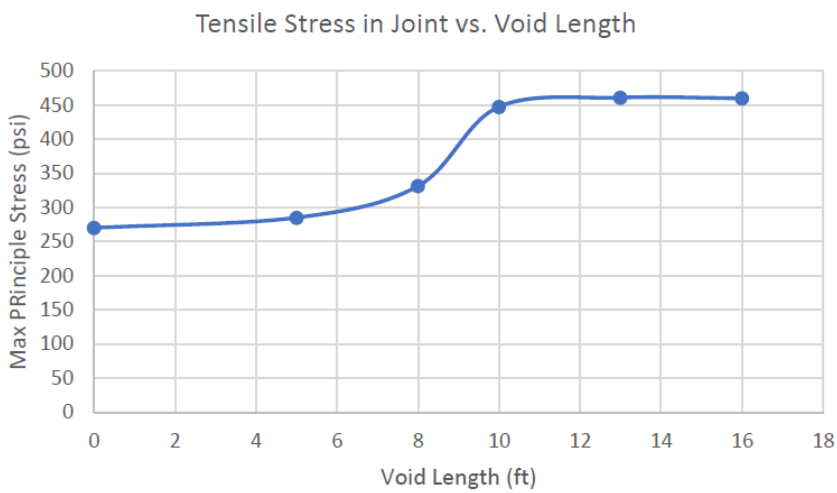

Figure 5.46. Concrete tensile stress in joint versus void length

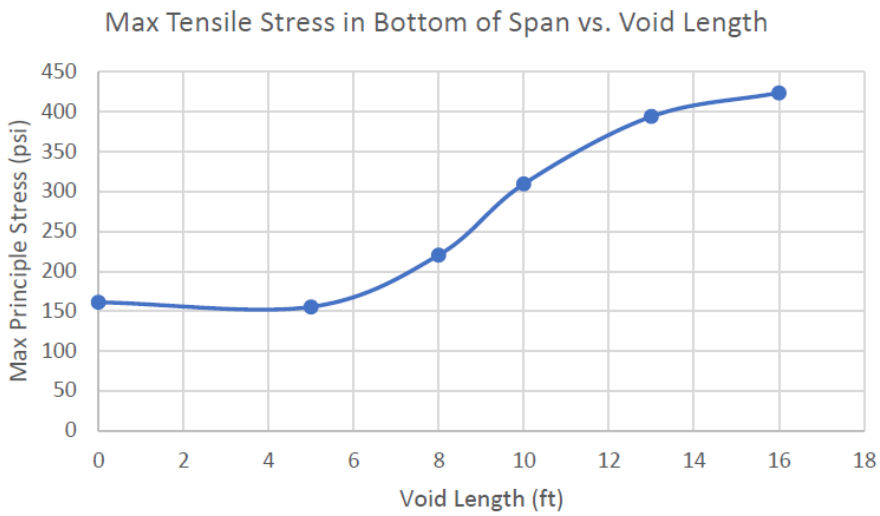

Figure 5.47. Maximum tensile stress in bottom of span versus void length

Stresses did not begin to drastically increase until voiding reached roughly 6 ft in length from the abutment. At this point, displacement began to increase more rapidly, indicating that the stiffness of the slab was being impacted by the loss of soil support underneath the slab. As the maximum displacement of the slab increased, the areas of extreme flexure within the slab began to experience much higher levels of tensile stress. Additionally, this settlement introduced rotation at the connection joint, increasing the tensile forces transferred through the steel dowels. In this case, due to the embedded nature of the tied connection bars in the joint, rotation is restricted, creating areas of high stress concentration. These forces are similar to those noted in the Jasper County model, although they manifest with a much lower magnitude as the voiding condition creates less rotation compared to a uniform settlement condition. Areas of notable stress increase were in the concrete at the dowel connections and in the bottom of the slab at the midpoint of the void.

Maximum stresses and peak displacement remained similar between the first two models, indicating that there is little increase in stresses in the slab for shorter void lengths. However, a clear increase in stresses in the connection joint began to occur between the 5 ft and 8 ft models, and peak stresses in the connection joint increased from 285 psi to 331 psi. However, the maximum vertical slab displacement in this range remained fairly similar to the base model, indicating that the slab remained structurally stiff and adequately spanned the erosion void.

The first major stress increase occurred between the 8 ft and 10 ft models. The tensile stress in the connection joint increased drastically from 331 psi to 447 psi, and it is at this point that the slab began to be at risk for early signs of concrete failure in the connection joint, as the tensile cracking stress for 4 ksi concrete is roughly 474 psi. It is in this range that the concrete at the connection joint began to fail, beginning to crack around 474 psi at a deflection of 0.13 in. The peak stress observed in the connection joint was recorded at 461 psi prior to the failure of the concrete in the joint for both the 13 ft and 16 ft models (Figure 5.48 and Figure 5.49), and it appears that the concrete in the connection joint may be susceptible cracking at a void length of around 11 ft.

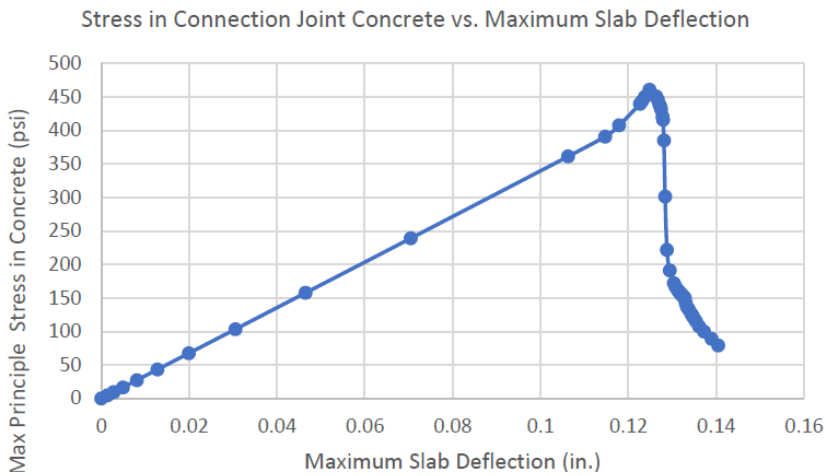

Figure 5.48. Tensile stresses in connection joint (13 ft void)

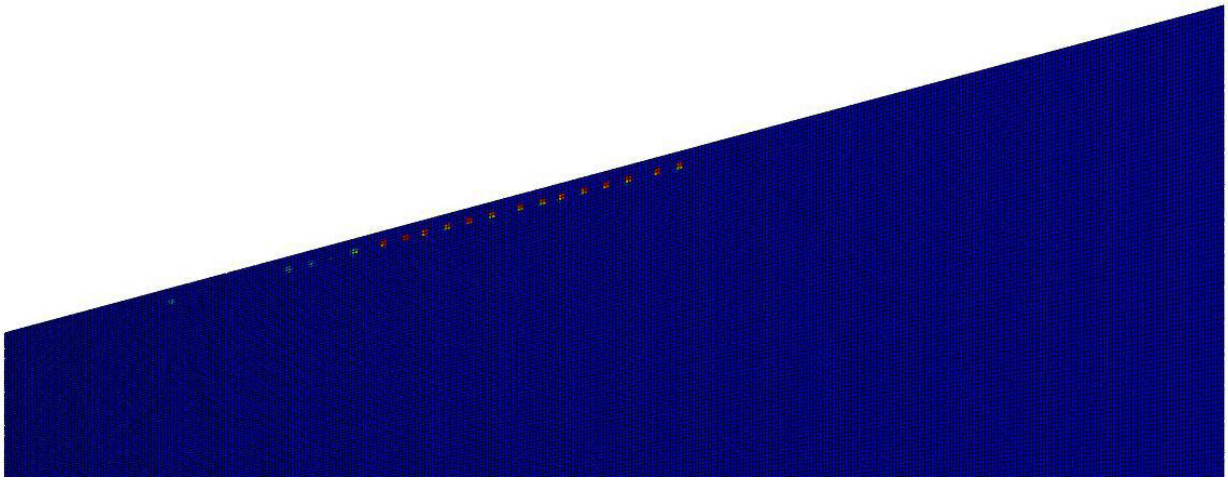

Figure 5.49. Locations of damage-based failure in 16 ft void model

Once the concrete in the connection joint begins to fail, it is anticipated that the displacement of the slab will become more drastic as the dowels will no longer be able to transfer force through the broken concrete in the slab. Once this occurs, the slab will begin to sink into the erosion void below, creating a bump between the approach slab and the abutment.

It is important to note that the modeling techniques utilized for this model designate the dowels as embedded beam elements that cannot physically pull out of the surrounding concrete, which likely creates high areas of stress concentration in the connection joint. Although the FE models indicate cracking and concrete damage in these areas of stress concentration, this is not necessarily indicative of failure in the actual field bridge. Therefore, it is important to pay attention to the transverse forces present in the slab, as this is the area where approach slabs appear to crack most easily based on the field investigations presented in the literature review.

The maximum principal stress in each model is shown in Figure 5.50. Between the base model and the model with the 5 ft void, tensile stresses in the area with the most vertical settlement remained around 157 psi. As with the stress increases observed in the connection joint, the tensile stresses mid-void began to increase between the 5 ft and 8 ft void models, reaching a maximum value of 220 psi. This value increased again for the 10 ft model, reaching a maximum stress of 309 psi. For the 13 ft and 16 ft models, stresses continued to increase at the middle of the erosion void, reaching 394 psi and 424 psi, respectively.

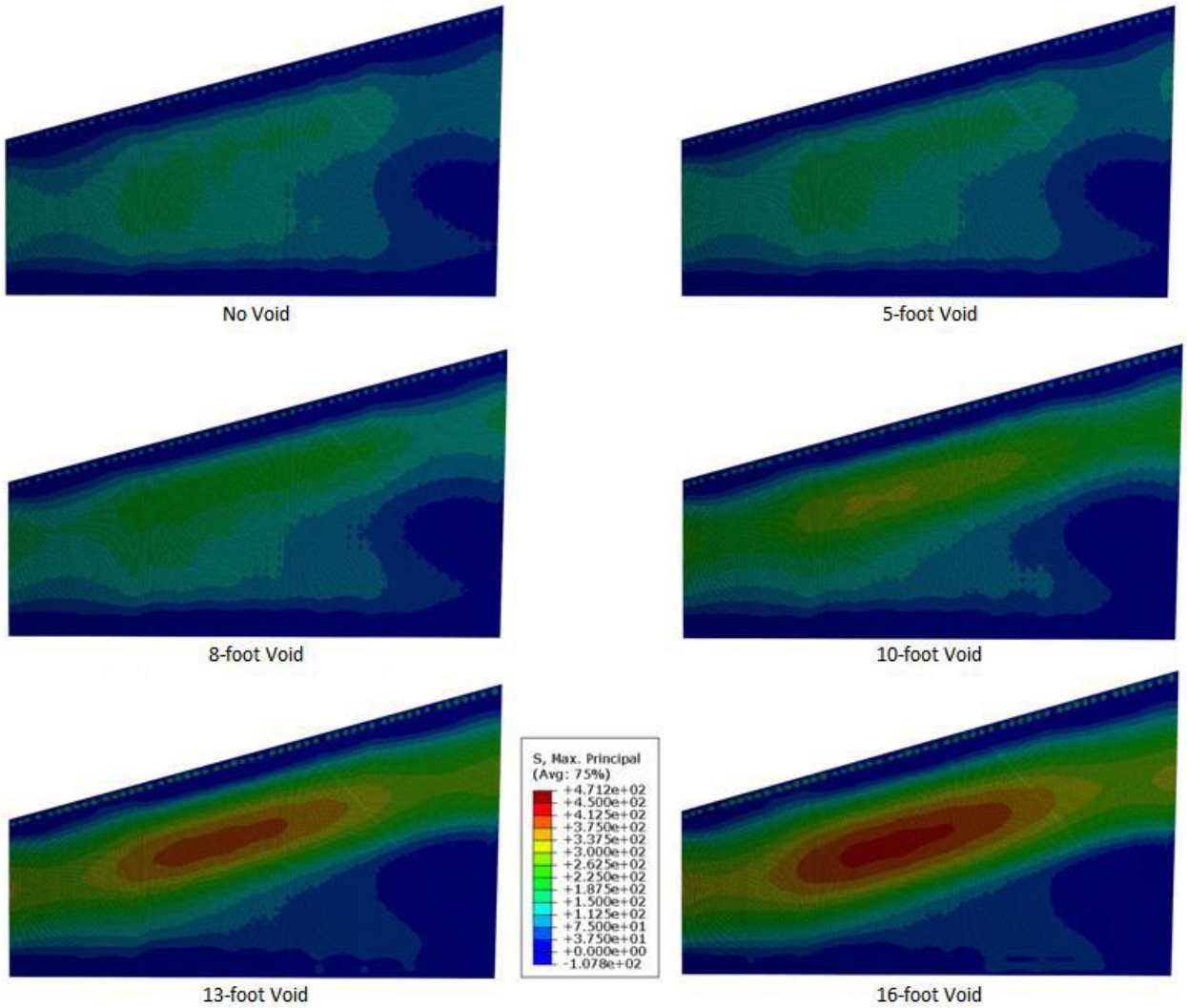

Figure 5.50. Maximum principal stress in each model

Due to the damage parameters used for these models, the 16 ft model failed to converge following the failure of the concrete in the connection joint. Thus, the model was not able to run sufficiently to determine the point at which the concrete in the middle of the slab would begin to crack. Given the peak stress of 424 psi observed at mid-void in the 16 ft model, relatively close to the number at which the concrete in the connection joint failed, it is possible that the slab may be subject to transverse cracking should the voiding extend beyond the 16 ft length included in

this study. However, it is worth noting that such an extreme example of voiding is rare and unlikely, as the majority of the slabs investigated previously had voids of less than 10 ft in length. Given the behavior of these models and the low likelihood of such extreme voiding cases, it is anticipated that the Story County bridge approach slabs are adequately designed to span standard voiding conditions should they occur during service.

5.4. Shelby County 118 FE Model

A third FE model was created to resemble a bridge located in Shelby County, Iowa (Shelby County 118). The 400 ft long and 44 ft wide bridge is located on US 59 over the West Nishnabotna River. The research activities for this bridge were limited to FE analysis, with no field monitoring anticipated. The Shelby County bridge was of interest because of its extremely high skew angle of 55 degrees. The south abutment is semi-integral, exceeding the current Iowa DOT skew limit of 45 degrees. Bridge construction utilized a self-expanding sealant system in the joint between the south approach abutment and the approach slab. The effects of the high skew at the joint location are unknown; therefore, a tied joint was not included in the design. The modeling techniques used for the previous two bridges (Jasper County and Story County) allowed for an investigation of the performance of a theoretical tied approach connection.

5.4.1. Model Features

The element types, materials, contact properties, and boundary conditions used to model this bridge were identical or similar to those of the Jasper County and Story County models. The Iowa DOT BR-205 Standard Road Plan approach connection in combination with the tie bar size and quantity taken from the J44 bridge plan standards were used to represent the tied approach connection. Twenty-two #8 stainless steel bars were spaced evenly across the joint and oriented vertically. Loading consisted of a 100°F temperature change per the Iowa DOT *LRFD Bridge Design Manual*, and the corresponding bridge abutment movement was determined by the bridge length and girder material. The 12 in. thick approach slab is 44 ft wide and 15 ft long at the short side due to skew. The model parts were assembled in the same manner as the previous FE models. A typical sleeper slab and a 2 ft thick soil layer were both modeled to be 1 ft wider than the approach slab to allow for sliding. The model's geometry and boundary conditions can be seen in Figure 5.51.

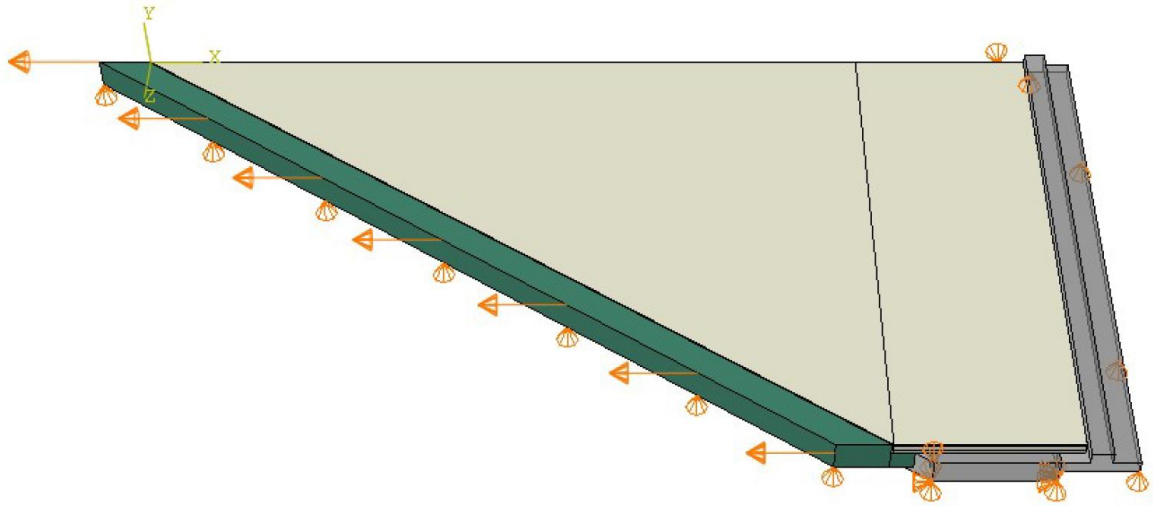

Figure 5.51. Shelby County 118—model geometry and boundary conditions

5.4.2. Shelby County 118 FE Results

The objective of the Shelby County 118 FE analysis was to further examine the effect of skew on a tied approach connection. As described in Section 6.2.3, a parametric study was completed using the Story County bridge as a base model and analyzing skews of 0, 15, and 30 degrees. It was found that the forces and stresses in the tie bars are, in general, distributed evenly across the tied joint for a rectangular slab with no skew. As the skew increases, the force distribution shifts and a gradient forms across the joint. The Shelby County 118 FE analysis examined the same concept for an extreme case of skew of 55 degrees.

The load-displacement curve presented in Figure 5.52 shows that the total force required to pull the slab during bridge contraction is 240 kips. The maximum shear force in any single one of the 22 tie bars is 16.8 kips, and the minimum is 4.1 kips. As expected, the maximum shear force occurs in the end bar at the acute bridge corner.

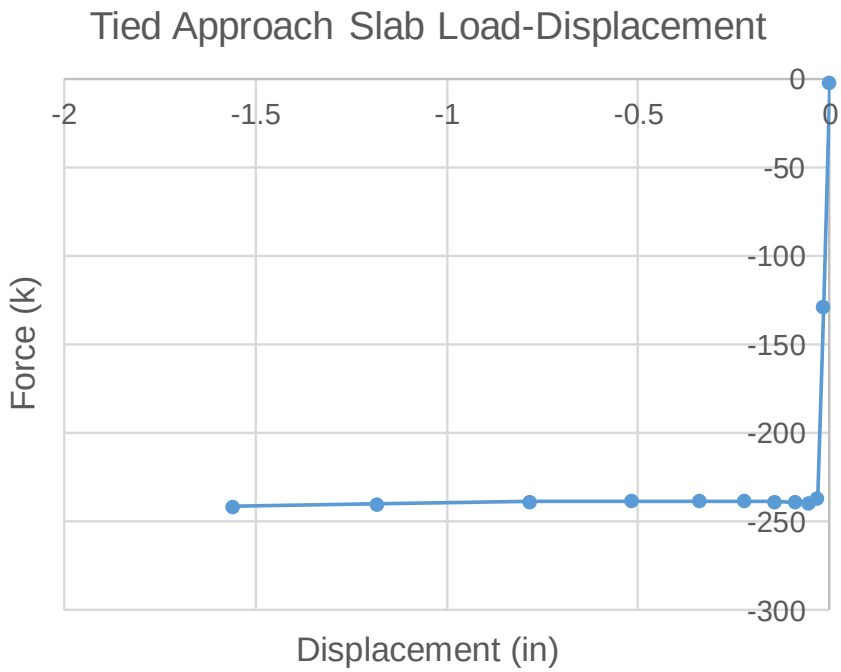

Figure 5.52. Shelby County 118—load displacement plot

The maximum principal concrete stress in the surface of the approach slab is shown in the contour plot in Figure 5.53. The contours follows the trends seen in the parametric study on skew angle for the Story County bridge. The maximum value occurs along the side of the slab on the longer side corresponding to the acute slab corner. The stress of 235 psi does not exceed the rupture modulus of 480 psi per the AASHTO *LRFD Bridge Design Specifications*.

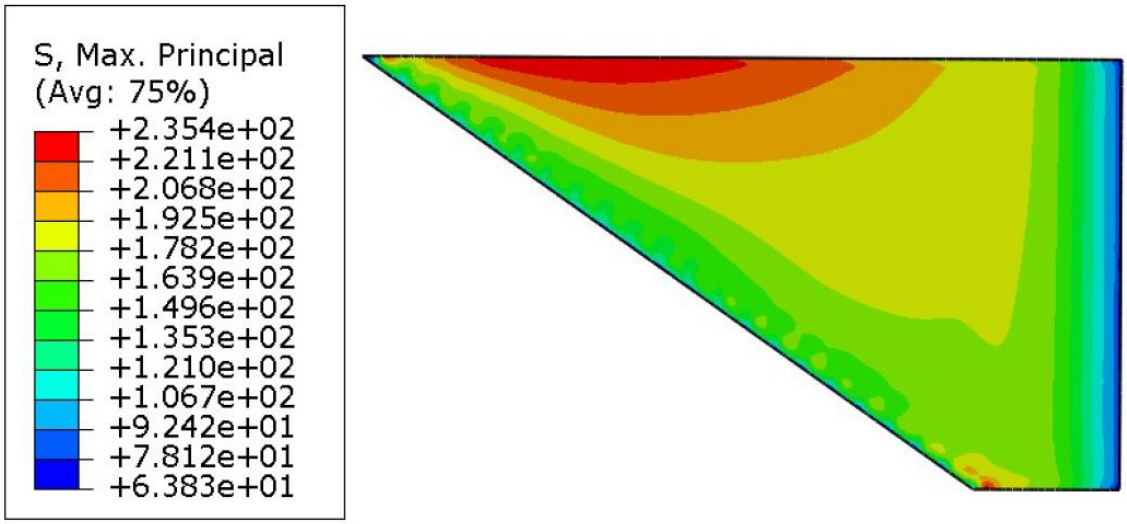

Figure 5.53. Shelby County 118—maximum principal stress

Trends in the force required to pull the slab are generally evident in the von Mises stress experienced by the tie bars. In the case of vertical bars, the shear force in the longitudinal direction accounts for the majority of the total stress. The von Mises stress distribution for all 22 bars is presented in Figure 5.54.

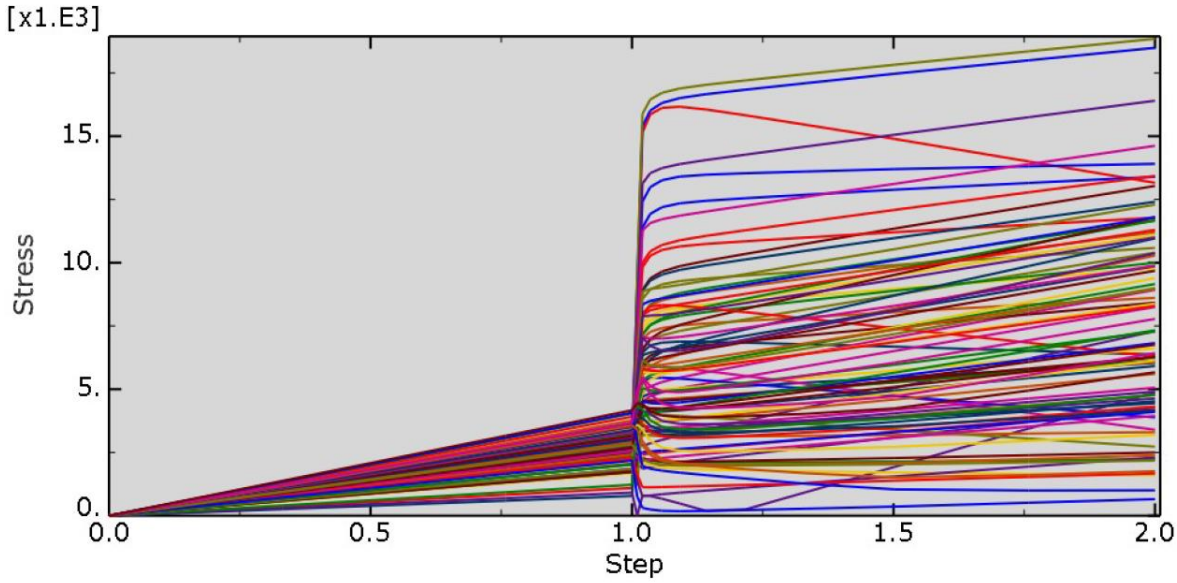

Figure 5.54. Shelby County 118—von Mises stress distribution

The stress distribution shows that the stress after the application of gravity to the model (the first loading step) is under 5 ksi for every bar. Some axial force remains in the bars during bridge contractions, as the maximum axial force in any single bar reached 8.7 kips. The transverse shear in the direction perpendicular to the bridge centerline shows opposite signs for bars at either end of the joint, since the slab contracts and attempts to pull the bars toward the middle. The von Mises stress in the bars ranges from 27.8 ksi to 1 ksi, illustrating a significant difference in magnitudes among the bars across the joint. Although the magnitudes observed in the Story County and Shelby County bridge models are not directly comparable due to differences in slab size and the number of tie bars used, the distribution plots for the Story County 30 degree skew model and the Shelby County 55 degree skew model both show that bar stresses are distributed throughout the range between maximum and minimum stresses.

5.5. Washington County FE Model

5.5.1. Purpose and Background

An important aspect of determining future changes to design details is the review and monitoring of previously built structures. During the routine inspections performed each year on Iowa's bridges, it has been noted that the approach slabs for a specific bridge in Washington County, Iowa, are experiencing issues such as spalling. As this bridge, which consists of precast approach slabs tied to an integral abutment, fits the scope outlined for this project, it was identified as a

useful subject for further inspection. As shown in Figure 5.55, the approach slabs for this bridge have experienced severe spalling directly above the tied connection dowels between the abutment and the approach slab.

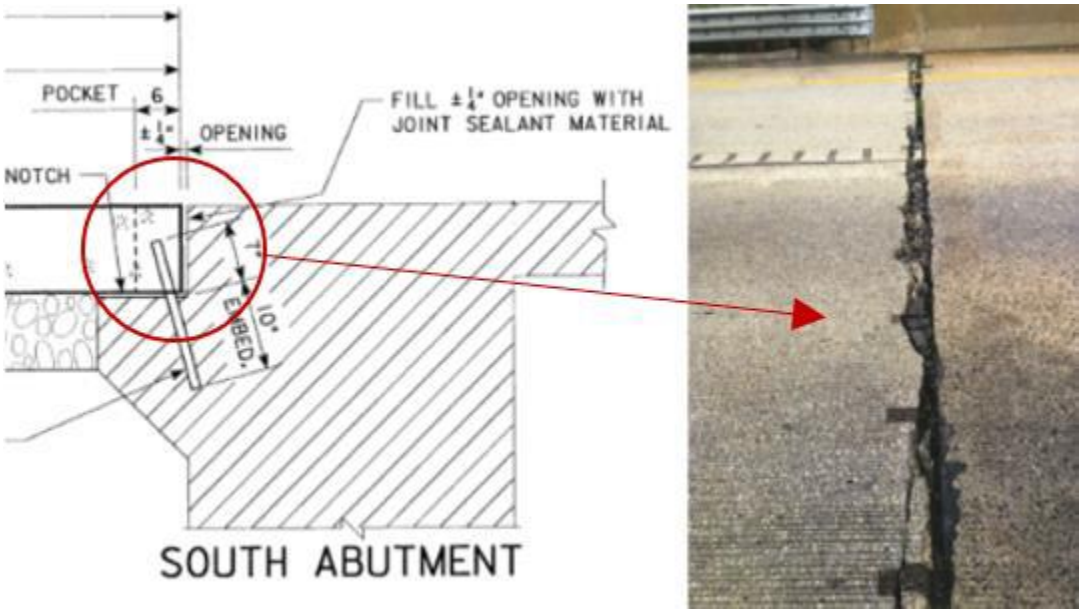

Figure 5.55. Washington County—south approach slab spalling location

The information found in the literature review indicates that this type of concrete failure at the connection point is possibly due to excess settlement. As the slab settles, it begins to rotate around the corner of the abutment seat. It is theorized that this behavior creates tensile stresses within the embedded connection dowels as the dowels attempt to hold the two pieces of concrete together. In turn, this could possibly create areas of high tensile stress concentration, which may result in concrete failure and pull-out of the connection dowels from the concrete. It was determined that a finite element investigation into the impact of settlement on this failure area may provide insight into why this failure occurred.

5.5.2. Design Details

Bridge 606890, the subject of this study, is a pretensioned prestressed concrete beam bridge with a total span length of 180 ft 6 in. and a width of 40 ft. The location is shown in Figure 5.56.

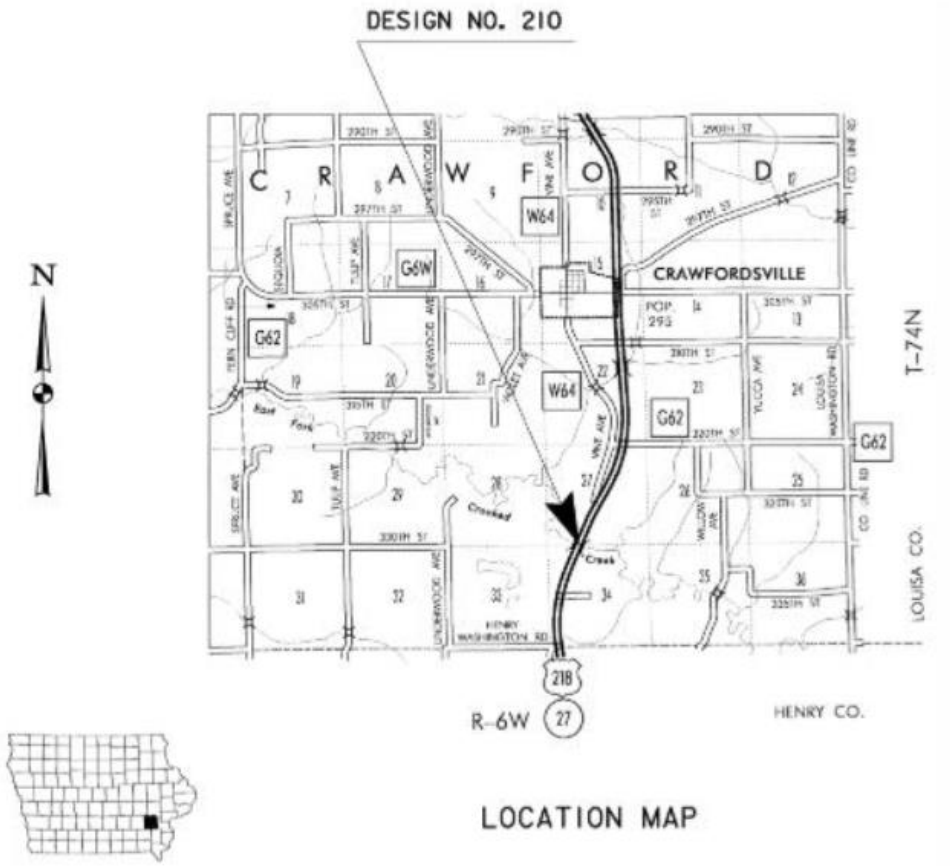

Figure 5.56. Bridge 606890 location map

The bridge was originally built in 1997 with integral abutments following Iowa DOT design 296. In 2012, the current tied approach slabs were installed following Iowa DOT design 210. The approach slab itself features six precast slabs connected to one another via dowels (Figure 5.57), and the slab adjacent to the abutment is connected to the integral abutment via angled dowels (Figure 5.58).

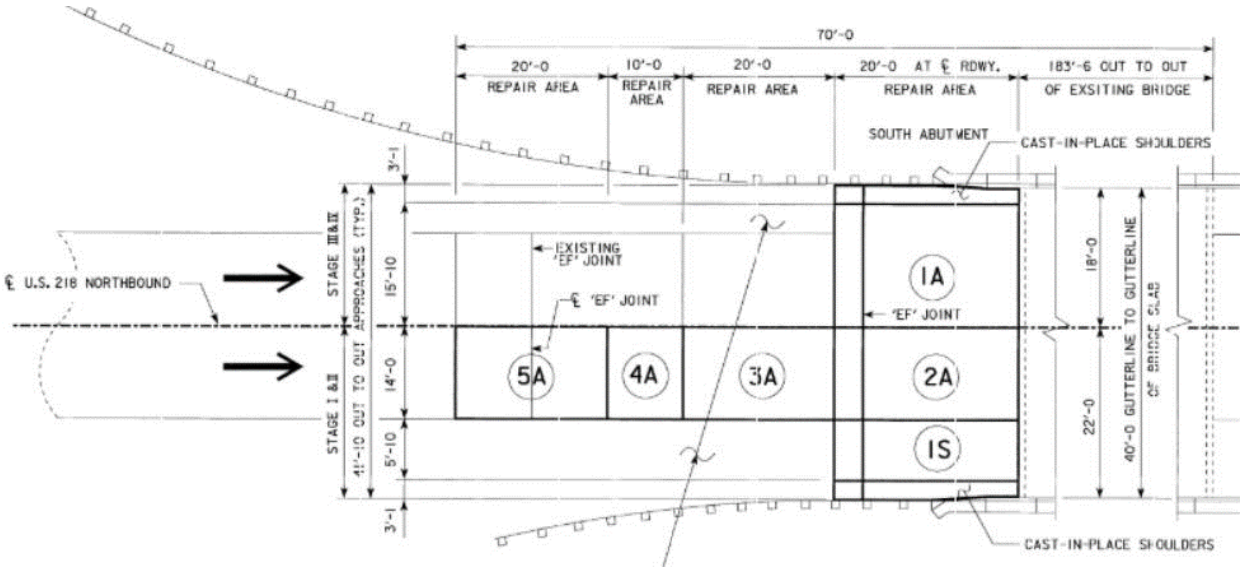

Figure 5.57. Washington County—general layout of precast panels

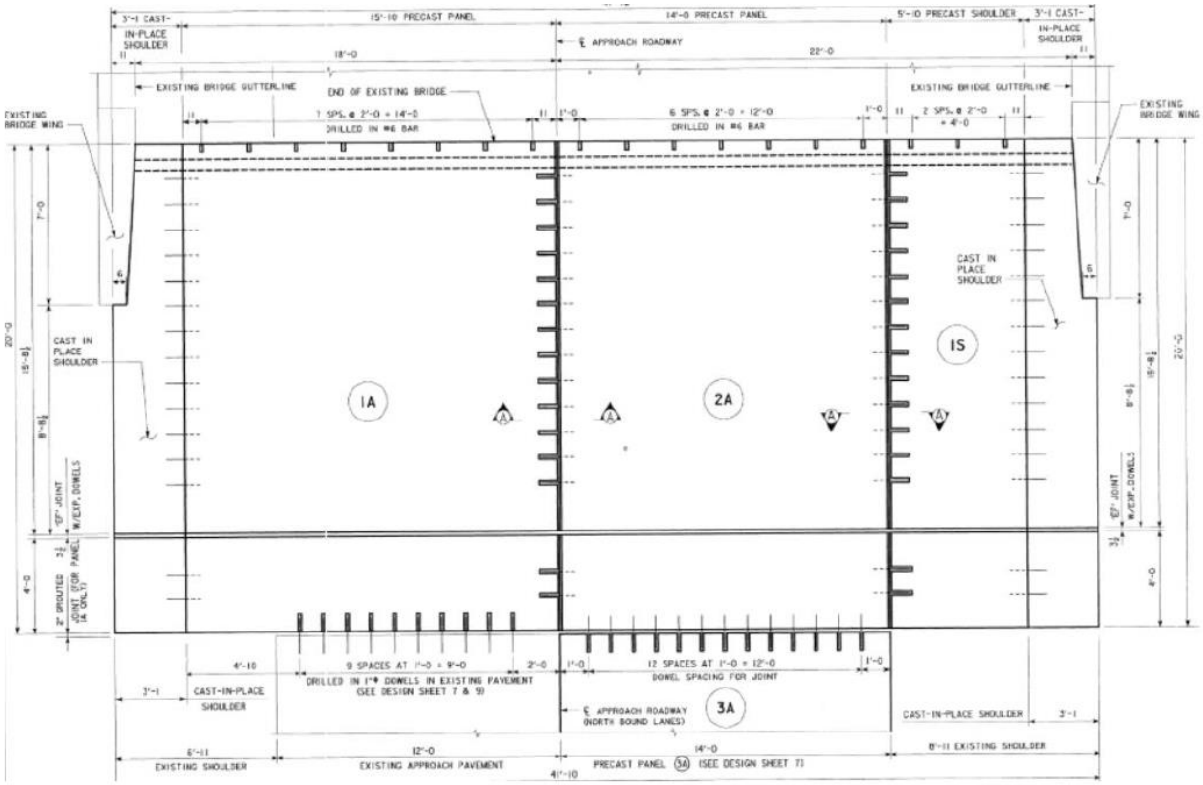

Figure 5.58. Washington County—layout of precast panels at abutment

There is no sleeper slab present in this design, and the slab is intended to slide across the underlying subbase as the bridge expands and contracts throughout the year. It is important to note that the design details utilized for this approach slab are not completely indicative of the standard design details used in most Iowa DOT approach slabs. Compared to those used in the

Story County and Jasper County models, these approach slabs use fewer connection dowels, a stronger (5 ksi) precast concrete, and a subbase consisting of a 2 in. sand cushion, which may be subject to higher levels of settlement compared to the standard modified subbase used for most approach slabs.

The tied dowels consist of eighteen 3/4 in. stainless steel bars embedded at an angle into both the approach slab and the abutment paving notch, and the approach slab itself rests upon a 2 in. sand cushion (Figure 5.59). The tied dowels are specified as having a 7 in. embedment into the approach slab and a 10 in. embedment into the abutment. The exact angle of the dowel itself is not given in either this plan set or the Iowa DOT design standard and was assumed based on the angle used in the Story County bridge. The required cover for the tied dowels is also not specified; it was assumed to be 2 in. per the standard cover specified in the general notes of the plan set. The abutment consists of 3.5 ksi concrete, and the precast approach slab panels consist of 5 ksi concrete.

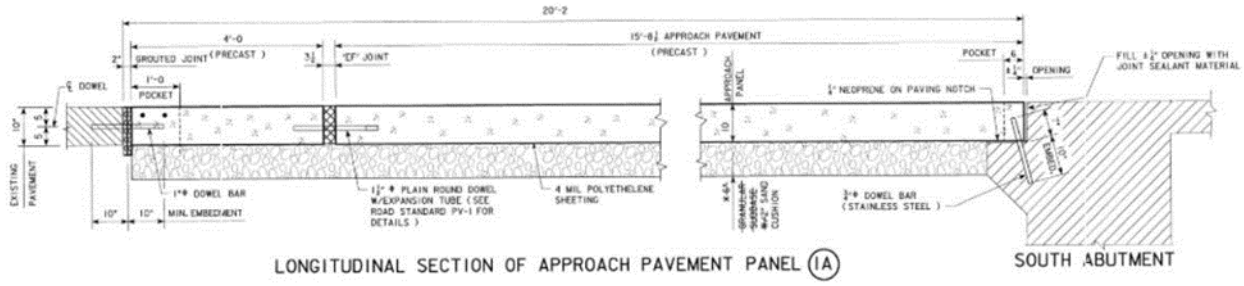

Figure 5.59. Washington County—longitudinal section of approach and abutment

All reinforcing steel for the bridge, abutment, and approach slab is indicated as 60 ksi steel (Figure 5.60). Connecting each of the precast panels is a set of EF joints with 1 1/2 in. plain round dowels with an expansion tube.

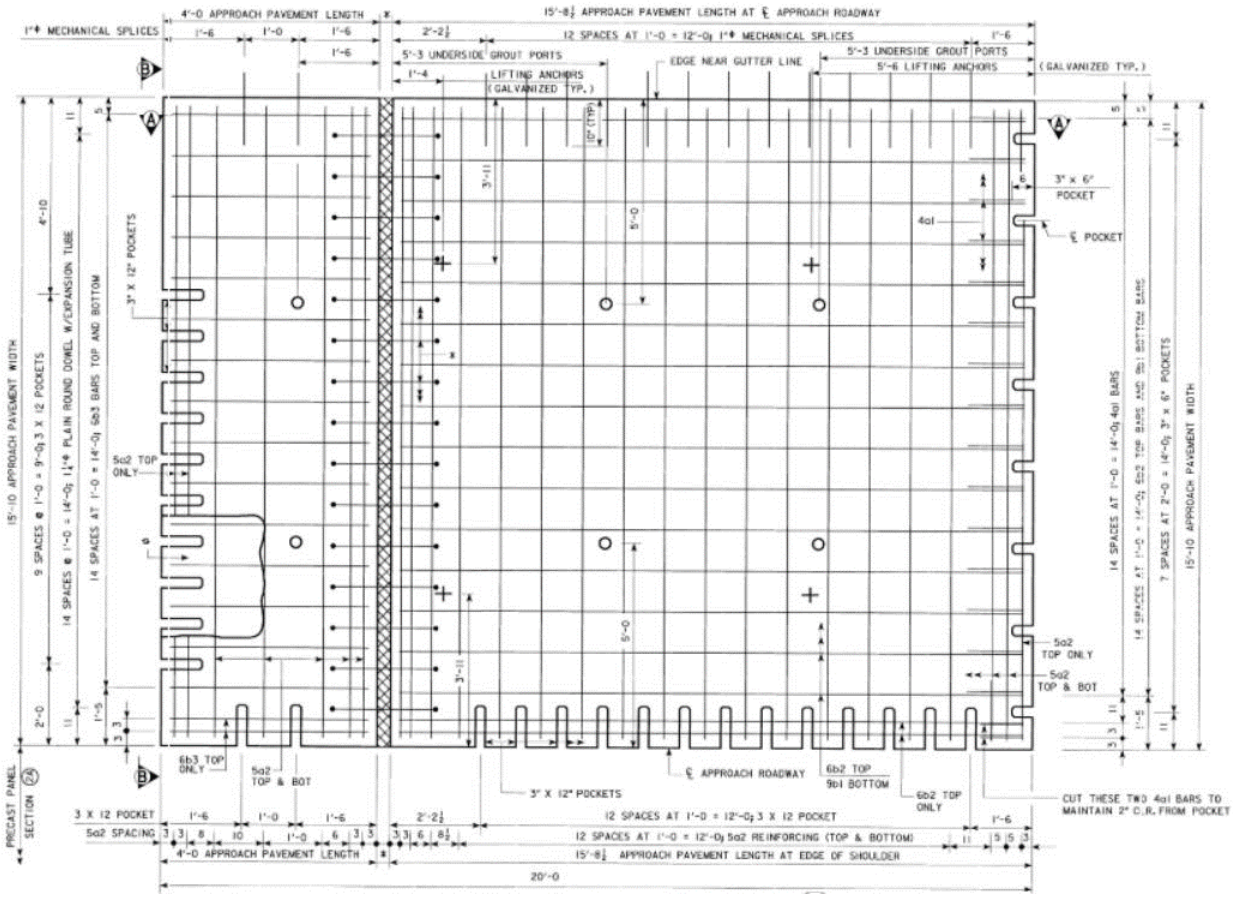

Figure 5.60. Washington County—rebar layout for Panel 1A

5.5.3. Finite Modeling Procedure

A base finite element model for the tied approach slabs in Bridge 606890 was created following the correlations and precedents set by the previous studies described in Sections 6.1 through 6.3 comparing field data to finite element models. By following a similar set of finite element modeling procedures and design considerations, it is reasonable to assume that, should these models exhibit behavior and stress distributions similar to those observed in the previous studies, the values given in the output should be an accurate representation of this approach slab. The goal of this study was to simulate and investigate the effect of the approach slab's settlement on the performance of the approach slab. Specifically, a key area of focus was the joint connecting the approach slab to the abutment, where clear signs of concrete failure occurred. Keeping with the previous studies, these models and their subsequent analyses were created and run in ABAQUS.

Instead of modeling the entire bridge, an effort that would drastically increase the runtime of the analysis, the base model for this approach slab consisted of the approach slab, the uppermost part of the abutment, the longitudinal and transverse slab reinforcement, the sand cushion beneath the slab, and the tied dowels connecting the abutment and the approach slab. The sand cushion was modeled via a thin shear layer and a series of linear springs, as with the Jasper County and Story

County models. The purpose of this model was to represent the approach slab, abutment, and connection as they were installed and currently operate in the field. Therefore, all approach slab elements were drawn with respect to the approach's plan set, and the abutment dimensions were obtained from the bridge's original plan set.

To simplify the geometry of this model, approach slab segments 1A, 2A, and 1S and the two shoulder slabs were drawn as one uniform mass. Since the segments were designed to function as a continuous slab following installation, this was intended to give an accurate representation of the approach slab's geometry. In addition, the shape of the complete slab was approximated with all sides at right angles to allow for better meshing. Because the main concerns of this model were the concrete and tied dowels near the slab-abutment connection, the precast segments on the other side of the EF joint were ignored, as a majority of the critical stress in the model should be a result of the applied movement from the bridge deck. The final shape of the approach slab is 41 ft 10 in. wide and 15 ft 8 1/2 in. long at the EF joint with a depth of 10 in. throughout the slab.

As noted above, the abutment geometry was drawn based on the original plan set from 1997. In an effort to simplify the model, the abutment geometry focused on the integral section and the approach slab seat; the abutment was cut below these areas of study and replaced with a boundary condition to simulate the support its embedment in the soil would provide.

To fully represent the impact of the reinforcing steel, all reinforcement was drawn with wire-truss elements to allow for a more useful model of stress distribution throughout the slab (Figure 5.61). In addition, each of the 18 connection dowels were modeled as wire-beam elements to allow for the full transmission of forces between the integral abutment and the approach slab.

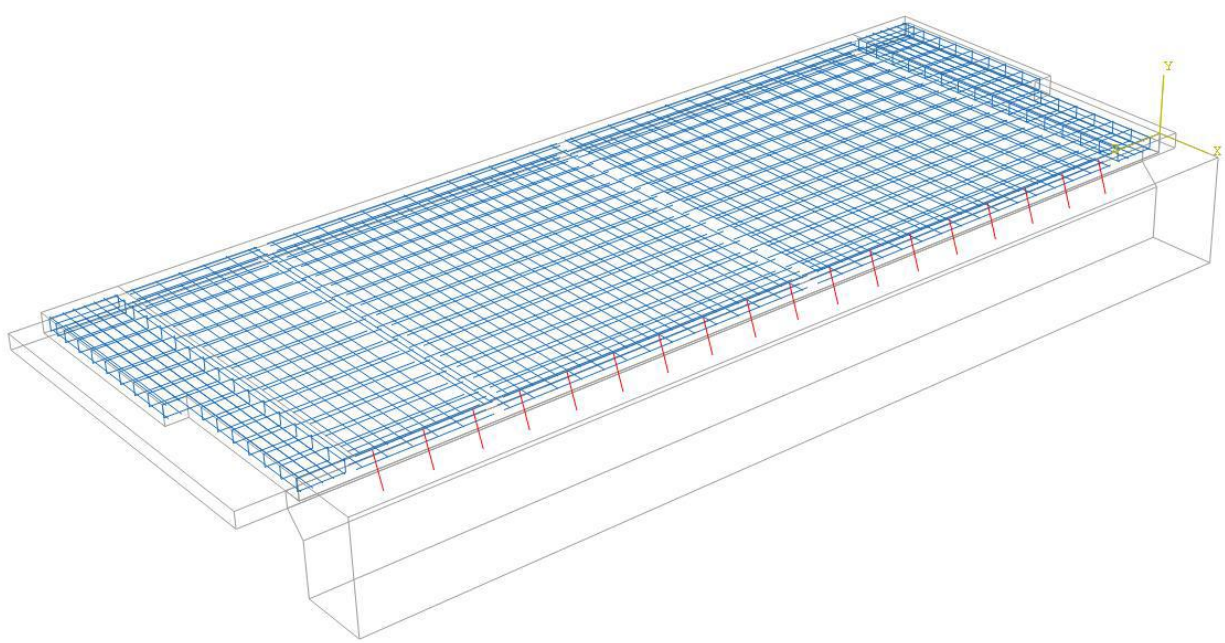

Figure 5.61. Washington County—rebar and connection dowels

Per the 2012 plan set for the approach slab, the compressive strength for this concrete was modeled as 5,000 psi. In addition, a Young's modulus of 3,605 ksi and a Poisson's ratio of 0.3 were used for linear-elastic behavior, and a density of 150 pcf was used for the slab concrete. Per the original plan set from 1997, concrete with a compressive strength of 3,500 psi was used for the modeled abutment. The material properties for the sand were determined based on standard values used by the Iowa DOT and numbers found in other literature.

To further cut down on analysis runtime, each model part was meshed separately (Figure 5.62). In addition, this allowed for the areas of particular interest (the approach slab and the dowels) to be meshed finer than the rest of the model, creating a more accurate representation of the internal stresses and strains within these critical parts. The connection dowels and concrete slab were meshed on a 1 in. grid, the abutment on a 4 in. grid, and the sand layer on a 2 in. grid.

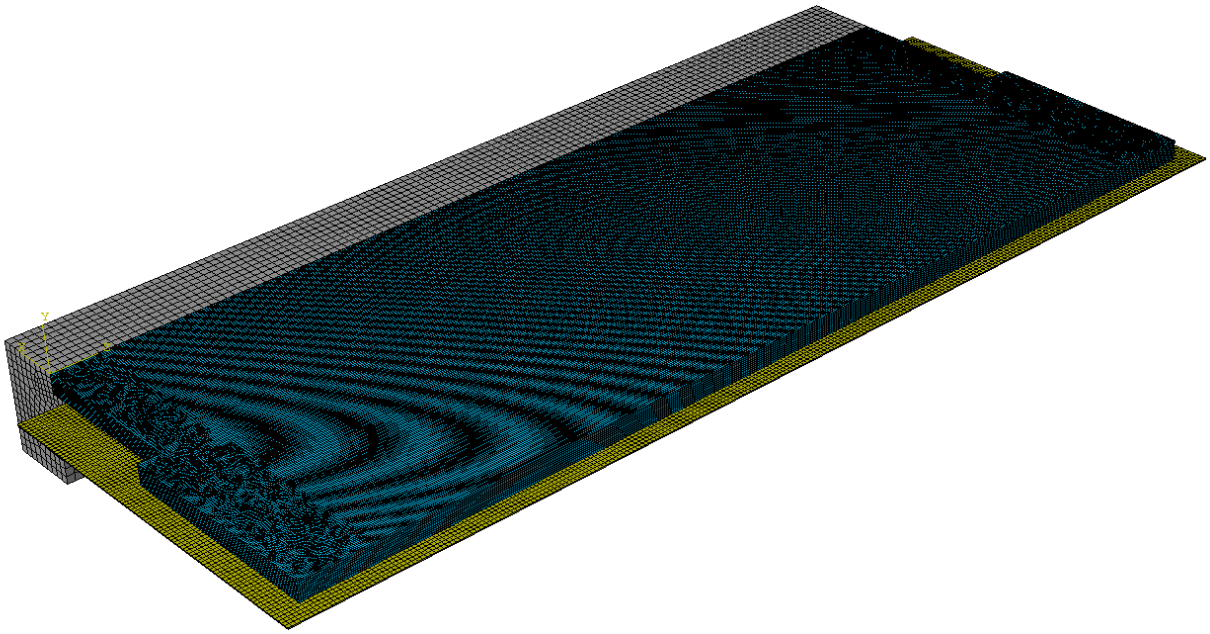

Figure 5.62. Washington County—general layout and meshing of model components

Loading for this model consisted of gravity and the maximum number of HL-93 load trucks that the approach slab would experience in the field. In this case, the maximum loading scenario for this approach slab would consist of two HL-93 trucks driving across the approach slab simultaneously. Each truck was modeled as two distributed strip loads of 36 kips each, totaling 72 kips for each truck (Figure 5.63). By evenly distributing these loads across the entire length of the slab, the analysis results were expected to be more representative of a slab settling slowly over time. Utilizing the same approach for the Jasper County and Story County models, a bed of linear springs was used to model the settlement of the slab as the loading condition was applied.

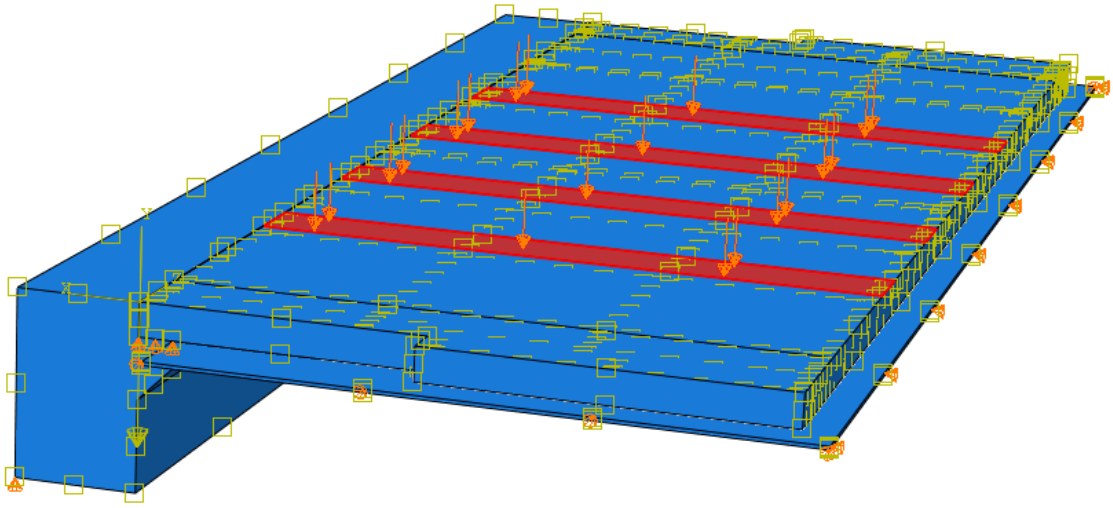

Figure 5.63. Washington County—loading scenario

5.5.4. Finite Element Study and Results

As with the previous analyses, an initial baseline model was run to determine how the model would behave assuming appropriate soil stiffness and minimal settlement. Following the stiffness values used for the previous models, a modulus of subgrade reaction of 250 pcf was used to calibrate the linear springs underneath the slab. This baseline model was run utilizing ABAQUS's Concrete Damaged Plasticity behavior to document any failures within the concrete.

As expected, this model displayed behavior similar to that of the Jasper County model. Because there is no sleeper slab to support the far end of the approach slab, the forces within the connection joint start to increase as soon as the slab begins to settle. Although the complete vertical displacement for this model only resulted in 0.014 in. at the far end of the slab, the maximum concrete tensile stresses within the connection joint were recorded as 181 psi (Figure 5.64). Due to the fact that the concrete used in this approach slab has a strength of 5 ksi compared to the lower strength of 4 ksi for the concrete used in the previous two models, it was expected that the Washington County model would reach a higher tensile value prior to cracking or damage.

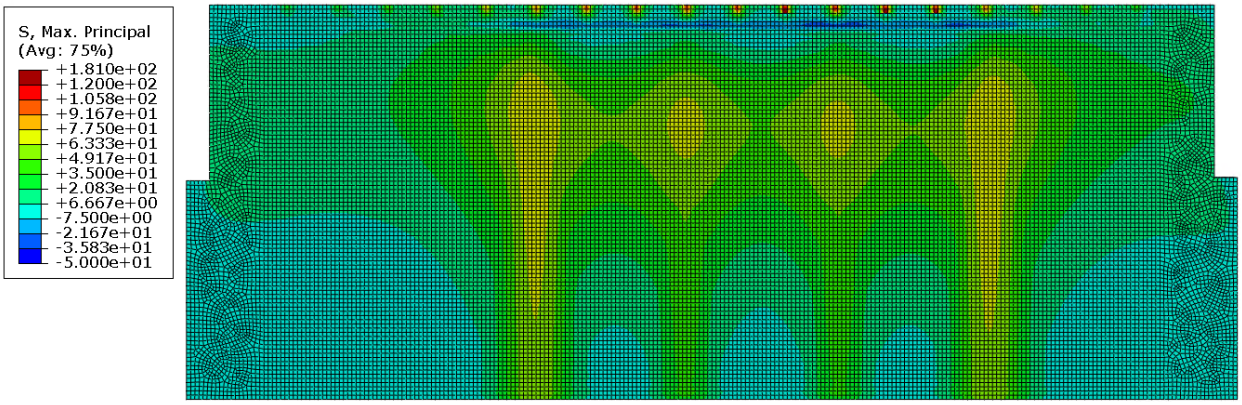

Figure 5.64. Washington County—stress concentrations on bottom of slab

Peak stresses of note elsewhere in the model occurred in the concrete along the top surface of the slab (Figure 5.65), likely as a result of the connection dowels attempting to restrict the rotation of the slab at the abutment seat. However, the highest stress value reached was only 43 psi.

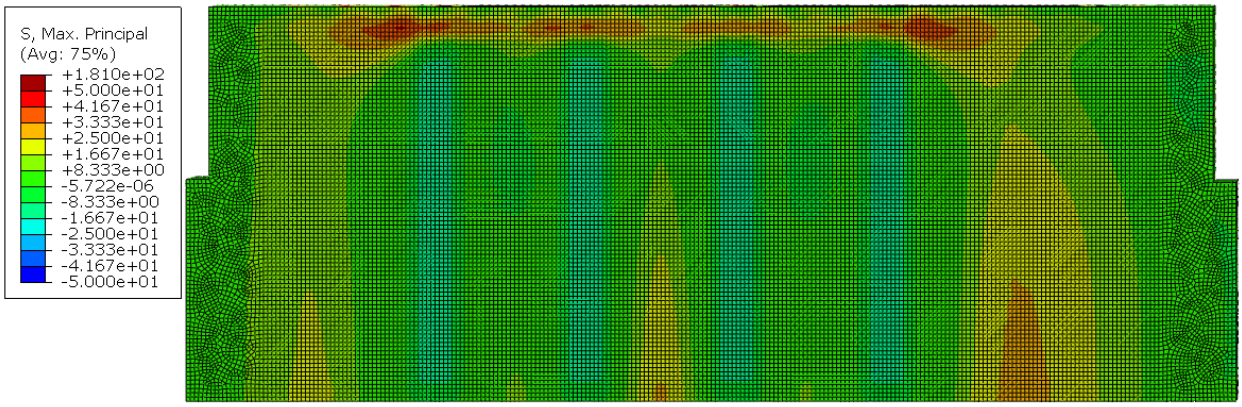

Figure 5.65. Washington County—areas of tensile stress on top surface of approach slab

Following the establishment of this base model, the stiffness value of the linear springs was reduced to simulate soil settlement in the model. However, as with the Jasper County model, the stress concentrations at the connection dowels led to failure at a mere 0.052 in. of settlement with a peak tensile stress of 524 psi (Figure 5.66). These results imply that significant forces are created in the connection joint should any settlement of the slab occur. This comes as a stark contrast to the voiding scenario observed with the Story County model, which is assumed to be supported on the far end by the sleeper slab.

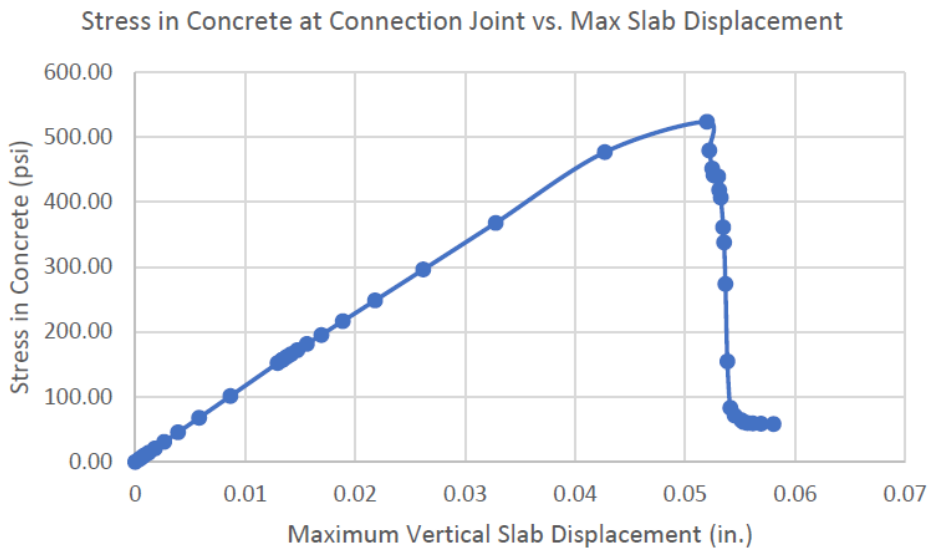

Figure 5.66. Concrete failure in Washington County connection joint

The stress concentrations and damage output provided by this FE model (Figure 5.67) may provide some insight into the failure observed in the Washington County field approach slabs.

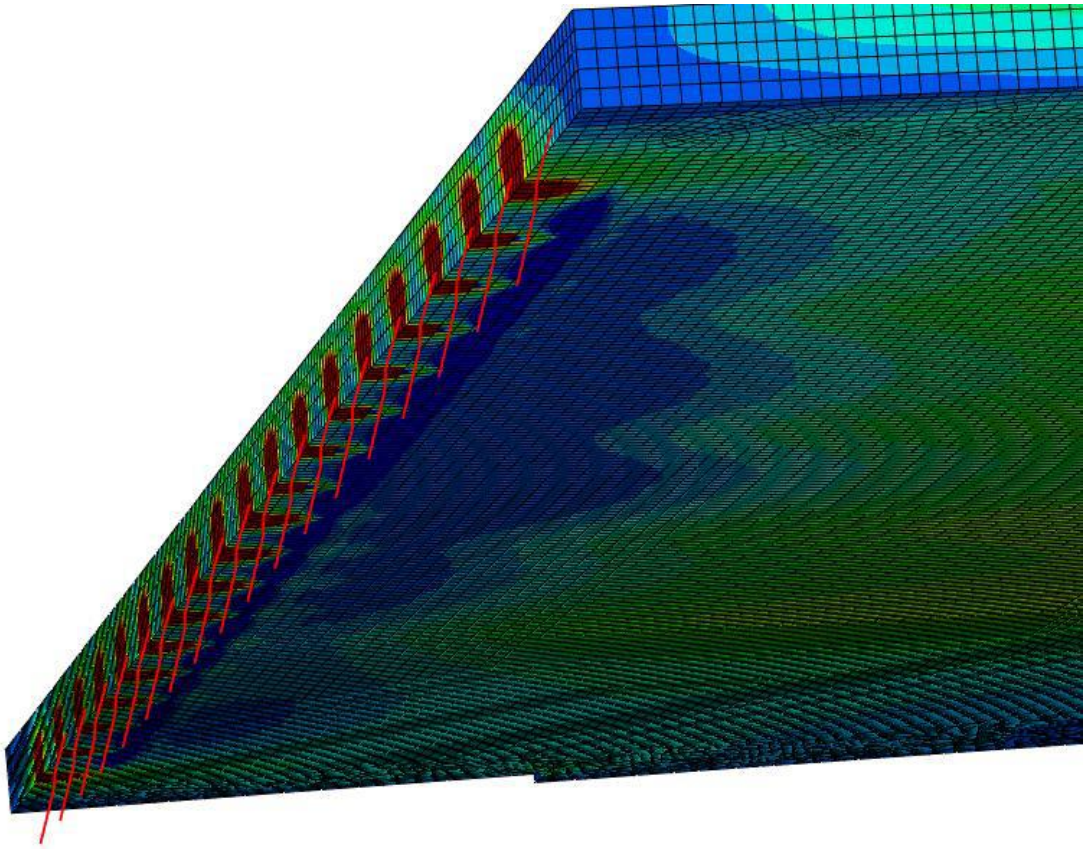

Figure 5.67. Washington County—stress concentrations in dowels and precast panels

While this model appears credible given the similarity of the failure observed in the model to the failure exhibited in the field, it is important to consider how the stress distributions in the approach slab would have developed in other circumstances. It is entirely possible that the stress concentrations displayed in the connection joint for the FE model are higher than those in the field slab. Unfortunately, the addition of damage parameters to the FE model creates an instability once several parts of the model begin to fail, and this leads to convergence issues.

Because these convergence issues do not allow the model to continue applying load after these failures, one option to further investigate stress distributions is to change the model to assume that the concrete in the slab exhibits linear-elastic behavior. Doing so would allow the model to continue to run following the point where the previous model failed due to tensile cracking. By noting the point at which different parts of the model reach appropriate levels of stress and strain to facilitate cracking, it is still possible to infer the point at which this approach slab begins to experience cracking at the connection joint.

After reformatting the model to assume a linear-elastic concrete, no other convergence issues were noted. The linear springs were calibrated with the applied load to provide a theoretical settlement of 1 in. to match the assumed settlement that the Washington County approach slab underwent prior to being mudjacked back to its original height. Following the completion of the simulation, the far, unsupported end of the slab settled 0.96 in. (Figure 5.68). The maximum principal stresses occurred in the same areas as those in the original iteration of the model.

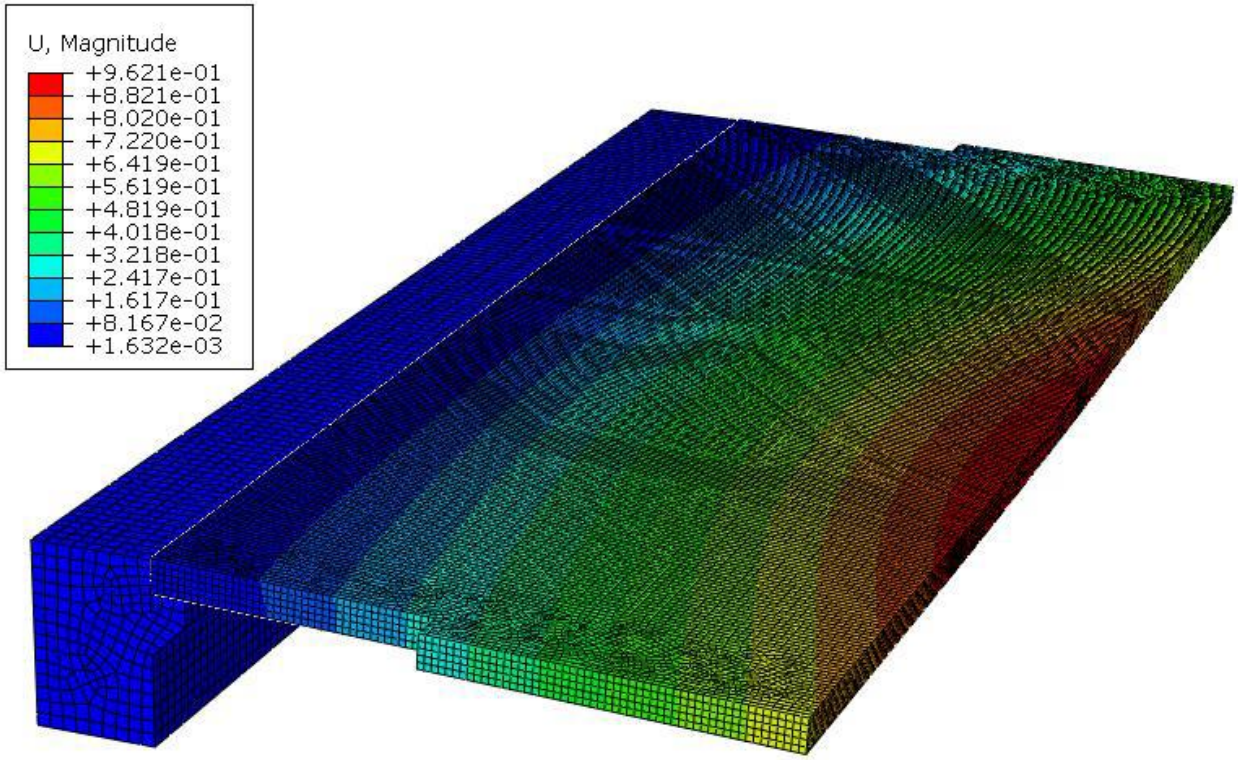

Figure 5.68. Washington County—approach slab settlement

Aside from the stress concentrations observed at the connection joint, 1 in. of settlement resulted in a concrete tensile stress of 475 psi in the area above the paving notch, where cracking was observed in the field (Figure 5.69). The high amount of tensile stress in this area is likely a result of the connection dowels restricting rotation of the slab. As the slab settles on one side and the connection dowels prevent this rotation, the top of the slab is put in flexure and subject to stress concentrations.

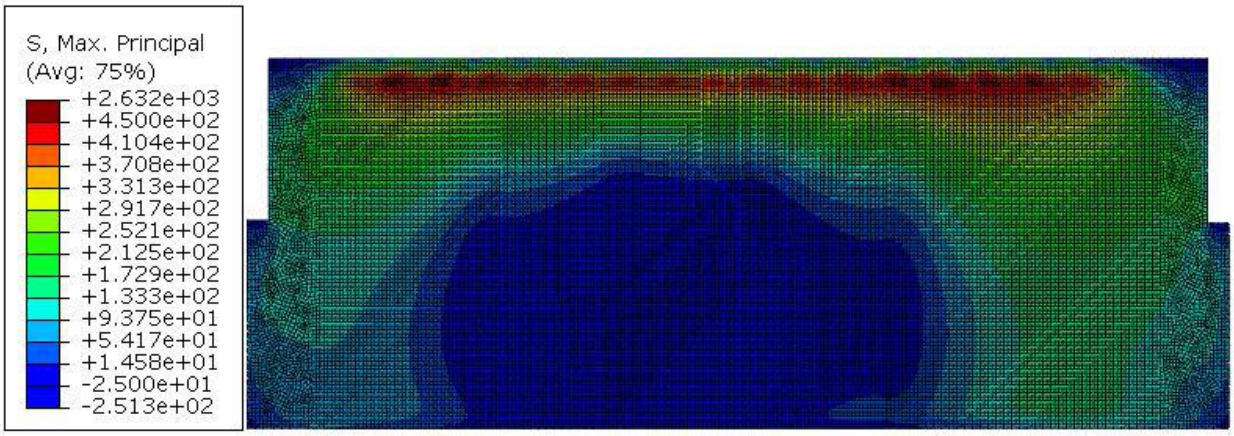

Figure 5.69. Washington County—stress concentrations after approach slab settlement

Based on the results presented for the FE models of the Washington County approach slabs, it appears that excessive settlement played a role in the premature tensile cracking observed at the tied connection joint between the approach slab and the integral abutment. As the approach slab settled during its first year or two of service, the portion of the slab sitting on top of the paving notch attempted to rotate and move upward from the face of the abutment seat. Due to the restraint placed on this rotation by the steel dowels embedded in the concrete of both the approach and the abutment, stress concentrations formed in two areas. The first of these forces was the result of the embedded dowel pulling on the underside of the slab as it attempted to rotate upward. The results of the FE modeling indicate that the forces due to this behavior became evident quickly, which may provide evidence as to why this approach slab connection experienced such significant cracking so soon after its initial construction. The second set of forces, again resulting from the embedded dowels, did not become especially notable until the slab had settled a maximum of approximately 1 in. Again, these forces appeared roughly in the same area as the spalled concrete in the field slab. As such, it is likely that the combination of excessive settlement and the resistance provided by the connection dowels created high stress concentrations that resulted in the concrete cracking observed in the field slab.

CHAPTER 6. CONCLUSIONS AND RECOMMENDATIONS

The objectives outlined in Chapter 1 provide a path to make important conclusions based on the completed work. The conclusions presented in this chapter are separated by the research task for which they were completed.

6.1. Literature Review

Much of the literature documented innovative approach slab and abutment details studied by other investigators with the goal of providing state DOTs and other transportation agencies with valuable information on the performance of said details. The main conclusions drawn from the comprehensive literature review described in this report are summarized below.

Many states are currently attempting to find ways to achieve the benefits of integral and semi-integral abutments while avoiding the issues associated with long bridges or high skew angles. One such example is the so-called Virginia Abutment used by VDOT, which employs an integral backwall separated from another backwall by a large void. A joint is placed at the end of the bridge, but the design prevents any water from reaching the bearings. The separation of the first backwall from the soil backfill eliminates most of the issues associated with integral abutments, especially for long bridges or those with high skews. The large void between the double backwalls allows easy drainage and maintenance, since it is large enough and open on the sides of the bridge to allow for clearing of debris. The concept of the Virginia Abutment would improve performance for bridges with conventional bearings, but it would not be necessary for situations where other abutment types would be acceptable that have less complexity in terms of constructability.

The deck-over-backwall concept is another abutment and approach slab detail that aims to realize the benefits of integral construction, including the elimination of a traditional joint at the deck end while also trying to eliminate the expansion of the bridge into the backfill. Research conducted by MDOT provides an example of deck-over-backwall construction that uses a layer of expanded polystyrene between the backwall top surface and the approach slab. The Butler County 118 demonstration bridge documented in Section 5.5 incorporates the deck-over-backwall concept at the east abutment.

VDOT uses an abutment type hierarchy for new bridge designs. Based on length and skew limitations, the process prioritizes integral abutments, semi-integral abutments, the deck-over-backwall concept, and finally the Virginia Abutment. The Iowa DOT provides a set of limitations on the use of integral abutments, but development of a similar hierarchy after finalizing investigation of new abutment details would prove beneficial in ensuring that a consistent and effective abutment type is chosen for a given project.

Corbels used to support the approach slab should be avoided if possible. The use of a corbel increases the difficulty of attaining proper backfill compaction next to the abutment, a key component of minimizing approach slab settlement. The Iowa DOT J-series bridge standards are

an example of the use of a paving notch as a part of the abutment. However, Story County 118 and the Iowa DOT H-series bridge standards include the use of a corbel. Corbels may not be eliminated easily for semi-integral abutment conversions in which the footing width of the existing abutment is predetermined.

Inclined tie bars are recommended for use with semi-integral abutments to allow approach slab rotation at the tied joint. Backfill settlement under the approach slab inevitably leads to a rotation at the end of the slab, which is best accommodated by inclined bars that do not transfer moment.

Buttresses and other bridge end guidance methods restrict thermal expansion to the longitudinal axis. Skewed bridges experience lateral earth pressure forces that cause rotation of the entire bridge superstructure after repeated thermal loading cycles. Transverse displacement complicates the behavior of tied approach slabs and other detailing aspects that may best be controlled by restricting expansion to the longitudinal axis.

The Iowa DOT BR-205 Standard Road Plan includes the use of a sleeper slab to support one end of the approach slab. A perforated subdrain is used under the EF joint in one direction from the sleeper slab and behind the abutment in the other direction from the sleeper slab. A joint exists between the approach slab and sleeper slab for which there is no subdrain. The formed curb at the side of the approach slab and sleeper slab is not continuous over the joint. An example from the literature shows drain collector pipes placed at the base of the sleeper slab. The lack of a subdrain at the sleeper slab for a tied approach slab conflicts with the design intent of having the entire bridge expansion accommodated at that location. The large movements expected at this location increase the possibility of surface water infiltration over time.

Approach slabs are designed to span the distance between the abutment and sleeper slab should a loss of support from the backfill occur. Sleeper slabs are placed on the same backfill material, so it follows that they may be susceptible to similar issues with settlement. It has been shown that a thicker approach slab (e.g., 16 in.) and sleeper slab supported by soil reinforced with two geogrid layers improved the road profile. Settlement of sleeper slabs was not found to be a critical parameter, but improvement of the soil support for the sleeper slab may be an option should the issue arise.

The abutment backfill details for the bridges assessed during the field monitoring portion of this research use a geotextile layer placed behind the abutment before filling with porous backfill. The geotextile is described as “permeable” per Iowa DOT IM 4196.01, which would allow for a hydraulic short circuit should drainage become blocked. Water would make its way underneath the abutment, possibly reaching the foundation piles. A geomembrane has been used in a similar manner to prevent such a hydraulic short circuit. However, the design choice of a geotextile may have been made in anticipation of blocked drainage to prevent accumulation of water behind the abutment. The choice of material should be evaluated with regard to the design intent.

6.2. Inspections

Seven different bridge designs that used tied approach slabs, including nine different structures, were inspected for condition as it relates to service life. The 1/4 in. preformed tied approach joints used at every location measured between 3/8 in. and 1 5/8 in. The joints were found to be opening over time and not performing as intended. Decreased joint widths at the opposite ends of the approach slabs highlight the fact that the approach slabs are shifting away from the tied connection. Multiple bridges using the Iowa DOT BR-205 Standard Road Plan have been let within the past few years. The road plan includes the use of a tied approach with vertical paving notch dowels. Future inspections should be completed to determine the effectiveness of the tied approach joints. Ideally, inspections would take place at least one year after initial construction to allow the bridges to experience one full seasonal temperature cycle.

The condition and performance of the joints between the wingwalls and the approach slab curbs appeared unsatisfactory on multiple occasions. Noted problems included a 6 in. deep void at the intersection of the approach to the deck joint and wingwall, separation of the approach slab and wingwall and opening of the joint, concrete cracking at the beginning of the approach slab curb, and frequent poor drainage resulting in buildup of debris at the beginning of the curb. The poor performance of the joints between the wingwalls and the approach slabs together with recommendations made based on a review of the literature indicate that barrier rails should be placed on top of the approach slab when the approach slabs are tied to the abutments. Strip seals are recommended for new construction of integral and semi-integral abutments. An example of a curb “kick-up” detail is provided, and a similar detail would be required to accommodate the continuous curb on the sleeper slab.

Abutment drainage was largely free of debris and able to drain water from behind the abutments should it infiltrate the deck joints. A single bridge, 310 Jasper Southbound (reconstructed in 2010), had drain exits for which the openings were reasonably close to the abutment and blocked by soil.

6.3. Field Monitoring

Field monitoring was completed for four different bridges in Iowa. The first was Jasper County 118, a 184×28 ft bridge with a 45 degree skew. The Jasper County 118 semi-integral abutment conversion was designed with the intent that the west abutment would be fixed and the east abutment would be moveable. Bridge displacement data captured by displacement transducers show movements of similar magnitudes for both abutments. Displacement transducers installed perpendicular to the bridge centerline measured transverse displacements equal to 81% and 120% of the longitudinal displacements for the semi-integral abutment bridge with a 45 degree skew.

Earth pressure sensors installed on the Jasper County 118 semi-integral abutment backwall just under the approach slab provided the range of pressures. The maximum pressure reached the calculated passive pressure value. A full yearly temperature cycle would prove invaluable for monitoring earth pressures during a warming period of bridge expansion.

The second bridge included for monitoring was Story County 118, a 375×60 ft integral abutment bridge with a 15 degree skew. Superstructure expansion of the Story County 118 bridge was captured using crackmeters installed at the tied approach joints and the approach-slab-to-sleeper-slab joints at both ends of the bridge. Displacement transducers require a fixed reference point, which would have been difficult to provide in this case given the fact that the Story County 118 bridge was new construction and embankment settlement can alter displacement readings. By assuming that the sleeper slabs are fixed in place, all expansion of the sleeper slabs and the superstructure was accounted for.

Crackmeters mounted on the Story County 118 bridge barrier rails measured movement in the tied approach slab joints without placing sensors on the road surface. While the initial data show that the joints experience cyclic opening and closing due to bridge expansion, the behavior is not simply a linear response. It is postulated that long-term monitoring may reveal additional joint expansion.

The third bridge included for monitoring was Polk County 120 over the Des Moines River that featured a 710.5×62 ft bridge deck with a skew angle of 15 degrees. The concrete temperatures in the east and west ends taken by averaging the temperatures measured by the strain gauges were plotted against the air temperatures measured by the datalogger. Joint expansion versus concrete temperature was also plotted, with positive values corresponding to bridge contraction, in which the approach slab pulls away from the sleeper slab. The movement between the approach slab and the abutment was found to be significantly low, indicating a good connection. A strong linear relationship with temperature indicates that the joint opens and closes depending on expansion and contraction of the bridge. As the temperature decreases, the bridge contracts and pulls on the approach slab, inducing tension.

The fourth bridge included for monitoring was Butler County 118, a new construction bridge located in Butler County, Iowa, with improved design features in its abutments. The bridge is 498 ft in length and 44 ft in width with five spans and a skew angle of 15 degrees. The west abutment was designed as an integral abutment, while the east abutment was constructed as a semi-stub abutment. This design decision was made to explore the potential for using semi-stub abutments in longer structures, possibly exceeding 1,000 ft in length.

Strain gauges were placed throughout the approach slab to measure strains induced by temperature effects and bending. Crackmeters were also installed to measure movement in the approach-slab-to-bridge-deck joint. Data collected from the bridge revealed patterns, particularly in the behavior of the top bars of the east approach slab. The joint expansion between the approach slab and the bridge deck showed a strong linear relationship with temperature. Also, the approach-slab-to-sleeper-slab joint graphs showed almost linear trends, indicating high tensile strains corresponding to low temperatures and high compressive strains corresponding to high temperatures.

The strain gauges close to the approach-slab-to-bridge-deck joint in the middle part of the approach slabs showed normal behavior in the bottom bars at both ends of the approach slabs, but the top bars on the east side exhibited high tensile strains, especially during warm weather. The strain plots for the acute and obtuse corners of the approach slabs indicated different patterns

on the east side, with the top bars at the acute corners consistently in tension and the bottom bars at the obtuse corners exhibiting normal behavior. The behavior recorded for the top bars in the east approach slab might be due to several factors, such as the presence of a minor transverse crack at the joint with the abutment and the working room gap between the abutment diaphragm and the backwall. The working room gap could possibly lead to a detrimental pivot point and crack development, which may be exacerbated by live loads and settlement effects.

6.4. Finite Element Analysis

Finite element models of bridge ends were developed to study the effect of bridge thermal movement and the response of the approach slabs. Various parameters, such as approach slab friction, soil stiffness, tie bar style, and bridge skew, were systematically investigated through FE simulations.

Load-displacement curves produced for the Jasper County bridge approach slab with a tied connection show a lateral force in the tied joint of a similar magnitude to the longitudinal force. The force develops very quickly, with only a fraction of the maximum displacement required to realize the movement of the slab in both directions. Tied joint design should therefore account for large lateral forces. As mentioned previously, limiting bridge expansion in the transverse direction using buttresses could eliminate transverse displacement of the slab. Moreover, the results of additional models indicated that there were stress concentrations at this connection point. However, this was not deemed concerning because the stress levels were still reasonably low.

Comparisons of the Story County bridge model with field monitoring data show similar magnitudes of strain induced in the tie bars. However, tied approach joint expansion was slightly underestimated in the model. The model shows a deformation in the tie bars before the strain reaches a plateau and the entire approach slab begins sliding. In contrast, continuous opening of the joint was observed in the instrumentation data.

Furthermore, a series of FE models was generated to investigate how the Story County approach slabs would accommodate settlement and voiding conditions. A range of lengths, i.e., 5, 8, 10, 13, and 16 ft, were used to gain insight into how the approach slab would fare when forced to span a variety of settlement trenches. The analysis revealed that the erosion void does not produce significant increases in tensile stress within the slab until the length reaches approximately 6 ft. Following this point, the results of the investigation determined that the approach slab would possibly experience tensile cracking at the connection joint with a settlement void length of 11 ft. It was also observed that transverse cracking would possibly begin to occur in the bottom of the slab with a void length of 16 ft. However, based on the void lengths observed in past studies, it is likely that the approach slab would be able to adequately span the voiding conditions typically observed in the field.

Increasing the coefficients of friction between the concrete approach slab and soil only served to increase the total force required to pull the slab. The stresses in the tie bars also increased proportionally, while the force distribution across the bars remained relatively unchanged. The

uncertainties involved in estimating approach slab friction were shown to have minimal effect on how forces are carried by the bars.

While soil stiffness did not affect the concrete or tie bar stresses during bridge contraction, it was found that stiffer soil can considerably increase concrete and tie bar stresses (i.e., maximum values) at the full range of thermal expansion. Inclined tie bars experienced lower stresses than vertical tie bars during bridge contraction while pulling the approach slab. Concrete stresses showed no notable trends with regard to bar orientation.

Skew drastically changes the stress distribution in the tie bars across the tied approach joint. Force is shifted towards the acute approach slab corner/obtuse bridge corner. Stresses were simultaneously lowered in the obtuse slab corner, resulting in a greater range of stresses for increased skew angles. These results were consistent with the case of an extreme skew angle of 55 degrees (which exceeds the current Iowa DOT skew limit of 45 degrees), for which the Shelby County bridge model exhibited a similar variation in stress in the tie bars across the width of the tied approach joint during bridge contraction.

REFERENCES

Abu-Hejleh, N., D. Hanneman, T. Wang, and I. Ksouri. 2008. Evaluation and recommendations for flowfill and mechanically stabilized earth bridge approaches. *Transportation Research Record: Journal of the Transportation Research Board*, Vol. 2045, pp. 51–61.

Aktan, H., and U. Attanayake. 2011. *High Skew Link Slab Bridge System with Deck Sliding over Backwall or Backwall Sliding over Abutments: Part II*. MDOT RC-1563. Western Michigan University, Kalamazoo, MI.

Aktan, H., U. Attanayake, and E. Ulku. 2008. *Combining Link Slab, Deck Sliding over Backwall, and Revising Bearings*. MDOT RC-1514. Western Michigan University, Kalamazoo, MI.

Arenas, A., G. Filz, and T. Cousins. 2013. *Thermal Response of Integral Abutment Bridges with Mechanically Stabilized Earth Walls*. Virginia Department of Transportation, Richmond, VA.

Bakeer, R., N. Mattei, B. Almalik, S. Carr, and D. Homes. 2005. *Evaluation of DOTD Semi-Integral Bridge and Abutment System*. Louisiana Transportation Research Center, Louisiana Department of Transportation and Development, Baton Rouge, LA.

Biana, I. 2010. A semi-integral composite bridge of high skew. *Bridge Engineering*, Vol. 163, No. BE3, pp. 115–124. https://doi.org/10.1680/bren.2010.163.

Bonczar, C., S. Brena, S. Civjan, J. DeJong, B. Crellin, and D. Crovo. 2005. Field data and FEM modeling of the Orange-Wendell Bridge. Integral Abutment and Jointless Bridges (IAJB 2005), March 16–18, Baltimore, MD, pp. 163–173.

Bonczar, C., S. Brena, S. Civjan, J. DeJong, and D. Crovo. 2005. Integral abutment pile behavior and design - Field data and FEM studies. Integral Abutment and Jointless Bridges (IAJB 2005), March 16–18, Baltimore, MD, pp. 174–184.

Briaud, J., R. James, and S. Hoffman. 1997. *NCHRP Synthesis 234: Settlement of Bridge Approaches (The Bump at the End of the Bridge)*. National Cooperative Highway Research Program, Washington, DC. http://onlinepubs.trb.org/Onlinepubs/nchrp/nchrp_syn_234.pdf.

Cai, C.S., G. Z. Voyiadjis, X. Shi. 2005. *Determination of Interaction between Bridge Concrete Approach Slab and Embankment Settlement*. FHWA/LA.05/403. Louisiana Transportation Research Center, Louisiana Department of Transportation and Development, Baton Rouge, LA.

Chen, Q., and M. Abu-Farsakh. 2016. Mitigating the bridge end bump problem: A case study of a new approach slab system with geosynthetic reinforced soil foundation. *Geotextiles and Geomembranes*, Vol. 44, No. 1, pp. 39–50.

Chen, Q. 2007. An Experimental Study on Characteristics and Behavior of Reinforced Soil Foundation. PhD dissertation. Louisiana State University, Baton Rouge, LA.

DeJong, A., W. Shi, B. Shafei, and T. Hosteng. 2021. Laboratory and numerical investigation of integral abutment connections with pile couplers. *Engineering Structures*, Vol. 248, Article No. 113159, pp. 1–12.

DeJong, A., W. Shi, B. Shafei, and T. Hosteng. 2021. Integral abutment connections with grouted reinforcing bar couplers and ultra-high performance concrete. *ASCE Journal of Bridge Engineering*, Vol. 26, No. 8, Article No. 04021042, pp. 1–15.

Dicleli, M., and S. Albhaisi. 2003. Maximum length of integral bridges supported on steel H-piles. *Engineering Structures*, Vol. 25, No. 12, pp. 1491–1504.

Dunker, K., and A. Abu-Hawash. 2005. Expanding the use of integral abutments in Iowa. 2005 Mid-Continent Transportation Research Symposium, August 18–19, Ames, IA.

Dupont, B., and D. Allen. 2002. *Movements and Settlements of Highway Bridge Approaches*. KTC-02-18/SPR-220-00-1F. Kentucky Transportation Center, University of Kentucky, Lexington, KY.

Fell, D. 2022. Comparative analysis of bridge abutment types. Williams Honors College, Honors Research Projects. 1540. University of Akron, Akron, OH.

Greimann, L., B. Phares, A. Faris, and J. Bigelow. 2008. *Integral Bridge Abutment-to-Approach Slab Connection*. Center for Transportation Research and Education, Ames, IA.

Hassiotis, S., Y. Khodair, E. Roman, and Y. Dehne. 2006. *Evaluation of Integral Abutments*. FHWA-NJ-2005-025. New Jersey Department of Transportation, Trenton, NJ.

Hoppe, E. K. Weakley, and P. Thompson. 2016. Jointless bridge design at the Virginia Department of Transportation. *Transportation Research Procedia*, Vol. 14 (2016), pp. 3943–3952.

Hoppe, E. J., and S. L. Eichenthal. 2012. *Thermal Response of a Highly Skewed Integral Bridge*. VCTIR 12-R10. Virginia Center for Transportation Innovation and Research, Charlottesville, VA.

Horvath, J. S. 2005. Integral-abutment bridges: Geotechnical problems and solutions using geosynthetics and ground improvement. Integral Abutment and Jointless Bridges (IAJB 2005), March 16–18, Baltimore, MD, pp. 281–291.

IDOT. 2012. Memorandum: 2012 Integral Abutment Bridge Policies and Details. Illinois Department of Transportation, Springfield, IL. https://idot.illinois.gov/content/dam/soi/en/web/idot/documents/doing-business/memorandums-and-letters/highways/bridges/abd-memos/abd123.pdf.

ITD. 2008. 11.6.1.3 Design Guidelines for Integral Abutments. *Idaho Transportation Department LRFD Bridge Design Manual*. Idaho Transportation Department, Boise, ID.

Kaniraj, S. 1988. *Design Aids in Soil Mechanics and Foundation Engineering*. 10th Ed. McGraw-Hill India, Uttar Pradesh, India.

Karim, R., and B. Shafei. 2022. Addition of partial-depth link slabs to bridge structures: Role of support conditions. *ASCE Journal of Bridge Engineering*, Vol. 27, No. 7, Article No. 04022049, pp. 1–12.

Karim, R., and B. Shafei. 2021. Performance of fiber-reinforced concrete link slabs with embedded steel and GFRP rebars. *Engineering Structures*, Vol. 229, Article No. 111590, pp. 1–12.

Kim, W., and J. A. Laman. 2011. Seven-year field monitoring of four integral abutment bridges. *Journal of Performance of Constructed Facilities*, Vol. 26, No. 1, pp. 54–64.

Kong, B., C. S. Cai, and Y. Zhang. 2016. Parametric study of an integral abutment bridge supported by prestressed precast concrete piles. *Engineering Structures*, Vol. 120, pp. 37–48. https://doi.org/10.1016/j.engstruct.2016.04.034.

LaFave, J. M., J. K. Riddle, M. W. Jarrett, B. A. Wright, J. S. Svatora, H. An, and L. A. Fahnestock. 2016. Numerical simulations of steel integral abutment bridges under thermal loading. *Journal of Bridge Engineering*, Vol. 21, No. 10. https://doi.org/10.1061/(ASCE)BE.1943-5592.0000919.

LaFave, J. M., L. A. Fahnestock, G. Brambila, J. K. Riddle, M. W. Jarrett, J. S. Svatora, B. A. Wright, and H. An. 2017. *Integral Abutment Bridges under Thermal Loading: Field Monitoring and Analysis*. FHWA-ICT-17-017. Illinois Center for Transportation, University of Illinois at Urbana–Champaign, Urbana, IL.

Lenke, L. R. 2006. *Settlement Issues – Bridge Approach Slabs*. New Mexico Department of Transportation, Albuquerque, NM.

Long, J. H., S. M. Olson, T. D. Stark, and E. A. Samara. 1998. Differential movement at embankment-bridge structure interface in Illinois. Paper No. 98-1575. *Transportation Research Record: Journal of the Transportation Research Board*, Vol. 1633, pp. 53–60.

Luna, R., J. Robison, and A. Wilding. 2004. *Evaluation of Bridge Approach Slabs, Performance and Design*. Missouri Department of Transportation, Jefferson City, MO.

Maruri, R. F., and S. Petro. 2005. Integral Abutments and Jointless Bridges (IAJB) 2004 survey summary. Integral Abutment and Jointless Bridges (IAJB 2005), March 16–18, Baltimore, MD, pp. 12–29.

Mekkawy, M. M., D. J. White, M. T. Suleiman, and S. Sritharan. 2005. Simple design alternatives to improve drainage and reduce erosion at bridge abutments. 2005 Mid-Continent Transportation Research Symposium, August 18–19, Ames, IA.

Miller, G. A., K. Hatami, A. B. Cerato, and C. Osborne. 2013. *Applied Approach Slab Settlement Research, Design/Construction*. FHWA-OK-13-09 2227. Oklahoma Department of Transportation, Oklahoma City, OK.

Mistry, V. C. 2005. Integral abutment and jointless bridges. Integral Abutment and Jointless Bridges (IAJB 2005), March 16–18, Baltimore, MD, pp. 3–11.

Nadermann, A., L. Greimann, and B. Phares. 2010. *Instrumentation and Monitoring of Precast Bridge Approach Tied to an Integral Abutment Bridge in Bremer County*. Bridge Engineering Center, Ames, IA.

Nassif, H. H., T. Abu-Amra., N. Suksawang, Y. Khodair, and N. Shah. 2009. Field investigation and performance of bridge approach slabs. *Structure and Infrastructure Engineering*, Vol. 5, No. 2, pp. 105–121.

Nassif, H., T. Abu-Amra, N. Shah. 2002. *Finite Element Modeling of Bridge Approach and Transition Slabs*. FHWA-NJ-2002-007. Center for Advanced Infrastructure and Transportation, Rutgers University, Piscataway, NJ.

Oliva, M. G., and G. Rajek. 2011. *Toward Improving the Performance of Highway Bridge Approach Slabs*. CFIRE 03-10. National Center for Freight and Infrastructure Research and Education, Madison, WI.

Olson, S. M., K. P. Holloway, J. M. Buenker, J. H. Long, and J. M. Lafave. 2013. *Thermal Behavior of IDOT Integral Abutment Bridges and Proposed Design Modifications*. FHWA-ICT-12-022. Illinois Center for Transportation, University of Illinois at Urbana–Champaign, Urbana, IL.

Olson, S. M., J. H. Long, J. R. Hansen, D. Renekis, and J. M. Lafave. 2009. *Modification of IDOT Integral Abutment Design Limitations and Details*. ICT-09-054. Illinois Center for Transportation, University of Illinois at Urbana–Champaign, Urbana, IL.

Phares, B. M., D. White, J. Bigelow, M. Berns, and J. Zhang. 2011. *Identification and Evaluation of Pavement-Bridge Interface Ride Quality Improvement and Corrective Strategies*. Institute for Transportation, Ames, IA.

Phares, B., and J. Dahlberg. 2015. *Performance and Design of Bridge Approach Panels in Wisconsin*. 0092-14-04. Wisconsin Department of Transportation, Madison, WI.

Potyondy, J. 1961. Skin friction between various soils and construction materials. *Geotechnique*, Vol. 11, No. 4, pp. 339–353.

Puppala, A., S. Saride, E. Archeewa, L. Hoyos, and S. Nazarian. 2009. *Recommendations for Design, Construction, and Maintenance of Bridge Approach Slabs: Synthesis Report*. FHWA/TX-09/0-6022-1. The University of Texas at Arlington, Arlington, TX.

Rende, N., and J. Donnelly. 2011. *Approach Slab Assessment – Full Testing Program Report*. WJE No. 2010.2389.2. Wiss, Janney, Elstner Associates, Inc., Northbrook, IL.

Reza, F. 2013. *Synthesis of Bridge Approach Panels Best Practices*. MN/RC 2013-09. Minnesota Department of Transportation, St. Paul. MN.

Robison, J. L., and Luna, R. 2004. Deformation analysis of modeling of Missouri bridge approach embankments. *Geotechnical Engineering for Transportation Projects*, Proceedings of GeoTrans 2004, July 27–31, Los Angeles, CA. American Society of Civil Engineers, Reston, VA. pp. 2020–2027.

Schaefer, V. R., and J. C. Koch. 1992. *Void Development under Bridge Approaches*. Report No. SD90-03. South Dakota Department of Transportation, Pierre, SD.

Seo, J., H. Ha, and J. L. Briaud. 2002. *Investigation of Settlement at Bridge Approach Slab Expansion Joint: Numerical Simulations and Model Tests*. FHWA/TX-03/0-4147-2. Texas Transportation Institute, College Station, TX.

Shi, W., B. Shafei, Z. Liu, and B. Phares. 2020. Longitudinal box-beam bridge joints under monotonic and cyclic loads. *Engineering Structures*, Vol. 220, Article No. 110976, pp. 1–11.

Thiagarajan, G., S. Ajgaonkar, M. Eilers, and C. Halmen. 2012. Cost-efficient and innovative design for bridge approach slab. *Transportation Research Record: Journal of the Transportation Research Board*, Vol. 2313, pp. 100–105. https://doi.org/10.3141/2313-11.

Varmazyar, M., R. Wozniak, and R. Walsh. 2017. Utilizing compressible inclusions and cement stabilised sand for integral bridges. Austroads Bridge Conference 2017, April 3–6, Melbourne, Australia.

Wahls, H. E. 1990. *NCHRP Synthesis 159: Design and Construction of Bridge Approaches*. National Cooperative Highway Research Program, Washington, DC.

Weakley, K. 2005. VDOT integral bridge design guidelines. Integral Abutment and Jointless Bridges (IAJB 2005), March 16–18, Baltimore, MD, pp. 61–70.

White, D. J., S. Sritharan, M. Suleimann, M. Mekkawy, and S. Chetlur. 2005. *Identification of the Best Practices for Design, Construction, and Repair of Bridge Approaches*. Center for Transportation Research and Education, Ames, IA.

White, D. J., M. M. Mekkawy, S. Sritharan, and M. T. Suleiman. 2007. "Underlying" causes for settlement of bridge approach pavement systems. *Journal of Performance of Constructed Facilities*, Vol. 21, No. 4, pp. 273–282.

White, H. 2007. *Integral Abutment Bridges: Comparison of Current Practice Between European Countries and the United States of America*. FHWA/NY/SR-07/152. New York State Department of Transportation, Albany, NY.

Yasrobi, S. Y., K. W. Ng, T. V. Edgar, and M. Menghini. 2016. Investigation of approach slab settlement for highway infrastructure. *Transportation Geotechnics*, Vol. 6, pp. 1–15.

THE INSTITUTE FOR TRANSPORTATION IS THE FOCAL POINT FOR TRANSPORTATION AT IOWA STATE UNIVERSITY.

InTrans centers and programs perform transportation research and provide technology transfer services for government agencies and private companies;

InTrans contributes to Iowa State University and the College of Engineering's educational programs for transportation students and provides K–12 outreach; and

InTrans conducts local, regional, and national transportation services and continuing education programs.

INSTITUTE FOR TRANSPORTATION

IOWA STATE UNIVERSITY

Visit **InTrans.iastate.edu** for color pdfs of this and other research reports.